Synthesis and Reactivity of Alkaline Earth and Aluminium Gallyl Complexes

José Adán Reyes Sánchez BSc MSci AMRSC

St Edmund Hall

Thesis submitted to the University of Oxford for the degree of Doctor of Philosophy in Inorganic Chemistry, June 2018.

The work described in this Thesis was carried out in the Chemistry Research Laboratory, University of Oxford from October 2013 to December 2017 under the supervision of Professor Philip Mountford. All work is my own unless stated to the contrary, and has not previously been submitted for any degree at this or any other university.

Jose Adan Reyes Sanchez

June 2018

Abstract

Jose Adan Reyes Sanchez Trinity 2018

St Edmund Hall D.Phil. Thesis

This Thesis describes the synthesis and characterisation of new alkaline earth metal and aluminium gallyl complexes. Experimental studies were performed to investigate their structure. The reactivity of these species was also studied.

Chapter 1 introduces metal-metal bonded complexes containing alkaline earth metals and aluminium and the use of gallium(I) analogues of N-heterocyclic carbenes in the synthesis of heterobimetallic complexes of gallium.

Chapter 2 describes the synthesis and reactivity of alkaline earth gallyl complexes supported by β-diketiminate ligands.

Chapter 3 presents the synthesis and reactivity of alkaline earth gallyl complexes supported by the carbazolide ligand CzOx.

Chapter 4 describes synthesis of aluminium-gallium bonded complexes supported by amidinate and β-diketiminate ligands and the attempted study of their reactivity.

Chapter 5 presents full experimental procedures and characterising data for the new complexes reported.

CD Appendix contains .cif files for all new crystallographically characterised complexes described.

Contents

Acknowledgements

First and foremost I would like to express my sincere gratitude to Professor Philip Mountford for giving me the opportunity to be part of his group and for all his invaluable support even before the start of my studies. I am also grateful for his advice and guidance during my time in Oxford. Thanks also for being an example of passion for science.

I would like to express my gratitude to the Mexican Council of Science and Technology (CONACYT, Scholarship 313866, Scholar 218287), the Mexican Secretariat of Public Education (SEP), the Department of Chemistry of the University of Oxford and St Edmund Hall, Oxford, for their financial support without which my DPhil studies would not have been possible.

Thanks to all members of the Mountford group, past and present, for creating a welcoming and friendly environment. Special thanks go to Dr Matthew Blake for his help, patience and guidance during the first three years of my DPhil. Thanks to Dr Liban Saleh for his help and advice on the tricks of lanthanides and gallyl magic! Special thanks also go to Dr Andrey Protchenko for his recommendations and for the many conversations we had sometimes during the late hours in the lab. Thanks to George Schenck for his perseverance and humour during his challenging Part II project. Thanks to Ross Green for being my always humorous colleague in the Team Metal-Metal Bond. Thanks also to Natália Vieira Reis for her company and never ending patience as part of being my fumehood neighbour.

I am grateful to Prof. Philip Mountford, Dr Matthew Blake, Dr Benjamin Clough and Dr Bowen Xie for their contribution to the collection and solving of X-ray crystallographic data. I am also thankful to Dr Nick Rees for the training and assistance in NMR spectroscopy I received.

Thanks to the Mexican friends I made in Oxford. Thanks to Dr Gabriela Espinoza Quintero and Dr Midori Amano Patiño for their friendship and the great moments since the beginning of my DPhil. Thanks to Andrea Brunner Bonilla and Karen Gamero Vega who joined us later and for your help and friendship in sometimes difficult moments. Thanks also to all the amazing friends I made outside the Department of Chemistry and Oxford. Special thanks to Juan Escobar, Matthew Schnelting, Patrick Lavelli, Andrew Gill, Denis O'Leary and Peter Feeny for all their

friendship and support at different stages of my time in Oxford. Thanks also to Prof. Henrike Lähnemann for her invaluable support in the recent months.

I would also like to express my gratitude to my parents, family and friends in Mexico for your love, support and encouragement. Special thanks go to my sisters Verónica and María de Jesús, and to Israel Rojas Rodríguez and Prof. Juventino García Alejandre for their support at the beginning of my DPhil studies.

Last but not least, I would like to express my deepest gratitude to my partner, Dr Iain Stephens for all his love and for making my life happier and brighter. I am also grateful for his unconditional support which has been crucial in the finalisation of my DPhil studies and this Thesis.

Abbreviations

General

Å	Ångstrom
atm	atmosphere(s)
avg.	average
ca.	*circa*, about
calcd.	calculated
cf.	*confer*, compared to
Cp_{cent}	computed cyclopentadienyl ring carbon centroid
CSD	Cambridge Structural Database
°	degrees
°C	degrees Celsius
d	day(s)
e.s.d	estimated standard deviation
g	gram(s)
h	hour(s)
K	Kelvin
mbar	millibar(s)
min	minute(s)
mL	millilitre(s)
mmol	millimole(s)
RT	room temperature
s	second(s)
vs.	versus

Chemical

Ae	alkaline earth metal
An	actinide
Ar	aryl group
bian	bis[(2,6-diisopropylphenyl)imino]acenaphthene
Bu	*n*-butyl
COD	cyclooctadiene
Cp	C_5H_5

Cp'	C_5H_4Me
Cp*	C_5Me_5
Cy	cyclohexyl
Dipp	2,6-diisopropylphenyl
DME	1,2-dimethoxyethane
dppe	$Ph_2PCH_2CH_2PPh_2$
en	ethylenediamine
Et	ethyl
Fp^-	$[CpFe(CO)_2]^-$
HMPA	$P(O)(NMe_2)_3$
^iPr	*iso*-propyl
L	a supporting ligand (set)
Ln	lanthanide
M	metal
Me	methyl
Mes	2,4,6-$C_6H_2Me_3$
NacNac	$[\{(Ar)NC(Me)\}_2CH]^-$
^nBu	*n*-butyl
P	generic phosphine ligand
Ph	phenyl
priso	$[(Ar)NC(NR_2)N(Ar)]^-$
Pz	pyrazolyl
R	generic aryl or alkyl
^tBu	*tert*-butyl
THF	tetrahydrofuran
TM	transition metal
TMEDA	tetramethylethylenediamine
Tol	4-C_6H_4Me
Tp	tris(pyrazolyl)hydroborate
X	Generic halide

Calculations

AIM	atoms-in-molecules
DFT	density functional theory
HOMO	highest occupied molecular orbital

LUMO	lowest unoccupied molecular orbital
MO	molecular orbital
MP2	Møller-Plesset perturbation theory (second order)
ρ	electron density
$\nabla^2\rho$	Laplacian of the electron density

Mass Spectrometry

EI	electron impact
m/z	mass to charge ratio
MS	mass spectrometry

Nuclear Magnetic Resonance Spectroscopy

$^{13}C\{^1H\}$	proton-decoupled ^{13}C
app	apparent
br	broad
COSY	correlation spectroscopy
d	doublet
DOSY	diffusion ordered spectroscopy
HMBC	heteronuclear multiple bond correlation
HMQC	heteronuclear single quantum correlation
Hz	Hertz
i	*ipso*
J	coupling constant
m	*meta*
m	multiplet
MHz	Megahertz
NMR	nuclear magnetic resonance
o	*ortho*
p	*para*
ppm	parts per million
q	quartet
s	singlet
sept	septet
t	triplet
VT	variable temperature

δ	chemical shift in ppm

Infrared Spectroscopy

br	broad
FT-IR	fourier transform infrared red
IR	infrared
cm^{-1}	wavenumber
m	medium
s	strong
w	weak
ν	frequency
ν(CO)	carbonyl absorption band

Notes

Literature compounds described in this Thesis are numbered **1.x**, **2.x**, **3.x**, **4.x** according to the Chapter in which they first occur. The new compounds described in this Thesis are numbered **1** – **53**.

X-ray crystallography data were collected, solved and refined by the author with help and guidance from Prof. Philip Mountford, Dr Matthew Blake, Dr Benjamin Clough and Dr Bowen Xie. Data for compounds **7**, **19**, **21-THF**, **29**, **40**, **41**, **44**, **49** and **51** were collected by Dr Benjamin Clough. Data for compounds **4.20**, **39**, **47** and **53** were collected by Dr Bowen Xie. Data for compounds **16**, **25** and **27** were collected by Dr Matthew Blake. Molecular drawings were produced by Prof. Philip Mountford.

Chapter One

Introduction

1.1 General Introduction

Molecular metal-metal bonds have been the subject of much research over the last five decades.[1, 2] This has enabled a better understanding of chemical bonding and the reactivity in intermetallic and more complex species. The practical applications of the metal-metal bonded species are of interest in the development of new materials[3-5] and the solution of current energy problems,[6, 7] amongst others.[8-10]

Nevertheless, despite their potential, research concerning the structure and reactivity of the species containing metal-metal bonds between elements of different blocks of the periodic table is still scarce particularly when compared to other areas of inorganic chemistry. This may be attributed to the elusiveness of their isolation and their extremely high reactivity. Relevant studies on metal-metal bonding in complexes include interactions in metallic clusters,[11] multiple metal-metal bonds[12, 13] and bridged intermetallic bonds.[14, 15] For the latter, also known as supported metal-metal bonds, it has been found that the presence of bridging ligands affects the nature, and even existence, of the intermetallic interactions.[16]

Different approaches for the synthesis of metal-metal bonded complexes include:[16] alkane or amine elimination, salt metathesis, adduct formation, reductive cleavage and oxidative addition. Due to the scope of this thesis, the present introduction will focus only on unsupported metal-metal bonds containing alkaline earth (Ae) metals, aluminium or gallium with particular emphasis on the latter.

1.2 Overview of alkaline earth metal complexes

1.2.1 Group 2 homobimetallic complexes

The high abundance and versatility of Group 2 metals have allowed their applications in a wide range of fields including catalysis,[17-19] medicine[20, 21] and materials.[22, 23] The same versatility has allowed the synthesis of metal-metal bonded complexes between Group 2 metals and *p* and *d* elements. Nevertheless, it was not until the last decade that the isolation of the first Group 2 homobimetallic complexes was possible as reported by Green *et al.*[24] To achieve the formation of the corresponding Mg-Mg dimers (**1.2**, **1.4**, Equations 1.1 and 1.2), magnesium iodide precursors were reduced utilising a potassium mirror.

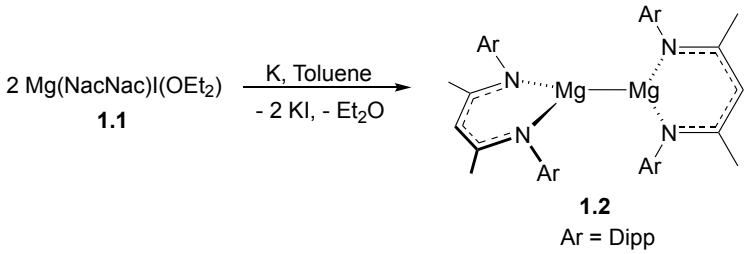

Equation 1.1[24]

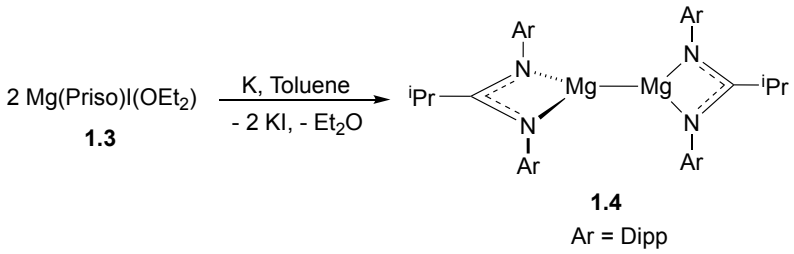

Equation 1.2[24]

The Group 2 homobimetallic complexes **1.2** and **1.4** represent the first complexes containing magnesium or any other Group 2 metal in the +1 oxidation state. Both compounds exhibit trigonal planar geometries in the solid state with Mg-Mg distances greater than the sum of two magnesium covalent radii (2.82(10) Å).[25] These complexes and their further steric modifications[26, 27] have been widely used in insertion reactions[28] and as mild reductants to access new metal-metal bonded compounds.[29, 30] The isolation of other Group 2 homobimetallic complexes containing metal-metal bonds, however, remains elusive.

1.2.2 Alkaline earth-main group complexes

One of the first Ae-main group metal bonded complexes was prepared by Westerhausen *et al*.[31] by reacting elemental calcium and Sn_2Me_6 in THF to form the calcium bis(stannide) species $Ca(SnMe_3)(THF)_4$ (**1.6**) (Equation 1.3). The presence of a Ca-Sn bond was inferred from solution NMR data and confirmed by X-ray analysis. The crystal structure of **1.6** revealed an octahedral geometry at calcium with the $SnMe_3$ ligands occupying axial positions. In addition, the measured Ca-Sn distance (3.2721(3) Å) was comparable to the ones observed in Ca-Sn binary phases and longer than the sum of the covalent radii of calcium and tin (Σr_{cov}(Ca, Sn) = 3.15(11) Å).[25]

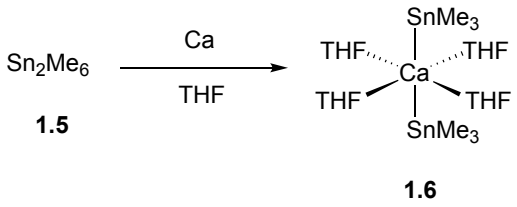

Equation 1.3[31]

Later on, a series of analogous complexes was prepared by Ruhlandt-Senge and Teng[32] by salt metathesis between $KGe(SiMe_3)_3$ (**1.7**) and AeI_2 (Ae = Ca, Sr, Ba) (Equation 1.4). For the Ca and Sr cases, three THF molecules are coordinated in the equatorial plane resulting in a trigonal bipyramidal structure. In contrast, as a result of its larger size, the Ba centre coordinates four THF molecules forming a distorted octahedral geometry around the metal.

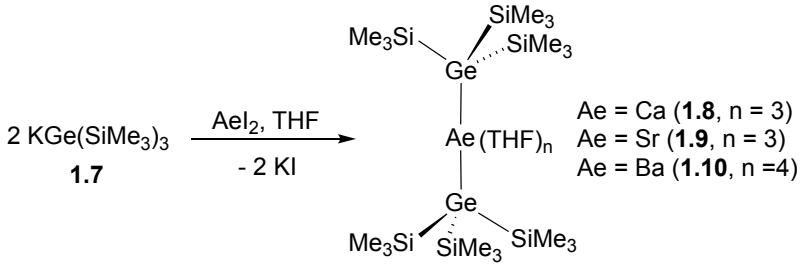

Equation 1.4[32]

Unsurprisingly, the intermetallic bond distances increase down the group due to the increasing atomic radius, with the Ba-Ge being the longest of the three cases (**1.8**, 3.022(2) Å; **1.9**, 3.147(5) Å; **1.10**, 3.398(9) Å). Related compounds containing Ge-Ae bonds have been reported by Lee *et al.* by means of oxidative addition of Ae (Mg, Ca) into a Ge-Ge bond in the four-membered inorganic heterocycle [(μ-SiClR)RGeGeRSiClR] ($R = SiMe^tBu_2$).[33]

The first Ae-Ga bonded species were synthesised by Jones and co-workers after reducing the gallium diiodide complexes $Ga(NArCR)I_2$ with either magnesium or calcium activated with a few drops of mercury (Equation 1.5).[34] The resulting complexes exhibited different geometries and coordination numbers depending on the metal. For example, the magnesium complex **1.11** contains an Ae centre coordinated to two gallyl fragments and three THF molecules resulting in a trigonal bipyramidal geometry around Mg. The calcium variants can coordinate one more THF molecule due to the increased atomic radius, forming the octahedral complexes **1.12** and **1.13**.

After the Jones *et al.* report, only a handful of Ae-Ga complexes have been isolated[35-37] and these will be discussed in detail later on.

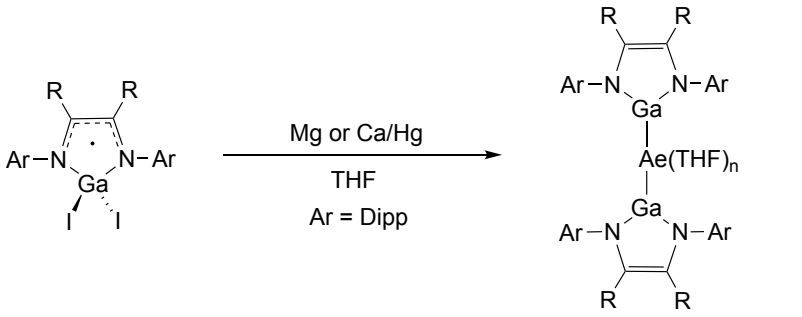

1.11 Ae = Mg, n = 3, R = H
1.12 Ae = Ca, n = 4, R = H
1.13 Ae = Ca, n = 4, R = Me

Equation 1.5[34]

More recently, Blom and co-workers[38] reported the synthesis of a Ae-Ge and Ae-Si complexes through adduct formation between Cp^*_2Ae and the N-heterocyclic carbene (NHC) analogues of silicon and germanium (Equation 1.6). These complexes showed rather weak donor-acceptor interactions as evidenced by their ^1H NMR spectra in which the sets of signals for the products did not shift considerably with respect to the starting materials. The structure of complex of **1.14** (Equation 1.6) was authenticated by X-ray diffraction exhibiting a Ca-Ge bond length of 3.1174(11) Å which is considerably longer the sum of their covalent radii (2.96(11) Å)[25], consistent with the described weak interaction. These complexes readily decompose into the Cp*Ae fragments coordinated to azabutadiene with the concomitant extrusion of germanium or silicon. Density Functional Theory (DFT) analyses supported the weak Ae-E interactions and the thermodynamic predisposition of **1.14-1.17** to release elemental Ge or Si.[38]

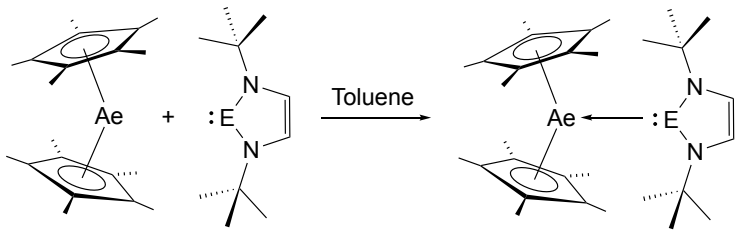

1.14 Ae = Ca, E = Ge
1.15 Ae = Sr, E = Ge
1.16 Ae = Ba, E = Si
1.17 Ae = Ba, E = Ge

Equation 1.6[38]

1.2.3 Alkaline earth-transition metal complexes

The first Ae-TM metal bonded compound was prepared by Felkin and co-workers[39] *via* formal oxidative addition of the Fe-Br bond in CpFeBr(dppe) (**1.18**) to activated Mg in THF to form CpFeMgBr(dppe)$(THF)_2$ (**1.19**) (Equation 1.7). The ^1H NMR spectrum and elemental analysis were in accordance with the formula CpFeMgBr(dppe)$(THF)_3$. One of the THF molecules was found to be easily displaced during recrystallisation. The crystal structure of **1.19** showed a distorted tetrahedral Mg centre with two THF molecules. The Mg-Fe distance of 2.593(7) Å is smaller than the sum of their covalent radii (2.73(8) Å)[25] and indicative of a significant covalent character according to the authors.[39]

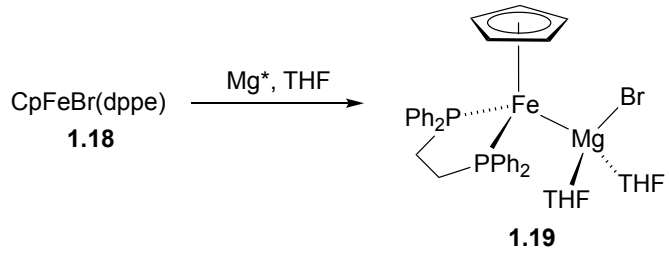

Equation 1.7[39]

The first compound with a bond between Mg and a 3rd row transition metal was reported in 1998 as $[Cp^*Ir(PMe_3)(H)MgPh]_2$ (**1.21**) (Equation 1.8).[40] To form **1.21**, one of the phenyl fragments in $MgPh_2(THF)_2$ removes one of the protons in $Cp^*(PMe_3)IrH_2$ (**1.20**). The complex **1.21** shows a dimeric structure in the solid state with a trigonal planar MgPh fragment bridging two iridium centres. The Mg-Ir distances in **1.21** are slightly different: 2.660(2) Å and 2.750(2) Å; nonetheless, both are shorter than the sum of the respective covalent radii (2.82(9) Å).[25] The reactivity of the reported dimer was shown to be versatile, *e.g.*, by forming $Cp^*(PMe_3)Ir(CO)$ upon reaction with CO_2 or the clean formation of the mixed isoptomer $Cp^*(PMe_3)Ir(H)(D)$ after the addition of D_2O to **1.21**.[40]

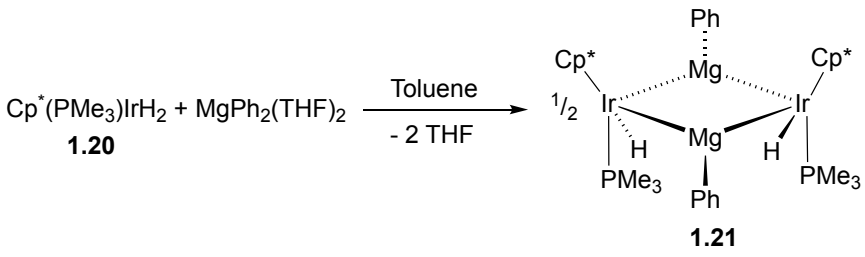

Equation 1.8[40]

More recently, the first complex containing a bond between calcium and a transition metal (TM) was synthesised by reacting a Ca/Hg amalgam with Fp_2 (Fp = $CpFe(CO)_2$) in THF by Blake *et al.* (**1.22**, Equation 1.9).[41] X-ray diffraction analysis of **1.22**, revealed a dimeric structure with an eight-membered ring formed by two $CaFp_2(THF)_3$ fragments bridged by isocarbonyl linkages. The iron atoms are in a tetrahedral environment with a Ca-Fe bond length of 3.0185(6) Å. This is shorter than the sum of the respective covalent radii (3.08(10) Å)[25] as opposed to Ca-main group compounds, for example **1.6** in Equation 1.3 (*vide supra*),[31] in which the Ca-Sn is longer than the sum of the respective covalent radii. DFT and IR analyses showed that **1.22** exists as a monomer in a THF solution and as a dimer in the solid state. In a further study,[42] this methodology was expanded to the isolation of the related $[MgFp_2(THF)]_2$, $[Mg\{Co(CO)_3(PCy_3)\}_2(THF)]_2$ and $[Ca\{Co(CO)_3(PCy_3)\}_2(THF)_2]_\infty$ complexes which, similarly to **1.22**, present eight membered rings and isocarbonyl linkages. The comprehensive experimental and computational study of these and other lanthanide related complexes showed a trend of decreasing Ae-TM interaction energies going down the group.[42]

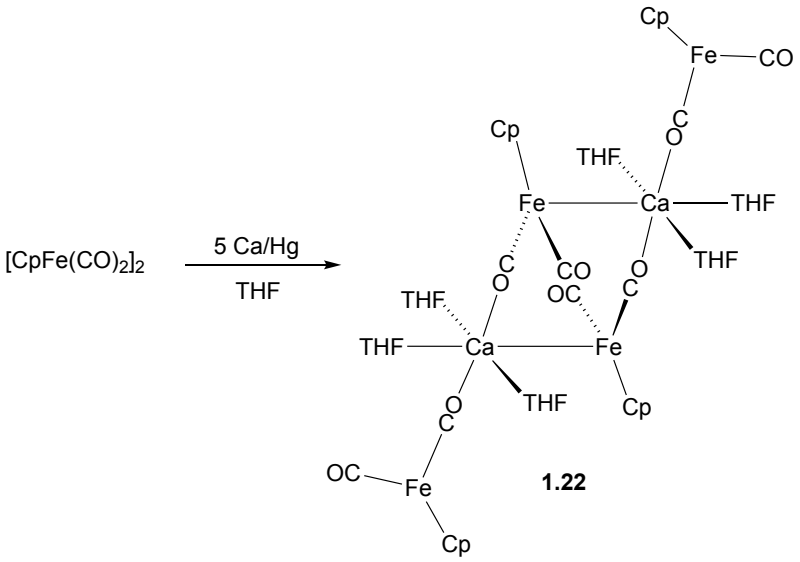

Equation 1.9[41]

1.3 Use of gallium(I) analogues of N-Heterocycle carbenes in metal gallyl complexes

The use of gallium(I) analogues of Arduengo or N-heterocycle carbenes (NHC) has proven useful in the isolation of complexes containing M-Ga bonds. Recently, Asay *et al.* reviewed the use of NHC analogues of groups 13 and 14 elements as ligands

along with some of their applications.[43] These gallium(I) analogues of NHCs are commonly found as 4- to 6-membered rings with the 5-membered heterocycle (**B**, Figure 1.1) being the most widely used. Similarly to the Arduengo carbenes, the gallium analogues of NHCs act as σ-donors *via* the lone pair in either neutral (**A** and **C**) or anionic (**B**) heterocycles. The formally vacant *p* orbital in the gallium atom can potentially confer π-acidity to the heterocycle although this is rather rare.[43-45] Interestingly, the gallium heterocycle can act as π-donor as found in the complex $\{(Me_3SiNCH_2CH_2)_3N\}U\{Ga(NArCH)_2\}(THF)$ (*vide supra*).[46] In the following sections some key examples of complexes containing the NHC analogues of gallium(I) will be discussed with special emphasis on the complexes containing structure **B**. Worthy to mention is the widely extended use of the Cp*Ga fragment[47] in the formation of Ga-M bonds, however, the discussion of its chemistry is beyond the scope of this thesis.

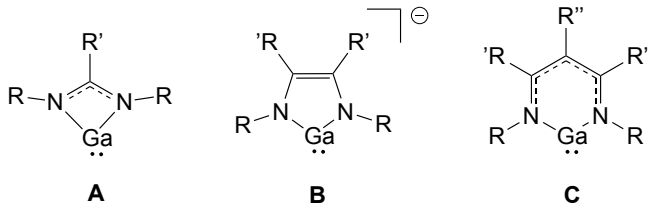

Figure 1.1. General structures of gallium(I) analogues NHCs

1.3.1 Four-membered gallium(I) heterocyles

To date, only one example of a four-membered gallium(I) analogue of NHCs has been reported.[48] This was synthesised by salt elimination between the lithium guanidinate, $Li[Cy_2NC(NDipp_2)]$ (**1.23**, Equation 1.10) and "GaI", which is a mixture of gallium iodides and gallium metal[49] that overall reacts as Ga(I) iodide.[50, 51]

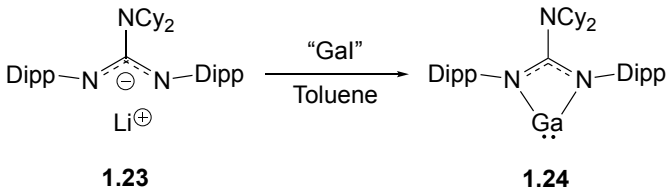

Equation 1.10[48]

Complex **1.24** is reported to be extremely air-sensitive although thermally stable decomposing at 158 ºC. DFT calculations described in the same report showed that

the HOMO and LUMO of **1.24** are mainly associated with the lone pair and the gallium p_z orbital, respectively. The lone pair has high 4*s* character although it is directional and points away from the heterocycle. The HOMO-LUMO gap is 67.4 kcal mol^{-1} which suggests that **1.24** should be a good σ-donor but a weak π-acceptor.[48, 52]

The four-membered gallium(I) heterocycle **1.24** has been predominantly used in the preparation of gallylene complexes of transition metals. These reactions proceed normally by the displacement of a weakly coordinating ligand. For instance, a series of group 10 gallylene complexes was synthesised by the reaction of **1.24** with the corresponding Ni and Pt precursors bearing olefins as labile ancillary ligands (Scheme 1.1).[53]

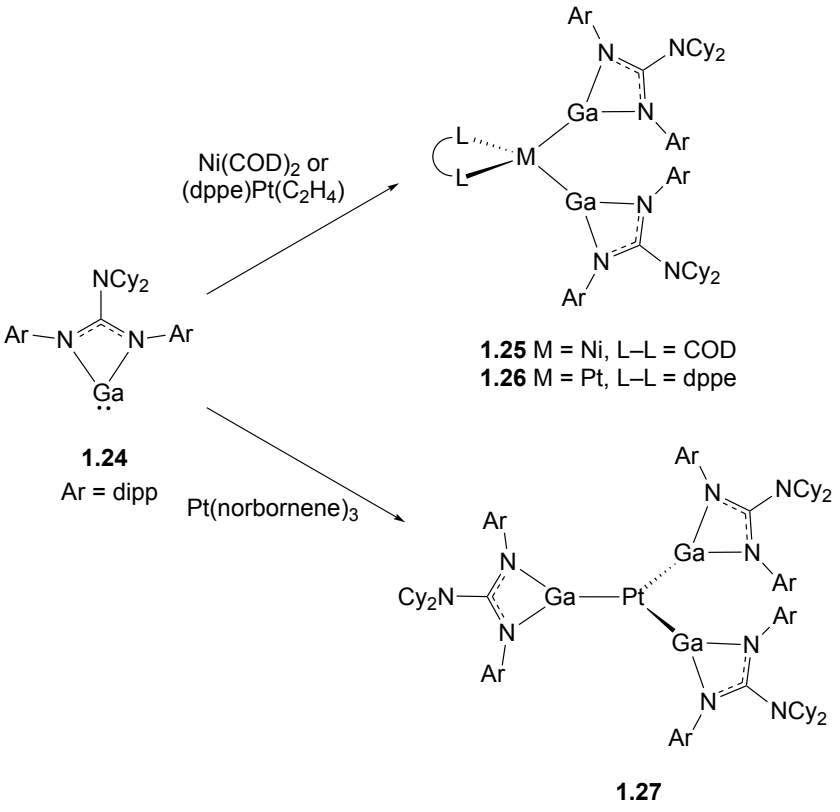

Scheme 1.1. Synthesis of group 10 gallylene complexes *via* ligand displacement by **1.24** with Ni and Pt precursors in toluene. Ar = Dipp.[53]

The synthesis of complexes **1.25** and **1.26** proceeded in toluene from the reaction of $Ni(COD)_2$ or $(dppe)Pt(C_2H_4)$ and **1.24** in either 1:2 or 1:4 ratios. In both cases, only two coordination sites were occupied by **1.24**, in contrast with the previously reported reaction between diyl gallyl precursors and $Ni(COD)_2$, where the homoleptic complex

is more likely to be formed.[54, 55] Although isolable, the tetrahedral d^{10} compounds **1.25** and **1.26** are unstable upon redissolving them in toluene apparently due to the loss of the gallium heterocycle. A better result is obtained with the substitution of norbornene with **1.24** to form the trigonal planar trisgallylene **1.27**. In all cases, a slight excess of **1.24** seems to be important for the stabilisation of **1.25-1.27** in solution and their further characterisation. DFT calculations and Charge Decomposition Analysis (CDA) for **1.27** revealed a polarised Pt-Ga bond in which the covalent component possesses a significant π contribution (*ca.* 40%). Such π contribution accounts for the HOMO and HOMO-1 which are formed by two nearly degenerate empty 4*p* orbital sets in the Ga atom and the $4d_{xy}$ or $4d_{x2-y2}$ orbitals of Pt.

Further reports have followed the same ligand displacement route to access Pt(II) gallyl complexes, *e.g.*, in the the formation of *cis*-[Pt(Ar^F)$_2${Ga(Cy_2NC(NDipp$_2$))}$_2$] (**1.28**), and *trans*-[Pt(2,4,6-$C_6H_2F_3$)$_2${Ga(Cy_2NC(NDipp$_2$))}$_2$] (**1.29**) by displacement of 1,5-hexadiene in the precursors.[56] Similarly to **1.25-1.27**, the low nucleophilicity of **1.24** made imperative its use in excess to stabilise **1.28** and **1.29** in non-coordinating solvents.

The use of **1.24** has been expanded to the preparation of gallylene complexes of other mid- to late-transition metals, namely, Co, Mo, Ru and Fe.[57] The carbonyls of these metals were chosen as starting materials aiming to displace CO with **1.24** (Scheme 1.2). Nonetheless, initial attempts to react **1.24** with $Fe(CO)_5$ were unsuccessful and $Fe_2(CO)_9$ was used instead as a more reactive source of $Fe(CO)_4$. The displacement of the $Fe(CO)_5$ occurred, successfully forming complex **1.30** (Scheme 1.2), which contains a Fe-Ga dative bond (2.272(1) Å). This is shorter than the ones found in some related Fe(CO)$_4${Ga(L)} compounds, and was attributed to the lower steric hindrance in **1.30**. In a similar manner, the displacement of one molecule PPh_3 from $Ru(CO)_2(PPh_3)_3$ led to the formation of **1.31** (Scheme 1.2). On the other hand, the use of cobalt and molybdenum carbonyls showed mixed results. The substitution of CO in $Co_2(CO)_8$ yielded a compound with cobalt centres symmetrically bridged by two gallium heterocycles and terminal carbonyls (**1.32**, Scheme 1.2). The Co-Ga distances (2.3801(8) and 2.3865(6) Å) are comparable to those found in the previously reported adduct $(CO)_3Co(\mu\text{-GaCp*})_2Co(CO)_3$ (**1.34**) (2.389(3) Å)[58] and shorter than the sum of the respective covalent radii (2.48(4) Å).[25] The reaction of $[CpMo(CO)_2]_2$ with **1.24**

only allowed the isolation of a hydroxo-bridged bisgallylene ligand coordinated to the Mo centre, presumably a hydrolysis product (**1.33,** Scheme 1.2).

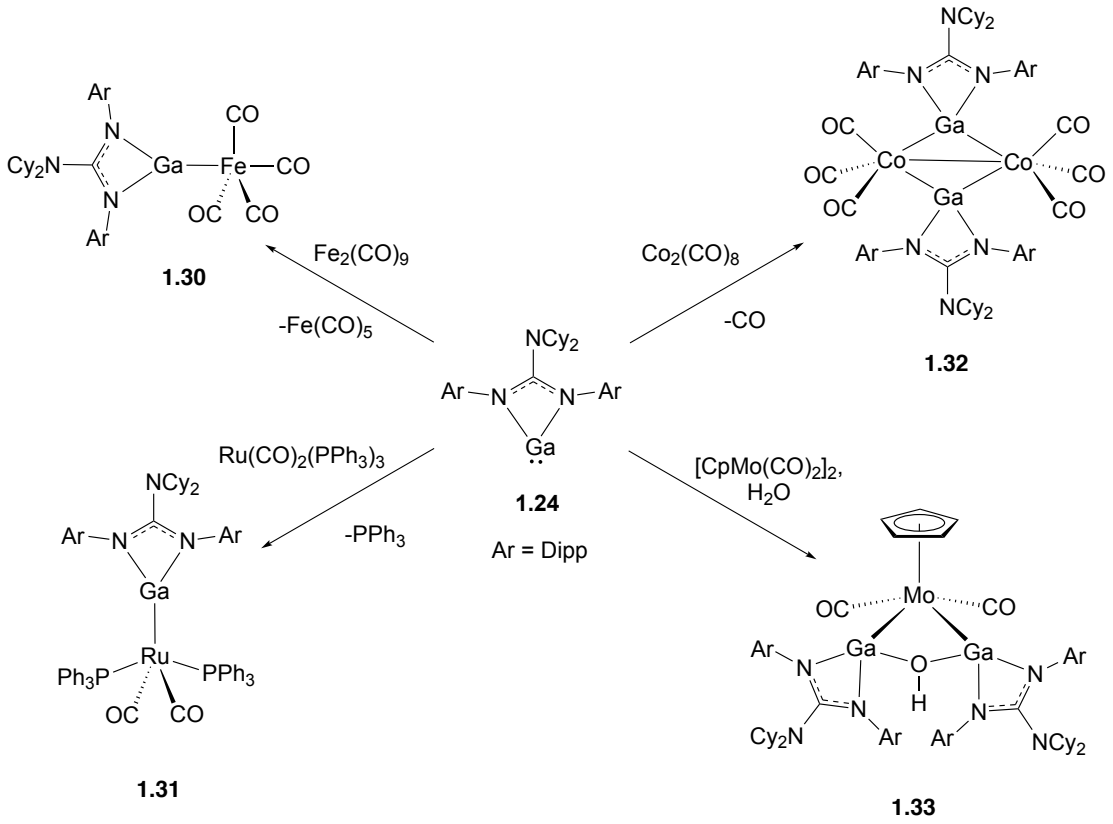

Scheme 1.2. Reactions of **1.24** with late transition metal carbonyls in toluene.[57]

Since 2009, when the aforementioned reactivity of **1.24** with metal carbonyls was reported,[57] neither this ligand nor any other four-membered gallium(I) heterocycle have been used in the preparation of other similar metal gallylene complexes. Notably, prior to the development of the chemistry of **1.24**, Jones, Aldridge and co-workers reported the reactions of a series of related amidinato complexes of group 13 metals with NaFp (Scheme 1.3).[59] All reactions led to the formation of Fe-group 13 bonded complexes with their halide atoms *anti* to the Cp-Fe bond, except for the indium complex **1.38**, which shows a conformation closer to *syn*. This was reported to be likely caused by the longer Fe-In bond in **1.38** which reduces its steric hindrance and allows a freer rotation around the Fe-M in contrast with **1.35-1.37**. Attempts to isolate the halide-free species by reaction of **1.35-1.38** with $Na[BAr^F{}_4]$ (Ar^F = 3,5-$(CF_3)_2C_6H_3$) were successful only with **1.36** yielding the desired compound **1.39** along with a small amount of its hydrolysis product **1.40**.

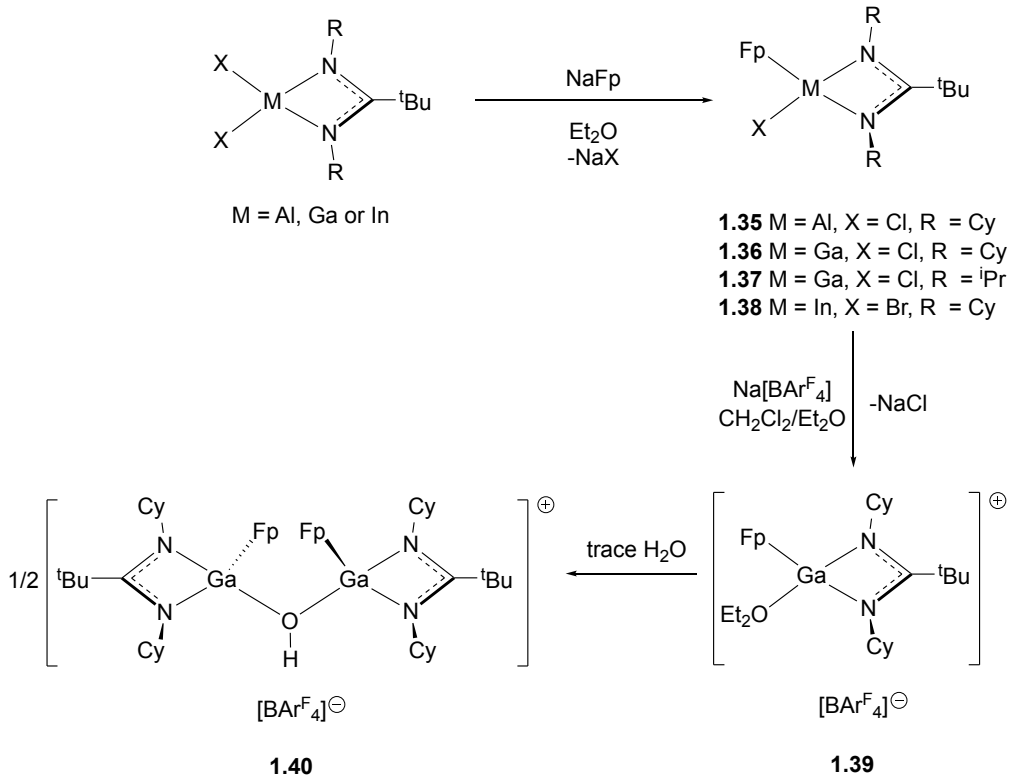

Scheme 1.3. Synthesis of Fe-group 13 complexes supported by amidinate ligands.[59]

1.3.2 Five-membered gallium(I) heterocyles

Five-membered gallium(I) heterocycles represent the most widely used gallium(I) analogues of NHCs.[43, 60] This translates into a huge variety of staring materials and metal gallyl complexes. Most of these are anionic and hence have been prepared as salts of alkali metals with tuning of the steric and electronic properties by modification of the substituents on the nitrogen or the vinyl carbons. A compilation of all these species is presented in the Figure 1.2.

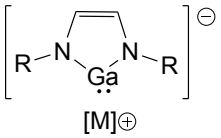

[M]⊕

1.41 [M] = [K(18-crown-6)(THF)$_2$], R = ^{t}Bu
1.46 [M] = 0.5 [K$_2$(18-crown-6)$_3$], R = Dipp

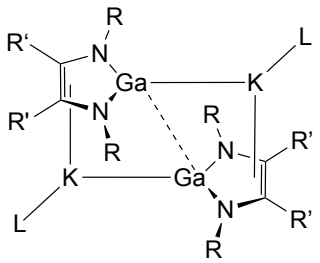

1.42 L = TMEDA, R = ^{t}Bu, R' = H
1.43 L = TMEDA, R = Dipp, R' = H
1.44 L = OEt$_2$, R = Dipp, R' = H
1.45 L = TMEDA, R = Dipp, R' = Me

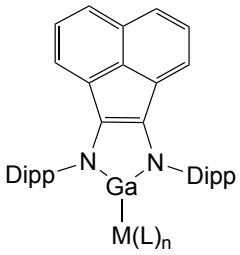

1.50 M = Li, L = OEt$_2$, n = 3
1.51 M = Na, L = OEt$_2$, n = 3
1.54 M = K, L = THF, n = 5

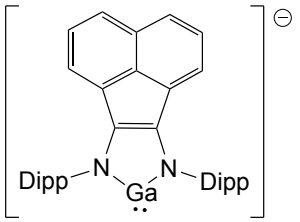

[Na(18-crown-6)(THF)$_2$]⊕
1.53

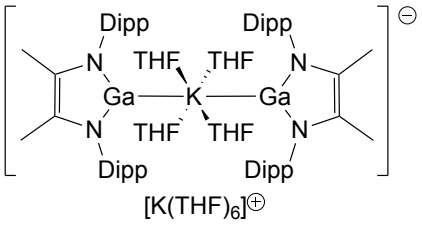

[K(THF)$_6$]⊕
1.57

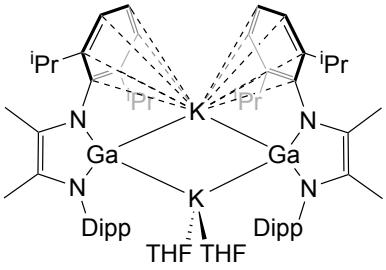

1.58

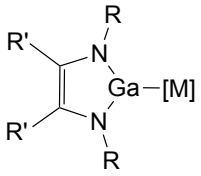

1.55 [M] = Li(THF)$_3$, R = Dipp, R' = Me
1.56 [M] = Na(THF)$_3$, R = Dipp, R' = Me
1.59 [M] = Na(TMEDA)(Toluene), R = Ar*, R' = H
1.60 [M] = Na(TMEDA), R = Ar*, R' = H
1.61 [M] = Na(TMEDA)(OEt$_2$), R = Ar*, R' = H
1.62 [M] = Na(THF)$_4$, R = Ar*, R' = H

Figure 1.2. Five membered gallium(I) analogues of NHCs. Ar* = 2,6-(Ph$_2$CH)$_2$-4-C$_6$H$_2$Me.[37, 61-67]

As observed, the stability and versatility of the five-membered heterocycles is richer than the 4- and 6-membered heterocycles as will be later seen. Species **1.41** (Figure 1.2) was the first of these complexes, reported in 1999 by Schmidt *et al*.[61] This was prepared by reducing the parent digallane(4) [Ga{N(^{t}Bu)CH)}$_2$]$_2$ with a potassium mirror in THF in the presence of 18-crown-6. Single crystal X-ray analysis

established the structure of **1.41** as an ion pair between the anionic heterocycle and a potassium complex with the crown ether and two THF molecules. The TMEDA analogue, **1.42**, was later isolated by following the same methodology.[62] In contrast, in the solid state **1.42** showed a dimeric structure stabilised by η^5-interactions between the heterocycle and K, which is also coordinated to a chelating TMEDA.

While being breakthroughs in the chemistry of gallium at that time, the syntheses of **1.41** and **1.42** were rather low yielding (**1.41**: 4%,[61] **1.42**: 18%[62]). The optimised synthesis of **1.42** along with the preparation of **1.43**-**1.46** was later reported by Baker *et al.*[63, 64] The direct reduction of the iodides $[Ga\{N^tBuCH)_2\}I]_2$ (**1.47**), $Ga\{NArCH)_2\}I_2$ (**1.48**) and $Ga\{NArCMe)_2\}I_2$ (**1.49**) instead of the corresponding digallanes(4) was key for the improved synthesis and isolation of these complexes. Complexes **1.43** and **1.44** possess a similar structure to **1.42** with the heterocycle being η^5-coordinated to a K(L) fragment (L = Et_2O or TMEDA). Additionally, a weak interaction between the gallium centres is reported with Ga···Ga distances of 2.8746(15) Å (**1.43**) and 2.8640(13) Å (**1.44**). The authors proposed that this contact could be due to a partial interaction of the lone pair of one gallium atom and the empty 4*p* orbital of the other gallium centre.[45] Such interactions are destroyed when **1.44** is treated with an excess of 18-crown-6 in THF generating **1.46** which exists as an ion pair in the solid state.

In 2008, Fedushkin *et al.* reported the high-yielding preparation of **1.50** and **1.51** *via* reduction of the parental digallane $[(dpp\text{-}bian)Ga]_2$ (dpp-bian = 1,2-bis((2,6-diisopropylphenyl)imino)acenaphthene) (**1.52**) with either lithium or sodium in Et_2O.[65] The gallium atoms in **1.50** and **1.51** are in distorted trigonal planar environments with a direct, unsupported Ga-M (M = Li or Na) bond. DFT calculations and Natural Bond Orbital (NBO) analysis of **1.50** suggested the donation of electron density from the lone pair of gallium to the empty 2*s* orbital of the lithium atom as the main contribution of that bond. Later in 2010, the same group reported the cleavage of the Ga-Na bond in **1.51** by addition of strongly coordinating ligands, *e.g.,* 18-crown-6, to form the ion pair **1.53**.[37] The same study describes the synthesis of **1.54** by reducing $[(dpp\text{-}bian)Ga]_2$ (**1.52**) with K in THF. Interestingly, although **1.54** and **1.42**-**1.45** bear the same substituent on the nitrogen atoms, **1.54** is not a dimer in the solid state and possesses a direct Ga-K bond similarly to its dpp-bian supported analogues **1.50** and **1.51**. This was reported to be caused by the presence of the fused

naphthalene fragment in **1.54**, which reduces the π-density in the metallacycle; such density is then less available to be donated in a η^5 coordination mode, favouring the situation where the potassium centre is electronically more satisfied by coordinating to the gallium lone pair and five THF molecules.

More recently, the syntheses of **1.55**-**1.58** (Figure 1.2) have been reported by Liu *et al.*, expanding the library of gallium(I) heterocycles with direct Ga-M bonds to Li, Na and K.[66] In their method, Liu and co-workers reacted the dichloride $Ga\{NArCMe)_2\}Cl_2$ with a series of reducing agents to form the corresponding gallium(I) NHC analogues. Reduction with either Li or Na in THF gave **1.55** and **1.56**, respectively, with unsupported Ga-M bonds (M = Li or Na) similar to Fedushkin's **1.50** and **1.51**. The use of potassium metal yielded the ion pair **1.57**, where the anion contains two gallyl heterocycles bridged by a $K(THF)_4$ unit. Surprisingly, the reduction of $Ga\{NArCMe)_2\}Cl_2$ with KC_8 gives **1.58** also possessing two bridged heterocycles in the solid state, although this time the metallacycles are joined by two potassium atoms which are in non-identical environments. Notably, the overall compositions in **1.57** and **1.58** are similar to **1.42**-**1.45**, the solid state structures are different.

For their part, Dange and co-workers have recently synthesised the first gallyl heterocycle containing the so-called "superbulky" Ga(NAr*CH) (Ar* = 2,6-$(Ph_2CH)_2$-4-C_6H_2Me) framework.[67] Initial attempts to reduce $Ga(NAr*CH)_2I_2$ with potassium were unsuccessful and a complex mixture was obtained instead. A better result was obtained when sodium in THF was used as reducing agent. Treatment of the reaction mixture with TMEDA/Et_2O and further crystallisation of the crude from toluene gives **1.59**. The ancillary ligands of sodium, particularly, of course, toluene, are labile, thus allowing the isolation of **1.60**, **1.61** and **1.62** by recrystallisation of **1.59** from TMEDA, Et_2O and THF respectively. All these complexes are monomeric in the solid state with the gallium atoms in distorted trigonal planar environments. The Ga-Na distances are affected by the degree of coordination of the sodium atoms. For instance, the shortest Ga-Na bond in the group (2.9404(13) Å) is found in **1.59** which features a weakly η^2-coordinated toluene, whilst **1.62** (in which sodium is coordinated to four THF molecules) has the longest Ga-Na bond (3.1208(16) Å).

The use of five-membered gallium(I) heterocycles has been expanded to the formation of gallyl complexes with elements of the four blocks of the periodic table and in some cases, similarities to the NHCs have been found. For instance, Baker and co-workers reported the reaction of $[K\{Ga(NArCH)_2\}(TMEDA)]_2$ (**1.43**) with nickelocene $NiCp_2$ to form the nickel bis(gallyl) complex, $[K(\mu\text{-}C_7H_8)(\mu\text{-}Cp)K(TMEDA)(\mu\text{-}Cp)Ni\{Ga(NArCH)_2\}]_\infty$ (**1.63**) (Scheme 1.4)[68] which resembles the Cp^- displacement reaction between $NiCp_2$ and 2 equivalents of the N-heterocyclic carbene $C(NMeCMe)_2$ (**1.64**) to form $[CpNi\{C(NMeCMe)_2\}_2][Cp]$ (**1.65**), as previously reported by Abernethy *et al*.[69]

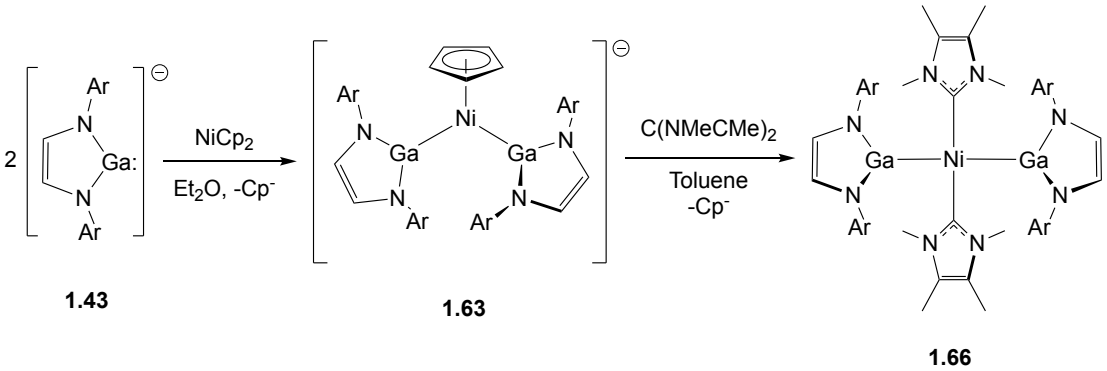

Scheme 1.4. Reactivity of nickelocene towards the five-membered gallium(I) NHC analogue (**1.43**). Cations omitted for clarity. Ar = Dipp.[68]

In the solid state, **1.63**, is a three-dimensional polymer with bridging Cp and Ar rings. The anionic component of **1.63** shows a nickel centre coordinated to gallyl fragments and one Cp to form a pseudo-trigonal planar environment. The average Ni-Ga bond distances (2.2175(11) Å) are shorter than the sum of their respective covalent radii (2.46(5) Å).[25] The gallyl fragments bond unsymmetrically to the nickel atom presumably due to steric hindrance. When $[K\{Ga(NArCH)_2\}(TMEDA)]_2$ (**1.43**) was reacted with Abernethy's bis(carbene) $[CpNi\{C(NMeCMe)_2\}_2][Cp]$ (**1.65**) no reaction occurred; in contrast, when **1.63** was reacted with $C(NMeCMe)_2$, elimination of KCp occurred and a square planar nickel(II) complex, **1.66**, was formed (Scheme 1.4). In **1.66**, the Ni-Ga bond distance (2.3242(6) Å) is slightly longer with respect to **1.63** as a result of the *trans* disposition of the ligands. The adaptation of this methodology to other neutral complexes with labile ligands allowed the formation of $[K(TMEDA)][Fe(CO)_4\{Ga(NArCH)_2\}]$ (**1.67**) by reaction of $Fe(CO)_5$ with $[K\{Ga(NArCH)_2\}(TMEDA)]_2$ (**1.43**).[70]

The oxidative addition to $(L)_nM$ fragments of the Ga-Ga bond of digallanes(4) has been another approach to access new gallyl complexes. The first of these additions involved the reaction between Cp_2Zr, generated *in situ* with ^{n}BuLi, and the digallane(4) $[Ga(NArCH)_2]_2$ (**1.68**) (Equation 1.11).[71]

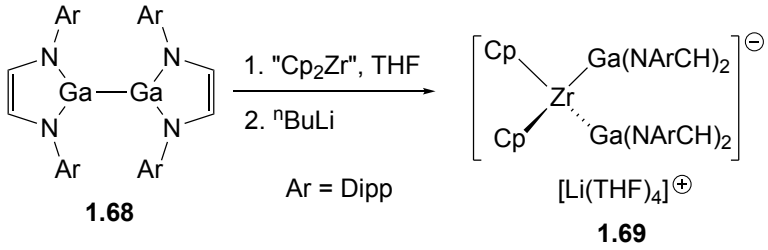

1.68 **1.69**

Equation 1.11[71]

The initial aim of the reaction between Cp_2Zr and $[Ga(NArCH)_2]_2$ (**1.68**) was to form the Zr(IV) bis(gallyl) $Cp_2Zr\{Ga(NArCH)_2\}_2$ (**1.70**). Instead, the paramagnetic Zr(III) complex **1.69** was isolated in *ca.* 10% presumably by reduction of **1.70** by an unintentional excess of ^{n}BuLi. Hence, the rational synthesis of **1.69** involved the addition of 1 equivalent of ^{n}BuLi in a second step as shown in Equation 1.11. Further attempts to form **1.70** from $CpZrCl_2$ and $[K\{Ga(NArCH)_2\}(TMEDA)]_2$ (**1.43**), or by oxidising **1.69** with $Ag[BF_4]$ or $[Cp_2Fe][PF_6]$ were unsuccessful. The authors suggest that this might be due to the unexpected transient stability of **1.70**. Complex **1.69** represents the first Zr-gallyl complex that has been structurally characterised. The analysis of the EPR spectrum showed that the hyperfine couplings to ^{69,71}Ga correspond to a very small unpaired spin density (1.25%) on the gallium atoms, suggesting minimal π back-donation from Zr(III) to Ga.

Oxidative addition reactions with other transition metals has successfully extended with **1.68** and other digallanes(4). In 2006, Aldridge, Jones *et al.* reported their findings on the oxidative addition of $[Ga(NArCH)_2]_2$ (**1.68**) to sandwich complexes (Scheme 1.5).[44] Upon mixing **1.68** with Cp'_2M complexes (M = Cr or V), the neutral monogallyl compounds **1.71** and **1.72** were isolated instead of the expected bisgallyl species, similarly to the aforementioned formation of **1.69**.[71] The mechanism to form **1.71** and **1.72** seems to be *via* comproportionation between the initially formed bisgallyl species and unreacted Cp'_2M. The coordination of a second gallyl can occur but only with **1.71**, presumably because of the larger covalent radius of V compared to Cr and the stability of **1.72** as an 18-electron complex.

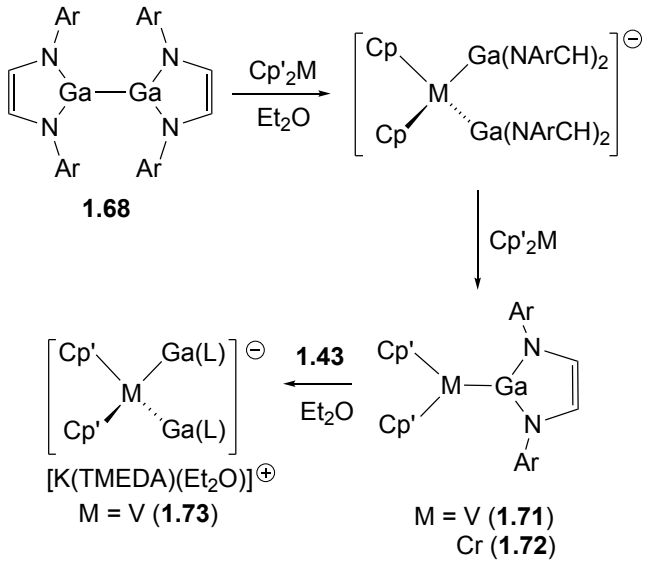

Scheme 1.5. Reactivity of the digallane(4) $[Ga(NArCH)_2]_2$ (**1.68**) with Cp'M species and further reactivity of the $Cp'_2V\{Ga(NArCH)_2\}$ complex (**1.71**). Cp' = C_5H_4Me; Ar = Dipp.[44]

More recently, Fedushkin *et al.* attempted similar transformations by reacting [(dpp-bian)Ga]$_2$ (**1.52**) with $Mo(CO)_6$ and $[CpMo(CO)_3]_2$ with a different behaviour in each case (Scheme 1.6).[72] $Mo(CO)_6$ reacted with **1.52** in THF at 100 ºC to give the paramagnetic monogallyl complex **1.74** after 15 h. In contrast, $[CpMo(CO)_3]_2$ reacted in milder conditions (80 ºC, 1 h) to form the diamagnetic complex **1.75**. The X-ray structure of **1.74** revealed that the Mo-CO distances are comparable except for the CO trans to the gallyl, which is shorter than the other carbonyls and seems to be indicative of minimal back-donation from Mo to $Ga(NArCH)_2$. The authors also note that on going from **1.52** to **1.74** and **1.75**, the C-N bond distances become longer and the C-C bonds of the gallacycle become shorter as a result of the consecutive increase of the electronic density in the ligand. Fedushkin *et al.* also observed that in **1.74**, the (dpp-bian)Ga fragment behaves as a two-electron donor ligand, [(dpp-bian)Ga:], akin to a carbenoid and in **1.75** its character is that of an anionic gallyl.[72, 73]

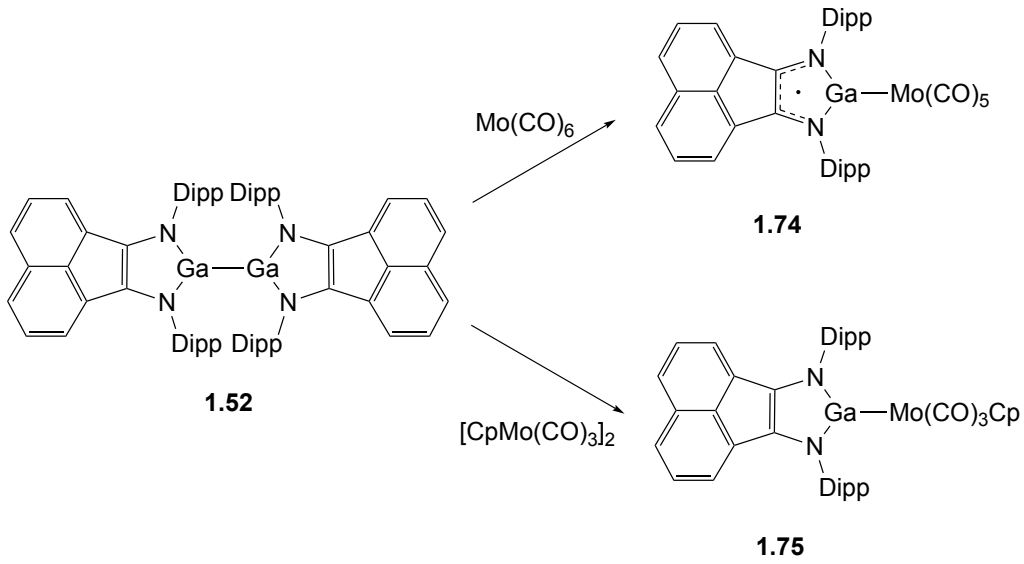

Scheme 1.6. Reactivity of the digallane(4) $[(dpp\text{-}bian)Ga]_2$ (**1.52**) with molybdenum carbonyls in THF.[72]

In addition to the ligand substitution and oxidative addition approaches, salt elimination reactions have been widely employed as routes to form new metal gallyl compounds. This has allowed the preparation of **1.76** and **1.77** (Scheme 1.7), which represent the first crystallographically characterised molecular compounds with Zn-Ga bonds.[74] Complex **1.76** was formed by reaction of $[K\{Ga(NArCH)_2\}(TMEDA)]_2$ (**1.43**) and the zinc amidinate complex $ZnCl\{^iPr_2NC(NAr)_2\}$ to form a mono(gallyl) neutral complex with the concomitant release of KCl. The tetrahedral bis(gallyl) variant, **1.77**, was prepared in the same way using $ZnCl_2(TMEDA)$ as starting material. In the solid state both complexes are monomeric and their Zn-Ga bond distances are in accordance with the sum of the respective covalent radii (1.22(5) Å). Nonetheless, **1.76** has a shorter Zn-Ga bond distance (2.3230(7) Å) than those of **1.77** (2.4399(12) Å average) due to the lower coordination number in the former.

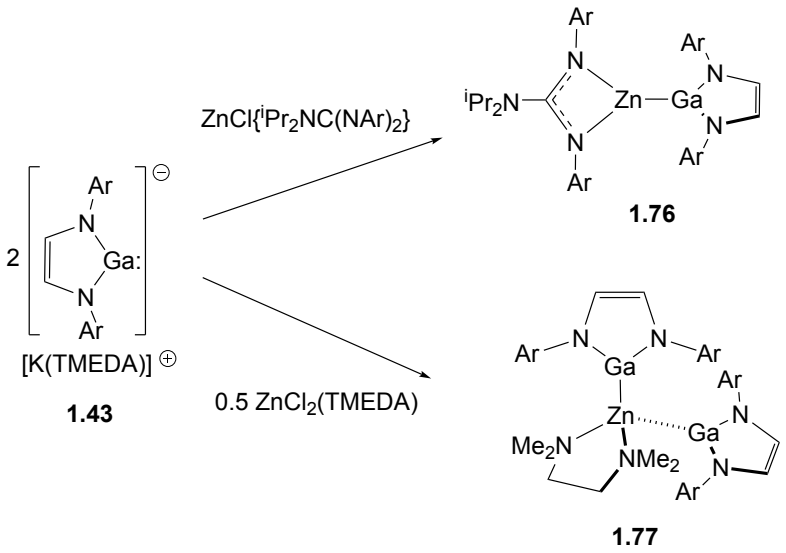

Scheme 1.7. Synthesis of Zn-Ga bonded complexes *via* salt metathesis in toluene.[74]

In 2007, Arnold, Jones *et al.* reported a salt metathesis reaction to form the first Nd-Ga bonded compound which also represents the first bond between gallium and an f-element.[75] This reaction proceeds by elimination of KI upon mixing the NHC stabilised Nd complex **1.78** with **1.43** as a source of the anionic gallium(I) heterocycle (Equation 1.12). The geometry around the Nd centre in **1.79** is that of a distorted trigonal bipyramid. All three anionic ligands occupy the equatorial positions and the neutral ligands are positioned axially. The Nd-Ga bond distance in **1.79** (3.2199(3) Å) is in accordance with the sum of the respective covalent radii (3.23(7) Å). On the other hand, the authors point out that the Nd-C_{NHC} bond distance of 2.669(2) Å is particularly long due to the presence of the nucleophilic gallyl. DFT calculations and NBO analysis of **1.79** suggested charge transfer from Ga(I) to Nd(III) and a Nd-Ga bond with some covalent character.

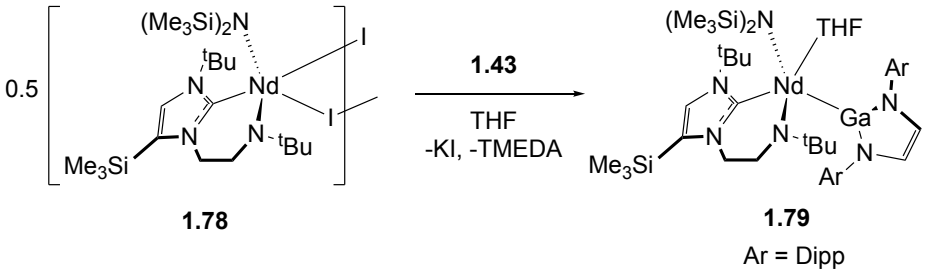

Equation 1.12[75]

One of the most breakthrough uses of $[K\{Ga(NArCH)_2\}(TMEDA)]_2$ (**1.43**) was reported by Liddle, Jones and co-workers in 2009.[46] The authors describe the

formation of the first U-Ga bonded complex by salt metathesis between **1.43** and the complex $\{Me_3SiNCH_2CH_2)_3N\}UCl(THF)$ (Equation 1.13). In the solid state, the complex $\{Me_3SiNCH_2CH_2)_3N\}U\{Ga(NArCH)_2\}(THF)$ (**1.80**), has an octahedral geometry at uranium. In the asymmetric unit of the crystal there are two molecules of **1.80** and, as a consequence of crystal packing forces, each exhibits a slightly different U-Ga bond length: 3.2115(8) and 3.2983(9), with the shortest U-Ga distance being closest to the sum of the covalent radii (3.18(8) Å). DFT calculations on a model of **1.80** revealed that the HOMO-2 and HOMO-3 are the main components of the polar covalent U-Ga bond. The HOMO-3 involves σ-donation from the Ga 4*sp* lone pair into an empty valence orbital of U. Surprisingly, the HOMO-2 corresponds to donation from a filled π-orbital in the gallyl to the $5f_{z2y}$ orbital of uranium and thus **1.80** represents the first group 13/*f* σ- and π-donation.

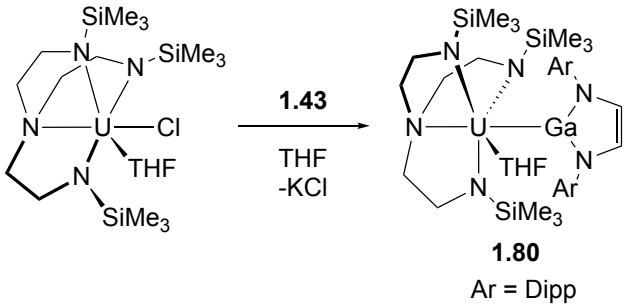

Equation 1.13[46]

1.3.3 Six-membered gallium(I) heterocyles

To date, only three six-membered gallium(I) NHC analogues have been reported (Equation 1.14). The first of these, **1.81**, was synthesised by Hardman *et al.* in 2000 by reaction of the lithiated ligand ^{Dipp}NacNacLi with "GaI", followed by treatment with potassium in toluene.[76]

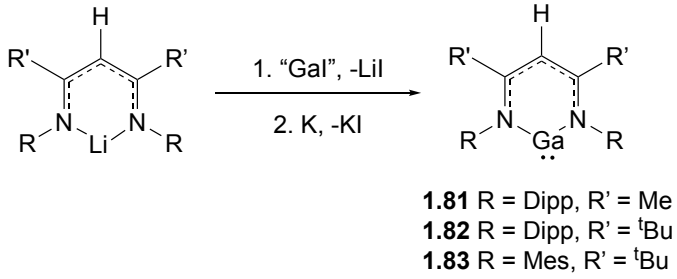

Equation 1.14[67, 76, 77]

Following Power's report, Choong and co-workers later added some steric modifications to the β-diketiminate backbone to form the gallacycles **1.82**[77] and **1.83**[67] of Equation 1.14. In all three cases, the metallacycle is almost planar with delocalisation within the ring.[67] In contrast to the neutral four membered analogue, **1.24**, the use the six-membered gallium(I) heterocycles, particularly **1.81**, has been extensively investigated.

One of the first reports on the use of **1.81** was made by Kempter *et al.* in 2005 (Scheme 1.8).[78] Upon reacting **1.81** with $(Ph_3P)AuCl$ the product of the insertion of **1.81** into the Au-Cl bond was obtained (**1.84**). Additionally, an excess of **1.81** acts as reducing agent but also as a neutral ligand by displacing the phosphine to form the gallyl-gallylene complex **1.85**. The geometry around the gold atom in **1.84** and **1.85** is almost linear with P-Au-Ga and Ga-Au-Ga angles of 174.64(5)º and 177.88(2)º respectively. In addition, the steric repulsion between the Dipp substituents and the increase in the polarisation of the Ga-N bonds in the (^{Dipp}NacNac)GaCl fragment reduces the planarity in the gallacycles in **1.84** and **1.85** with respect to **1.81**. The same group later synthesised the chloride free complex $[Au\{Ga(^{Dipp}NacNac)\}_2][BAr^F{}_4]$ (**1.86**) by halide abstraction of **1.85** with $Na[BAr^F{}_4]$.[79]

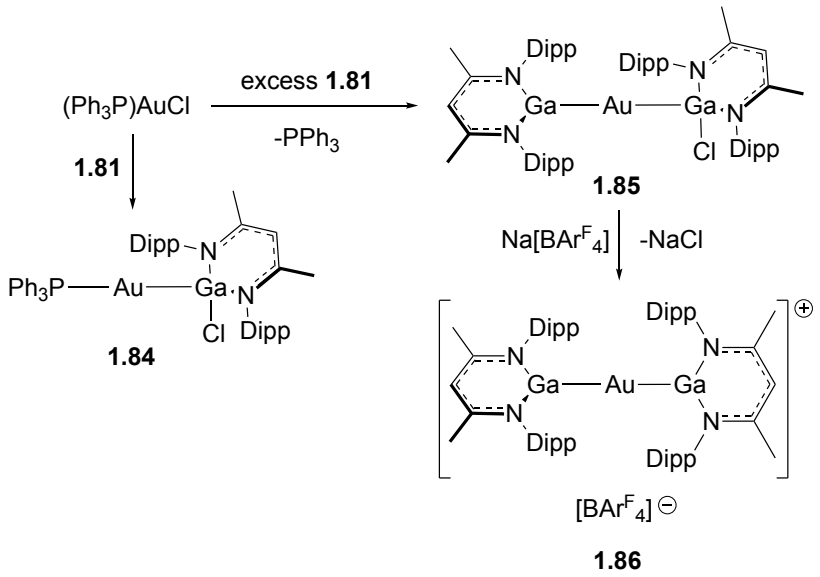

Scheme 1.8. Reactions of the 6-membered gallium(I) NHC analogue **1.81** with $(Ph_3P)AuCl$ in hexane[78] and further halide abstraction.[79]

In 2007, Kempter *et al.* applied the ligand displacement approach to form a series of new Pt-Ga complexes from Pt(0) olefin complexes.[80] The addition of (^{Dipp}NacNac)Ga

(**1.81**) to Pt(1,5-COD)$_2$ gives the monosubstituted product, **1.87**, which also exhibits isomerisation of the remaining 1,5-COD ligand (Scheme 1.9). Although the ^{1}H and ^{13}C NMR spectra of **1.87** could not be unequivocally assigned, the structure could be elucidated by single crystal X-ray diffraction. In the solid state, **1.87** features a trigonal planar geometry around the Pt atom with two gallylene fragments and one 1,3-COD ligand. The Pt-Ga bonds are similar (2.346(1) and 2.342(1) Å) and shorter than the sum of the respective covalent radii (2.58(6) Å).[25] The COD ligand in **1.87** can be further substituted with other neutral donors, *e.g.,* CO or isonitriles. Additionally, the *trans*-dihydride derivative could be prepared by treatment of **1.87** with excess H_2 (**1.88**, Scheme 1.9). This reaction also produces the complete hydrogenation of the COD ligand. The formation of the *cis*-silane Pt{Ga(^{Dipp}NacNac)}$_2$(H)(SiEt$_3$) (**1.89**) by reaction of **1.87** with HSiEt$_3$ suggests the formation of **1.88** *via* a *cis*-hydride. The Ga-Pt-Ga fragment in the complex **1.88** exhibits a linear geometry with an angle of 180.00(5)º. In addition, the Pt-Ga interaction in **1.88** apparently becomes stronger than in **1.87** since it shortens to 2.3040(15) Å.

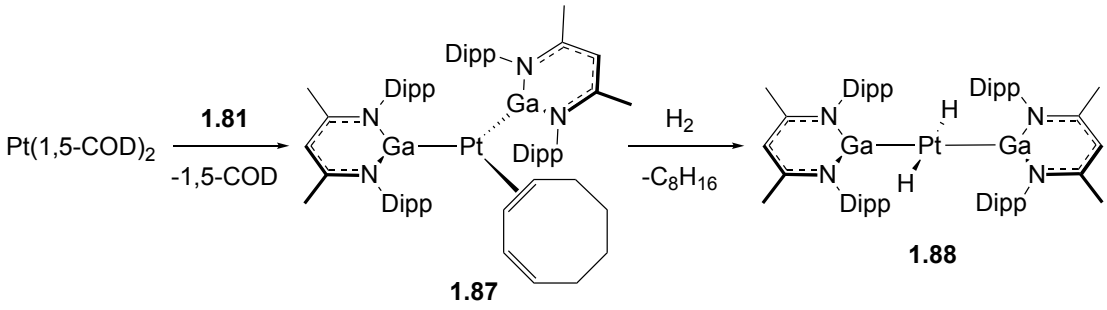

Scheme 1.9. Formation of a platinum bis(gallyl) complex (**1.86**) and its further reactivity with H_2.[80]

The use of (^{Dipp}NacNac)Ga (**1.81**) has proven useful in the isolation of the first Hg-Ga and Pb-Ga bonds. These were formed by reacting chlorides or triflate salts of Hg and Pb with **1.81** (Scheme 1.10).[81] Addition of **1.81** to Me$_3$PbCl gives the oxidative addition of the Pb-Cl bond to the gallium centre forming **1.90**. In the solid state, **1.90** shows a distorted tetrahedral geometry for both the Ga and Pb centres. The Pb-Ga distance is 2.5974(10) Å and is shorter than the sum of the covalent radii of Pb and Ga (2.68(6) Å).[25] When Hg(SC$_6$F$_5$) is used, **1.81** oxidatively adds the Hg-S bonds yielding the linear complex **1.91**. This was isolated as two conformers with the S(C$_6$F$_5$) moieties in either *anti* (***anti*-1.91**, Scheme 1.10) or *gauche* conformations

with comparable structural factors. In both cases, the Hg-Ga distances (*anti*: 2.5339(6) Å, *gauche*: 2.5332(5) Å) are within the range of the sum of the respective covalent radii (2.54(6) Å).[25]

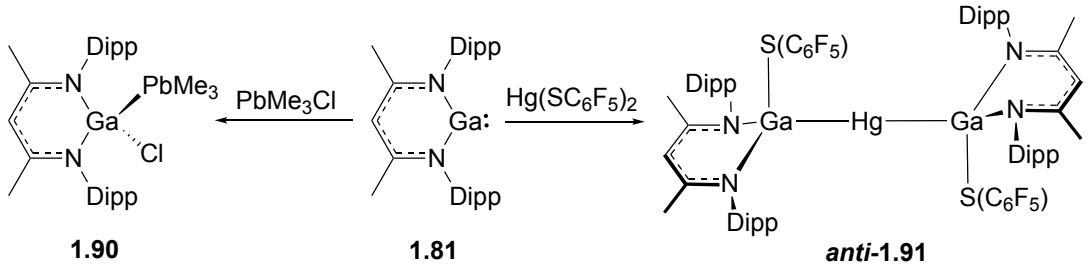

1.90 **1.81** ***anti*-1.91**

Scheme 1.10. Formation of Pb- and Hg-Ga bonded complexes *via* oxidative addition.[81]

Use of **1.81** as an ancillary ligand, has made possible the stabilisation of novel species, *e.g.,* a Bi=Bi double bonded complex by Prabusankar *et al.*[82] This was synthesised upon mixing **1.81** and either bismuth triflate or aryloxide (Equation 1.15). In both cases, the doubly bonded GaBi=BiGa complexes (**1.92** and **1.93**) were formed along with [(^{Dipp}NacNac)Ga(OR)$_2$] R = C_6F_5 or SO_2CF_3 as by-products. Both **1.92** and **1.93** have similar distances and angles and are monomeric in the solid state. In **1.92**, the GaBi=BiGa chain exhibits a planar geometry with Bi=Bi and Bi-Ga bond distances of 2.8111(2) Å and 2.655(1) Å, respectively. The bismuth atoms apparently exhibit π-interactions with the aromatic rings of the Dipp fragments in the gallium heterocycles. DFT calculations for a series of model compounds gave Wiberg bond indices of 1.91 and 0.99 for the the Bi=Bi and Bi-Ga bonds, respectively. In the Quantum Theory of Atoms in Molecules (QTAIM) calculations the Laplacian distribution, $\nabla^2\rho(r)$, shows critical points for the Bi=Bi and Bi-Ga bonds and an area of charge concentration in the latter suggesting a non-polar covalent bond. The relevance of the use of **1.81** as a ligand is indicated by the fact that attempts to synthesise NHC analogues of **1.92** and **1.93** by the authors were unsuccessful and such species still remain elusive to date.

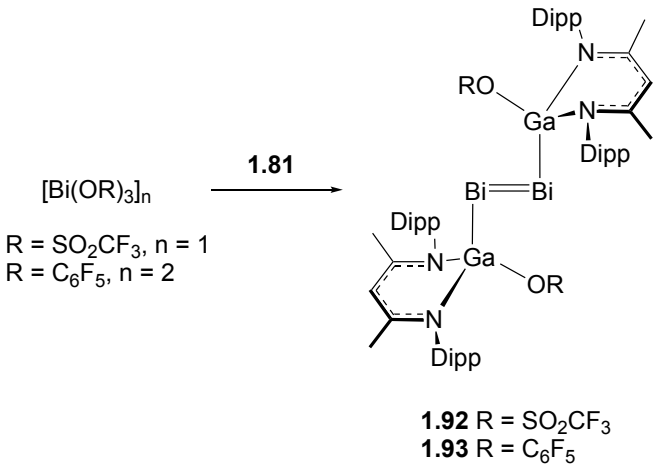

Equation 1.15. By-products omitted for clarity.[82]

It is worthwhile also to mention the more recent dehydrogenation of (^{Dipp}NacNac)GaH$_2$ (**1.94**) as an approach to incorporate the gallium(I) heterocycle **1.81** into M(L) complexes by Turner and co-workers. In their initial studies, addition of (^{Dipp}NacNac)GaH$_2$ to metal carbonyls gave the gallylene metal species with extrusion of H_2 (Equation 1.16).[83] This contrasts with the reactivity of (^{Dipp}NacNac)AlH$_2$ which typically generates the σ-alane κ^1 and κ^2 hydride complexes, *e.g.*, W(CO)$_5${κ^1-H$_2$Al(^{Dipp}NacNac)}[84] or Cr(CO)$_4${κ^2-H$_2$Al(^{Dipp}NacNac)}[85]. Indeed, the related gallane Cp'Mn(CO)$_2${κ^1-H$_2$Ga(^{Dipp}NacNac)} can be observed and isolated prior to the formation of **1.95**. On the other hand, the reactions with zero-valent metal precursors led to the direct formation of the donor-acceptor complexes **1.96-1.98**. The mechanism for the formation of a modelled **1.96** was studied by DFT calculations. These suggested that the initial step goes through Ga-H oxidative addition to the iron centre to form the complex (CO)$_4$Fe(H){(H)Ga(^{Me}NacNac)} instead of the expected either κ^1 and κ^2 gallane species as occurs with **1.95**. A rotation around the Fe-Ga bond generates a transition state with the hydride fragments in *anti* conformation prior to their release as H_2 and the formation of the modelled **1.96** complex (CO)$_4$Fe{Ga(^{Me}NacNac)}.

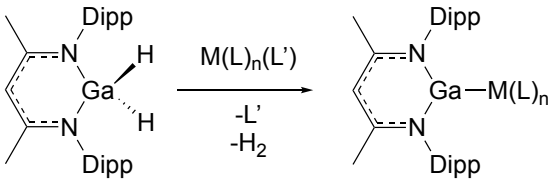

1.94

1.95 $M(L)_n = Cp'Mn(CO)_2$
1.96 $M(L)_n = Fe(CO)_4$
1.97 $M(L)_n = Mo(CO)_5$
1.98 $M(L)_n = W(CO)_5$

Equation 1.16[83]

The dehydrogenation approach was later extended to rhodium(I) cationic complexes supported by phosphines. By changing the supporting ligands at the rhodium atom, it was possible to tune the hydride transfer from gallium to rhodium ultimately identifying and studying the species involved in such migration (**1.99**-**1.101**, Scheme 1.11).[86] The use of an aromatic bidentate phosphine on the rhodium centre gives a square planar rhodium(I) complex with bridging hydrides and a weak Rh···Ga interaction (**1.99**) determined by single crystal X-ray and neutron diffraction analyses. In contrast, the use of a monodentate electron-donating phosphine, PCy_3, gives a dihydride octahedral rhodium(III) complex, agostically stabilised (**1.101**). An intermediate situation is found with the use of chelating bisphosphines with electron-donating substituents, which favours the formation of five-coordinate Rh species (**1.100**). The phosphorus, gallium and bridging hydrogen atoms are found to be coplanar with rhodium in **1.100** as expected. The structural parameters in **1.100**, *e.g.,* Rh-Ga, Rh-H, R-Ga distances amongst others, are in between those found in the aforementioned Rh(I) and R(III) complexes thus, **1.100** can be regarded as a structural "snapshot" in going from **1.90** to **1.101**.

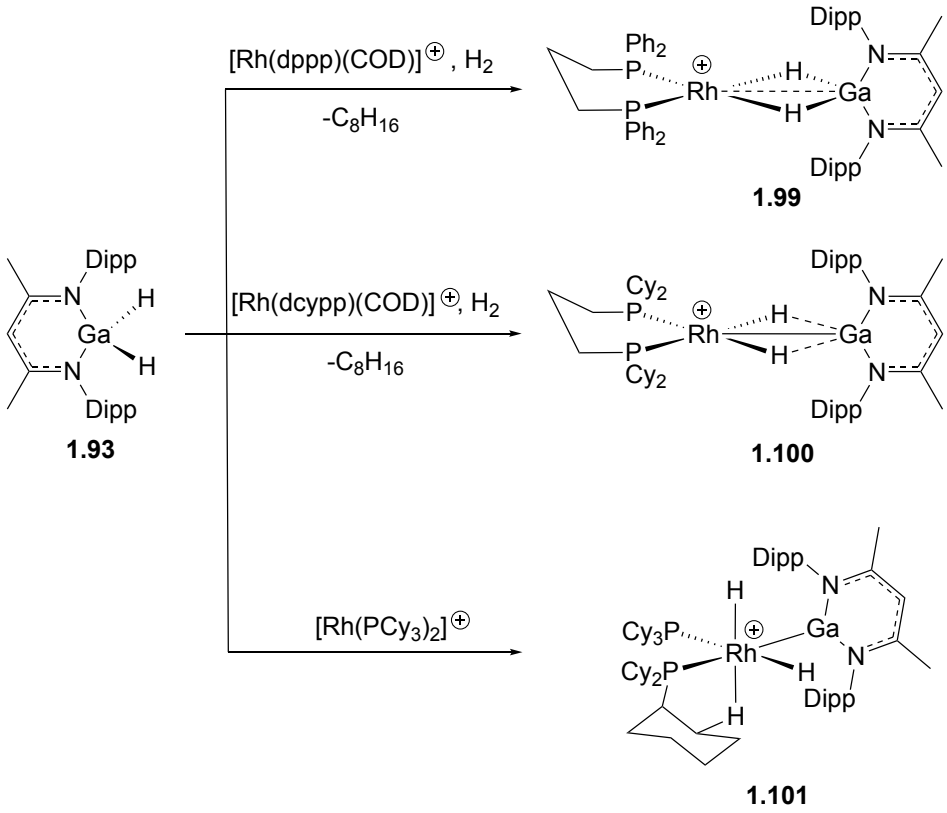

Scheme 1.11. Ga-H activation by rhodium(I) cationic complexes. Counterions omitted for clarity.[86]

1.4 Aluminium-metal bonded complexes

1.4.1 Aluminium-transition metal bonded complexes

To date, there are no reported examples of unsupported bonds between aluminium and *s*-block elements with the interactions between those metals only having been observed in multinuclear ligand-bridged species.[87] A different scenario occurs with regards to the bonding of aluminium to other elements. Concerning the bonding of Al to transition metals, the majority of the reported compounds involve either Fe-Al or Pt-Al bonded species formed by adduct formation or salt elimination. In this context, one of the first reported Al-TM compounds was formed as a donor-acceptor complex after reaction between Ph_3Al and $[Fp][NEt_4]$ (Equation 1.17).[88] As a result of the coordination of the aluminium σ-donor, the asymmetric stretch of the CO ligands in **1.102** shifts to higher frequencies compared to those of $[Fp][NEt_4]$. In the solid state, the complex $[FpAlPh_3][NEt_3]$ exhibits a distorted tetrahedral geometry around the Al centre with an Al-Fe bond distance of 2.510(2) Å, which falls within the sum of the respective covalent radii (2.53(5) Å).[25]

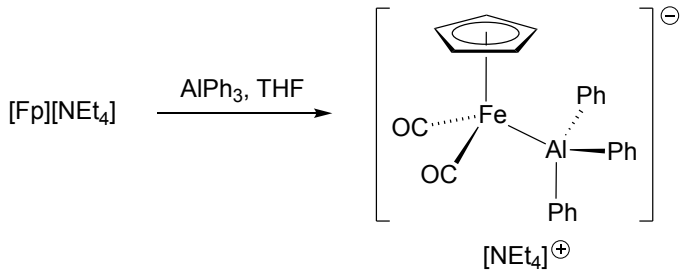

1.102

Equation 1.17[88]

A series of complexes analogous to **1.102** have been synthesised by salt elimination by Riddlestone *et al*.[89] In this case, NaFp was used as the source of the anionic iron fragment which was treated with a series of aluminium guanidinato and amidinato complexes to form the monosubstituted products in moderate yields (Equation 1.18). The change of the substituents in going from **1.103** to **1.105** does not have a direct effect in the Fe-Al bond distances, which lie in the 2.340(1)-2.364(2) Å range. An increase in the Fe-Al bond distance is observed only after the use of more sterically demanding substituents as those in Cp*Fe(CO)$_2${Al(^{Dipp}NacNac)} (**1.106**) which exhibits a Fe-Al bond distance of 2.480(1) Å. All Fe-Al bond distances in **1.103**-**1.106** were found to be significantly shorter than that of the previously described donor-acceptor complex **1.102** (2.510(2) Å).[88] Attempts to react **1.103**-**1.105** with a second equivalent of NaFp were unsuccessful apparently due to steric hindrance. Nevertheless, substitution of the chloride in **1.103** is possible with the use of the smaller MeLi to form FpAl{^{i}Pr$_2$NC(NCy)$_2$}Me.[89]

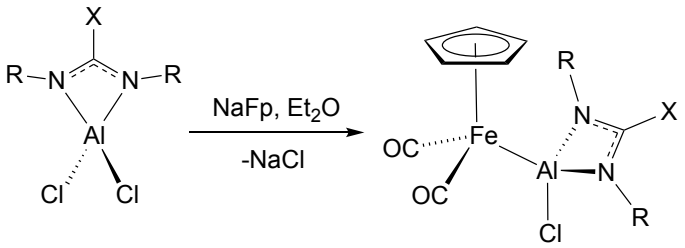

1.103 R = Cy, X = N^{i}Pr$_2$
1.104 R = ^{i}Pr, X = N^{i}Pr$_2$
1.105 R = ^{i}Pr, X = Ph

Equation 1.18[89]

A combined salt elimination-adduct formation approach was recently employed to form a Fe-Al complex by reaction of a boryl aluminium bromide precursor with $K_2[Fe(CO)_4]$ (Equation 1.19).[90] The IR spectrum of **1.107** shows strong bands for both terminal and bridging carbonyls. This was confirmed by the X-ray structure, which revealed Al-Fe donor-acceptor species bridged through isocarbonyl linkages forming an eight-membered ring, similarly to the previously mentioned **1.22**,[41] *vide supra*. The geometry around the Al centre is distorted tetrahedral whereas the one around Fe is trigonal bipyramidal with a Fe-Al bond distance of 2.394(1) Å.

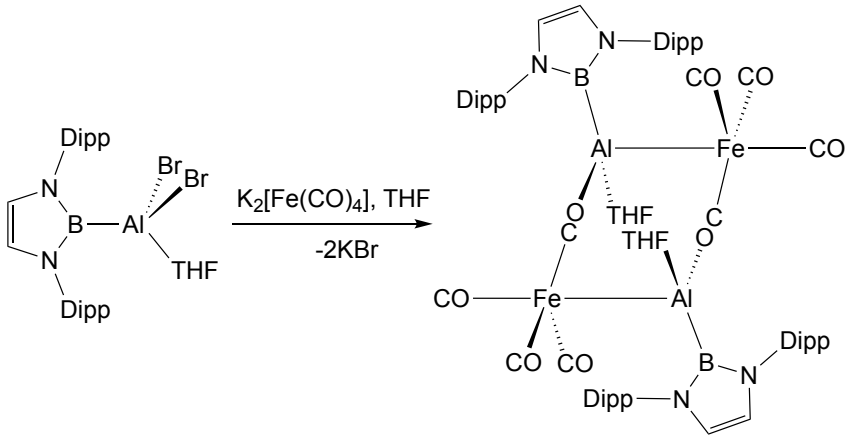

Equation 1.19[90]

The adduct formation approach has also assisted the formation of Pt-Al bonds. For instance, Bauer and co-workers have reported the Lewis pair between a NHC and phosphine stabilised platinum(0) complex (**1.108**) and aluminium(III) chloride (Equation 1.20).[91] The Lewis pair **1.109** has a T-shaped geometry in the solid state with a wide average Cl-Al-Pt angle (117.72(6)º) resulting from the steric repulsion between the chloride atoms and the substituents on the ligands. Furthermore, the C-Pt-P angle decreases compared to the parent complex **1.108** as a result of the charge donation to aluminium (**1.108**: 175.71(7)º, **1.109**: 165.97(1)). The effect of the coordination of Al to Pt was also studied by calculations which showed an increase in the natural charge on the platinum in **1.109** compared to the parent complex **1.108**. After analysis of the calculated parameters between **1.109** and other L_2PtAlX_3 complexes, a trend was found in which the Bond Dissociation Energy (BDE) of the Pt-Al bond decreases with the group of the halides used.

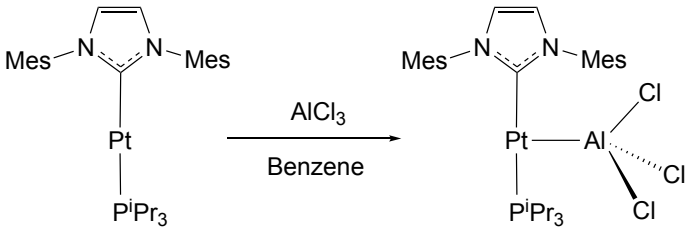

1.108 **1.109**

Equation 1.20[91]

A related Al-Pt Lewis pair, this time involving charge transfer from aluminium to platinum, was reported by Nagata *et al.*[92] The *in situ* reduction of aluminium(II) precursors in the presence of $Pt(PCy_3)_2$ yielded Al-Pt donor-acceptor complexes (**1.110** and **1.111**, Equation 1.21). The formed species represent the first reported two coordinate alumylene platinum compounds. The platinum fragments in **1.110** and **1.111** adopt a terminal position and the geometries around the aluminium centres are linear. The Al-Pt bond distances (**1.110**: 2.2857(18) Å, **1.111**: 2.2829(13) Å) are shorter than the sum of the respective covalent radii (2.57(6) Å)[25] and are slightly shorter than previously reported Al-Pt species presumably due to the low coordination number of Al. DFT calculations of a real molecule of **1.110** showed a mostly electrostatic interaction between the ArAl and $Pt(PCy_3)_2$ fragments. Additionally, the NBO analysis revealed σ-donation from 3*s*(Al) to 6*s*(Pt) and π-back donation from 5*d*(Pt) to 3*p*(Al).

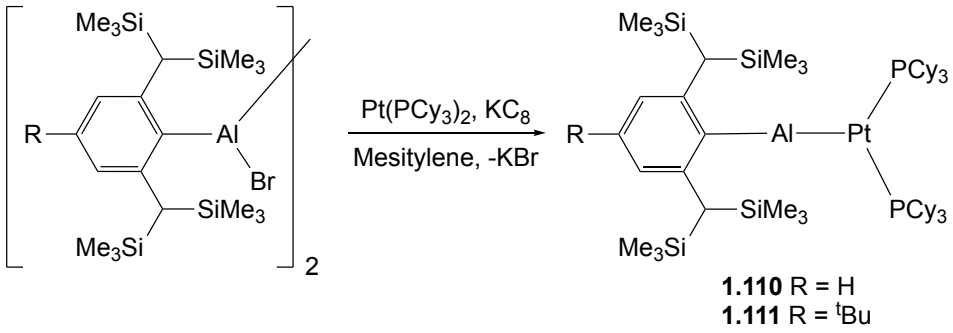

1.110 R = H
1.111 R = ^{t}Bu

Equation 1.21[92]

1.4.2 Aluminium-*p*-block metal bonded complexes

With respect to the bonding of aluminium to other main group metals, the first of these compounds was reported in 1985 by Veith and Frank.[93] Such a complex was isolated as an adduct between a tin-nitrogen cubane and aluminium chloride (**1.112**, Figure 1.3). The geometry around the Al centre in **1.112** is tetrahedral with average

Al-Sn bond distances of 2.780(4) Å. Interestingly, only two $AlCl_3$ units coordinate to the cubane as attempts to saturate the other two Sn centres in the structure were unsuccessful. Nearly three decades later, Zeckert reported the second Al-Sn bonded species, this time by forming a Lewis pair between $AlMe_3$ and a paddle-like Yb-Sn complex, **1.113** (Figure 1.3).[94] The Sn-Al bond distances in **1.113** (2.8317(10) Å) are slightly longer than **1.112**. Complexes **1.112** and **1.113** are the only Al-Sn species structurally authenticated to date.

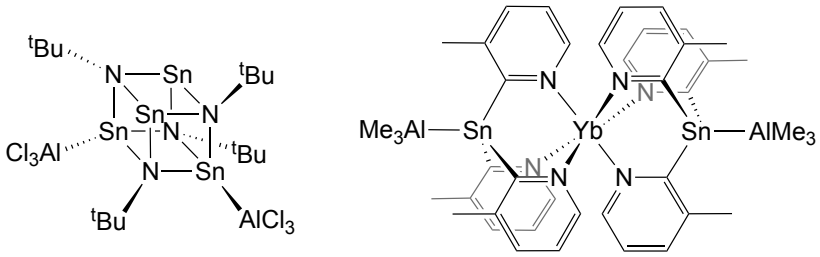

1.112 **1.113**

Figure 1.3. Al-Sn bonded species[93, 94]

After Veith and Frank's report,[93] the study on the bonding of aluminium to other main group metals has been extended to other metals in particular to the heavier Sb and Bi. For instance, in 2014, Ganesamoorthy *et al.* reported the preparation of a Al-Sb and Al-Bi bonded species by oxidative addition of the E-E bond in E_2Et_4 (E = Sb or Bi) to (^{Dipp}NacNac)Al (**1.114**, Scheme 1.12).[95] In a the same year, Ganesamoorthy *et al.* also reported the synthesis of similar bismuth species by reaction of $BiEt_2$ with **1.114** which instead activates the Bi-C bond upon heating at 75 ºC forming (^{Dipp}NacNac)Al(BiEt)(Et) **1.117** (Scheme 1.12).[96] The second Bi-C bond in **1.117** can be further activated by prolonged heating with the extrusion of elemental Bi, and $BiEt_3$. In **1.115-1.117** there is a deviation in the planarity of the aluminium metallacycle due to the oxidation of Al which adopts a tetrahedral geometry. The authors note that despite the possibility of conjugation of the lone pair of Bi in **1.117** and the empty 3*p* orbital of Al, this is not observed and the Bi atom rather adopts a trigonal pyramidal conformation. The Al-E bonds in these complexes (**1.115**: 2.6878(5) Å, **1.116**: 2.7679(8) Å, **1.117**: 2.7549(6) Å) are longer than those of Lewis acid-base adducts, and are more in agreement with other Al-E σ-bonded species.

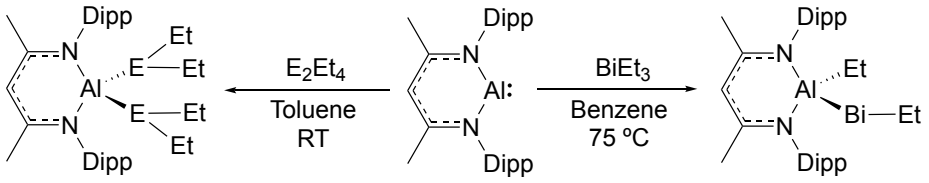

1.115 E = Sb
1.116 E = Bi

1.114

1.117

Scheme 1.12. Synthesis of Al-Sb (**1.115**) and Al-Bi (**1.116** and **1.117**) species by oxidative addition of E-E and E-C bonds to the (^{Dipp}NacNac)Al (**1.114**) precursor.[95, 96]

In a similar fashion, Erickson *et al.* have prepared a germylalane complex assisted by insertion of Ge(Ar^{Mes2})$_2$ into the Al-C bond of $AlMe_3$ (Equation 1.22).[97] The complex **1.118** bears tetrahedral germanium and pyramidal aluminium centres. The authors suggested that a weak coordination of the aluminium centre to a flanking aryl could cause the aluminium geometry to be displaced from planarity. The bulkiness of the terphenyl ligands also restrict the rotation around the Ge-Al bond since the ^{1}H NMR spectrum shows different environments for the methyl substituents on the aluminium atom and the mesityl moieties.

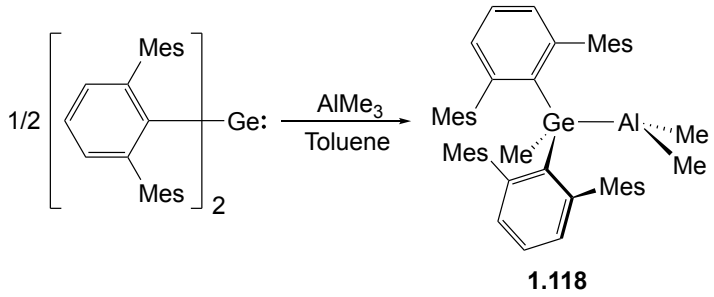

1.118

Equation 1.22[97]

Aluminium has also been bonded to other group 13 metals though this has been limited mostly to the formation of adducts. For instance, the Al-In and Al-Ga complexes **1.119** and **1.120** (Equation 1.23) were prepared by coordination of the [Cp*M]$_6$ (M = Ga or In) species to the Lewis acid Al(^{t}Bu)$_3$.[98] In the resulting species and as a result of the coordination, the signal of the Cp* substituents shifts to high field and that of the *tert*-butyl substituents in Al shifts to low field. In the solid state, the geometry around the Ga and In atoms is distorted linear (Cp*$_{centr}$-Ga-Al: 172.2º, Cp*$_{centr}$-In-Al: 170.0º). As expected, the M-Al bond distance in **1.119** (2.629(2) Å) is shorter than that of **1.120** (2.845(2) Å) due to the increase in the atomic radius. Both

M-Al bond distances are longer than the sum of the respective covalent radii (Ga-Al: 2.43(5) Å, In-Al: 2.63(6) Å).[25]

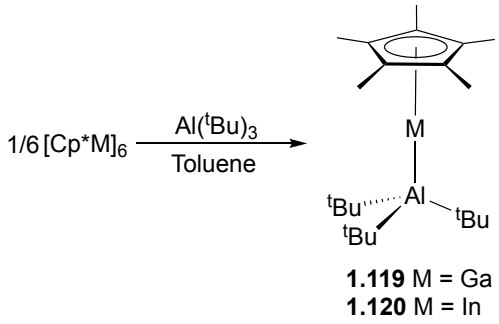

Equation 1.23[98]

1.4.3 Aluminium-*f*-element bonded complexes

Similar to the bonding of aluminium to group 13 metals, to date, only three unsupported lanthanide- or actinide-bonded species to aluminium are known and all of these have been synthesised as donor-acceptor species (Figure 1.4). The first of these involve bonding to lanthanides and were reported by Gamer *et al.* in 2006.[99] The Ln-Al (Ln = Eu, **1.121**; Ln =Yb, **1.122**) complexes were prepared by heating Cp^*_2Ln and $[Cp^*Al]_4$ at 120 ºC without any solvent for two weeks. In the crystal structure, the aluminium centres exhibit a distorted linear geometry with angles of 161.82(1)º (**1.121**) and 171.79(1)º (**1.122**). The Eu-Al and Yb-Al bond distances of 3.3652(10) Å and 3.1981(11) Å, respectively, are longer to the sum of the Ln and Al covalent radii (Σr_{cov}(Eu, Al): 3.19(7) Å, Σr_{cov}(Yb, Al): 3.08(9) Å).[25] DFT calculations revealed a very low BDE for both complexes (*ca.* 36 kJ mol^{-1}) which reflects of the poor stability of these species in solution. The same calculations showed a HOMO mainly composed by the 4*f* orbital of the Ln atom. The interaction in these complexes is predominantly ionic with negligible covalency or charge transfer according to this study.

In 2008, Minasian and co-workers reported the first molecular interaction between a group 13 metal and an actinide (**1.123**, Figure 1.4).[100] This compound possess a pseudo-tetrahedral geometry around U with U-Al bond lengths (3.121(3) Å) comparable to the sum of the covalent radii (3.17(8) Å).[25] Preliminary DFT studies of a model of **1.123** (Cp_3U-AlCp) suggest that there is a significant covalency due to the charge transfer from Al to U with a Wiberg bond index of 0.487 and no π-bonding.

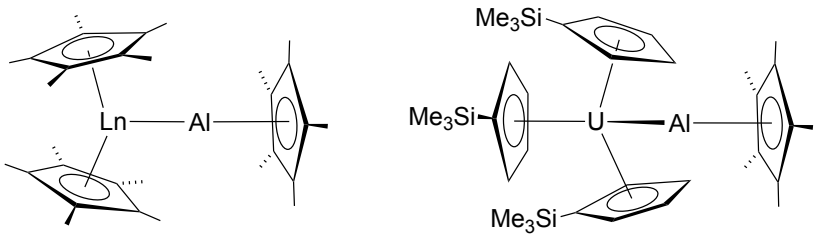

1.121 Ln = Eu
1.122 Ln = Yb

1.123

Figure 1.4. Unsupported aluminium-f-element bonded complexes.[99, 100]

1.5 Summary and objectives

This Chapter presented a general overview of group 2- and aluminium-metal bonded compounds. The use of NHC analogues of gallium(I) was introduced and described as a tool to access metal-gallium complexes or their use in further synthetic transformations such as the stabilisation of Bi=Bi double bonds. As described, despite the variety of unsupported molecular metal-metal bonds and the development of gallium containing ligands, only a very small number of group 2- and aluminium-gallium bonded complexes is known. Moreover, as with the majority of metal-metal bonded species, the reactivity of Ae-Ga compounds is, to date, unknown.

The work in this Thesis is aimed to expand the study of these species by means of the synthesis of new Ae- and Al-Ga bonded compounds and an investigation of their reactivity with small molecules.

1.6 References

1. S. T. Liddle, *Molecular Metal-Metal Bonds: Compounds, Synthesis, Properties*, Wiley, Weinheim, 2015.
2. F. A. Cotton, C. A. Murillo and R. A. Walton, *Multiple Bonds between Metal Atoms*, Springer-Verlag, New York, 2005.
3. O. A. Efremova, M. A. Shestopalov, N. A. Chirtsova, A. I. Smolentsev, Y. V. Mironov, N. Kitamura, K. A. Brylev and A. J. Sutherland, *Dalton Trans.*, 2014, **43**, 6021.
4. J. Crespo, A. Falqui, J. Garcia-Barrasa, J. M. Lopez-de-Luzuriaga, M. Monge, M. E. Olmos, M. Rodriguez-Castillo, M. Sestu and K. Soulantica, *J. Mater. Chem. C*, 2014, **2**, 2975.
5. S. S.-Y. Chui, S. M.-F. Lo, J. P. H. Charmant, A. G. Orpen and I. D. Williams, *Science*, 1999, **283**, 1148.

6. P. Luo, P.-L. Karsenti, G. Brisard, B. Marsan and P. D. Harvey, *Chem. Commun.*, 2015, **51**, 17305.
7. A. M. Brown, L. J. Antila, M. Mirmohades, S. Pullen, S. Ott and L. Hammarström, *J. Am. Chem. Soc.*, 2016, **138**, 8060.
8. M. Kampa, M.-E. Pandelia, W. Lubitz, M. van Gastel and F. Neese, *J. Am. Chem. Soc.*, 2013, **135**, 3915.
9. G. Wang, Y. S. Ceylan, T. R. Cundari and H. V. R. Dias, *J. Am. Chem. Soc.*, 2017, **139**, 14292.
10. I. G. Powers and C. Uyeda, *ACS Catal.*, 2017, **7**, 936.
11. P. O. Braunstein, L. A.; Raithby, P. R., *Metal clusters in chemistry*, Wiley-VCH, Weinheim, 1999.
12. P. A. Rudd, S. Liu, N. Planas, E. Bill, L. Gagliardi and C. C. Lu, *Angew. Chem. Int. Ed.*, 2013, **52**, 4449.
13. S. Ndambuki and T. Ziegler, *Int. J. Quantum Chem.*, 2013, **113**, 753.
14. M. Bortz, R. Bau, J. J. Schneider and S. A. Mason, *J. Cluster Sci.*, 2001, **12**, 285.
15. D. R. Laws, R. M. Bullock, R. Lee, K.-W. Huang and W. E. Geiger, *Organometallics*, 2014, **33**, 4716.
16. B. Oelkers, M. V. Butovskii and R. Kempe, *Chem. Eur. J.*, 2012, **18**, 13566.
17. S. Harder, F. Feil and K. Knoll, *Angew. Chem. Int. Ed.*, 2001, **40**, 4261.
18. M. H. Chisholm, J. C. Gallucci and K. Phomphrai, *Inorg. Chem.*, 2005, **44**, 8004.
19. Y. Sarazin, D. Roşca, V. Poirier, T. Roisnel, A. Silvestru, L. Maron and J.-F. Carpentier, *Organometallics*, 2010, **29**, 6569.
20. R. Radha and D. Sreekanth, *J. Magnesium Alloys*, 2017, **5**, 286.
21. F. Witte, I. Abeln, E. Switzer, V. Kaese, A. Meyer-Lindenberg and H. Windhagen, *J. Biomed. Mater. Res., Part A*, 2008, **86A**, 1041.
22. J. K. Park, C. H. Kim, S. H. Park, H. D. Park and S. Y. Choi, *Appl. Phys. Lett*, 2004, **84**, 1647.
23. S. Harder, *Alkaline-Earth Metal Compounds*, Springer-Verlag, Berlin, 2013.
24. S. P. Green, C. Jones and A. Stasch, *Science*, 2007, **318**, 1754.
25. B. Cordero, V. Gomez, A. E. Platero-Prats, M. Reves, J. Echeverria, E. Cremades, F. Barragan and S. Alvarez, *Dalton Trans.*, 2008, 2832.

26. A. J. Boutland, D. Dange, A. Stasch, L. Maron and C. Jones, *Angew. Chem. Int. Ed.*, 2016, **55**, 9239.
27. S. J. Bonyhady, C. Jones, S. Nembenna, A. Stasch, A. J. Edwards and G. J. McIntyre, *Chem. Eur. J.*, 2010, **16**, 938.
28. A. J. Boutland, A. Carroll, C. Alvarez Lamsfus, A. Stasch, L. Maron and C. Jones, *J. Am. Chem. Soc.*, 2017, **139**, 18190.
29. A. Rit, J. Campos, H. Niu and S. Aldridge, *Nat. Chem.*, 2016, **8**, 1022.
30. J. Hicks, E. J. Underhill, C. E. Kefalidis, L. Maron and C. Jones, *Angew. Chem. Int. Ed.*, 2015, **54**, 10000.
31. M. Westerhausen, *Angew. Chem. Int. Ed. Engl.*, 1994, **33**, 1493.
32. W. Teng and K. Ruhlandt-Senge, *Organometallics*, 2004, **23**, 952.
33. V. Y. Lee, K. Takanashi, M. Ichinohe and A. Sekiguchi, *Angew. Chem. Int. Ed.*, 2004, **43**, 6703.
34. C. Jones, D. P. Mills, J. A. Platts and R. P. Rose, *Inorg. Chem.*, 2006, **45**, 3146.
35. M. Wiecko, P. W. Roesky, P. Nava, R. Ahlrichs and S. N. Konchenko, *Chem.Commun.*, 2007, 927.
36. O. Bonello, C. Jones, A. Stasch and W. D. Woodul, *Organometallics*, 2010, **29**, 4914.
37. I. L. Fedushkin, A. N. Lukoyanov, A. N. Tishkina, G. K. Fukin, K. A. Lyssenko and M. Hummert, *Chem. Eur. J.*, 2010, **16**, 7563.
38. B. Blom, A. Said, T. Szilvási, P. W. Menezes, G. Tan, J. Baumgartner and M. Driess, *Inorg. Chem.*, 2015, **54**, 8840.
39. H. Felkin, P. J. Knowles, B. Meunier, A. Mitschler, L. Ricard and R. Weiss, *J. Chem. Soc., Chem. Commun.*, 1974, 44.
40. J. T. Golden, T. H. Peterson, P. L. Holland, R. G. Bergman and R. A. Andersen, *J. Am. Chem. Soc.*, 1998, **120**, 223.
41. M. P. Blake, N. Kaltsoyannis and P. Mountford, *J. Am. Chem. Soc.*, 2011, **113**, 15358.
42. M. P. Blake, N. Kaltsoyannis and P. Mountford, *J. Am. Chem. Soc.*, 2015, **137**, 12352.
43. M. Asay, C. Jones and M. Driess, *Chem. Rev.*, 2011, **111**, 354.

44. S. Aldridge, R. J. Baker, N. D. Coombs, C. Jones, R. P. Rose, A. Rossin and D. J. Willock, *Dalton Trans.*, 2006, 3313.
45. N. J. Hardman, C. Cui, H. W. Roesky, W. H. Fink and P. P. Power, *Angew. Chem. Int. Ed.*, 2001, **40**, 2172.
46. S. T. Liddle, J. McMaster, D. P. Mills, A. J. Blake, C. Jones and W. D. Woodul, *Angew. Chem. Int. Ed.*, 2009, **48**, 1077.
47. D. Loos and H. Schnöckel, *J. Organomet. Chem.*, 1993, **463**, 37.
48. C. Jones, P. C. Junk, J. A. Platts and A. Stasch, *J. Am. Chem. Soc.*, 2006, **128**, 2206.
49. B. J. Malbrecht, J. W. Dube, M. J. Willans and P. J. Ragogna, *Inorg. Chem.*, 2014, **53**, 9644.
50. M. L. H. Green, P. Mountford, G. J. Smout and S. R. Speel, *Polyhedron*, 1990, **9**, 2763.
51. R. J. Baker and C. Jones, *Dalton Trans.*, 2005, 1341.
52. J. Overgaard, C. Jones, D. Dange and J. A. Platts, *Inorg. Chem.*, 2011, **50**, 8418.
53. S. P. Green, C. Jones and A. Stasch, *Inorg. Chem.*, 2007, **46**, 11.
54. C. Gemel, T. Steinke, D. Weiss, M. Cokoja, M. Winter and R. A. Fischer, *Organometallics*, 2003, **22**, 2705.
55. C. Gemel, T. Steinke, M. Cokoja, A. Kempter and Roland A. Fischer, *Eur. J. Inorg. Chem.*, 2004, **2004**, 4161.
56. G. J. Moxey, C. Jones, A. Stasch, P. C. Junk, G. B. Deacon, W. D. Woodul and P. R. Drago, *Dalton Trans.*, 2009, 2630.
57. C. Jones, A. Stasch, G. J. Moxey, P. C. Junk and G. B. Deacon, *Eur. J. Inorg. Chem.*, 2009, 3593.
58. P. Jutzi, B. Neumann, G. Reumann and H.-G. Stammler, *Organometallics*, 1998, **17**, 1305.
59. C. Jones, S. Aldridge, T. Gans-Eichler and A. Stasch, *Dalton Trans.*, 2006, 5357.
60. R. J. Baker and C. Jones, *Coord. Chem. Rev.*, 2005, **249**, 1857.
61. E. S. Schmidt, A. Jockisch and H. Schmidbaur, *J. Am. Chem. Soc.*, 1999, **121**, 9758.

62. E. S. Schmidt, A. Schier and H. Schmidbaur, *J. Chem. Soc., Dalton Trans.*, 2001, 505.
63. R. J. Baker, R. D. Farley, C. Jones, M. Kloth and D. M. Murphy, *J. Chem. Soc., Dalton Trans.*, 2002, 3844.
64. R. J. Baker, C. Jones, D. P. Mills, G. A. Pierce and M. Waugh, *Inorg. Chim. Acta*, 2008, **361**, 427.
65. I. L. Fedushkin, A. N. Lukoyanov, G. K. Fukin, S. Y. Ketkov, M. Hummert and H. Schumann, *Chem. Eur. J.*, 2008, **14**, 8465.
66. Y. Liu, S. Li, X.-J. Yang, Q.-S. Li, Y. Xie, H. F. Schaefer and B. Wu, *J. Organomet. Chem.*, 2011, **696**, 1450.
67. D. Dange, S. L. Choong, C. Schenk, A. Stasch and C. Jones, *Dalton Trans.*, 2012, **41**, 9304.
68. R. J. Baker, C. Jones and J. A. Platts, *J. Am. Chem. Soc.*, 2003, **125**, 10534.
69. C. D. Abernethy, J. A. C. Clyburne, A. H. Cowley and R. A. Jones, *J. Am. Chem. Soc.*, 1999, **121**, 2329.
70. R. J. Baker, C. Jones and J. A. Platts, *Dalton Trans.*, 2003, 3673.
71. R. J. Baker, C. Jones and D. M. Murphy, *Chem. Commun.*, 2005, 1339.
72. I. L. Fedushkin, V. G. Sokolov, A. V. Piskunov, V. M. Makarov, E. V. Baranov and G. A. Abakumov, *Chem. Commun.*, 2014, **50**, 10108.
73. I. L. Fedushkin, V. G. Sokolov, V. M. Makarov, A. V. Cherkasov and G. A. Abakumov, *Russ. Chem. Bull.*, 2016, **65**, 1495.
74. C. Jones, R. P. Rose and A. Stasch, *Dalton Trans.*, 2007, 2997.
75. P. L. Arnold, S. T. Liddle, J. McMaster, C. Jones and D. P. Mills, *J. Am. Chem. Soc.*, 2007, **129**, 5360.
76. N. J. Hardman, B. E. Eichler and P. P. Power, *Chem. Commun.*, 2000, 1991.
77. S. L. Choong, W. D. Woodul, A. Stasch, C. Schenk and C. Jones, *Aust. J. Chem.*, 2011, **64**, 1173.
78. A. Kempter, C. Gemel and R. A. Fischer, *Inorg. Chem.*, 2005, **44**, 163.
79. A. Kempter, C. Gemel, N. J. Hardman and R. A. Fischer, *Inorg. Chem.*, 2006, **45**, 3133.
80. A. Kempter, C. Gemel and R. A. Fischer, *Chem. Eur. J.*, 2007, **13**, 2990.
81. G. Prabusankar, C. Gemel, M. Winter, R. W. Seidel and R. A. Fischer, *Chem. Eur. J.*, 2010, **16**, 6041.

82. G. Prabusankar, C. Gemel, P. Parameswaran, C. Flener, G. Frenking and R. A. Fischer, *Angew. Chem. Int. Ed.*, 2009, **48**, 5526.
83. J. Turner, J. A. B. Abdalla, J. I. Bates, R. Tirfoin, M. J. Kelly, N. Phillips and S. Aldridge, *Chem. Sci.*, 2013, **4**, 4245.
84. I. M. Riddlestone, S. Edmonds, P. A. Kaufman, J. Urbano, J. I. Bates, M. J. Kelly, A. L. Thompson, R. Taylor and S. Aldridge, *J. Am. Chem. Soc.*, 2012, **134**, 2551.
85. J. A. B. Abdalla, I. M. Riddlestone, J. Turner, P. A. Kaufman, R. Tirfoin, N. Phillips and S. Aldridge, *Chem. Eur. J.*, 2014, **20**, 17624.
86. J. A. B. Abdalla, A. Caise, C. P. Sindlinger, R. Tirfoin, A. L. Thompson, A. J. Edwards and S. Aldridge, *Nat. Chem.*, 2017, **9**, 1256.
87. T. Y. Her, C. C. Chang, G. H. Lee, S. M. Peng and Y. Wang, *Inorg. Chem.*, 1994, **33**, 99.
88. J. M. Burlitch, M. E. Leonowicz, R. B. Petersen and R. E. Hughes, *Inorg. Chem.*, 1979, **18**, 1097.
89. I. M. Riddlestone, J. Urbano, N. Phillips, M. J. Kelly, D. Vidovic, J. I. Bates, R. Taylor and S. Aldridge, *Dalton Trans.*, 2013, **42**, 249.
90. D. Dange, C. P. Sindlinger, S. Aldridge and C. Jones, *Chem. Commun.*, 2017, **53**, 149.
91. J. Bauer, H. Braunschweig and R. D. Dewhurst, *Chem. Rev.*, 2012, **112**, 4329−4346.
92. K. Nagata, T. Agou and N. Tokitoh, *Angew. Chem. Int. Ed.*, 2014, **53**, 3881.
93. M. Veith and W. Frank, *Angew. Chem. Int. Ed. Engl.*, 1985, **24**, 223.
94. K. Zeckert, *Dalton Trans.*, 2012, **41**, 14101.
95. C. Ganesamoorthy, D. Bläser, C. Wölper and S. Schulz, *Angew. Chem. Int. Ed.*, 2014, **53**, 11587.
96. C. Ganesamoorthy, D. Blaser, C. Wolper and S. Schulz, *Chem. Commun.*, 2014, **50**, 12382.
97. J. D. Erickson, J. C. Fettinger and P. P. Power, *Inorg. Chem.*, 2015, **54**, 1940.
98. S. Schulz, A. Kuczkowski, D. Schuchmann, U. Flörke and M. Nieger, *Organometallics*, 2006, **25**, 5487.
99. M. T. Gamer, P. W. Roesky, S. N. Konchenko, P. Nava and R. Ahlrichs, *Angew. Chem. Int. Ed.*, 2006, **45**, 4447.

100. S. G. Minasian, J. L. Krinsky, V. A. Williams and J. Arnold, *J. Am. Chem. Soc.*, 2008, **130**, 10086.

Chapter Two

Synthesis and reactivity of β-diketiminate supported alkaline earth gallyl compounds

2.1 Overview

In this chapter, the synthesis and reactivity of new alkaline earth gallyl compounds will be described. These compounds were synthesised *via* salt elimination reactions between the corresponding alkaline earth iodide complexes and the gallium(I) NHC analogue $[K\{Ga(NArCH)\}_2(Et_2O)]_2$ (**1.44**). Some preliminary studies of the effects of steric modifications at the supporting ligand of the alkaline earth metals were performed by G. Schenck, a Part II student in the Mountford group, under the direct supervision of the author. The features of the Ae-Ga complexes presented in this Chapter will be compared to pertinent literature examples. Furthermore, the reactivity of these complexes with small molecules, namely carbodiimides, isobutene epoxide, Me_3NO and alkyl iodides will also be described. The precedents to the synthesis and reactivity of Ae-Ga complexes reported in the literature along with the characteristics of ^{R}NacNac supported metal complexes will be discussed in the initial sections of this chapter.

2.2 Introduction

2.2.1. Effects of the steric and electronic modifications of the β-diketiminate ligands

The β-diketiminates, also known as 1,3-diketiminates or ^{R}NacNac (R indicates a generic substituent set) due to their similarities to acac (acetylacetonate or 1,3-diketones), are a group of widely used anionic bidentate ligands. Their extended applications rely on their facile preparation, generally by condensation of aromatic amines and 1,3-diketones, and the possibility to tune their properties, and those of their complexes, by modifying the substituents on the nitrogen α to the coordinated metal and the β- and γ- carbons (Figure 2.1).

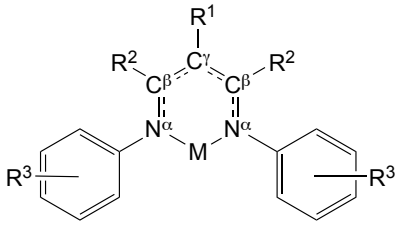

Figure 2.1. General structure of ^{R}NacNac complexes.

Recently, Chen and co-workers have reviewed the use of ^{R}NacNac ligands in complexes of transition metals and the trends in the electronic and steric effects

brought about by varying the substituents in the three aforementioned positions.[1] Other analyses have focused on the effect of such modifications on the catalytic properties of ^{R}NacNac complexes of first row transition metals[2] and the chemistry of platinum group metals.[3]

According to Chen *et al.*,[1] the steric properties of the ^{R}NacNac complexes can be tuned by varying the substituents on the β-carbon, changing the size of the subsitituents of the *ortho*-position of the N-aryl or by relocating such moieties to *meta*- and *para*-positions. For instance, the increase of the steric bulk of the substituents of the β-C in particular, pushes the N-aryl towards the metal, forcing this to remain closer to the metallacycle. On the other hand, the *o*-substitution in the aromatic rings of ^{R}NacNac with bulky fragments increases the distance between the metal and its ligands.[1] In terms of the effects on the structure, the reduction of the steric demands of the ^{R}NacNac ligands results in dimerisation or oligomerisation of their complexes or the increase in the coordination number of the metal centre when this interacts with small ligands.[4] Additionally, these structural modifications affect the reactivity of the formed complexes since some intermediates or transition states would be more stable than others depending on the respective conformations and their accessibility. One example of these effects, is the ligand controlled reactivity of vanadium chloride complexes supported by ^{R}NacNac ligands (Scheme 2.1).[5] The use of methyl substituents in the β-carbon of the ligand gives a vanadium(I) dimer (**2.3**, Scheme 2.1). In contrast, the use of the bulkier phenyl fragment in the same position yields the product of the C-NDipp bond cleavage (**2.4**, Scheme 2.1). The authors propose that complex **2.2** of Scheme 2.1 is reduced to form the transient complex $\{HC(C(Ph)NDipp)_2\}V$ in which the Ph substituents of the β-C push the NDipp fragment towards the electron deficient vanadium centre. This leads to coordination of the C-NDipp bond to vanadium and the further cleavage of that bond to form the azabutadienyl complex **2.4**.

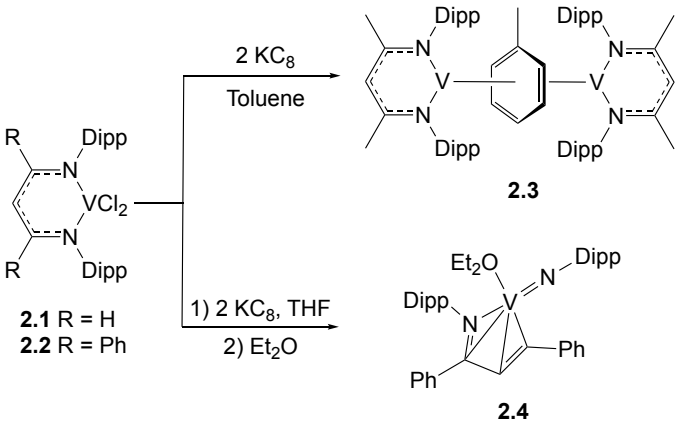

Scheme 2.1. Reactivity of ^{R}NacNac complexes of vanadium with KC_8.[5]

The variations on the *o*-substituent in the N-aryl can also lead to different products in reactions under the same conditions. For instance, the oxidation of chromium complexes with small substituents on the *ortho* positions of the N-aryl gives a μ-oxo complex (**2.5**, Scheme 2.2).[6] In contrast, the increase of the steric bulk in the same position leads to the dinuclear hydroxo chromium complex bridged by a C-C bond in the *o*-substitutent (**2.6**, Scheme 2.2). This is presumably due to the steric hindrance in the coordination sphere of chromium in **2.6** preventing the formation of the oxo-bridge as in **2.5**, instead, the benzylic hydrogen atom is abstracted by the oxygen atom in the intermediate Cp(^{R}NacNac)Cr(O) with concomitant C-C coupling.

As mentioned, the modifications of the ^{R}NacNac ligand also entail electronic effects. In their analysis Chen and co-authors describe that these effects are observed when modifications occur in the γ-C although the substitution in other positions can also have an effect in the electronic properties of (NacNac)M systems.[1] Generally, the use of electron withdrawing groups allows the complex to have a more positive reduction potential consistent with the decrease of the electronic density on the ligand and the metal centre. Additionally, electron withdrawing substituents enhance the stabilisation of metals in low oxidation states. In contrast, more negative reduction potentials and stabilisation of high oxidation states are more likely to be accessed with the use of electron-donating substitutents.[1]

The influence of the substituents is also observed in the spectroscopic properties of ^{R}NacNac supported complexes. In this regard, the presence of ligands sensitive to the changes in the electronic features of the complex such as CO or even the γ-C and γ-H in the ^{R}NacNac ligand can serve as probes to qualitatively determine these effects. For

example, substitution with the electron-withdrawing CF_3 group at the β-C of (^{R}NacNac)Cu(CO) complexes reduces the M-CO back-bonding which translates into higher wavenumbers for the ν(CO).[7] Relatedly, the substitution of CF_3 for CH_3 in the β-C of (NacNac)Ru(η^6-Ar) species deshields the γ-C causing a downfield shift in its proton resonance.[8]

As with the steric effects of the substituents, the changes in the electronic properties of the substituents affect the reactivity of the β-diketiminato complexes. For instance, electron-withdrawing groups increase the acidity of the metal centre, this reduces the rate constant of the oxidative addition of MeI to Cp(^{R}NacNac)Cr complexes compared to the faster addition when electron-donating substituents are present in the same positions.[9]

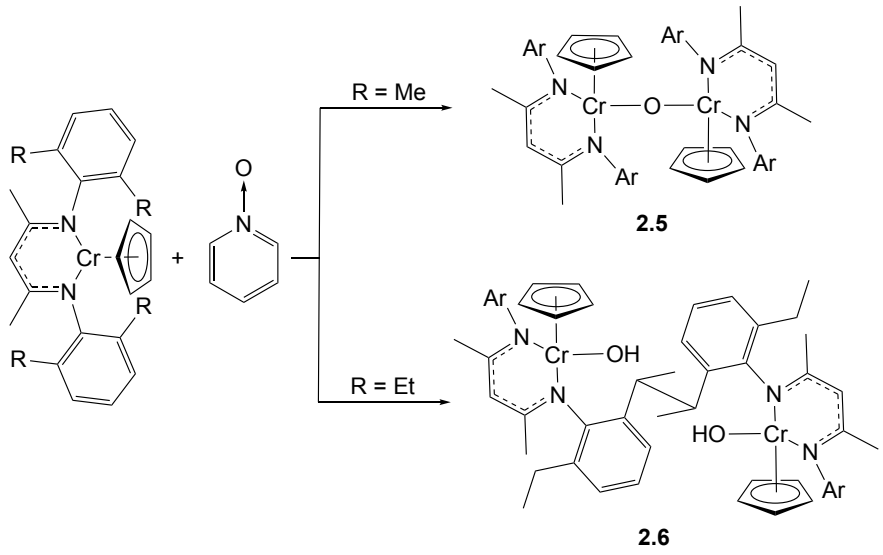

Scheme 2.2. Ligand controlled reactivity of Cp(^{R}NacNac)Cr complexes with pyridine *N*-oxide.[6]

2.2.2. Alkaline earth-gallium bonded complexes

In Chapter 1, the synthesis of the first Ae-Ga bonded species (**1.11**-**1.13**, Scheme 2.3) by Jones *et al.* was briefly described.[10] Initial attempts to form these compounds by salt metathesis between [K(TMEDA){Ga(NArCH)$_2$}]$_2$ (**1.43**) and the corresponding AeI_2 iodides in THF only yielded complex mixtures. Eventually the desired complexes were accessed upon reduction of the gallium diiodide complexes with either Mg or Ca metals previously activated with a small amount of mercury (Scheme 2.3). As described, depending on the size of the ionic radius of the alkaline earth metal, the coordination of three (Mg) or four (Ca) THF molecules occurred with a

direct effect on the geometry of the formed complexes. The formation of **1.11**-**1.13** proceeds through further reductions of the diiodides **1.48** or **1.49** (Scheme 2.3) to form paramagnetic intermediates of the type **2.7**, followed by the diamagnetic digallanes(4) **2.8** and finalised with the insertion of the Ae atom into the Ga-Ga bond in **2.8**. This mechanism was proposed after the observation of **2.7** and **2.8** in the early stages of the reactions and it is also supported by the alternative formation of **1.11** and **1.12** by reaction of the intermediates **2.7** or **2.8** (R = H) with either magnesium or calcium. In terms of their structural properties in the solid state, **1.11** has a magnesium centre in a distorted trigonal bipyramidal environment with two gallyls and one THF molecule in the equatorial positions; another two THF molecules in the axial positions complete the trigonal bipyramid. In contrast, the calcium analogues **1.12** and **1.13** exhibit an octahedral geometry around the Ca atom with four THF molecules occupying equatorial positions and two gallyls in axial positions. The Ae-Ga bond distances in **1.11** (2.7174(15) Å), **1.12** (3.1587(6) Å) and **1.13** (3.1988(12) Å) are slightly longer than the sum of their respective covalent radii (Mg-Ga: 2.63(8) and Ca-Ga: 2.98(10) Å).[11] Despite Sr and Ba being more electropositive than Mg and Ca, the reactions with those heavier alkaline earth metals and **1.48** stopped in the formation of **2.8** and according to the authors, this could be due to a kinetic factor in the last step.[10]

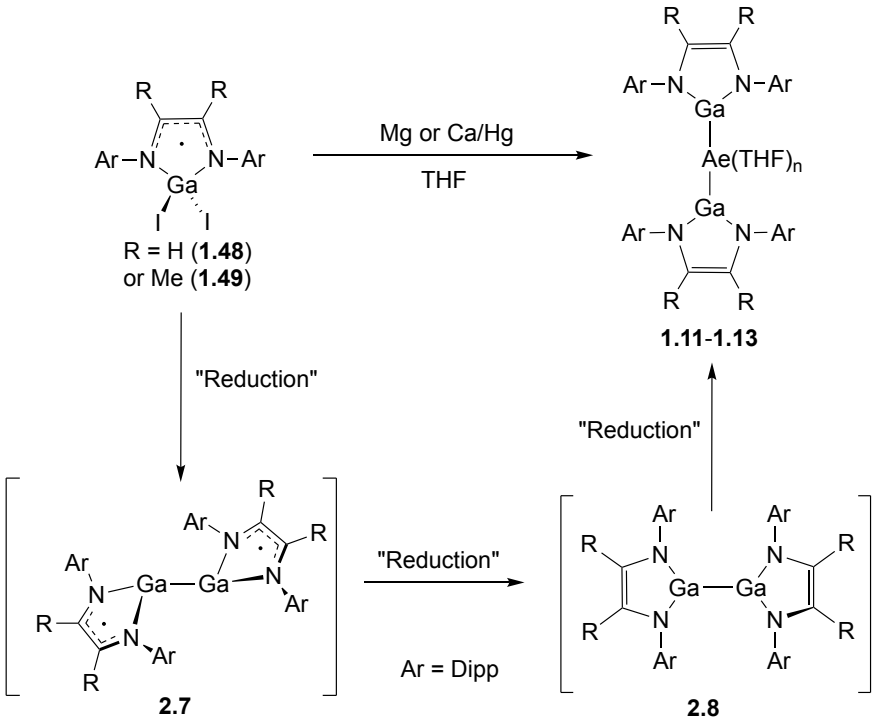

Scheme 2.3. Reduction of $Ga(ArNCR)I_2$, where R = H (**1.48**) or Me (**1.49**), to form the complexes $Ae\{Ga(ArNCR)_2\}_2(THF)_n$ *via* intermediates **2.7** and **2.8**. For Ae = Mg, R = H (**1.11**) and n = 3. For Ae = Ca, R = H (**1.12**) or Me (**1.13**) and n = 4.[10]

The outstanding Sr-Ga and Ba-Ga complexes along with a new Ca-Ga species were later isolated by Wiecko and co-workers by changing the set of ligands and the approach.[12] In their report, Wiecko *et al.* formed the acceptor-donor complexes between $(\eta^5\text{-}C_5Me_5)Ga$ and the metallocenes $(\eta^5\text{-}C_5Me_5)_2M$ (M = Ca, Ba) and $(\eta^5\text{-}C_5Me_5)_2Sr(THF)_x$ (Scheme 2.4). The formation of **2.9** and **2.11** proceeds selectively as opposed to **2.10** which is formed along with its THF-free analogue. The increase in covalent radius down the group favours the coordination of a THF molecule in **2.10** compared to **2.9** and the coordination of two gallyl fragments in **2.11**. The fact that strontium coordinates one THF molecule instead of two gallyl moieties is presumably to due to strontium being too small to coordinate two $(\eta^5\text{-}C_5Me_5)Ga$ units. The observed Ae-Ga distances (Ca-Ga: 3.183(2) Å, Sr-Ga: 3.4348(7) Å, Ba-Ga: 3.5911(5) Å) increase down the group. Furthermore, the Ae-Ga bonds are longer than the sum of respective covalent radii (Ca-Ga: 2.98(10) Å, Sr-Ga: 3.17 (10) Å, Ba-Ga 3.37(11) Å).[11] The chemical shifts of **2.9**-**2.11** are very similar to those of the starting materials which is characteristic of a weak Ae-Ga interaction. This was supported by DFT and

second order Møller-Plesset (MP2) calculations for **2.9** which suggested a weak Ca-Ga bond presumably stabilised by van der Waals dispersive forces.

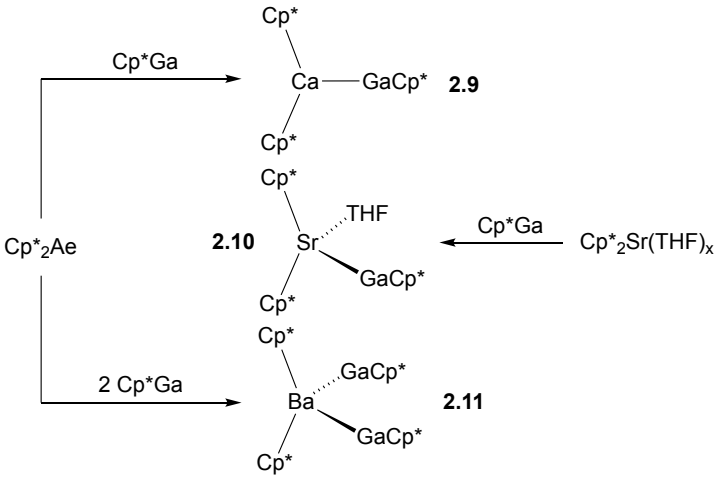

Scheme 2.4. Synthesis of Ae-Ga by adduct formation between (η^5-C_5Me_5)Ga and the metallocenes [Cp*$_2$Ae] (Cp* = η^5-C_5Me_5).[12]

Almost in parallel, the groups of Jones and Fedushkin reported the synthesis of Ae-Ga species through different routes. Fedushkin *et al.* accessed a series of Ae-Ga (Ae = Mg, Ca, Sr and Ba) complexes after inserting the Ae metals into the Ga-Ga bond of the digallane(4) [(dpp-bian)Ga]$_2$ (**1.52**) (Equation 2.1).[13] Complex **2.15** could be alternatively prepared by salt metathesis between BaI_2 and either $Na(Et_2O)_3${Ga(dpp-bian)} (**1.51**) or $K(THF)_5${Ga(dpp-bian)} (**1.54**). The quality of X-ray data of **2.12**-**2.14** was poor although good enough to establish the connectivity in these complexes. The X ray structure of **2.15** showed a pentagonal-bipyramidal geometry around the Ba centre with the THF molecules in the equatorial and the Ga(dpp-bian) units in the axial positions. The obtuse Ga-Ba-Ga angle of 156º is presumably caused by steric repulsion between the THF molecules and the 2,6-^{i}Pr$_2$-C_6H_3 substituents of the gallyls. Similarly to Jones' Mg (**1.11**) and Ca (**1.12**) analogues (*vide supra*), the Ba-Ga bond distances (3.6433(5) Å and 3.5964(7) Å) are longer than the sum of the respective covalent radii and similar to those of Cp*$_2$Ba(GaCp*)$_2$ (**2.11**).

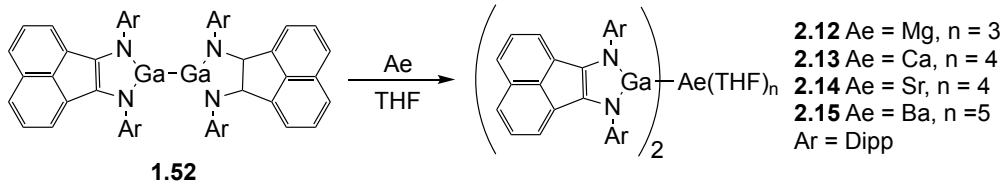

1.52

Equation 2.1.[13]

For their part Bonello, Jones *et al.* revisited the synthesis of the Ca, Sr and Ba analogues of **1.11** and **1.12** in THF using TMEDA as ancillary ligand.[14] These were prepared by salt elimination between the corresponding AeI_2 (Ae = Ca, Sr, Ba) iodides and $[K(TMEDA)\{Ga(NArCH)_2\}]_2$ (**1.43**) in an excess of TMEDA (Scheme 2.5). Attempts to synthesise the Mg analogue of **2.16-2.18** were unsuccessful. In order to obtain a related TMEDA complex by salt elimination, $Mg(^{Dipp}NacNac)I(Et_2O)$ was used as the source of the magnesium. Complexes **2.16-2.18** exist in equilibrium with their *cis* isomers in solution with *trans:cis* ratios of ca. 80:20. In the solid state all exhibit octahedral geometries with two gallyl fragments occupying axial positions and the TMEDA ligands in the equatorial plane. The Ae-Ga bond distances increase down the group and are longer than the sum of the Ae and Ga covalent radii as observed in other Ae-Ga complexes (*vide supra*). Unexpectedly, the Ca-Ga distances in **2.16** (3.2568(8) Å and 3.1983(8) Å) are longer than those of Wiecko's $Cp^*_2Ca(GaCp^*)$ (**2.9**) donor-acceptor complex (3.183(2) Å).[12] On the other hand, the ^{Dipp}NacNac supported complex **2.19** exhibits a distorted tetrahedral geometry around the Mg centre. The Mg-Ga bond length of **2.19** is 2.7470(7) Å which is slightly longer than that of $Mg\{Ga(NArCH)_2\}_2(THF)_3$ (**1.11)**, despite the higher coordination number in the latter. Additionally, the TMEDA ligand is κ^1-coordinated to Mg. In solution **2.19** exhibits fluxionality at -50 ºC with a slow exchange regime between two isomers. One of them is thought to be reminiscent of the solid state structure and the second one is presumably a more symmetric form of **2.19**, *e.g.,* a polymer formed by bridging TMEDA units. Further attempts to isolate the ^{Dipp}NacNac supported Ca analogue of **2.19** led to the bis(gallyl) complex **2.16**. The authors propose that the calcium gallyl species is formed initially and then redistributes to **2.16** and the homoleptic $Ca(^{Dipp}NacNac)_2$ (**2.20**).

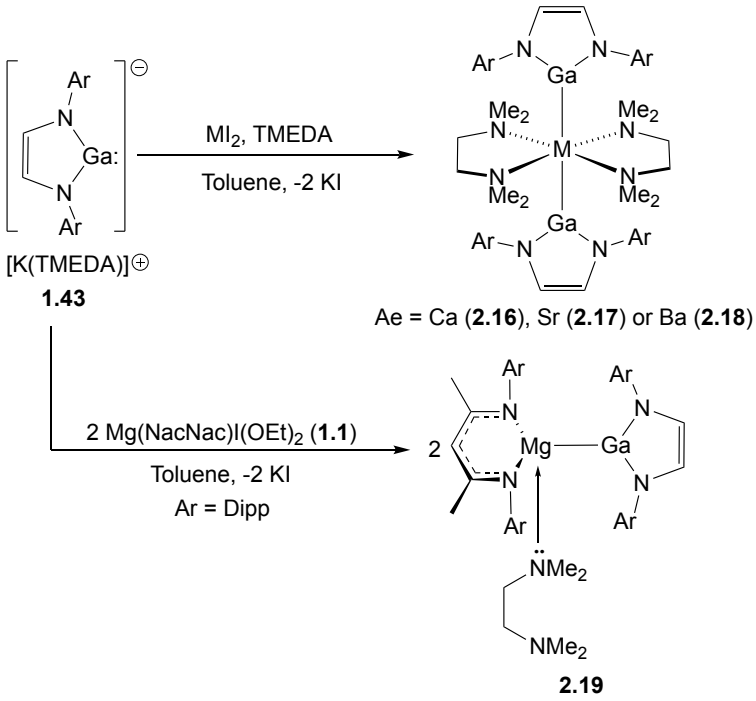

Scheme 2.5. Synthesis of Ae-Ga bonded complexes *via* salt elimination with TMEDA as ancillary ligand.[14]

2.2.3. Reactivity of Ae-M and M-Ga(NArCH)$_2$ bonded complexes

To date there are no reported investigations on the reactivity of Ae-Ga complexes in the literature. However, the reactivity of Ae-M or M-Ga (M = metal) complexes has been widely explored. For instance, the reactivity of Green's Mg^{I}-Mg^{I} dimer (**1.2**) was initially assessed in the activation of N_2 or H_2 although these reactions did not proceed. A positive result was obtained when **1.2** was reacted with the carbodiimide CyNCNCy which led to the corresponding insertion product (**2.21**, Equation 2.2).[15] The authors propose that this reaction could proceed *via* initial coordination of the carbodiimide to one of the Mg atoms, followed by the double reduction of the coordinated CyNCNCy and ending with its insertion into the metal-metal bond to form **2.21**. In the solid state, the Mg(^{Dipp}NacNac) rings in **2.21** become parallel and orthogonal to the plane of CyNCNCy in contrast to their conformation in the parent **1.2** where the magnesiacycles are almost orthogonal. Complex **1.2** has been extensively used in insertion reactions with other unsaturated compounds including alkenes,[16, 17] nitriles,[18] isocyanates and azides.[19]

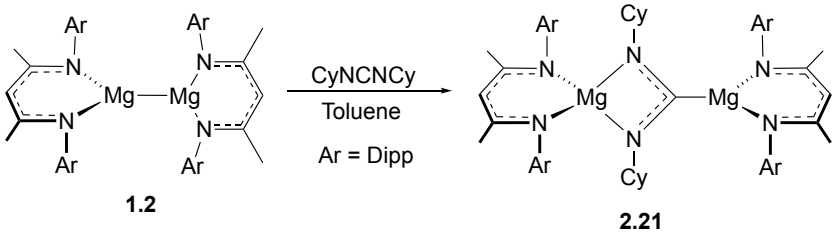

1.2 **2.21**

Equation 2.2.[15]

More recently the insertion of carbodiimides has been extended to heteronuclear species such as the Mg(^{Dipp}NacNac)Fp(THF) (**2.22**) complex by Blake *et al.,* this time with 1,3-di-*p*-tolylcarbodiimide (Equation 2.3).[20] The crystal structure of **2.23** could not be obtained although its spectroscopic properties allowed the study of the interactions in this complex. For instance, the increase in the ν(CO) frequencies in the IR spectrum of **2.23** compared to those of **2.22** suggested charge transfer from the Fe to the carbodiimide. Complex **2.22** was also reacted with iodomethane rapidly yielding (^{Dipp}NacNac)MgI(THF) and MeFp.

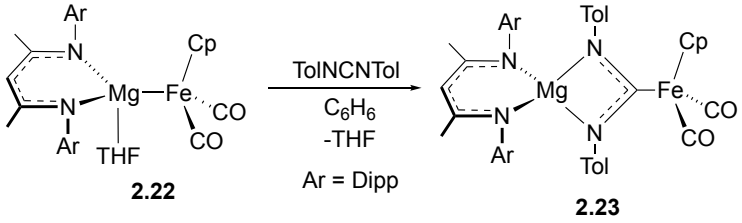

2.22 **2.23**

Equation 2.3.[20]

The insertion of carbodiimides also has been successfully applied to Ln-Ga complexes. For instance, the cationic amidinate supported species Ln{$Me_3CH_2C(NCy)_2$}$_2${Ga(NArCH)$_2$}(THF) (Ln = Y or Lu) can insert one molecule of CyNCNCy into the Ln-Ga bond (Equation 2.4).[21] As with **2.22**, the THF ligand in **2.24** and **2.25** is displaced upon reaction of these complexes with CyNCNCy. The same procedure can successfully be applied to scandium and other carbodiimides and these reactions represent the first structurally characterised net insertions into a M-Ga bond. It is noteworthy that previously reported reactions of M-Ga species were driven by the non-innocence of the supporting ligand[22, 23] or coordination to the metal centre.[23]

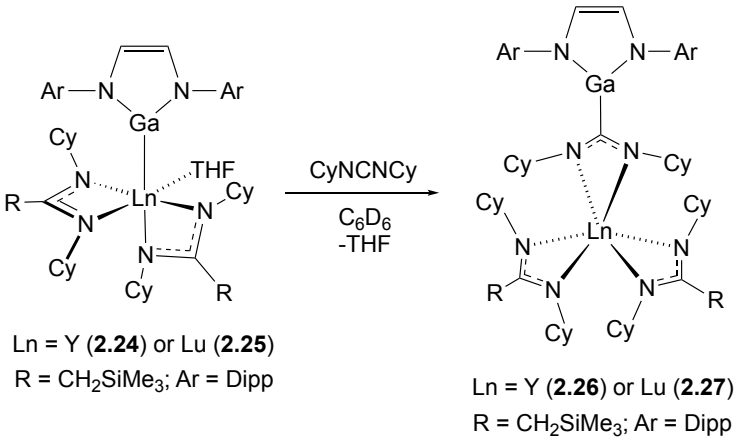

Equation 2.4.[21]

Recently, Xiong and co-workers reported the direct insertion of chalcogens into the Ge-Ga bond of donor-acceptor complexes (Scheme 2.6).[24] The addition of S or Se to THF solutions of the Ge-Ga adduct (**2.28**, Scheme 2.6) yields the product of the addition of these chalcogenides with one atom of either S (**2.29**) or Se (**2.30**) inserted into the Ge-Ga bond. In their report, the authors propose that the mechanism starts with the initial oxidation of the Ge(0) centre to form species of the type **A** of Scheme 2.6; the migration of the $GaCl_3$ unit from Ge to the chalcogenide forms the intermediate **B** which undergoes a second oxidation to form the final product. This mechanism was supported by DFT calculations and by the fact that the use of 1/8 equivalents of Se_8 in acetonitrile or one equivalent of activated Te in THF slows these reactions and makes possible the isolation of the intermediates of the type **B** with these elements.

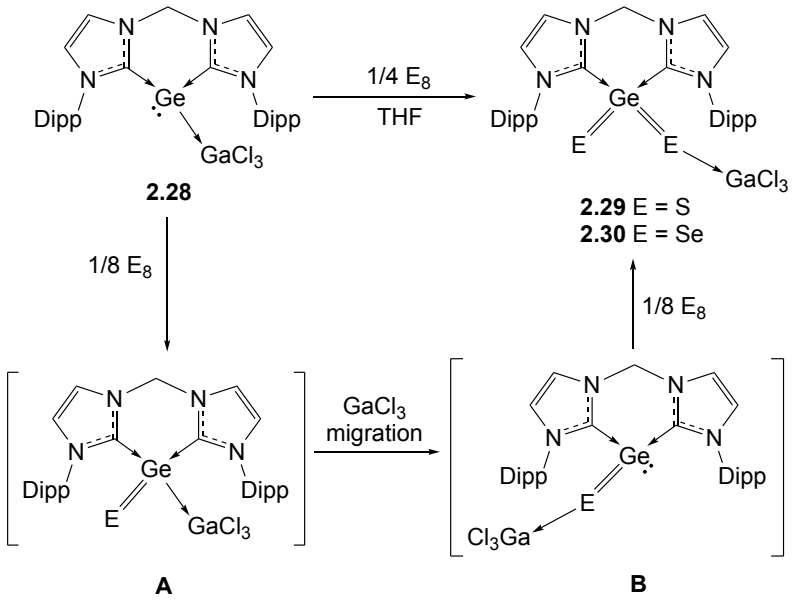

Scheme 2.6. Oxidation of Ge-Ga donor-acceptor complexes with S and Se.[24]

2.3 Synthesis of Ae(^Dipp^NacNac){Ga(NArCH)$_2$}(THF) complexes

The first attempts to synthesise Ae-Ga complexes were inspired by the aforementioned work of Bonello *et al*.[14] Initial tests towards the synthesis of this type of complex involved the reaction between solutions of Mg(^Dipp^NacNac)I(THF) (**2.31**) and [KGa(NArCH)$_2$(Et$_2$O)]$_2$ (**1.44**) in toluene to form an orange solution which was left to react for 16 h. Removal of volatiles from the reaction mixture and washing with hexane resulted in an orange solid. Analysis of the ^{1}H NMR spectrum of the solid revealed consumption of the starting materials and a new set of signals for both the ^{Dipp}NacNac and diazabutadiene frameworks along with digallane(4) [Ga(NArCH)$_2$]$_2$ (**1.68**), which is a known decomposition product in reactions with **1.44** or its analogues.[21, 25] In order to reduce the formation of **1.68**, toluene was added to a solid mixture of **1.44** and **2.31** at -78 ºC. The mixture was then allowed to warm up to RT and the reaction time was reduced to 1 h. After washing with hexane, the desired complex was obtained with the absence of **1.68** (**1**, Equation 2.5).

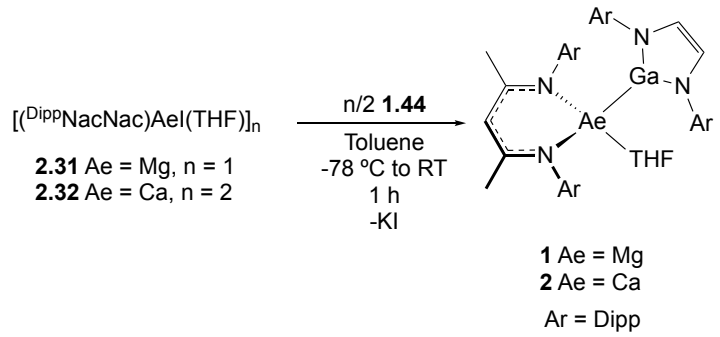

Equation 2.5

Complex **1** is the THF analogue of the Mg-Ga complex reported by Bonello (*vide supra*)[14] and therefore shares some similarities. **1** shows a characteristic upfield shift at 6.42 ppm for the vinyl proton as a result of the new chemical environment for the gallyl fragment (*cf.* 6.48 ppm for **1.44**). This upfield shift also occurred in the formation of other M-Ga$(NArCH)_2$ complexes and is within the range of the aforementioned Ae-Ga compounds and other species bearing the Ga$(NArCH)_2$ heterocycle.[14, 21, 26] The γ-H resonance of the ^{Dipp}NacNac ligand shifts from 4.84 ppm in **2.31** to 4.79 ppm in **1** which reflects the coordination of Mg to a less electronegative element than iodine in **2.31**. Compared to Bonello's Mg(^{Dipp}NacNac){Ga$(NArCH)_2$}(κ^1-TMEDA) (**2.19**), **1** shows sharper signals in the ^{1}H NMR spectrum.

Interestingly, Mg(^{Dipp}NacNac){Ga$(NArCH)_2$}(κ^1-TMEDA) (**2.19**) cannot be formed by adding TMEDA to a solution of **1** as THF seems to be a better Lewis base than TMEDA in this system. Nevertheless, the opposite reaction, *i.e.,* the substitution of TMEDA by THF, could be performed after adding THF to **2.19** in C_6D_6. The higher coordinating strength of THF was also observed during the synthesis of **2.19**. Thus **2.19** could not be formed by reacting Mg(^{Dipp}NacNac)I(THF) (**2.31**) and [KGa$(NArCH)_2$(TMEDA)]$_2$ (**1.43**), even in the presence of an excess of TMEDA and the Et_2O precursor Mg(^{Dipp}NacNac)I(Et_2O) **1.1** had to be employed as reported.[14] TMEDA is known as a strongly basic ligand and the displacement of THF by TMEDA in Mg[27, 28] and other metal[29, 30] complexes has been observed, nonetheless because of the steric crowding in the Mg(^{Dipp}NacNac){Ga$(NArCH)_2$}(L) species, TMEDA only coordinates through one of the nitrogen atoms as observed in Bonello's Mg-Ga complex and therefore is easily displaced for the less coordinating but sterically less demanding THF.

The methodology to form **1** was attempted for the synthesis of the calcium and strontium analogues. Overall it was observed that going down in the group, the stability of the Ae-Ga complexes decreased as judged by the amount of $[Ga(NArCH)_2]_2$ (**1.68**) after work up being higher for Ca and Sr. This is not surprising considering the larger atomic radii of Ca and Sr and the reduction of their Lewis acidity which makes them prone to side reactions, *e.g.,* Schlenk equilibria and redistribution.[31-33] For instance, attempts to synthesise $Ca(^{Dipp}NacNac)\{Ga(NArCH)_2\}(TMEDA)$ by Bonello and co-workers were unsuccessful and instead yielded the homoleptic $Ca(^{Dipp}NacNac)_2$ (**2.20**) (*vide supra*).[14] Eventually, we found that the complex $Ca(^{Dipp}NacNac)\{Ga(NArCH)_2\}(THF)$ (**2**, Equation 2.5) could be obtained after leaving the initial reaction mixture stir for 30 min at -78 ºC followed by warming up to RT and stirring for a further 1 h (see Chapter 5 for details). Unfortunately, after several attempts to optimise the conditions to synthesise $Sr(^{Dipp}NacNac)\{Ga(NArCH)_2\}(THF)$ (**3**), the redistribution products **1.68** and $Sr(^{Dipp}NacNac)_2$ (**2.33**) could not be removed or their formation inhibited and therefore **3** was only characterised in solution.

Similarly to **1**, complexes **2** and **3** exhibit singlets for the vinyl protons of the gallyl fragment which overall shift towards lower field as the Ae metal in the $Ae(^{Dipp}NacNac)\{Ga(NArCH)_2\}(THF)$ complexes changes from Mg (6.43 ppm) to Ca (6.45 ppm) to Sr (6.48 ppm). A similar trend is present in the TMEDA supported Ae-Ga complexes,[14] the Cp*Ga resonance of the donor-acceptor complexes prepared by Wiecko *et al.*[12] and the vinyl proton of related amidinate supported $Ln\text{-}Ga(NArCH)_2$ species.[21] As with **1**, the γ-H resonance of the ^{R}NacNac ligand of **2** and **3** shifts to higher field than the parent iodides upon coordination of the $Ae(^{Dipp}NacNac)$ fragments to gallium. As expected in ^{R}NacNac supported compounds (*vide supra*), a trend in which the resonance of the γ-H shifts upfield in going from **1** to **3** is also present due to the reduction of the electronegativity of the Ae metal in the ring (δ_H (ppm) **1**: 4.79; **2**: 4.70; **3**: 4.65).

Complexes **1**-**3** are extremely air and moisture sensitive, and prolonged handling results in decomposition. Exposure of **1**-**3** to vacuum for periods longer than 4 h results in the formation of the digallane(4) $[Ga(NArCH)_2]_2$ (**1.68**), the homoleptic species $Ae(^{Dipp}NacNac)_2$[34] and other minor unknown species presumably due to the

loss of THF. Additionally, leaving C_6D_6 solutions of these complexes overnight leads to rearrangement into the Ae(^{Dipp}NacNac)$_2$ homoleptic species and **1.68**.

2.4 Synthesis of Mg(^{R}NacNac){Ga(NArCH)$_2$}(THF) (R = Ph, Mes)

In order to study the effect of the reduction of the steric crowding around the Mg-Ga bond, the use of less sterically demanding substituents in the N-aryl of Mg gallyl complexes was envisaged. To reduce the steric congestion, the substitution of phenyl and mesityl for Dipp in the nitrogen of ^{R}NacNac was intended. Initial tests in the NMR tube scale in C_6D_6 involved reactions of **1.44** with either Mg(^{Mes}NacNac)I(THF) (**2.34**) or Mg(^{Ph}NacNac)I(THF) (**4**) (Equation 2.6). Upon mixing, the formation of a precipitate was evident and orange solutions are formed after settling of the salt. The changes observed in the ^{1}H NMR spectra of **5** and **6** with respect to their starting materials were similar to the ones observed with **1**. Comparing the ^{1}H NMR spectra of **5** and **6** with that of **1** it is noticeable that the resonance of the γ-H proton of the least substituted Mg(^{Ph}NacNac){Ga(NArCH)$_2$}(THF) **6** is shifted to higher field (4.70 ppm) than its more substituted congeners, Mg(^{Mes}NacNac){Ga(NArCH)$_2$}(THF) **5** and Mg(^{Dipp}NacNac){Ga(NArCH)$_2$}(THF) **1**, which both exhibit singlet resonances for their γ-H at 4.79 ppm. Conversely, the resonance of the vinyl proton in these compounds shifts downfield as the steric demand of the N-aryl decreases (δ_H (ppm) **1**: 6.42; **5**: 6.46; **6**: 6.58).

The scaling up of the synthesis of **5** and **6** was attempted adapting the methodology to isolate **1**. Complex **5** could be prepared in 74% yield. In contrast, the less substituted and less sterically hindered **6** turned out to be unstable on exposure to vacuum. This was observed after removing volatiles under vacuum from a fresh sample of **6** in an NMR tube and then redissolving the sample it in C_6D_6. The ^{1}H NMR spectrum of the redissolved mixture revealed the decomposition of **6** into [Ga(NArCH)$_2$]$_2$ (**1.68**) and Mg(^{Ph}NacNac)$_2$ (**2.35**)[35] up to 50%. The decomposition of **6** is presumably due to the loss of THF and to the presence of a less sterically encumbering set of ligands which no longer protects the Mg-Ga bond. The lack of substituents in the N-aryl could also form a more thermodynamically stable homoleptic magnesium species (**2.35**). Hence, **6** was characterised only in solution by NMR spectroscopy.

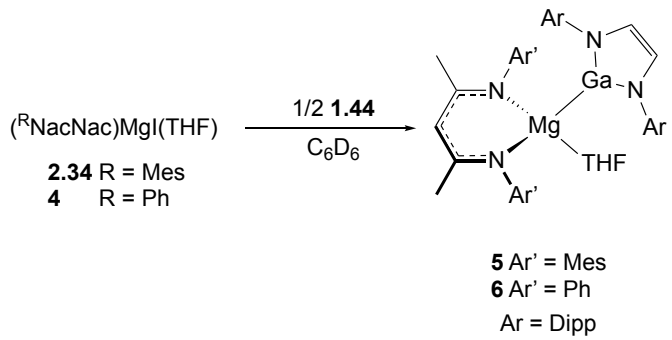

Equation 2.6

2.5 Reactivity of Ae(^{R}NacNac){Ga(NArCH)$_2$}(THF) complexes

2.5.1 Reactions of alkaline earth gallyl complexes with carbodiimides

The first attempts to study the reactivity of the aforementioned Ae-Ga compounds involved the activation of CO_2 and SO_2; unfortunately, these reactions led to the formation of complex and intractable mixtures with [Ga(NArCH)$_2$]$_2$ (**1.68**) being the only identifiable product. The use of carbodiimides which are isoelectronic with CO_2 was then explored. Upon addition of 1 equivalent of *N,N'*-diisopropylcarbodiimide (^{i}PrNCN^{i}Pr) to a C_6D_6 solution of **1**, a change in the colour of the reaction mixture from orange to yellow was observed**.** The ^{1}H NMR of the sample showed the complete consumption of the starting materials and the formation of a new species (**7**, Equation 2.7). An upfield shift for the resonance of the vinyl proton from 6.43 ppm in **1** to 6.13 ppm in the product **7** evidenced the formation of the insertion product. This upfield shift, resulting from the coordination of Ga to a *sp*^{2} carbon is in the range of other related systems containing the C_{sp2}-Ga(NArCH)$_2$ moiety.[21, 25, 36] Conversely, the γ-H resonance in **7** shifts downfield with respect to its parent **1**. The ^{1}H NMR spectrum also showed only one environment for the protons in the isopropyl fragments of the carbodiimide suggesting the formation of a symmetric product. The THF ligand appears as free in the ^{1}H NMR spectrum of this sample; this was further confirmed after removing the volatiles from a fresh sample of **7** at low pressure and redissolving the resulting mixture in C_6D_6. No apparent change was found in the ^{1}H NMR spectrum of the product and the THF resonances were absent, supporting the incorporation of the carbodiimide to the Mg-Ga complex with displacement of THF. The synthesis of complex **7** could be successfully scaled up in good yield (84%). Following this result, the study in solution of the insertion of ^{i}PrNCN^{i}Pr into the less hindered analogues of **1**, Mg(^{Mes}NacNac){Ga(NArCH)$_2$}(THF) (**5**) and

Mg(^{Ph}NacNac){Ga(NArCH)$_2$}(THF) (**6**, Equation 2.7). Similar upfield shifts for the vinyl proton of the products are found when ^{i}PrNCN^{i}Pr is added to solutions of either **5** or **6** with upfield shifts for the vinyl protons and downfield shifts for the γ-H resonances of **8** and **9**.

Additionally, and in order to further explore the similarities of the Mg-Ga bonding in these complexes with respect to the crystallographically authenticated Mg(^{Dipp}NacNac){Ga(NArCH)$_2$}(TMEDA) **2.19**, a C_6D_6 solution of **2.19** was treated with 1 equivalent of ^{i}PrNCN^{i}Pr forming the expected insertion product **7** and releasing TMEDA. This result, along with the displacement of TMEDA by THF in **2.19** to form **1** (*vide supra*) and the characterising data supports the formulation and the proposed structure of **1** and its analogues.

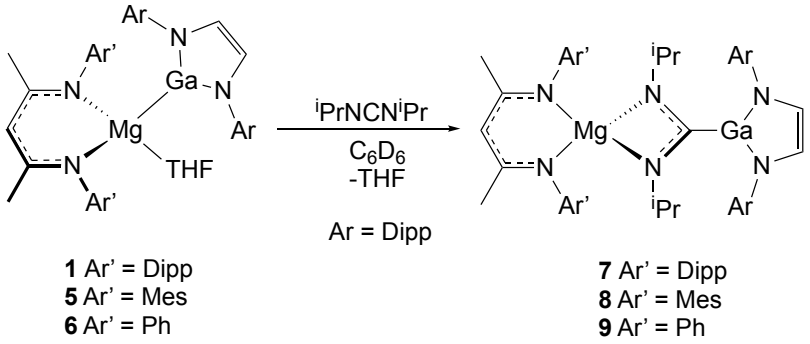

1 Ar' = Dipp
5 Ar' = Mes
6 Ar' = Ph

7 Ar' = Dipp
8 Ar' = Mes
9 Ar' = Ph

Equation 2.7

Diffraction-quality crystals of **7** were grown from a saturated solution of C_6D_6 at RT. The solid state structure confirmed the insertion of ^{i}PrNCN^{i}Pr into the Mg-Ga bond of **1** or **2.19**. The molecular structure and selected distances and angles are shown in Figure 2.2 and Table 2.1.

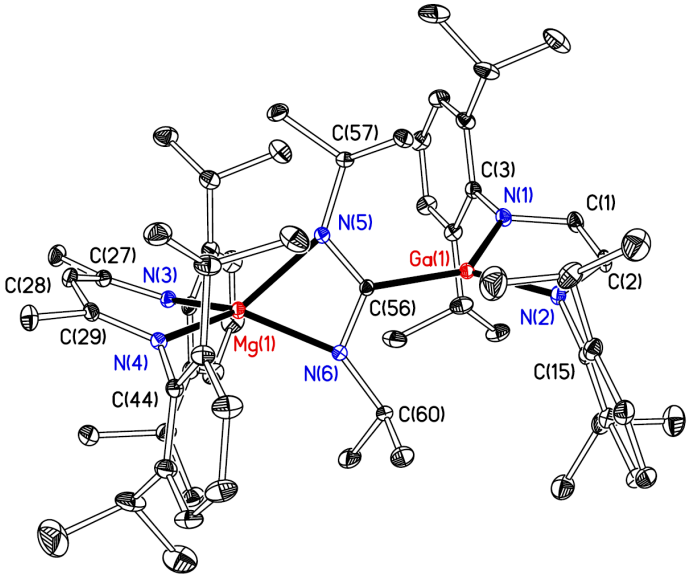

Figure 2.2. Displacement ellipsoid plot (20 % probability) of Mg(^{Dipp}NacNac){(N^iPr)$_2$CGa(NArCH)$_2$}(THF) (**7**). H atoms omitted for clarity.

Table 2.1. Selected distances (Å) and angles (°) for Mg(^{Dipp}NacNac){(N^iPr)$_2$CGa(NArCH)$_2$}(THF) (**7**).

Mg(1)-N(3)	2.0600(14)	Ga(1)-N(2)	1.8472(13)
Mg(1)-N(4)	2.0451(14)	Ga(1)-C(56)	1.9799(15)
Mg(1)-N(5)	2.0968(14)	C(56)-N(5)	1.3263(19)
Mg(1)-N(6)	2.0684(14)	C(56)-N(6)	1.327(2)
Ga(1)-N(1)	1.8486(13)		
N(3)-Mg(1)-N(4)	93.94(6)	N(1)-Ga(1)-N(2)	90.25(6)
N(5)-Mg(1)-N(6)	65.64(5)		

The geometry at the four-coordinate Mg centre is distorted tetrahedral, with the coordinated ^{Dipp}NacNac and a bidentate galla-amidinate. The distances between Mg(1) and the surrounding nitrogen atoms are comparable those of the only two structurally authenticated magnesium metal-amidinates Mg(^{Dipp}NacNac){(NCy)$_2$CMg(^{Dipp}NacNac)} (**2.21**)[15] and Mg(^{Mes}NacNac){(N^iPr)$_2$CMo(NSi^iPr_3)(Ar*)} (Ar* = 2,6,4-C_6H_2{$CHPh_2$}$_2Pr^i$) (**2.36**).[37] The N(5)-Mg(1)-N(6) angle (65.64(5)º) is also comparable to that of **2.36** (66.56(9)º). The N(1)-Ga(1) and N(2)-Ga(1) distances are shorter than those of

Bonello's Mg(^{Dipp}NacNac){Ga(NArCH)$_2$}(TMEDA) (**2.19**) complex[14] which is also a precursor to **7**. In addition, the N(1)-Ga(1)-N(2) angle (90.25(6)º) is notably wider than that of **2.19** (85.55(6)º). These structural changes involving widening in the N-Ga-N and shortening of the Ga-N distances upon coordination of the gallium atom to a sp^2 carbon have been previously investigated in the aforementioned insertions into Ln-Ga bonds[21] and have been rationalised in terms of Bent's rule.[38] Upon coordination of gallium to an element more electronegative than magnesium, *i.e.,* carbon in **7**, the *s* character of gallium directed towards carbon depletes and the *p* character increases. This leaves more *s* character in the Ga-N bonds which widens the N-Ga-N angle. Indeed, the N(1)-Ga(1)-N(2) of 90.25(6)º is one of the widest N-Ga-N angles in systems containing five-membered NHC analogues of gallium(I) being comparable to that of (η^1-C_5Me_5)Ga(NArCH)$_2$ (90.07(14)º)[39] or related complexes with gallium coordinated to even more electronegative elements, *e.g.,* K(μ-Cl)$_2$Ga(NArCMe)$_2$(THF)$_4$ (90.20(1)º).[40] Conversely, the coordination of gallium to a more electropositive element results in more acute N-Ga-N angles; for instance, the N-Ga-N angles in **7** and **2.19** are wider than that of [KGa(NArCH)$_2$(Et$_2$O)]$_2$ (**1.44**) (81.88(9)º).[41] As mentioned, only two structures of insertions into Mg-M bonds have been reported. Complex **7** represents the first structurally authenticated net insertion into a Mg-Ga bond and indeed any Ae-Ga bond.

The reactions of carbodiimides with Mg-Ga complexes were further extended to other carbodiimides, namely, CyNCNCy and TolNCNTol (Equation 2.8). The insertion reactions with either CyNCNCy or TolNCNTol and **1** in C_6D_6 were successful and the synthesis of the complexes **10** and **11** was scaled up in good yields (68-92%). The product of the incorporation of CyNCNCy to **1**, **10**, has chemical shifts for the vinyl and γ-H protons, 6.13 ppm and 4.82 ppm, respectively, similar to its less hindered analogue **7** (δ_{vinyl}: 6.13 ppm and $\delta_{\gamma\text{-H}}$: 4.80 ppm). The insertion of the aromatic carbodiimide TolNCNTol forms the complex **11** with a slight upfield resonance for the vinyl proton (6.12 ppm) and downfield shift of the resonance of its γ-H (4.88 ppm) with respect of its analogues **7** and **10** bearing alkyl substituents on the nitrogen of the amidinate (4.80 ppm and 4.82 ppm, respectively).

After these results, further study of the reactions of **5** and **6** with TolNCNTol was then performed. Similar observations are found when TolNCNTol is added to a solution of **6**. The resulting complex (**12**, Equation 2.8) was characterised in solution and presents

resonances for its vinyl and γ hydrogens at 6.25 ppm and 4.88 ppm, respectively. Surprisingly, the addition of TolNCNTol to a C_6D_6 solution of **6** yielded the redistribution products $[Ga(NArCH)_2]_2$ (**1.68**) and $Mg(^{Mes}NacNac)_2$ (**2.37**)[35] instead of the desired insertion. The reason for the unexpected reactivity of **6** with TolNCNTol is unknown although it clearly cannot be due to steric factors since the product of the more and less sterically hindered Mg-Ga complexes **11** and **12** could be successfully achieved.

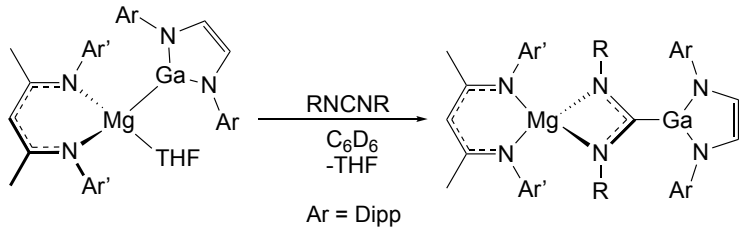

Equation 2.8

Following the study of the insertion of carbodiimides with magnesium complexes, these reactions were extended to the calcium complex **2** (Equation 2.9). Inspection of the ^1H NMR spectra of complexes **13-14** revealed the clean formation of the insertion products. Notably, the THF ligand remains coordinated to the calcium centre as opposed to the magnesium congeners, due to the larger atomic radius of calcium which affords the accommodation of the ^{R}NacNac, galla-amidinate and THF ligands. As with the ^{Dipp}NacNac supported Mg analogues **7**, **10** and **11**, the tolyl containing insertion product **15**, exhibits the most upfield shifted resonance for the vinyl proton (6.22 ppm) compared to its alkyl substituted congeners **13** (6.33 ppm) and **14** (6.28 ppm). All other trends present in the ^{Dipp}NacNac supported complexes, *e.g.* downfield shift of the γ-H upon insertion of the carbodiimides, are present in the calcium complexes **7-11**. The synthesis of **13-15** could be scaled up in good yields (61-76%).

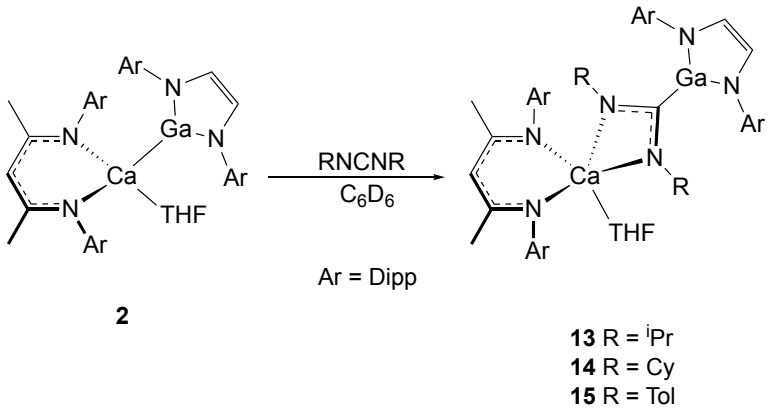

2

13 R = ^{i}Pr
14 R = Cy
15 R = Tol

Equation 2.9

Attempts to crystallise **15** from a concentrated C_6H_6 solution at RT, yielded, after two weeks, diffraction quality crystals. Unexpectedly, the solution of the structure revealed a bis(galla-amidinate). The molecular structure, selected bond distances and angles are shown in Figure 2.3 and Table 2.2. The solid state structure will be discussed later on. This bisgalla-amidinate complex **16** is presumably formed in a Schlenk equilibrium when **15** is in solution (Scheme 2.7). Species **16** could be independently synthesised by the double insertion of TolNCNTol and the known bis(gallyl) calcium complex $Ca\{Ga(NArCH)_2\}_2(THF)_4$ (**1.12**)[10] in 61% yield (Scheme 2.7). Additionally, heating a C_6D_6 solution of **15** at 80 ºC for 6 h formed $Ca\{(NTol)_2CGa(NArCH)_2\}_2(THF)_2$ (**16**) and $Ca(^{Dipp}NacNac)_2$ (**2.20**)[34] in small amounts (< 5%) within a complex mixture.

As mentioned, complex **16** can also be formed by the reaction of 2 equivalents of TolNCNTol with $Ca\{Ga(NArCH)_2\}_2(THF)_4$ (**1.12**). To date, there are no precedents of structurally authenticated double insertions of carbodiimides into metal-metal bonds. Nonetheless, the formation of related bis(amidinate) or bis(guanidinate) complexes *via* double insertion of carbodiimides, particularly with calcium complexes, is not uncommon.[42-44] Complex **16** exhibits a resonance at 5.82 ppm for its vinyl protons, which shifts downfield with respect to the parent complex $Ca\{Ga(NArCH)_2\}_2(THF)_4$ (**1.12**) (5.78 ppm), in contrast to what is observed in all the ^{R}NacNac supported insertion products.

Complex **16** crystallises in the triclinic space group *P*-1 with one molecule per unit cell. The geometry around the calcium atom is octahedral with the galla-amidinates occupying the equatorial positions and the THF ligands in the axial positions. The N(3)-Ca(1)-N(4) angle (56.28(5)º is comparable to that of Ca{(N(*o*-

Tol))$_2$CH}$_2$(THF)$_2$ (average 56.35(4)º)[45] and other related calcium bisamidinate complexes.[43, 46, 47] The N(1)-Ga(1)-N(2) angle (90.90(6)º) is significantly wider than that of the parent bis(gallyl) complex **1.12** (83.68(11)º), which reflects the same widening effect of the N-Ga-N angle in **7** upon coordination of gallium to carbon to form the corresponding insertion complex.

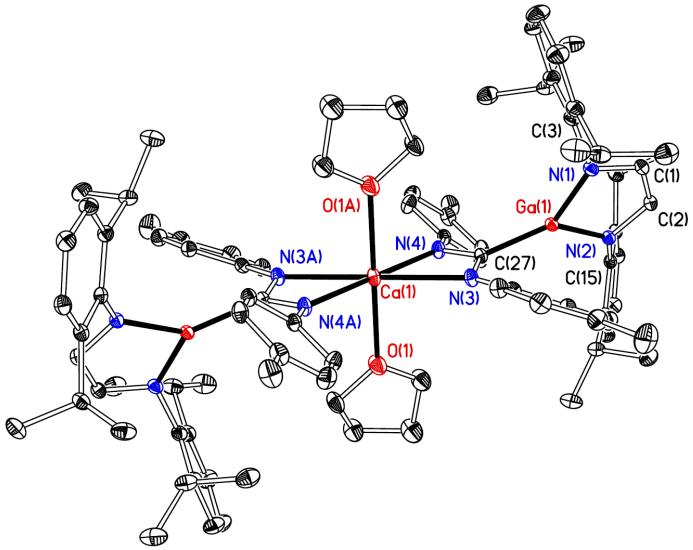

Figure 2.3. Displacement ellipsoid plot (20 % probability) of Ca{(NTol)$_2$CGa(NArCH)$_2$}$_2$(THF)$_2$ (**16**). H atoms omitted for clarity. Atoms carrying the suffix 'A' are related to their counterparts by the symmetry operator 1-x, 1-y, 1-z)

Table 2.2. Selected distances (Å) and angles (º) for Ca{(NTol)$_2$CGa(NArCH)$_2$}$_2$(THF)$_2$ (**16**).

Ca(1)-N(3)	2.3914(14)	Ga(1)-N(1)	1.8636(13)
Ca(1)-N(4)	2.3975(14)	Ga(1)-N(2)	1.8675(14)
Ca(1)-O(1)	2.3867(16)	Ga(1)-C(27)	1.9856(15)
N(3)-Ca(1)-N(4)	56.28(5)	N(4)-Ca(1)-O(1)	88.02(5)
N(3)-Ca(1)-O(1)	91.41(6)	N(1)-Ga(1)-N(2)	90.90(6)

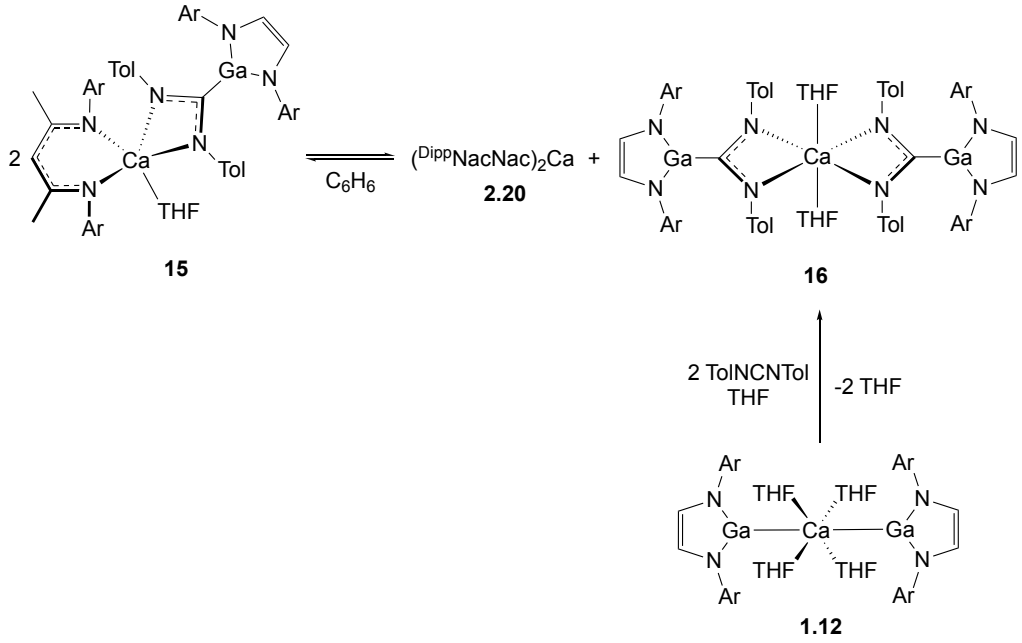

Scheme 2.7. Proposed formation of the Ca{(NTol)$_2$CGa(NArCH)$_2$}$_2$(THF)$_2$ (**16**) complex by redistribution of complex **15** and independent synthesis of species **16** by the double insertion of TolNCNTol into the Ca-Ga bonds of **1.12**. Ar = Dipp.

2.5.2 Reactions with isobutene epoxide and Me_3NO

The study of the reactivity of complex **1** was also explored with epoxides aiming to open their ring and insert them into the Ae-Ga bonds. A C_6D_6 solution of **1** was reacted with 1 equivalent of isobutene epoxide (Scheme 2.8). Surprisingly, this reaction yielded the oxygen abstraction product **17** instead of the insertion product. This is supported by the observation of free isobutene in the ^{1}H NMR of the reaction mixture and the absence of the resonances of the olefin after removal of volatiles. This same reaction was tested with the Ca-Ga complex **2** yielding the oxygen abstraction product and the release of isobutene. In both cases, there is no overall release of THF according to the ^{1}H NMR spectrum. This is consistent with **1** yielding a product that is substituting only one position in the Mg coordination sphere, as opposed to the observed release of THF in the formation of carbodiimides. It is also noteworthy that the resonance for the vinyl proton considerably shifts upfield to 6.03 ppm in **17** and 6.04 ppm in **18**. The shifts to higher field with respect to the parent complexes (**1**: 6.45 ppm, **2**: 6.45 ppm) have been observed in the insertion complexes **7**-**15**. In those cases, the resonance of the vinyl proton is in the range 6.12-6.33 ppm for the ^{Dipp}NacNac supported species. The even more shifted resonance of the oxygen abstraction products **17** and **18** is in agreement with the coordination of a more

electronegative atom to gallium (*cf.* 5.73 ppm for the vinyl resonance in [K(μ-O){Ga(NArCH)$_2$}(TMEDA)]$_2$).[48] The synthesis of complex **18** was scaled up and the product could be isolated in good yield (64%). The elemental analysis of **18** is consistent with its formulation.

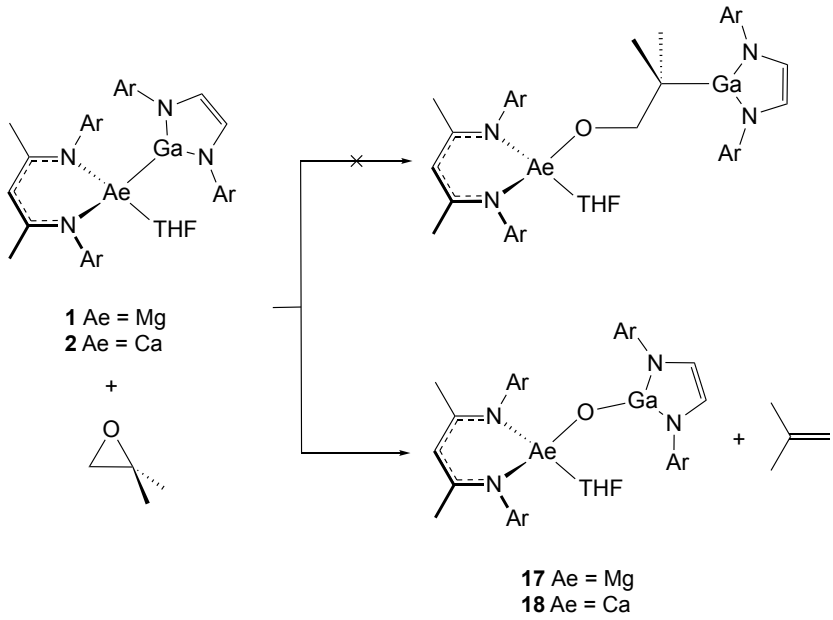

Scheme 2.8. Reactions of Mg(^{Dipp}NacNac){Ga(NArCH)$_2$}(THF) (**1**) and Ca(^{Dipp}NacNac){Ga(NArCH)$_2$}(THF) (**2**) with isobutene epoxide in C_6D_6. Ar = Dipp.

To gain further insight into the identity of **17** and **18**, their alternative syntheses by means of reactions of the Ae-Ga complexes **1** and **2** with oxygen donors other than epoxides was envisaged. When Me_3NO is added to C_6D_6 solutions of **1** and **2**, the species **17** and **18** are formed correspondingly and free Me_3N is observed as a by-product in the ^{1}H NMR spectra. The use of pyridine *N*-oxide or triphenyl phosphine oxide as oxygen donors gave **17** and **18** only in very small quantities (<1 %) within complex mixtures. Additionally, a series of reactions with **18** in the NMR tube scale aiming to identify and isolate species containing a OGa(NArCH)$_2$ fragment were attempted. The use of trimethylsilyl iodide forms [(^{Dipp}NacNac)CaI(THF)]$_2$ (**2.32**,[34] Equation 2.10). However, the fate of the gallyl fragment could not be determined since the characteristic resonance for the vinyl proton of the OGa(NArCH)$_2$ fragment disappears and several trimethylsilyl resonances appear in the 0.00-0.50 ppm region, suggesting multiple reaction pathways.

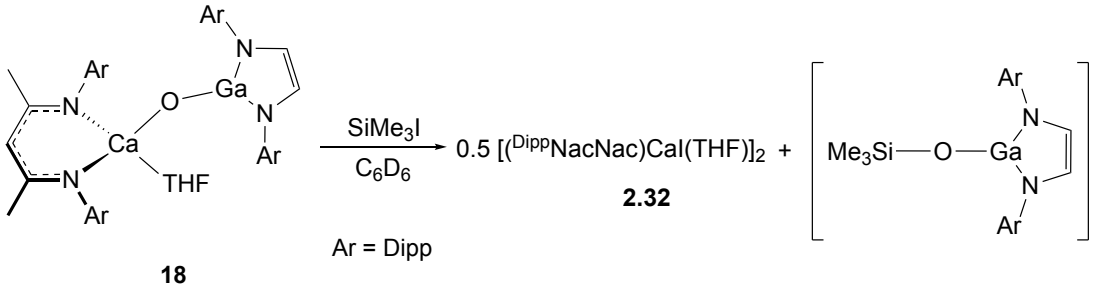

Equation 2.10

There are no known oxygen abstraction reactions by complexes containing unsupported metal-metal bonds. This reactivity is rare even within related metal-metal bonded species as the complete incorporation of the epoxide to the complex is more common[49, 50] and the formation of oxo-bridged species is preferably accessed with the use of other oxidants, e.g., O_2,[51, 52] P_2O_5,[53] or N_2O.[54] The closest approach to the oxygen transfer to a metal-metal bond has been reported by Baranger and co-workers.[55] In this study, the authors reported the atom transfer reactions between a bridged Zr-Ir complex and thiiranes and epoxides. When styrene epoxide was added to the Zr-Ir complex, the reaction led to the oxygen abstraction product $Cp_2Zr(\mu\text{-}^tBuN)(\mu\text{-}O)IrCp^*$ **2.38** along with the release of styrene and $Cp^*Ir N^tBu$ as by-products (Equation 2.11). Attempts to form **2.38** were also possible with the use of pyridine *N*-oxide and N_2O as oxygen donors

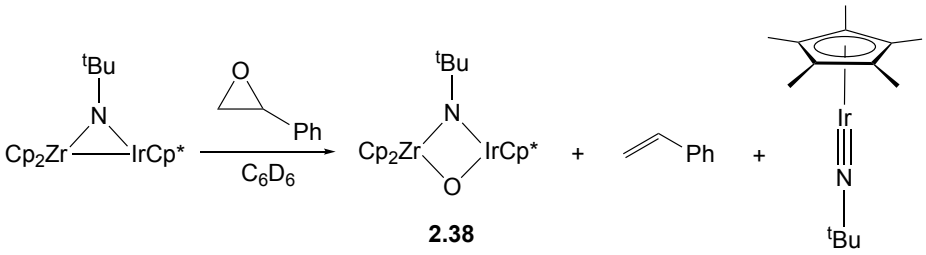

Equation 2.11.[55]

2.5.3 Reactions with alkyl iodides

Following previous reports on the cleavage of polarised metal-metal bonds by reaction with alkyl iodides,[20] the reactions of complexes **1** and **2** were studied with MeI. The addition of 1 equivalent of MeI to these complexes yielded complex mixtures where the corresponding alkaline earth iodide complexes, **2.31** and **2.32**, and the digallane(4) **1.68** could be identified (Scheme 2.9). However, the number of products in the mixture impeded the identification of the expected complex $MeGa(NArCH)_2$.

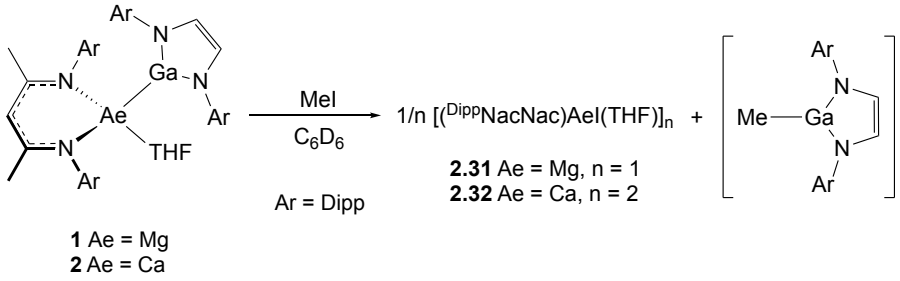

Scheme 2.9. Reactions of alkaline earth gallyl complexes **1** and **2** with MeI.

The use of Me_3SiI with Mg(^{Dipp}NacNac){Ga(NArCH)$_2$}(THF) (**1**) also gave a complex mixture containing **2.31** and **1.68**. However, a product with a vinyl resonance at 6.33 ppm could be identified. The amount of such gallyl containing product $(Me_3Si)Ga(NArCH)_2$ (**19**) is 45% with respect to **2.31**. Additionally, the reaction of Me_3SiI with the base free potassium gallyl K[Ga(NArCH)$_2$] (**20**) on the NMR tube scale selectively yields **19** allowing its identification in the reaction of Me_3SiI with **1**. Following these results, the synthesis of **19** was successfully scaled up in 84% yield (Scheme 2.10). As mentioned, complex **19** exhibits a resonance for its vinyl proton at 6.33 ppm which as expected is upfield with respect to the same resonance in **1**.

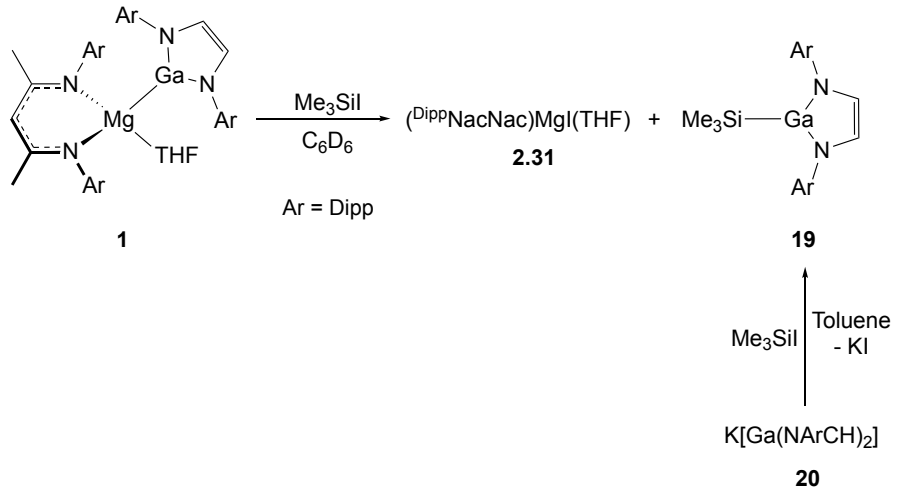

Scheme 2.10. Reaction of the magnesium gallyl complex **1** with Me_3SiI and independent synthesis of $(Me_3Si)Ga(NArCH)_2$ **(19)**.

Crystals of **19** suitable for X-ray diffraction were grown from a saturated benzene solution. The solid state structure confirms the identity this complex (Figure 2.4). Table 2.3 presents selected distances and angles for **19**. The Ga(1)-Si(1) bond length of **19** (2.3640(4) Å) is longer than the sum of the respective covalent radii (2.33(4)

Å)[11] yet shorter than those of the related complex {K(Et$_2$O)}Si{Ga(NArCH)$_2$}$_2$(NArSiMe$_3$) (**2.39**) (2.438(1) Å and 2.452(1) Å)[56] which is the only reported structure with a "Si-Ga(NArCH)$_2$" moiety. Moreover, the Ga(1)-Si(1) bond distance is comparable to that of Si(SiMe$_3$)$_3$GaCl$_2$(THF) (2.362(1) Å) which possesses one of the shortest Si-Ga bonds. Expectedly, the N(1)-Ga(1)-N(2) angle (88.47(4)) is wider than that of Mg(^{Dipp}NacNac){Ga(NArCH)$_2$}(TMEDA) (**2.19**) (85.55(6)º).[14]

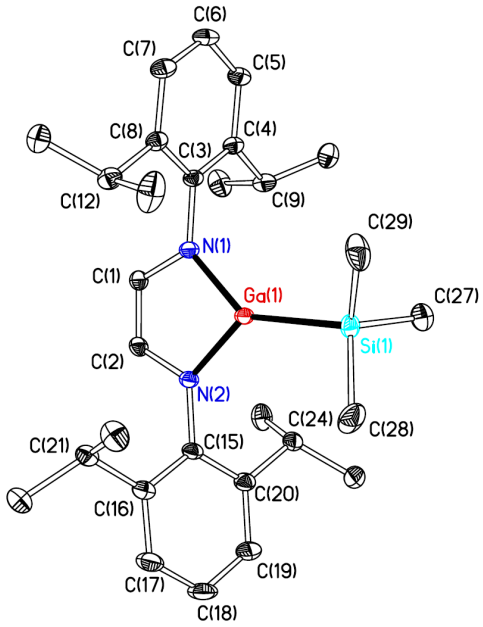

Figure 2.4. Displacement ellipsoid plot (20% probability) of (Me$_3$Si)Ga(NArCH)$_2$ (**19**). H atoms omitted for clarity.

Table 2.3. Selected distances (Å) and angles (°) for (Me$_3$Si)Ga(NArCH)$_2$ (**19**).

Si(1)-C(27)	1.8624(15)	Ga(1)-Si(1)	2.3640(4)
Si(1)-C(28)	1.8708(17)	Ga(1)-N(1)	1.8501(10)
Si(1)-C(29)	1.8689(17)	Ga(1)-N(2)	1.8559(10)
Ga(1)-Si(1)-C(27)	109.28(5)	Ga(1)-Si(1)-C(29)	110.62(8)
Ga(1)-Si(1)-C(28)	107.02(6)	N(1)-Ga(1)-N(2)	88.47(4)

2.6 Summary and conclusions

In this chapter, the synthesis of a new series of alkaline earth gallyl complexes was presented. The stability of the magnesium gallyl complex and the optimisation of the synthesis conditions of the calcium gallyl complex allowed their isolation as opposed to the strontium gallyl complex which was characterised in solution. Steric modifications to the N-aryl of the (^{R}NacNac)Mg{Ga(NArCH)$_2$}(THF) complexes suggests that the reduction of the steric demand is prejudicial to the stability of these complexes. In addition to the synthesis, the reactivity of alkaline earth gallyl complexes was tested for the first time. The reactions of these complexes with carbodiimides lead to insertion products. These reactions proved successful in a wide scope of substituents in either the carbodiimides or the magnesium gallyl complexes. The first structurally authenticated net insertion into a Ae-Ga bond was performed with ^{i}PrNCN^{i}Pr and either (^{Dipp}NacNac)Mg{Ga(NArCH)$_2$}(THF) (**1**) or (^{Dipp}NacNac)Mg{Ga(NArCH)$_2$}(TMEDA) (**2.19**). The formation of **1** from the structurally authenticated **2.19** and the identical reactivity of **1** and **2.19** with carbodiimides, suggests their structural similarities. The stability of the Ae-Ga complexes and their insertion products decreases with the group. This could be inferred from the increased sensitivity of the calcium and strontium gallyl complexes or the redistribution of Ca(^{Dipp}NacNac){(NTol)$_2$Ga(NArCH)$_2$} in solution, which lead to the isolation of a bisgalla-amidinate complex Ca{(NTol)$_2$CGa(NArCH)$_2$}$_2$(THF)$_2$ (**16**). The independent synthesis of **16** represents the first structurally authenticated net insertion of carbodiimides into two metal-metal bonds. The reactions of the magnesium and calcium gallyl complexes with isobutene epoxide yielded the rather rare oxygen abstraction products. On the other hand, the reactions of the Mg and Ca gallyl species with MeI yields the expected formation of the alkaline earth iodide complexes although the fate of the gallyl fragment could not be determined. In contrast, the reaction of complex **1** with Me$_3$SiI allows the identification of the gallyl containing product, (Me$_3$Si)Ga(NArCH)$_2$, which was both independently synthesised and structurally authenticated.

2.7 References

1. C. Chen, S. M. Bellows and P. L. Holland, *Dalton Trans.*, 2015, **44**, 16654.
2. R. L. Webster, *Dalton Trans.*, 2017, **46**, 4483.
3. D. Zhu and P. H. M. Budzelaar, *Dalton Trans.*, 2013, **42**, 11343.

4. P. G. Hayes, W. E. Piers, L. W. M. Lee, L. K. Knight, M. Parvez, M. R. J. Elsegood and W. Clegg, *Organometallics*, 2001, **20**, 2533.
5. K.-C. Chang, C.-F. Lu, P.-Y. Wang, D.-Y. Lu, H.-Z. Chen, T.-S. Kuo and Y.-C. Tsai, *Dalton Trans.*, 2011, **40**, 2324.
6. K. C. MacLeod, B. O. Patrick and K. M. Smith, *Inorg. Chem.*, 2012, **51**, 688.
7. L. M. R. Hill, B. F. Gherman, N. W. Aboelella, C. J. Cramer and W. B. Tolman, *Dalton Trans.*, 2006, 4944.
8. D. F. Schreiber, Y. Ortin, H. Müller-Bunz and A. D. Phillips, *Organometallics*, 2011, **30**, 5381.
9. W. Zhou, L. Tang, B. O. Patrick and K. M. Smith, *Organometallics*, 2011, **30**, 603.
10. C. Jones, D. P. Mills, J. A. Platts and R. P. Rose, *Inorg. Chem.*, 2006, **45**, 3146.
11. B. Cordero, V. Gomez, A. E. Platero-Prats, M. Reves, J. Echeverria, E. Cremades, F. Barragan and S. Alvarez, *Dalton Trans.*, 2008, 2832.
12. M. Wiecko, P. W. Roesky, P. Nava, R. Ahlrichs and S. N. Konchenko, *Chem.Commun.*, 2007, 927.
13. I. L. Fedushkin, A. N. Lukoyanov, A. N. Tishkina, G. K. Fukin, K. A. Lyssenko and M. Hummert, *Chem. Eur. J.*, 2010, **16**, 7563.
14. O. Bonello, C. Jones, A. Stasch and W. D. Woodul, *Organometallics*, 2010, **29**, 4914.
15. S. P. Green, C. Jones and A. Stasch, *Science*, 2007, **318**, 1754.
16. C. Jones, L. McDyre, D. M. Murphy and A. Stasch, *Chem. Commun.*, 2010, **46**, 1511.
17. A. J. Boutland, A. Carroll, C. Alvarez Lamsfus, A. Stasch, L. Maron and C. Jones, *J. Am. Chem. Soc.*, 2017, **139**, 18190.
18. M. Ma, A. Stasch and C. Jones, *Chem. Eur. J.*, 2012, **18**, 10669.
19. S. J. Bonyhady, C. Jones, S. Nembenna, A. Stasch, A. J. Edwards and G. J. McIntyre, *Chem. Eur. J.*, 2010, **16**, 938.
20. M. P. Blake, N. Kaltsoyannis and P. Mountford, *Chem. Commun.*, 2013, **49**, 3315.
21. L. M. A. Saleh, D. Phil Thesis, University of Oxford, 2014.
22. C. Jones, D. P. Mills, R. P. Rose and A. Stasch, *Dalton Trans.*, 2008, 4395.

23. C. Jones, D. P. Mills, R. P. Rose, A. Stasch and W. D. Woodul, *J. Organomet. Chem.*, 2010, **695**, 2410.
24. Y. Xiong, S. Yao, M. Karni, A. Kostenko, A. Burchert, Y. Apeloig and M. Driess, *Chem. Sci.*, 2016, **7**, 5462.
25. S. P. Green, C. Jones, K. A. Lippert, D. P. Mills and A. Stasch, *Inorg. Chem.*, 2006, **45**, 7242.
26. A. V. Protchenko, D. Dange, A. D. Schwarz, C. Y. Tang, N. Phillips, P. Mountford, C. Jones and S. Aldridge, *Chem. Commun.*, 2014, **50**, 3841.
27. T. Alonso, S. Harvey, P. C. Junk, C. L. Raston, B. Skelton and A. H. White, *Organometallics*, 1987, **6**, 2110.
28. C. Loh, C. Glock, S. Ziemann, H. Görls, S. Krieck and M. Westerhausen, *Z. Naturforsch., B: J. Chem. Sci.*, 2013, **68**, 518.
29. D. B. Collum, *Acc. Chem. Res.*, 1992, **25**, 448.
30. P. B. Hitchcock, T. H. Lee and G. J. Leigh, *Inorg. Chim. Acta*, 2003, **349**, 159.
31. M. R. Crimmin, M. Arrowsmith, A. G. M. Barrett, I. J. Casely, M. S. Hill and P. A. Procopiou, *J. Am. Chem. Soc.*, 2009, **131**, 9670.
32. J. S. Wixey and B. D. Ward, *Dalton Trans.*, 2011, **40**, 7693.
33. B. Sedai, M. J. Heeg and C. H. Winter, *Organometallics*, 2009, **28**, 1032.
34. S. Harder, *Organometallics*, 2002, **21**, 3782.
35. S. J. Bonyhady, C. Jones, S. Nembenna, A. Stasch, A. J. Edwards and G. J. McIntyre, *Chem. Eur. J.*, 2010, **16**, 938.
36. R. J. Baker, C. Jones, M. Kloth and J. A. Platts, *Organometallics*, 2004, **23**, 4811.
37. J. Hicks, C. E. Hoyer, B. Moubaraki, G. Li Manni, E. Carter, D. M. Murphy, K. S. Murray, L. Gagliardi and C. Jones, *J. Am. Chem. Soc.*, 2014, **136**, 5283.
38. H. A. Bent, *Chem. Rev.*, 1961, **61**, 275.
39. T. Pott, P. Jutzi, B. Neumann and H.-G. Stammler, *Organometallics*, 2001, **20**, 1965.
40. Y. Zhao, Y. Liu, Q.-S. Li and J.-H. Su, *Dalton Trans.*, 2016, **45**, 246.
41. R. J. Baker, R. D. Farley, C. Jones, M. Kloth and D. M. Murphy, *J. Chem. Soc., Dalton Trans.*, 2002, 3844.
42. J. R. Lachs, A. G. M. Barrett, M. R. Crimmin, G. Kociok‐Köhn, M. S. Hill, M. F. Mahon and P. A. Procopiou, *Eur. J. Inorg. Chem.*, 2008, **2008**, 4173.

43. Tareq M. A. Al–Shboul, G. Volland, H. Görls and M. Westerhausen, *Z. Anorg. Allg. Chem.*, 2009, **635**, 1568.
44. F. Feil and S. Harder, *Eur. J. Inorg. Chem.*, 2005, **2005**, 4438.
45. M. L. Cole, G. B. Deacon, C. M. Forsyth, K. Konstas and P. C. Junk, *Dalton Trans.*, 2006, 3360.
46. A. G. M. Barrett, M. R. Crimmin, M. S. Hill, P. B. Hitchcock, S. L. Lomas, M. F. Mahon and P. A. Procopiou, *Dalton Trans.*, 2010, **39**, 7393.
47. W. S. M.Westerhausen, *Z. Naturforsch., B: J. Chem. Sci.*, 1992, **47b**, 453.
48. R. J. Baker, C. Jones and M. Kloth, *Dalton Trans.*, 2005, 2106.
49. A. Sisak and E. Halmos, *J. Organomet. Chem.*, 2007, **692**, 1817.
50. E. Simón‐Manso and C. P. Kubiak, *Angew. Chem. Int. Ed.*, 2005, **44**, 1125.
51. Z. Padelkova, P. Svec, V. Pejchal and A. Ruzicka, *Dalton Trans.*, 2013, **42**, 7660.
52. C. L. Gross, J. L. Brumaghim and G. S. Girolami, *Organometallics*, 2007, **26**, 2258.
53. H. Braunschweig, R. Dörfler, J. Mies, K. Radacki and M. Schmitt, *J. Organomet. Chem.*, 2012, **699**, 26.
54. A. F. R. Kilpatrick, J. C. Green and F. G. N. Cloke, *Organometallics*, 2015, **34**, 4816.
55. A. M. Baranger, T. A. Hanna and R. G. Bergman, *J. Am. Chem. Soc.*, 1995, **117**, 10041.
56. A. V. Protchenko, A. D. Schwarz, M. P. Blake, C. Jones, N. Kaltsoyannis, P. Mountford and S. Aldridge, *Angew. Chem. Int. Ed.*, 2013, **52**, 568.

Chapter Three

Synthesis and reactivity of carbazolide supported alkaline earth gallyl compounds

3.1 Overview

In this chapter, the synthesis of alkaline earth gallyl complexes supported by a bulky tridentate carbazolide ligand is presented. This carbazolide ligand was used with the objective of increasing the stability of the Ae-Ga complexes. The reactivity of these complexes with carbodiimides, styrene oxide and alkyl iodides was explored and compared with that of the ^{R}NacNac supported complexes presented in the previous chapter. Moreover, the reactivity with bulkier epoxides, isocyanates, azides and Fp containing species was also examined and these results are correspondingly discussed. The relevant examples of the use of carbazolides and related ligands along with the initial attempts to stabilise Ae-Ga complexes is also presented.

3.2 Introduction

3.2.1 Carbazolide supported metal compounds

The use of carbazolides as ligands has been developed in the last decade due to their capability to sterically stabilise complexes along with their electronic properties and the possibility to tune their chirality effects. In this context, the initial development of carbazole bis(oxazoline) ligands by Inoue and Nakada[1, 2] has found multiple applications in asymmetric catalysis. This has been possible due to the relative ease of tuning its chirality by changing the substituents in the oxazoline fragments (R^2 and R^3 in Figure 3.1) along with the facile preparation by condensation between carbazole derivatives and amino alcohols. Moreover, when coordinated to metals the C-N bond in the oxazoline fragment is less prone to attack by nucleophiles.

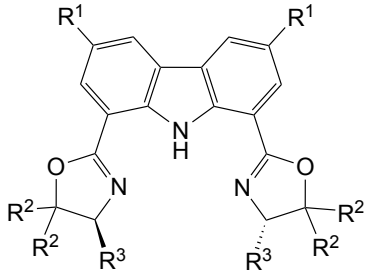

3.1 R^1 = Ph, R^2 = Me, R^3 = H
3.2 R^1 = Ph, R^2 = ^{i}Pr, R^3 = H
3.3 R^1 = Ph, R^2 = Me, R^3 = Me
3.4 R^1 = Cl, R^2 = ^{i}Pr, R^3 = H

Figure 3.1. Structure of the carbazolides synthesised by Inoue and Nakada.[1, 2]

Further applications of these ligands have included mimicking the properties of other systems. For example, the formation of iron complexes supported by a carbazolide

ligand has been envisaged as a way to emulate the properties of iron heme complexes without the difficulties entailed in the preparation of porphyrins.[3] Despite being tridentate, carbazole bis(oxazoline) ligands are planar and exhibit long π-conjugation like porphyrins. These non-heme iron complexes were prepared by reaction between $FeCl_2 \cdot H_2O$ and the *in situ* deprotonated carbazolides (Equation 3.1). The products of this reaction were iron(III) complexes and the authors adduce the oxidation of iron by oxygen during synthesis or work up.[3] When used in catalytic amounts, complex **3.5** affords the epoxidation of *trans*-stilbene in moderate to high enantioselectivities akin to metalloporphyrins.

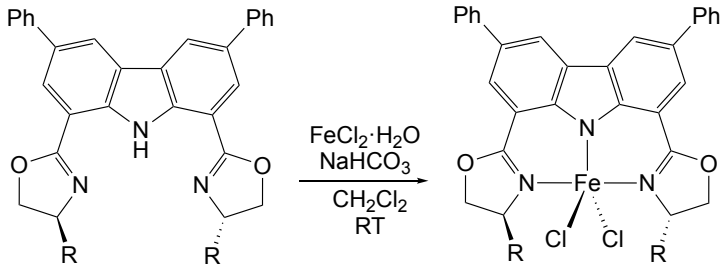

Equation 3.1[3]

Modifications in the carbazole and oxazoline fragments by Zou and co-workers generated the carbazolide H-CzOx (**3.7**, Scheme 3.1) which allows the stabilisation of lanthanide chlorido complexes without formation of homoleptic species (**3.8**-**3.10**, Scheme 3.1).[4] The $Ln(CzOx)Cl_2(THF)$ complexes can be further alkylated by reacting them with $LiCH_2SiMe_3$ to form the dialkyl complexes **3.11**-**3.13**. Alternatively, **3.11**-**3.13** could be formed directly from **3.7** and the corresponding $Ln(CH_2SiMe_3)_3(THF)_2$ species, although this route was low yielding as the ionic radius of the lanthanides increased. As expected, the dichlorido complexes are octahedral and the dialkyl complexes are trigonal bipyramidal in the solid state. In the $Ln(CzOx)Cl_2(THF)$ complexes, the Ln-Cl distance of the bond *trans* to the nitrogen of the carbazole fragment is longer than that of the Ln-Cl *trans* to the THF. The authors adduce this lengthening to an electronic cause, presumably a *trans* influence. The reactivity of complexes **3.11**-**3.13** was further tested in the polymerisation of alkenes although this resulted in no activity by these complexes. A further report established the use of **3.7** in the formation of a series of Yb(II) complexes as a way to illustrate the versatility of **3.7** to stabilise complexes in different oxidation states.[5]

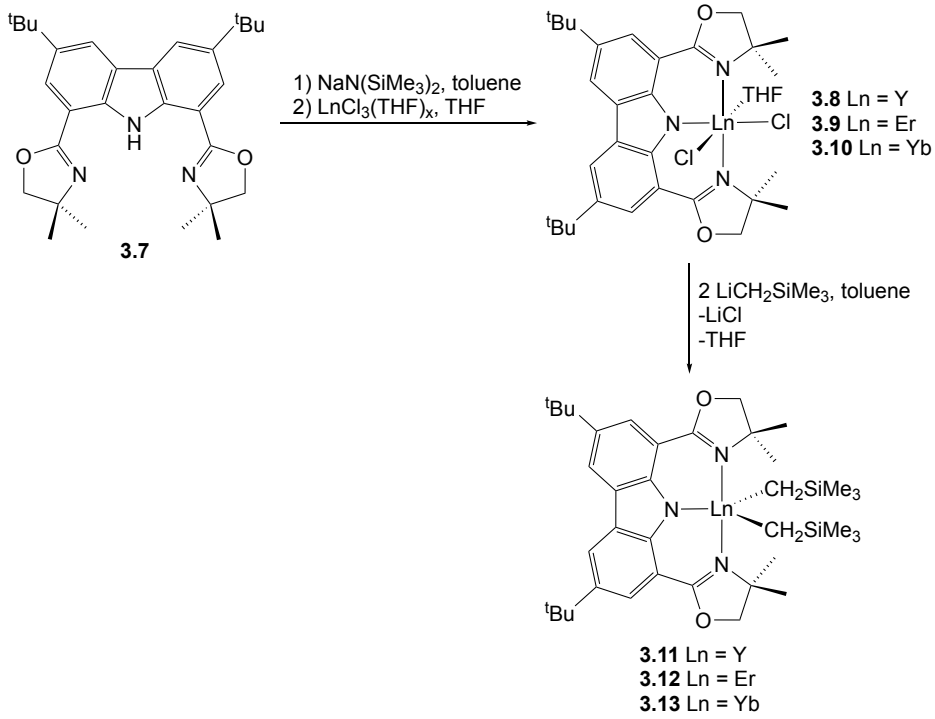

Scheme 3.1. Formation of bis(oxazoline) carbazolide supported lanthanide complexes.[4]

More recently, Core and Mountford expanded the use of the carbazolide **3.7** to group 2 and rare earth metals aiming to further use them as catalysts for the ring opening polymerisation of lactides.[6] The formation of a magnesium complex Mg(CzOx)I(THF) (**3.14**) proceeded through direct reaction of **3.7** and the corresponding Grignard reagent in Et_2O followed by dissolution of the obtained mixture in THF (Scheme 3.2). The calcium analogue Ca(CzOx)I(THF)$_2$ (**3.16**) was formed *via* the salt elimination between the potassium salt of **3.14**, K(CzOx) (**3.15**), and CaI_2 in THF. According to ^{1}H NMR and X-ray analyses, the magnesium complex **3.14** coordinates one THF molecule whilst the calcium analogue **3.16** contains two THF molecules due to the larger atomic radius of Ca. The versatility of the carbazolide ligand allowed the formation of a wide range of complexes with anionic ligands other than iodides as well as imposition of chirality by steric tuning of the substituents of the carbon α to the nitrogen in the oxazoline.

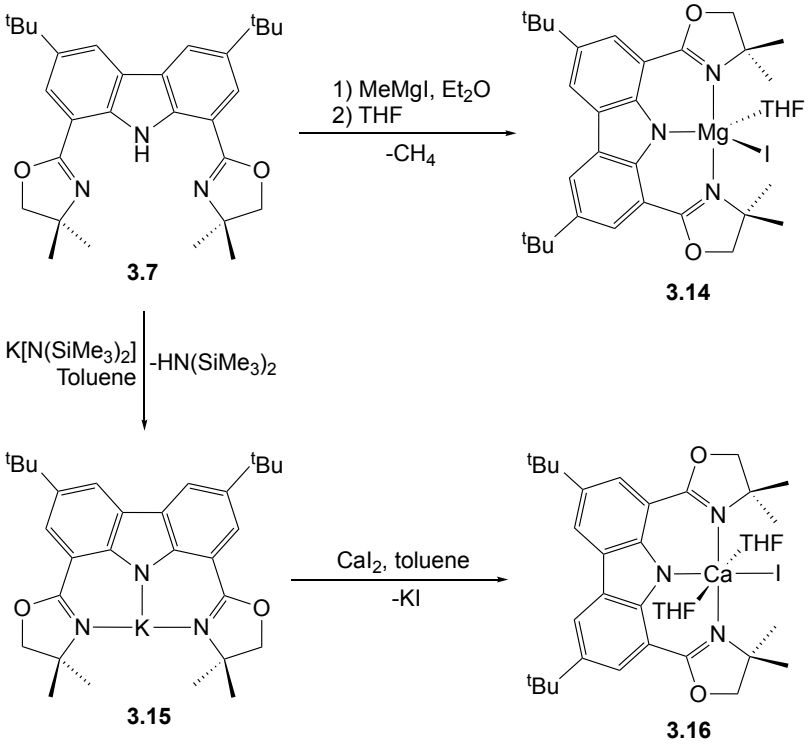

Scheme 3.2. Formation of group 2 iodide complexes stabilised by bis(oxazoline) carbazolides.[6]

The installation of phosphines on the arms of carbazolide by Grüger *et al.* has allowed the access to the PNP donor **3.17** of Scheme 3.3 and its use in the stabilisation of transiton metal complexes.[7] As presented in Scheme 3.3, reaction of the PNP ligand with Ir(acac)(COD) yields an Ir(I) complex. In this case, the acac serves as internal base to deprotonate the PNP ligand *in situ.* The formed complex **3.18** is also stabilised by COD which along with the carbazolide results in a trigonal bipyramidal complex. Interestingly, the PNP ligand coordinates to Ir in a facial fashion instead of the expected meridional occupancy. The hydrogenation of **3.18** by H_2 at 70 ºC yields the dihydride complex **3.19**. Similarly to **3.18**, the dihydride complex presents a trigonal bipyramidal geometry in the solid state, however, the PNP carbazolide here coordinates to the metal in a meridional fashion. Treatment of **3.18** with an excess of diphenylacetylene allows the transfer of hydrogen from the complex to the alkyne to release *trans*-stilbene and to form the η^2-diphenylacetylene adduct (**3.20**). Additionally, the hydrogenation proceeds catalytically in an excess of H_2 and diphenylacetylene. The high reactivity of **3.19** also permits the C-H bond activation in C_6H_6 and THF and the activation of the C-Cl bond of chlorobenzene. Other systems

similar to **3.17** in iron complexes have been successfully applied in the hydrogenation of alkenes[8] or the fixation of dinitrogen.[9]

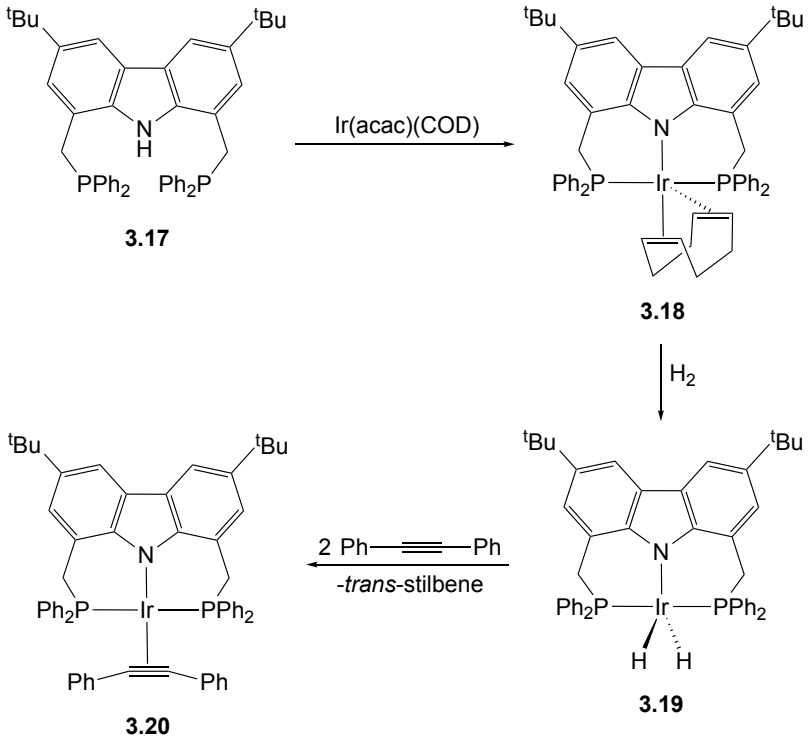

Scheme 3.3. Synthesis and reactivity of an iridium(I) complex stabilised by a PNP carbazolide ligand.[7]

Despite their proved usefulness, the benefits of the use of carbazolide ligands have not been exploited in the stabilisation of metal-metal bonded species. Relatedly, one of the few reports on the use of carbazolyls as supporting ligands was made by Mansaray *et al.* in 2011.[10] Lithiation of 3,6-di-*tert*-butylcarbazole (HCz) followed by addition of InCl to the reaction mixture yields the tetranuclear $In_2\{In_2(Cz)_6\}$ complex (**3.21**, Equation 3.2). The mixed valence In^{I}/In^{II} complex **3.21** exhibits an In-In bond length of 2.759(1) Å which is shorter than two In covalent radii (2.84(7) Å)[11] and comparable to other In-In bonded complexes. When the more sterically demanding 1,3,6,8-tetra-*tert*-butylcarbazole is used, the presence of the *tert*-butyl fragments in the vicinity of the nitrogen atom of the carbazolyl prevents the formation the In-In bonded complex and a polymeric complex bridged by In···arene interactions is obtained instead.[10]

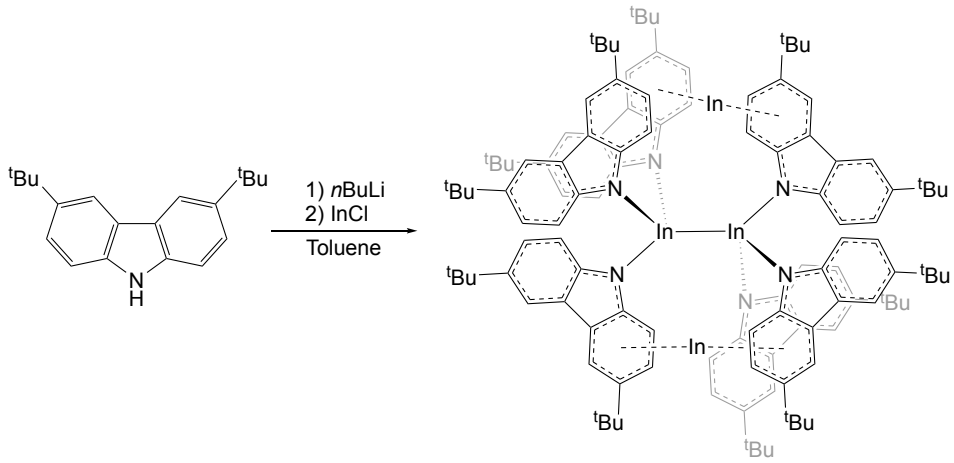

3.21

Equation 3.2[10]

The closest approach to a carbazolide assisted metal-metal bonded complex involved the reduction of a CNC pincer Pd(II) complex with KC_8 (Scheme 3.4).[12] In the solid state, the Pd(0) complex **3.22** exhibits a dimeric structure with two Pd-K contacts of lengths 3.2376(5) Å and 3.6166(5) Å, the former contact being shorter than the sum of the covalent radii of Pd and K (3.42(13) Å).[11] Unexpectedly, the ^{1}H NMR spectrum of **3.22** shows only one set of signals despite the asymmetrical coordination environment at the potassium atom in the solid state structure. Diffusion Ordered Spectroscopy (DOSY) analysis suggested that the dimeric structure dissociates after redissolving crystals of **3.22** in THF. The use of the less reactive lithium graphite as reducing agent or the reduction of the reaction time allows the observation in solution of a Pd(I)-Pd(I) complex (**3.23**, Scheme 3.4). The structure of **3.23** was proposed from the analysis of its ^{1}H and ^{13}C NMR spectra and the comparison of these with related Pd(I)-Pd(I) complexes.

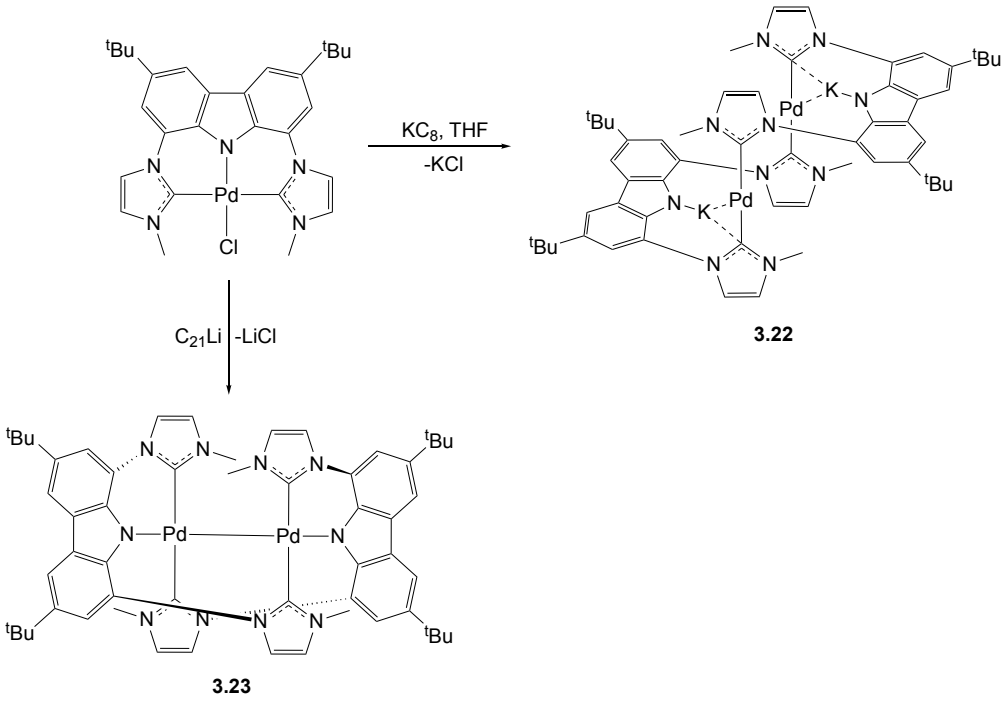

Scheme 3.4. Reagent controlled reactivity of a CNC pincer Pd(II) complex.[12]

3.3 Synthesis of Ae(CzOx){Ga(NArCH)$_2$}(THF)$_x$ complexes

The study of the synthesis and reactivity of Ae(NacNac){Ga(NArCH)$_2$(THF) complexes presented in Chapter 2, showed that generally these complexes are sufficiently stable in solution to allow their characterisation, nonetheless, leaving solutions of these complexes overnight or the exposure to prolonged vacuum resulted in the formation of disproportionation species such as homoleptic complexes of the type Ae(NacNac)$_2$ and the digallane(4) [Ga(NArCH)$_2$]$_2$ (**1.68**) presumably due to loss of THF. In order to increase the stability of the Ae{Ga(NArCH)$_2$} core the use of the bulky tri-dentate HCzOx (**3.7**) was envisaged as a supporting ligand for the alkaline earth metals in these species using complexes Mg(CzOx)I(THF) (**3.14**) and Ca(CzOx)I(THF)$_2$ (**3.14**) as the source of the alkaline earth metals.

Based on the previous work on the synthesis of alkaline earth metal complexes supported by the carbazolide CzOx[6] and in order to enhance the solubility of the Mg(CzOx)I(THF) (**3.14**) complex, THF was chosen as solvent. Addition of a THF solution of 0.5 eq. of [KGa(NArCH)$_2$(Et$_2$O)]$_2$ (**1.44**) to a solution of 1 eq. of Mg(CzOx)I(THF) (**3.14**) formed a clear orange solution which was left to react for 1 h. After work up in a similar way to the ^{R}NacNac supported analogues, the ^{1}H NMR of the resulting solid in THF-d_8 showed a mixture of products from which

$[Ga(NArCH)_2]_2$ (**1.68**) could be identified. Additionally, the ^1H NMR of this mixture revealed the absence of protio THF. Attempts to optimise the synthesis by cooling the initial solutions to -78 ºC followed by reaction for 1 h and work up or using coordinating co-solvents including HMPA, DME and pyridine did not offer any improvement in the selectivity of this reaction. Interestingly, analysis of the NMR tube-scale reaction between $[KGa(NArCH)_2(Et_2O)]_2$ (**1.44**) and Mg(CzOx)I(THF) (**3.14**) in THF-d_8 allowed the observation of only one set of signals for what seemed to be the desired Mg-Ga complex and the absence of $[Ga(NArCH)_2]_2$ (**1.68**). The gallyl resonance of the Mg-Ga complex appears at 5.88 ppm and remains the same after the addition of 1 eq. of the aforementioned co-solvents. Decomposition of the mixture is observed only after removal of volatiles and redissolution in THF-d_8. On the other hand, dissolving samples of either $Mg(^{Dipp}NacNac)\{Ga(NArCH)_2\}(THF)$ (**1**) or $[KGa(NArCH)_2(Et_2O)]_2$ (**1.44**) in THF-d_8 also showed a gallyl resonance at 5.88 ppm in both cases thus suggesting complete dissociation of the metal gallyl species in THF solutions. The prejudicial effect of THF as solvent has been previously observed in the synthesis of the $Ln\{Me_3SiCH_2C(NCy)_2\}_2\{Ga(NArCH)_2\}(THF)$ complexes described in Chapter 2[13] and the origin of such influence could be derived from the dissociation of the [M]-$Ga(NArCH)_2$ species in that solvent and the lack of stabilisation of these ions and the formation of homobimetallic species, *e.g.,* $[Ga(NArCH)_2]_2$ (**1.68**), once the solvent is removed.

Following this result, the NMR tube-scale reaction between $[KGa(NArCH)_2(Et_2O)]_2$ (**1.44**) and Mg(CzOx)I(THF) (**3.14**) was repeated, but this time in C_6D_6 which showed the clean formation of the complex $Mg(CzOx)\{Ga(NArCH)_2\}$ (**21**). The vinyl resonance for the gallyl fragment shifts downfield from 6.48 ppm in **1.44** to 6.50 ppm in **21**. Notably, THF is released in the formation of **21** since is observed as free in the ^1H NMR of the reaction mixture. This is presumably due to the steric hindrance around the Mg centre. The coordination of the $Ga(NArCH)_2$ to Mg also has an effect in the resonances of the methyl protons of the oxazoline fragment which change from a singlet in **3.14** to two singlets in **21**. Upon removal of volatiles, the resonances for THF disappear and the signals for the product remain unchanged. The synthesis of **21** was successfully scaled up in toluene in 77% yield (Equation 3.3).

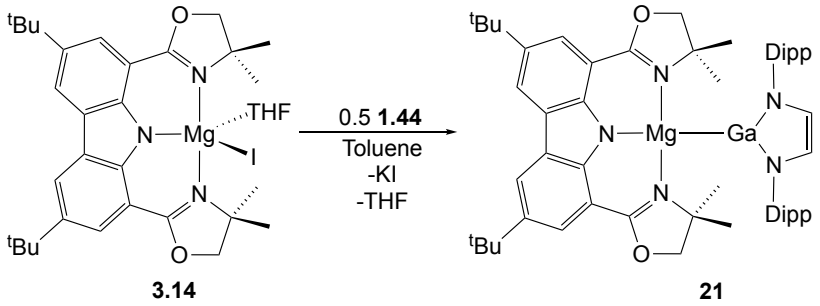

Equation 3.3

The Mg(CzOx){Ga(NArCH)$_2$ (**21**) complex appeared to be more stable than the ^{Dipp}NacNac supported analogue complex Mg(^{Dipp}NacNac){Ga(NArCH)$_2$(THF) (**1**) as solutions of **21** left overnight formed the redistribution product [Ga(NArCH)$_2$]$_2$ (**1.68**) in quantities of less than 5% with respect to **21** and after heating these samples at 80 ºC for a 2 h the amount of **1.68** did not increase considerably.

Complex **21** is sparingly soluble in benzene and attempts to grow single crystals of this compound were unsuccessful as a microcrystalline powder was formed with every attempt. However, the THF adduct (**21-THF**) could be obtained by slow evaporation of a concentrated 90:10 toluene/THF solution at RT. The molecular structure and selected distances and angles for **21-THF** are shown in Figure 3.2 and Table 3.1.

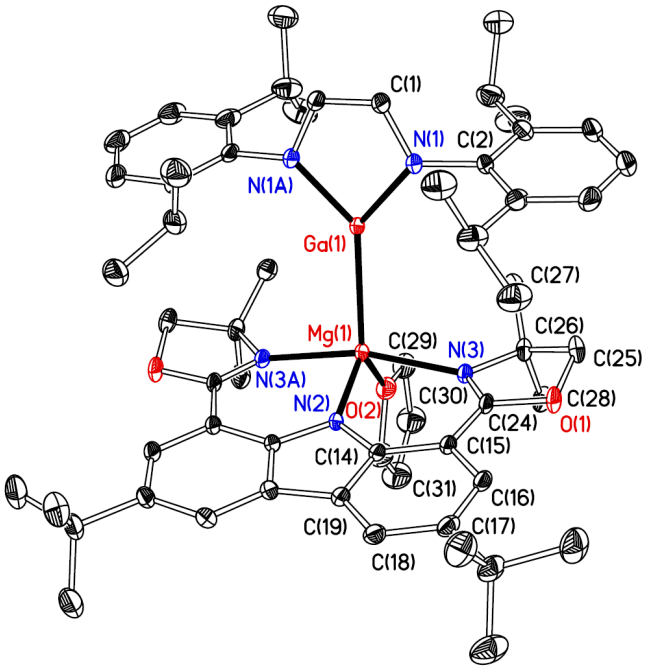

Figure 3.2. Displacement ellipsoid plot (20 % probability) of Mg(CzOx){Ga(NArCH)$_2$}(THF) (**21-THF**). Atoms carrying the suffix 'A' are related to their counterparts by the symmetry operator x, 3/2-y, z. H atoms omitted for clarity.

Table 3.1. Selected distances (Å) and angles (°) for Mg(CzOx){Ga(NArCH)$_2$}(THF) (**21-THF**).

Mg(1)-Ga(1)	2.7458(14)	Mg(1)-O(2)	2.174(4)
Mg(1)-N(2)	2.050(4)	Ga(1)-N(1)	1.930(2)
Mg(1)-N(3)	2.219(2)		
N(2)-Mg(1)-N(3)	86.70(7)	O(2)-Mg(1)-Ga(1)	130.96(11)
N(2)-Mg(1)-Ga(1)	112.68(11)	N(3)-Mg(1)-N(3A)	164.86(14)
N(3)-Mg(1)-Ga(1)	97.56(7)	N(1)-Ga(1)-N(1A)	84.05(14)

Complex **21-THF** exhibits a distorted trigonal bipyramidal geometry around the Mg centre. As usual for complexes with trigonal bipyramidal geometries, the more electronegative ligands (oxazolines) occupy the apical positions.[14] The nitrogen of the carbazole moiety, the gallyl fragment and a THF molecule occupy the equatorial positions. Despite the higher coordination number of Mg in **21-THF** compared to the

tetra-coordinated Mg centre in Mg(^{Dipp}NacNac){Ga(NArCH)$_2$(κ^1-TMEDA) (**2.19**), the Mg-Ga bond distance in **21-THF** (2.7458(14) Å) is slightly shorter than that of **2.19** (2.7470(7) Å).[15] Similarly to **2.19** and other Ae-Ga bonded complexes, the Mg-Ga bond distance in **21-THF** is longer than the sum of the respective covalent radii (2.63(8) Å).[11] The Mg(1)-O(2) bond distance (2.174(4) Å) is comparable to the Mg-O_{THF} bond distance in other pentacoordinated Mg complexes (*cf.* 2.178(2) for Mg(CH_2SMe)$_2$(THF)$_3$[16] and 2.172(6) Mg{(μ-3,5-Me_2Pz)$_2$GaCy$_2$)}Cl(THF)$_2$[17]). The Mg(1)-O(2) is longer than that of the only carbazolide supported Mg-THF complex (CzOx)Mg(BH_4)(THF) (**3.24-THF**) (2.083(2) Å) in which THF also occupies an equatorial position within a *pseudo*-trigonal bipyramidal geometry around Mg.[6] The Mg(1)-N(2) and Mg(1)-N(3) bond distances (2.050(4) Å and 2.219(2) Å, respectively) are comparable to the equivalent bond distances in **3.24-THF** (2.043(3) Å and 2.2526(19) Å, respectively).[6] The N(3)-Mg(1)-N(3A) angle (164.86(14)º) deviates from linearity more than in **3.24-THF** (172.08(10)º)[6] presumably due to the higher steric demand of the Ga(NArCH)$_2$ fragment compared to BH_4 pushing the Mg centre further away from the carbazolide. The N(1)-Ga(1)-N(1A) angle (84.05(14)º) is narrower than that of the only reported Mg mono(gallyl) Mg(^{Dipp}NacNac){Ga(NArCH)$_2$(κ^1-TMEDA) (**2.19**) (85.55(6)º)[15] and more comparable to those of the bis(gallyl) Mg{Ga(NArCH)$_2$}$_2$(THF)$_3$ (**1.11**) (84.56(15)º and 84.09(15)º) which also exhibits a trigonal bipyramidal geometry around Mg.[18] However, the N(1)-Ga(1)-N(1A) angle is expectedly wider than that of the parent potassium gallyl [KGa(NArCH)$_2$(Et_2O)]$_2$ (**1.44**) (81.88(9)º)[19] or its TMEDA analogue [KGa(NArCH)$_2$(TMEDA)]$_2$ (**1.43**) (82.05(15)º).[19]

Addition of 1 eq. of THF to a C_6D_6 solution of **21** aiming to observe **21-THF** in solution did not change the shifts of either **21** or THF which remains free. This result, along with the release of THF in the formation of **21** suggests a weak Mg-THF interaction. Notably, the crystals for complex (CzOx)Mg(BH_4)(THF) **3.24-THF** are reported to be obtained from diffusion of pentane into a THF solution of the THF-free complex, (CzOx)Mg(BH_4) (**3.24**), similarly to **21-THF**. It is proposed that the **3.24-THF** complex is formed initially and then the THF molecule is removed when the reaction mixture is exposed to vacuum, followed by work up to obtain **3.24**.[6]

Following the isolation of **21**, attempts to obtain the calcium analogue under similar conditions allowed the formation of the complex Ca(CzOx){Ga(NArCH)$_2$}(THF)$_2$

(**22**) according to Equation 3.4. Upon formation of **22** and similarly to **21**, the vinyl resonance shifts to 6.54 ppm which is upfield with respect to the same resonance in **1.44**. The steric hindrance in the calcium gallyl complex is seemingly reduced with respect to **21** since both THF molecules remain coordinated and the methyl protons of the oxazoline moiety appear as a singlet instead of the two singlets observed in **21**. Complex **22** could be isolated on the gram scale in 73% yield. As with **21**, **22** is more stable in solution that its ^{R}NacNac supported analogue with no major change in the composition of a C_6D_6 solution of **22** when this is left standing overnight. As inferred by comparison of the stabilities in solution between **1** and **21** or **2** and **22**, the use of the carbazolide CzOx as supporting ligand improves the stability of the Ae-Ga complexes.

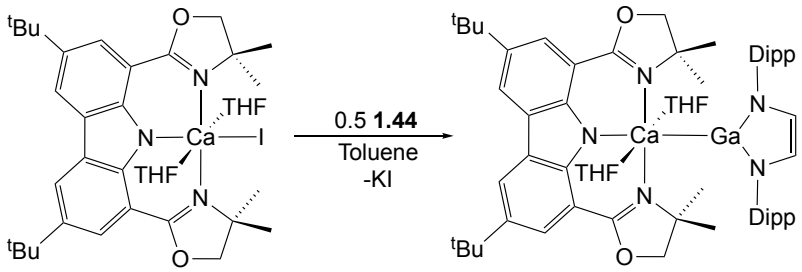

Equation 3.4

3.4 Reactivity of Ae(CzOx){Ga(NArCH)$_2$(THF)$_x$ complexes

3.4.1 Reactions with carbodiimides

As with **1**, initial attempts to study the reactivity of Mg(CzOx){Ga(NArCH)$_2$} (**21**) started with CO_2 and CS_2 which gave intractable complex mixtures. After this, the reactivity with the isoelectronic carbodiimides was performed as illustrated in the Equation 3.5. After the addition of 1 eq of ^{i}PrNCN^{i}Pr to a C_6D_6 solution of **21** there is an upfield shift of the resonance of the vinyl proton from 6.50 ppm in **21** to 6.21 ppm in its insertion product (**23**, Equation 3.5) as a result of coordination of the gallium centre to a sp^2 carbon. A similar upfield shift is also observed when CyNCNCy reacts with **21** to form **24** (Equation 3.5). These upfield shifts are reminiscent to the ones observed in the insertion reactions of the Mg(^{R}NacNac){Ga(NArCH)$_2$(THF) complexes described in the Chapter 2 or the insertions of carbodiimides into the Ln-Ga bonds of the previously reported Ln{Me$_3$SiCH$_2$C(NCy)$_2$}$_2${Ga(NArCH)$_2$}(THF) species.[13] With the formation of **23**, the steric hindrance in the vicinity of the Mg

centre is seemingly reduced since the resonance for the methyl protons of the oxazoline fragment appear as a sharp singlet instead of two singlets in the parent **21**. The reactions yielding **23** and **24** could be successfully scaled up in moderate yields (48% and 54%, respectively) and the elemental analyses and the spectroscopic data are in accordance with their proposed structures.

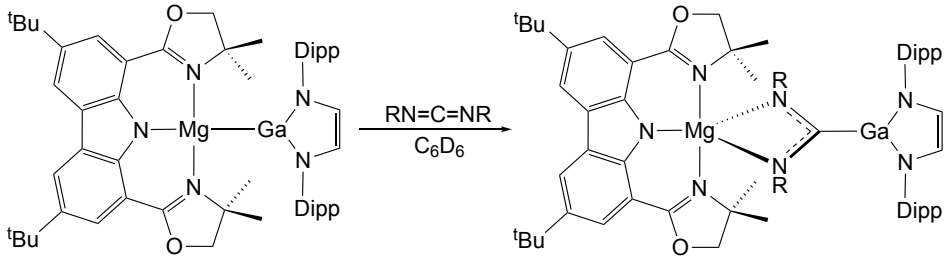

21 **23** R = ^{i}Pr
24 R = Cy

Equation 3.5

An attempt to insert TolNCNTol did not appear to be successful as this reaction did not seem to proceed and ultimately led to decomposition of **21** after 4 days. It is possible that this is due to the steric clash between the carbazolide, the Dipp substituents and the carbodiimide. However, this is not entirely certain since the same reaction with CyNCNCy, which bears a bulkier substituent than TolNCNTol, proceeds successfully and in a selective manner. This result suggests that there may also be an electronic effect that inhibits the insertion of TolNCNTol into the Mg-Ga bond of **21**. In previously studied insertions of carbodiimides, it has been proposed that the coordination of the carbodiimide to the metal centre is the first step in these reactions.[13, 20, 21] In some cases, the coordination of carbodiimides is preceded by decoordination of a labile ancillary ligand, *e.g.* THF, to leave a vacant coordination site for the carbodiimide.[13] Indeed, the carbodiimide can compete with THF for the coordination to Mg; for example, the reaction of [Mg(^{Dipp}NacNac)(THF)]$_2$ with CyNCNCy in THF does not proceed[22] whilst the same reaction with the base free complex [Mg(^{Dipp}NacNac)]$_2$ in a non-donor solvent yields the desired insertion product.[20] In the reaction of **21** with carbodiimides the release of such labile ancillary ligand is not required and their coordination and insertion would follow the route proposed in Scheme 3.5 adapted from the aforementioned studies. However, the initial coordination of TolNCNTol is presumably weaker than those performed by CyNCNCy or ^{i}PrNCN^{i}Pr as the lone pair in the nitrogen in TolNCNTol is delocalised

into the aromatic ring of the tolyl fragment. The delocalisation makes the lone electron pair of nitrogen less available for the coordination of the carbodiimide to the Mg centre. Evidently, the delocalisation of the lone pair is not present in the alkyl carbodiimides which act as better σ donors and insert into the Mg-Ga bond. Comparison of the reactions of TolNCNTol with Mg(^{Dipp}NacNac){Ga(NArCH)$_2$}(THF) (**1**) and Mg(CzOx){Ga(NArCH)$_2$} (**21**), suggests that the insertion of TolNCNTol is then both dependant on steric and electronic effects and that such reaction can be achieved when the steric hindrance is reduced. This is also supported by the fact that the insertion of TolNCNTol can be performed with Ca(CzOx){Ga(NArCH)$_2$}(THF)$_2$ (**22**) (*vide infra*), which is sterically less impeded due to the larger covalent radius of calcium along with the potential lability of two THF molecules.

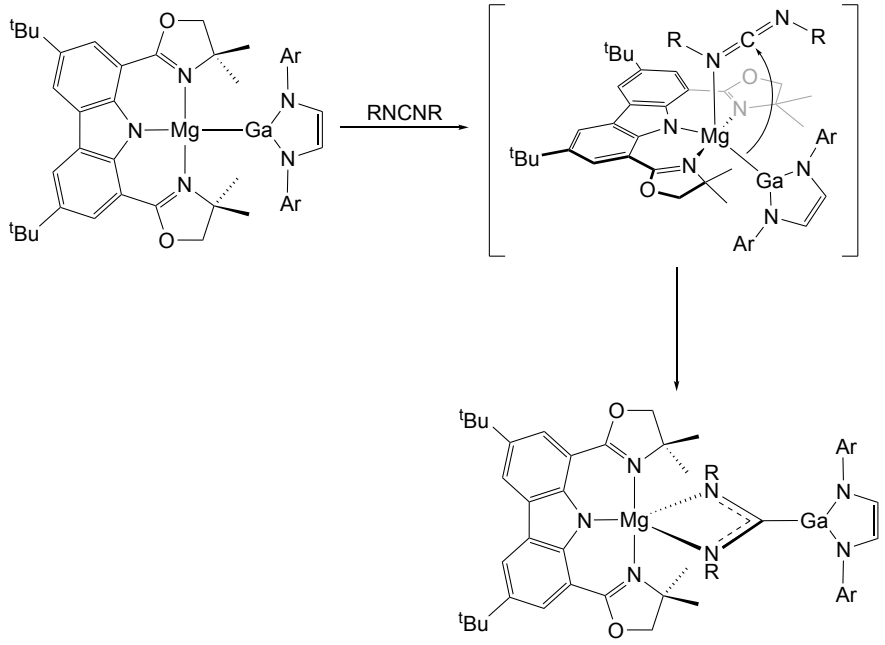

Scheme 3.5. Proposed mechanism for the insertion of carbodiimides. Ar = Dipp.

As mentioned, the insertions of ^{i}PrNCN^{i}Pr, CyNCNCy and TolNCNTol carbodiimides were also attempted with Ca(CzOx){Ga(NArCH)$_2$}(THF)$_2$ (**22**) successfully forming the desired products (**25**-**27**, Equation 3.6). The shifts in the resonance of the vinyl protons of the insertion products **25**-**27** are in agreement with the upfield shifts observed in the formation of **23** and **24**. Upon insertion, one of the THF molecules remains coordinated to the Ca centre according to the ^{1}H NMR spectra of the reaction mixtures. The insertion products **25**-**27** were isolated in 51-83% yields and the elemental analyses are in accordance with their formulations.

Additionally, crystals suitable for X ray diffraction for complexes **25** and **27** were obtained by slow evaporation of concentrated hexane and benzene solutions, respectively. The molecular structures and selected distances and angles are shown in Figures 3.3 and 3.4 and Tables 3.2 and 3.3.

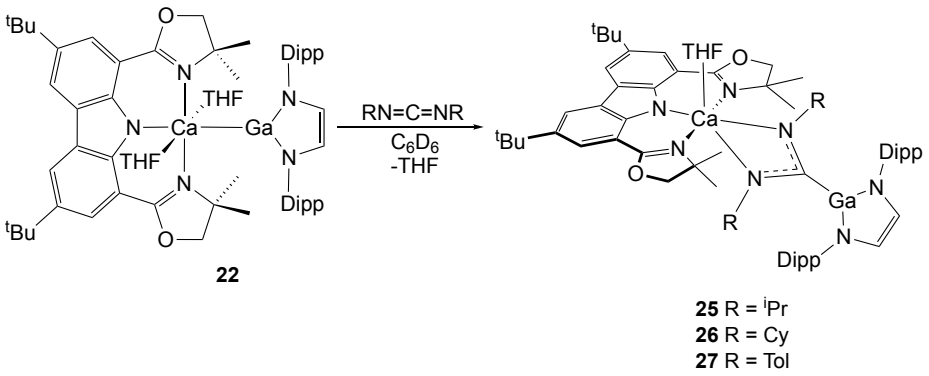

Equation 3.6

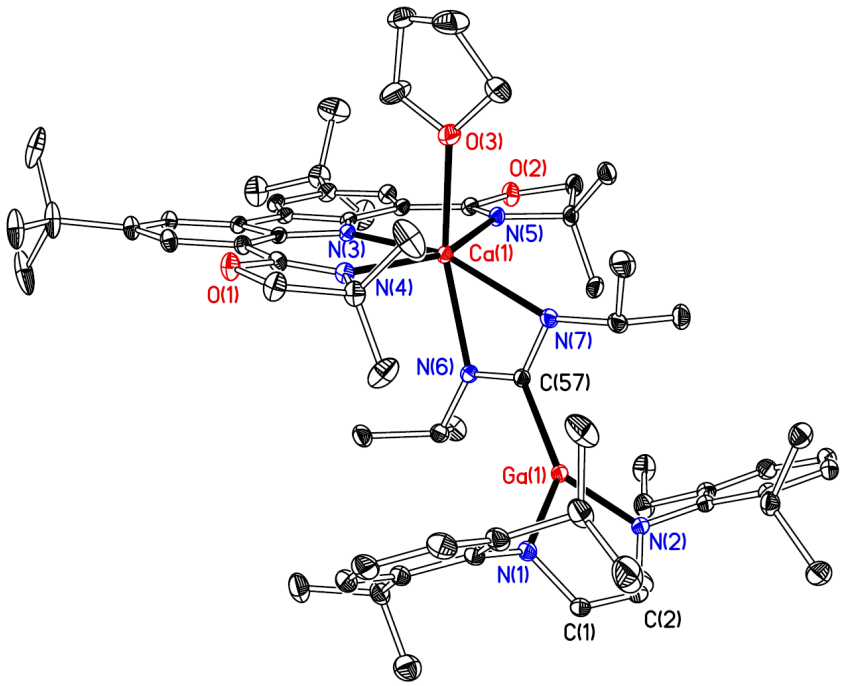

Figure 3.3. Displacement ellipsoid plot (20 % probability) of Ca(CzOx){(N^{i}Pr)$_2$CGa(NArCH)$_2$}(THF) (**25**). H atoms omitted for clarity.

Table 3.2. Selected distances (Å) and angles (°) for Ca(CzOx){(N^{i}Pr)$_2$CGa(NArCH)$_2$}(THF) (**25**).

Ca(1)-N(3)	2.4060(10)	Ga(1)-N(1)	1.8660(11)
Ca(1)-N(4)	2.4941(10)	Ga(1)-N(2)	1.8593(11)
Ca(1)-N(5)	2.4721(10)	Ga(1)-C(57)	2.0055(12)
Ca(1)-N(6)	2.3666(11)	N(6)-C(57)	1.3158(16)
Ca(1)-N(7)	2.5252(11)	N(7)-C(57)	1.3338(16)
Ca(1)-O(3)	2.4171(11)		
N(3)-Ca(1)-N(4)	78.67(3)	N(6)-C(57)-N(7)	119.34(11)
N(3)-Ca(1)-N(5)	78.17(3)	N(1)-Ga(1)-N(2)	89.39(5)
N(4)-Ca(1)-N(5)	156.11(4)	N(1)-Ga(1)-C(57)	135.58(5)
N(6)-Ca(1)-N(7)	55.63(4)	N(2)-Ga(1)-C(57)	135.02(5)
N(3)-Ca(1)-O(3)	94.35(4)		

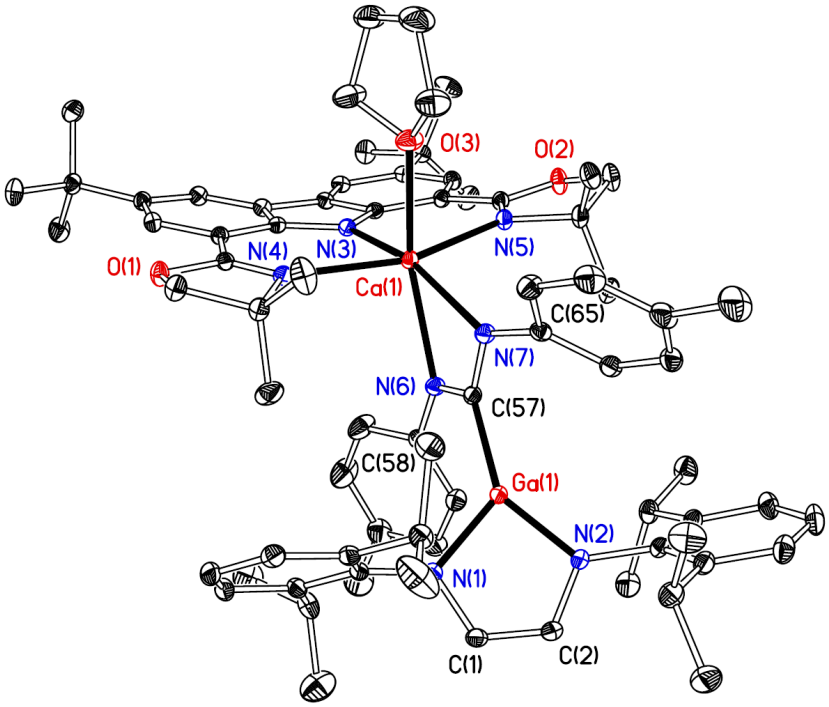

Figure 3.4. Displacement ellipsoid plot (20 % probability) of Ca(CzOx){(NTol)$_2$CGa(NArCH)$_2$}(THF) (**27**). H atoms omitted and solvent of crystallisation omitted for clarity.

Table 3.3. Selected distances (Å) and angles (°) for Ca(CzOx){$(NTol)_2CGa(NArCH)_2$}(THF) (**27**).

Ca(1)-N(3)	2.3954(13)	Ga(1)-N(1)	1.8683(13)
Ca(1)-N(4)	2.4702(14)	Ga(1)-N(2)	1.8676(14)
Ca(1)-N(5)	2.4551(14)	Ga(1)-C(57)	2.0055(16)
Ca(1)-N(6)	2.4290(14)	N(6)-C(57)	1.324(2)
Ca(1)-N(7)	2.5018(14)	N(7)-C(57)	1.340(2)
Ca(1)-O(3)	2.4126(13)		
N(3)-Ca(1)-N(4)	78.23(4)	N(6)-C(57)-N(7)	115.74(14)
N(3)-Ca(1)-N(5)	78.91(5)	N(1)-Ga(1)-N(2)	89.96(6)
N(4)-Ca(1)-N(5)	156.44(5)	N(1)-Ga(1)-C(57)	127.52(6)
N(6)-Ca(1)-N(7)	54.45(4)	N(2)-Ga(1)-C(57)	141.84(6)
N(3)-Ca(1)-O(3)	96.73(5)		

The solid state structures of **25** and **27** confirm their proposed structures and the observed retention of one THF molecule. Complexes **25** and **27** exhibit distorted octahedral geometries around the calcium atom. The Ca(1)-N(3) distances (2.4060(10) Å for **25** and 2.3954(13) Å for **27**) are comparable to that of the related *pseudo* six-coordinate complex Ca(CzOx)$(BH_4)(THF)_2$ (**3.25**) (2.399(2) Å).[6] In general, the bond distances between calcium and the donor atoms of the neutral ligands are slightly longer in **25** than in **27**. For instance the Ca(1)-N(4) distance in **25** is 2.4941(10) Å and in **27** is 2.4702(14) Å. Similarly, the Ca(1)-O(3) distance in **25** is 2.4171(11) Å whereas the same bond distance in **27** is 2.4126(13) Å. The deviation of the linearity of the N(4)-Ca(1)-N(5) angle is similar in both complexes and comparable to that of **3.25** (156.93(11)º).[6] The galla-amidinates seemingly coordinate in a less symmetric fashion in **25** and **27** than in the insertion products Mg(^{Dipp}NacNac){$(N^iPr)_2CGa(NArCH)_2$} (**7**) or Ca{$(NTol)_2CGa(NArCH)_2$}$_2(THF)_2$ (**16**). For instance, in **7** the two Mg-N^{i}Pr distances are similar between them (2.0968(14) Å and 2.0684(14) Å), whereas in **25** the disparity between the Ca(1)-N(6) (2.3666(11) Å) and Ca(1)-N(6) (2.5252(11)Å) bond distances is more pronounced. Additionally, the Ca-NTol distances in **16** (2.3914(14) Å and 2.3975(14) Å), which

comparably to **27** exhibits a distorted octahedral geometry around the Ca atom, are less dissimilar than the Ca(1)-N(6) (2.4290(14)Å) and Ca(1)-N(7) (2.5018(14) Å) bond distances in **27**. This unsymmetrical chelation by the galla-amidinates in **25** and **27** could be due to the occupation of different positions of the calcium octahedron by the NRC (R = ^{i}Pr or Tol) fragments of the galla-amidinates: axial and equatorial in **25** and **27** *vs* only equatorial in **16**, and to the steric demand of the coordinated THF in these complexes, which pushes away the CNR fragment that is closer to it resulting in the elongation of the Ca(1)-N(7) bond. The N(1)-Ga(1)-N(2) angles in **25** (89.39(5)º) and **27** (89.96(6)º) are comparable to those found in **7** (90.25(6)º) and **16** (90.90(6)º) and as with these complexes the particularly wide angle in **25** and **27** is presumably due to the coordination of gallium to carbon. Unfortunately, it was not possible to obtain crystals of the parent complex **22** to make a direct comparison, nonetheless, the N(1)-Ga(1)-N(2) angles of **25** and **27** are wider than those of literature Ca-Ga bonded complexes, *e.g.* $Ca\{Ga(NArCH)_2\}_2(THF)_4$ (**1.12**) (83.68(11)º)[18] and $Ca\{Ga(NArCH)_2\}_2(TMEDA)_2$ (**2.16**) (83.4(1)º and 83.6(1)º).[15] The N(1)-Ga(1)-N(2) angles of **25** and **27** are also wider than of $[KGa(NArCH)_2(Et_2O)]_2$ (**1.44**) (81.88(9)º).[19] The Ga(1)-C(57) distances are the same in both of **25** and **27** and their Ga(1)-N(1) and Ga(1)-N(2) bond distances are similar, suggesting that the $Ca(CzOx)\{(NR)_2C\}$ fragment has the same effect in the structural parameters of the gallacycles irrespective of the substituents of the employed carbodiimide.

3.4.2 Reactions with iodides

Similarly to **1** and **2**, complex **21** was reacted with a MeI in the NMR tube-scale to form a new carbazolide based product, seemingly the base-free magnesium iodide complex (CzOx)MgI **28** (Scheme 3.6). As with to **1** and **2**, reactions with MeI did not lead to the observation of the $MeGa(NArCH)_2$ complex. The same reactivity is observed with the use of ^{t}BuI, AcI and I_2 which leads only to the observation of **28** and $[Ga(NArCH)_2]_2$ (**1.68**). The base-free magnesium complex (CzOx)MgI (**14**) was independently prepared by reacting MeMgI with the ligand CzOx-H in Et_2O, which does not coordinate to the Mg centre. The ^{1}H NMR spectrum of **14** matches the resonances observed in the reactions of **21** with iodides.

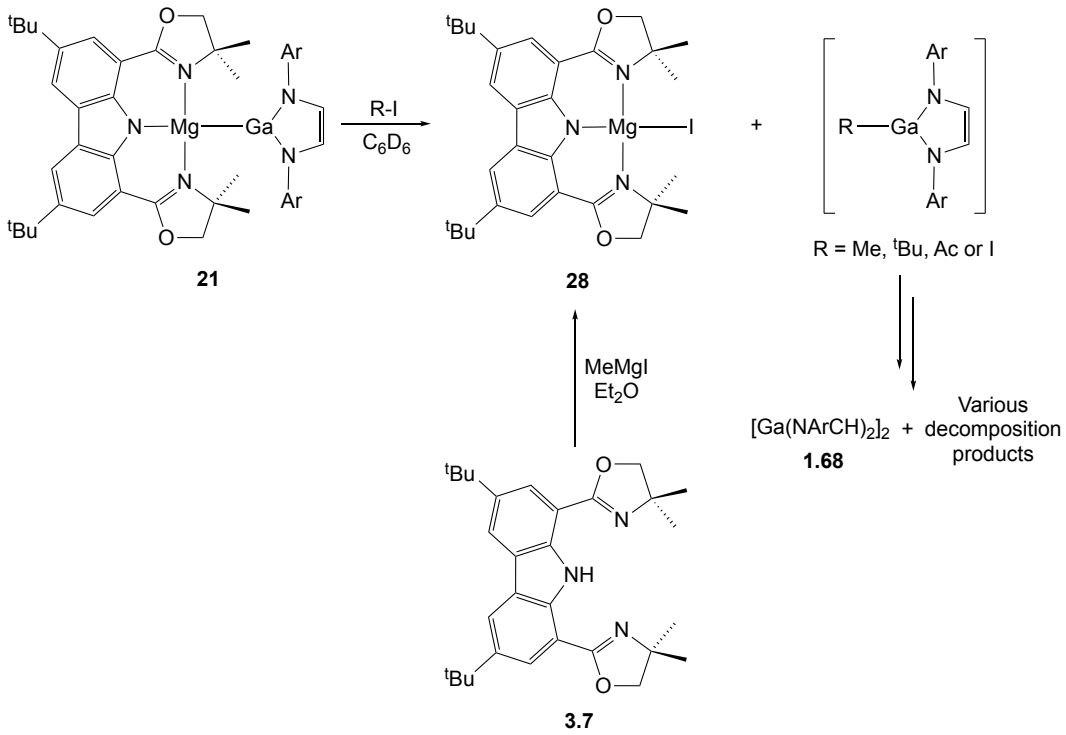

Scheme 3.6. Reactions of Mg(CzOx){Ga(NArCH)$_2$} (**21**) with iodides and independent synthesis of the base free magnesium complex (CzOx)MgI (**14**).

The complex Ca(CzOx){Ga(NArCH)$_2$}(THF)$_2$ (**22**) reacts with MeI in a similar way to its magnesium counterpart **21** this time without loss of THF and therefore regenerating (CzOx)CaI(THF)$_2$ (**3.16**, Equation 3.7). Somewhat surprisingly, reacting **24** with I_2 forms the homoleptic calcium complex $(CzOx)_2Ca$ and free diazabutadiene according to the ^{1}H NMR spectrum of the reaction mixture.

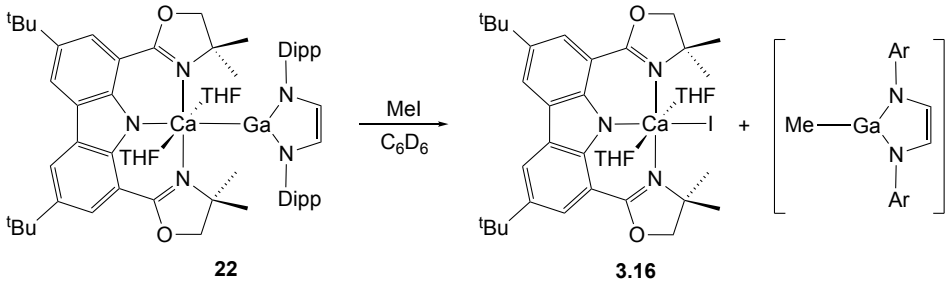

Equation 3.7

These attempts to obtain alkyl gallyls from reactions of Ae-Ga complexes with iodides suggest the instabilities of the expected RGa(NArCH)$_2$ (R = Me, ^{t}Bu, Ac, I) compounds towards possible redistribution due to the reducing power of the Ga(NArCH)$_2$ fragment which can lead to the formation of the diamagnetic $[Ga(NArCH)_2]_2$ (**1.68**) or the paramagnetic $[GaI(NArCH)_2]_2$.[23]

As with **1**, the reaction of **21** with $SiMe_3I$ forms (CzOx)MgI **28** and $(Me_3Si)Ga(NArCH)_2$ (**19**, Equation 3.8) which is presumably a more stable product than its alkyl analogues as suggested by its achievable identification and isolation (see Chapter 2). A small amount of digallane (18% with respect to **19**) is also observed, which overall makes a less complex mixture than the one seen with **1** and $SiMe_3I$.

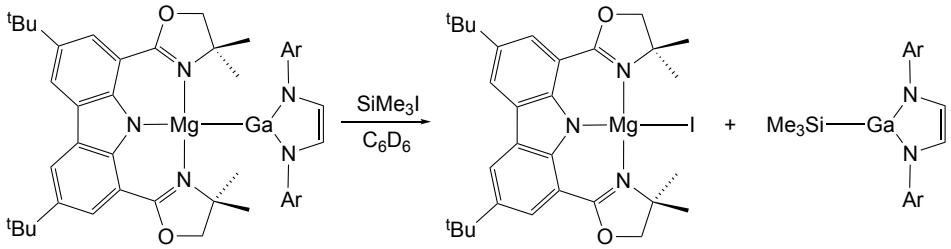

21 **28** **19**

Equation 3.8

3.4.3 Reactions with isobutene epoxide and oxygen donors

Aiming to compare the reactivity of the (CzOx)Ae{Ga(NArCH)$_2$}(THF)$_n$ complexes with that of **1** and **2** in the presence of oxygen donors, the reactions of **21** and **22** with isobutene epoxide were envisaged. The addition of isobutene epoxide to a solution of **21** in C_6D_6 gave an immediate change in the colour of the mixture from an orange suspension to a yellow solution. Analysis of the ^{1}H NMR of the mixture showed the release of isobutene and the oxygen abstraction product (CzOx)Mg{(μ-O)Ga(NArCH)$_2$} (**29**, Equation 3.9) similarly to **1** and **2** although in a more selective manner, being isobutene and **29** the only products in this reaction. The vinyl resonance in **29** (6.01 ppm) compares to that of its ^{Dipp}NacNac analogue (6.02 ppm).

Alternately, reacting **21** with Me_3NO gives the oxygen abstraction product although less selectively as some digallane and other minor unknown species are present. The use of other oxygen donors such as Ph_3PO or TEMPO with **21** gave **29** in rather small quantities (< 5%) within complex mixtures.

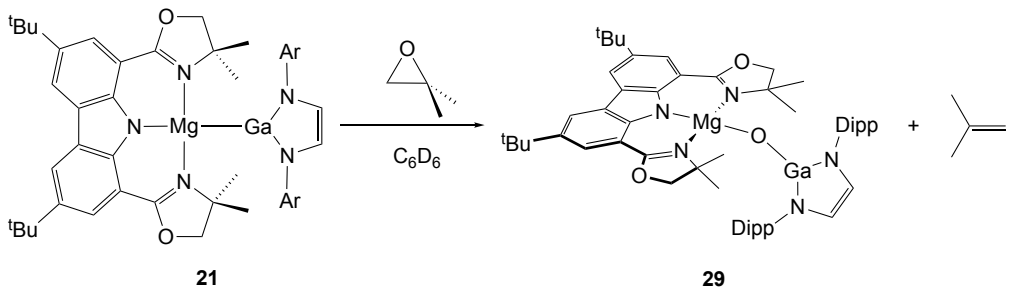

Equation 3.9

Complex **29** was isolated in moderate yield (45%) from the reaction of Mg(CzOx){Ga(NArCH)$_2$} (**21**) with isobutene epoxide in toluene. The ^{1}H and ^{13}C NMR spectra and elemental analysis are in accordance with the proposed structure. Additionally, diffraction-quality crystals of **29** were grown from a concentrated benzene solution at RT. The molecular structure and selected distances and angles are shown in Figure 3.5 and Table 3.4.

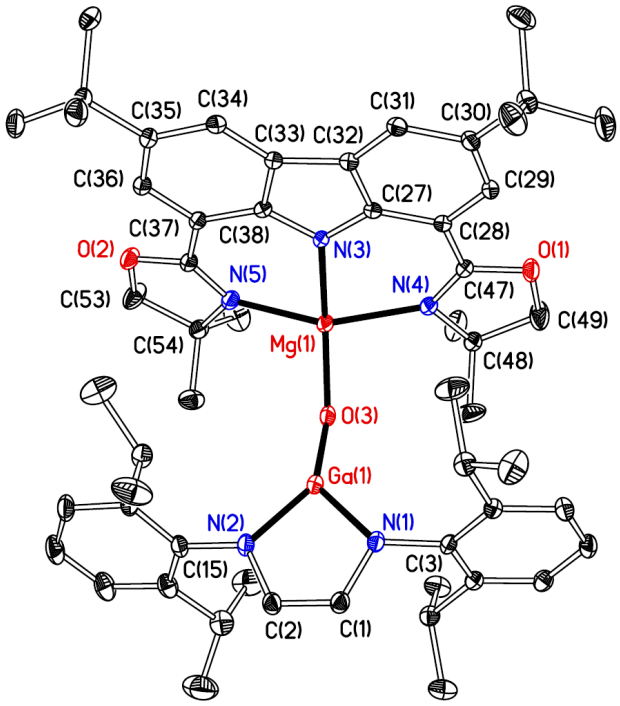

Figure 3.5. Displacement ellipsoid plot (20 % probability) of Mg(CzOx){(μ-O)Ga(NArCH)$_2$} (**29**). H atoms and second disordered component of the oxo-bridge omitted for clarity.

Table 3.4. Selected distances (Å) and angles (°) for Mg(CzOx){(μ-O)Ga(NArCH)$_2$} (**29**).

Mg(1)-O(3)	1.880(4)	Ga(1)-O(3)	1.747(4)
Mg(1)-N(3)	2.002(2)	Ga(1)-N(1)	1.853(2)
Mg(1)-N(4)	2.152(3)	Ga(1)-N(2)	1.839(2)
Mg(1)-N(5)	2.146(3)		
N(3)-Mg(1)-N(4)	86.57(10)	N(5)-Mg(1)-O(3)	104.5(3)
N(3)-Mg(1)-N(5)	87.68(10)	Mg(1)-O(3)-Ga(1)	138.3(4)
N(4)-Mg(1)-N(5)	146.68(12)	N(1)-Ga(1)-N(2)	90.81(11)
N(4)-Mg(1)-O(3)	98.0(2)		

The solid state structure of **29** reveals a distorted tetrahedral geometry around the Mg centre. This environment is formed by the tridentate carbazolide and a bridging oxygen atom. Despite the plethora of oxo-bridged intermetallic species and the oxophilicity of alkaline earth metals, there are no known Mg-O-Ga species and only four Group 2-Group 13 bimetallic structures with a single oxo-bridge are known. Of these, three contain the Mg-O-Al motif[24, 25] with the fourth containing a Ca-O-B core.[26] The Ga(1)-O(3) distance is shorter than the Mg(1)-O(3) distance consistent with a smaller covalent radius of Ga. The Mg(1)-O(3) bond distance (1.880(4) Å) is comparable to those found in Mg{(μ-O)Al(^{Dipp}NacNac)Me}(NSiMe$_3$)(THF)$_2$ (**3.26**) (1.850(2) Å) and Mg{(μ-O)Al(^{Dipp}NacNac)Me}$_2$(THF)$_2$ (**3.27**) (1.873(2)Å).[25] The Ga(1)-O(3) distance (1.747(4) Å) is the shortest Ga-O bond distance in a heterobimetallic oxo-bridged complex to date. Related complexes contain Ga-O bond distances in the order of Ga(1)-O(3), *e.g.,* [Ga(^{Mes}NacNac)Cl]$_2$(μ-O) (1.783(1)Å)[27] or Ga(^{Dipp}NacNac)Cl(μ-O)(SiMe$_3$) (1.789(2) Å).[28] The Mg(1)-O(3)-Ga(1) angle (138.3(4)º) is significantly different from the Mg-O-M angle in other species, for example, Mg{(μ-O)Al(^{Dipp}NacNac)Me}(NSiMe$_3$)(THF)$_2$ (150.2(1)º)[25] and [Mg(O^{t}Bu){GaH$_2$(O^{t}Bu)$_2$}]$_2$ (98.5(1)º).[29] Complex **29** contains the N(4)-Mg(1)-N(5) angle (146.68(12)º) that deviates considerably from linearity (*cf.* 164.86(14)º in the parent **21**) as a result of the Mg-OGa interaction which pushes the Mg atom further away from the plane of the carbazole. As observed in previous systems, the coordination of gallium to an atom more electronegative than Mg, significantly

increases the N(1)-Ga(1)-N(2) angle from 84.05(14)º in **21** to 90.81(11)º in **29**. As described in Chapter 2, the oxygen abstraction by metal-metal bonded species is an uncommon process. Notably, the analogous complex Mg{(μ-O)Al(^{Dipp}NacNac)Me}(NSiMe$_3$)(THF)$_2$ (**3.26**) was prepared by reaction of Mg{N(SiMe$_3$)$_2$} with Al(^{Dipp}NacNac)(OH)Me (Equation 3.10).[25]

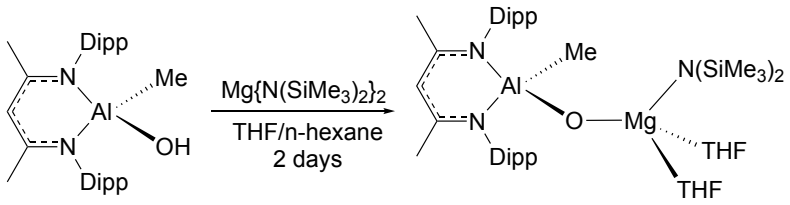

3.26

Equation 3.10[25]

3.4.3.1 Reactions with bulkier epoxides

This reactivity of **21** was further studied with epoxides bulkier than isobutene epoxide, namely cyclohexene epoxide ($C_6H_{10}O$) and *exo*-norbornene epoxide ($C_7H_{10}O$). Addition of 1 eq. of any of those two epoxides to solutions of **21**, results in a change in the colour of the reaction mixture from an orange suspension to a yellow cloudy solution is observed. However, analysis of the ^{1}H NMR spectra of the reaction mixtures did not suggest the release of free cyclohexene or norbornene. Furthermore, removal of volatiles did not show any change in the resonances of the products thus suggesting complete incorporation of the epoxides to the Mg gallyl complex forming the complexes Mg(CzOx){($C_6H_{10}O$)Ga(NArCH)$_2$} (**30**) and Mg(CzOx){($C_7H_{10}O$)Ga(NArCH)$_2$} (**31**) as illustrated in Equation 3.11. The syntheses of **30** and **31** could be scaled up in moderate yields (75% and 83%, respectively). After isolation, heating of fresh C_6D_6 solutions of **30** and **31** at 60 ºC for 24 h did not result in the release of norbornene or cyclohexene. The low solubility of these compounds in benzene impeded their crystallisation. Notably, in both cases the vinyl resonance shifts upfield (**30**, 6.08 ppm; **31**, 6.22 ppm) and is in the range of the shifts of the previously described insertion products, *e.g.,* Mg(CzOx){(N^{i}Pr)$_2$CGa(NArCH)$_2$} **23** (6.21 ppm) or the literature compounds ArGa(NArCH)$_2$ (Ar = C$_6$H$_3$^{i}Pr$_2$-2,6; 6.14 ppm)[30] and (η^1-Cp*)Ga(NArCH)$_2$ (5.70 ppm in THF-d_8)[31] thus suggesting coordination of gallium to carbon in accordance with the proposed structures of these products in Equation 3.11.

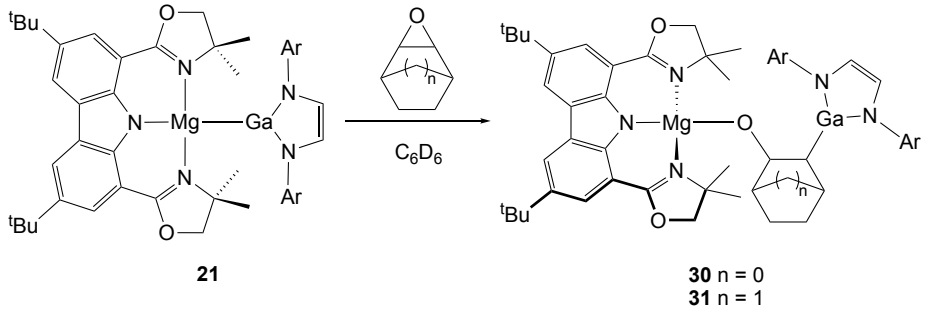

Equation 3.11

The incorporation of cyclohexene and *exo*-norbornene epoxides is reminiscent of the ring opening of *exo*-norbornene epoxide by the imido complex $Cp_2Zr(N^tBu)(THF)$ (**3.27**).[32] Addition of 1 eq. of *exo*-norbornene epoxide to a C_6D_6 solution of **3.27** allows the observation of the epoxide complex $Cp_2Zr(N^tBu)(C_7H_{10}O)$ (**3.28**, Scheme 3.7) consistent with an exchange of the THF and *exo*-norbornene epoxide ligands. Heating of the mixture at 45 ºC leads to the formation of the ring opening product **3.29** presumably formed *via* a zwitterionic intermediate.

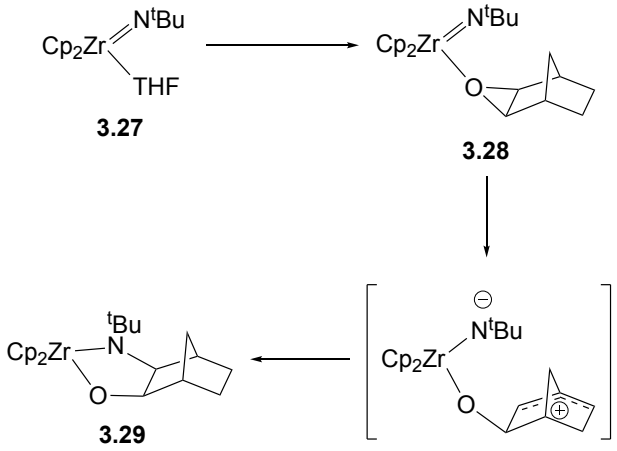

Scheme 3.7. Ring opening of *exo*-norbornene epoxide by a zirconocene imido complex.[32]

3.4.4 Reactions with isocyanates

Inspired by the previously studied insertion of *tert*-butyl isocyanate into the Mg^I-Mg^I bond of $[(L)Mg]_2$ complexes by Jones and Stasch,[33-35] the study of the reactivity of **21** and **22** with commercially available isocyanates was envisaged. Addition of 1 eq. of ^{t}BuNCO to a C_6D_6 solution of $Mg(CzOx)\{Ga(NArCH)_2\}$ (**21**) resulted in the full consumption of the isocyanate and its incorporation to a single product $Mg(CzOx)\{(^tBuN)(O)CGa(NArCH)_2\}$ (**32**, Equation 3.12). Removal of volatiles does

not show a change in the resonances for the backbone of **32**. Addition of a second equivalent of ^{t}BuNCO to **32** or the addition of two equivalents of ^{t}BuNCO to a C_6D_6 solution of **21** did not yield the product of a double insertion in contrast with the Mg^{I}-Mg^{I} dimers which insert two equivalents of isocyanates.[33-35] Complex Mg(CzOx){(^{t}BuN)(O)CGa(NArCH)$_2$} (**32**) could be isolated in good yield (85%).

Inspection of the ^{1}H NMR spectrum of **32** shows an upfield shifted resonance of the vinyl proton to 6.16 ppm. The methylene protons of the oxazoline fragment are diasterotopic in **32** and appear as two doublets with ^{2}J = 8.3 Hz instead of a singlet. This could be caused by the coordination of the nitrogen of the inserted isocyanate to the Mg centre, which removes the mirror symmetry in the carbazolide and differentiates the methylene protons of the oxazoline depending on their position towards and away from the N^{t}Bu fragment. A similar behaviour has been previously observed in the complex Mg(CzOx){N(SiMe$_3$)$_2$} (**3.30**) in which the methylene protons of the oxazoline are also diasterotopic and present a geminal coupling of ^{2}J = 8.0 Hz as a result of the different orientation of such protons with respect to the N(SiMe$_3$)$_2$ ligand.[6] Complex **32** also shows a characteristic shift for the CO carbon of the isocyanate at 180.43 ppm consistent with its insertion and coordination to gallium (*cf.* 179.25 ppm for NCN in Mg(CzOx){(N^{i}Pr)$_2$CGa(NArCH)$_2$} **23**).

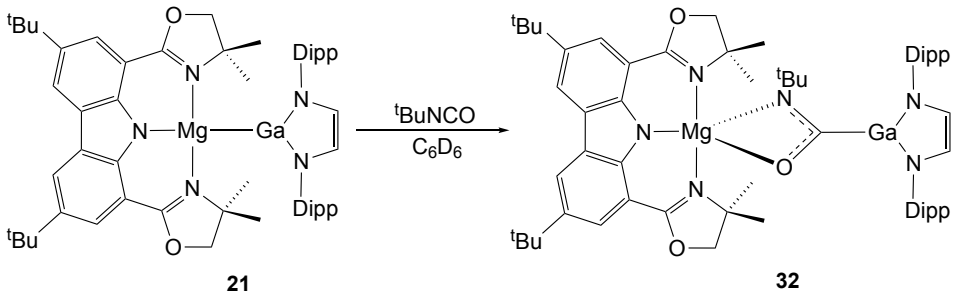

21 **32**

Equation 3.12

Attempts to synthesise the calcium analogue of **32** in C_6D_6 resulted in the formation of a complex mixture. Nonetheless, a better result was obtained with the use of EtNCO which allows the observation of Ca(CzOx){(EtN)(O)CGa(NArCH)$_2$}(THF) (**33**, Equation 3.13). Upon insertion, only one of the THF molecules is displaced from the calcium centre as observed in the insertion of carbodiimides into the Ca-Ga bond of Ca(CzOx){Ga(NArCH)$_2$}(THF)$_2$ (**22**). Similarly to Mg(CzOx){(^{t}BuN)(O)CGa(NArCH)$_2$} (**32**), the vinyl proton in **33** shifts upfield to 5.84 ppm. Likewise, complex **33** presents a resonance for the CO carbon of the

inserted EtNCO at 169.85 ppm (*cf.* 177.48 ppm for NCN in Ca(CzOx){(NTol)$_2$CGa(NArCH)$_2$}(THF), **27**). Complex **32** was further isolated by reaction of Ca(CzOx){Ga(NArCH)$_2$}(THF)$_2$ (**22**) with EtNCO in toluene in good yield (73%).

Relatedly, the single insertion of isocyanates has been reported into Mg-H[36] and Mg-C[37] bonds to form complexes Mg(^{Dipp}NacNac){OC(H)NDipp} (**3.31**) and Mg{(NEt$_2$)$_2$AlMe$_2$}(NPhCMeO) (**3.32**), respectively, which possess structures similar to those proposed for **32** and **33**. In terms of the connectivity in complexes **32** and **33**, another possibility is the formation of a magnesium amido complex featuring a bridging carbonyl group. In this respect, the only structurally authenticated gallium complex containing an acyl fragment, [Ga(^{t}Bu)$_2${μ-(C(^{t}Bu)O)}]$_2$, is reported to exhibit a δ_{CO} at 310.3 ppm, which markedly differs from those of **32** and **33**.

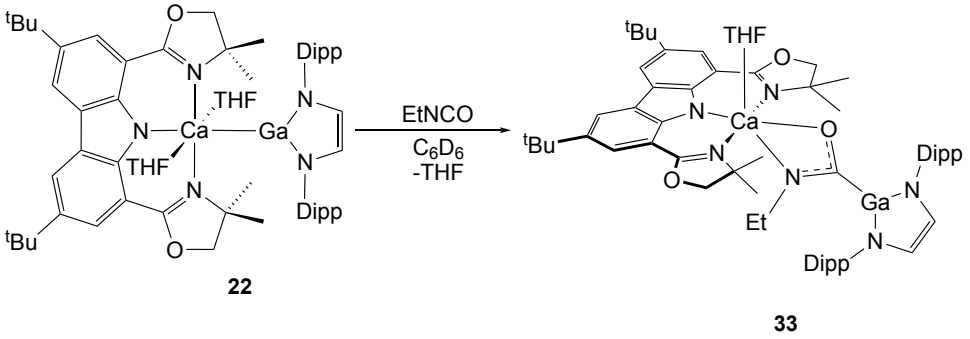

Equation 3.13

3.4.5 Reactions with azobenzene

Addition of 1 eq. of azobenzene to a C_6D_6 solution of Mg(CzOx){Ga(NArCH)$_2$} (**21**) cleanly forms the product of the addition of azobenzene to the magnesium gallyl complex Mg(CzOx){N(Ph)N(Ph)Ga(NArCH)$_2$} (**34**, Equation 3.14). The ^{1}H NMR spectrum shows a shift to 5.91 ppm, which is upfield with respect of the vinyl resonance of **21**. The spectrum also shows a desymmetrisation of azobenzene with two environments for its aromatic protons which altogether integrate together for only one molecule of azobenzene with respect to the backbones of the (CzOx)Mg and Ga(NArCH)$_2$ fragments. This complex which seems to be the product of the insertion of azobenzene *via* oxidation of the Ga(NArCH)$_2$ fragment, is rather unstable in solution as it forms a complex mixture within one hour. Nonetheless, this reaction could be scaled up by allowing a mixture of **21** and azobenzene in C_6H_6 react for 10 min at RT, followed by immediate removal of volatiles. The ^{1}H NMR spectrum of

complex **34** can be reproduced by dissolving aliquots of the isolated product stored in a glovebox for up to three days before it starts showing multiple resonances in the aromatic region indicative of its decomposition in the solid state. The possibility of **34** being merely the coordination of azobenzene to Mg appears to be less likely since the interaction of NAr fragments with the Mg centre is presumably weak as observed in the lack of reactivity of **21** with TolNCNTol (*vide supra*). Furthermore, the upfield shift of the vinyl proton suggests substitution of Mg by a more electronegative element in the coordination sphere of Ga, *i.e.,* the loss of the Mg-Ga interaction. Nonetheless, the coordination of azobenzene to Mg in **21** could be the initial step in the formation of **34**.

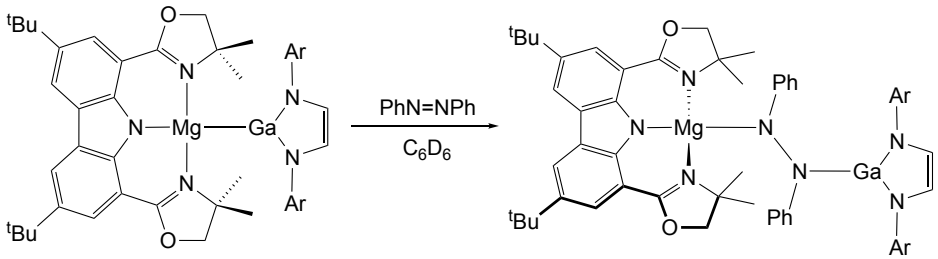

21 **34**

Equation 3.14

3.4.6 Reactions with azides

Addition of trimethylsilyl azide to a C_6D_6 solution of Mg(CzOx){Ga(NArCH)$_2$} (**21**) gave a clean reaction which is in agreement with the insertion of the $NSiMe_3$ fragment into the Mg-Ga bond of **21** to form complex Mg(CzOx){N(SiMe$_3$)Ga(NArCH)$_2$} (**35**, Equation 3.15). The presence of the bulky $NSiMe_3$ fragment in the vicinity of the carbazolide reduces the symmetry of the oxazoline moiety since its methylene protons appear as diasterotopic with ^2J = 8.3 Hz similar to the previously described carbazolide supported magnesium complexes containing the $NEMe_3$ (E = C or Si) moiety, *i.e.,* Mg(CzOx){(^{t}BuN)(O)CGa(NArCH)$_2$} (**32**) complex (^2J = 8.3 Hz) and the related magnesium amido complex Mg(CzOx){N(SiMe$_3$)$_2$} (**3.30**) (^2J = 8.0 Hz).[6] In addition, the methyl protons of the oxazoline fragment appearing as two doublets as it occurs in **3.30**[6] is in contrast with the sharp singlet observed in other insertion products. Indeed, complex **35** can be seen as the gallyl derivative of **3.30**. The synthesis of complex **35** could be scaled up and its elemental analysis is in accordance with its formulation.

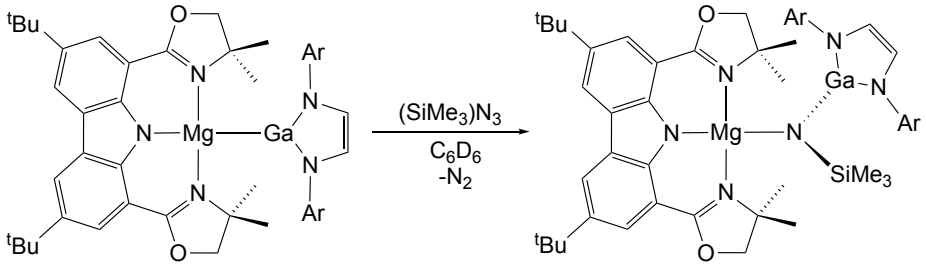

21 **35**

Equation 3.15

Adaptation of the reaction of $(SiMe_3)N_3$ with $Ca(CzOx)\{Ga(NArCH)_2\}(THF)_2$ (**22**) did not selectively form the desired insertion product and formed a complex mixture instead. A cleaner reaction was obtained when phenyl azide was used which selectively forms $Ca(CzOx)\{N(Ph)Ga(NArCH)_2\}(THF)_2$ (**36**, Equation 3.16). The synthesis of complex **36** could be further scaled up in moderate yield (66%). The ^1H NMR spectrum of **36** shows the presence of two coordinated THF molecules which is consistent with the substitution of the $Ga(NArCH)_2$ fragment by a monodentate ligand. For instance, in the above discussed reaction of $Ca(CzOx)\{Ga(NArCH)_2\}(THF)_2$ (**22**) with iodomethane, the calcium iodide complex is formed with retention of both THF molecules. In a similar manner to $Mg(CzOx)\{N(SiMe_3)Ga(NArCH)_2\}$ (**35**) the vinyl proton of **36** shifts upfield to 6.18 ppm (*c.f.* 6.19 ppm for **35**).

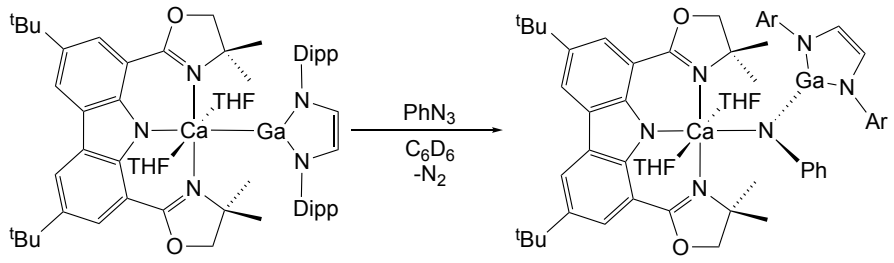

22 **36**

Equation 3.16

3.4.7 Reactions with derivatives of the $CpFe(CO)_2$ fragment

To further extend this reactivity, 1 eq. of FpI (Fp = $CpFe(CO)_2$) was added to a solution of **21** in C_6D_6 showing the formation of the base free Mg iodide complex Mg(CzOx)I (**28**) and a new species, seemingly the $FpGa(NArCH)_2$ (**37**, Scheme 3.8) complex along with digallane and the Fp_2 dimer as by-products. To corroborate the formation of **37**, its synthesis was independently performed by reacting FpI and 0.5

eq. of $[KGa(NArCH)_2(Et_2O)]_2$ (**1.44**) in C_6D_6 and its ^1H NMR spectrum confirmed its formation in the reaction of **21** with FpI. The synthesis of complex **37** was in turn scaled up to in moderate yield (54%) as a black solid.

Complex **37** exhibits a vinyl resonance at 6.52 ppm which is downfield compared to its parents $[KGa(NArCH)_2(Et_2O)]_2$ **1.44** (6.48 ppm) or $Mg(CzOx)\{Ga(NArCH)_2\}$ (**21**) (6.50 ppm) and any of the insertion derivatives of **21** and **22** presented thus far. The vinyl shift in **37** is consistent with the coordination of the Fp fragment to gallium and is comparable to that found in the Fe-Ga complex $[K(TMEDA)][Fe(CO)_4\{Ga(NArCH)_2\}]$ (**3.32**, 5.95 ppm, CD_3CN).[38] Additionally, the Cp fragment appears as a singlet at 3.97 ppm and is in the range of literature Fp[Ga] complexes, for example FpGa(dpp-bian) (**3.33**, 4.00 ppm)[39] or $FpGa(^tBu)_2$ (**3.34**, 4.13 ppm, toluene-d_8).[40] Compound **37** presents a resonance for the carbonyl ligands at 212.7 ppm in the $^{13}C\{^1H\}$ spectrum, which is comparable to the resonance for the same fragment in **3.32** (217.4 ppm, CD_3CN)[38] or **3.34** (216.1 ppm, toluene-d_8).[40] In the IR spectrum, complex **37** presents two strong bands positioned at 2010 cm^{-1} and 1953 cm^{-1}, corresponding to $\nu_{sym}(CO)$ and $\nu_{anti}(CO)$, respectively, characteristic of terminal carbonyls. This compares with the two bands observed for $FpB(NArCH)_2$ (1992 cm^{-1}, 1932 cm^{-1} (KBr)),[41] $FpC(NMesCH)_2$ (2049 cm^{-1}, 2004 cm^{-1} (CH_2Cl_2 solution)),[42] $FpGa(^tBu)_2$ (1980 cm^{-1}, 1928 cm-1 (CsI))[40] and $FpAl\{N(CMe_2CH_2)_2CH_2\}_2$ (1982 cm^{-1}, 1927 cm^{-1} (hexane solution)).[43]

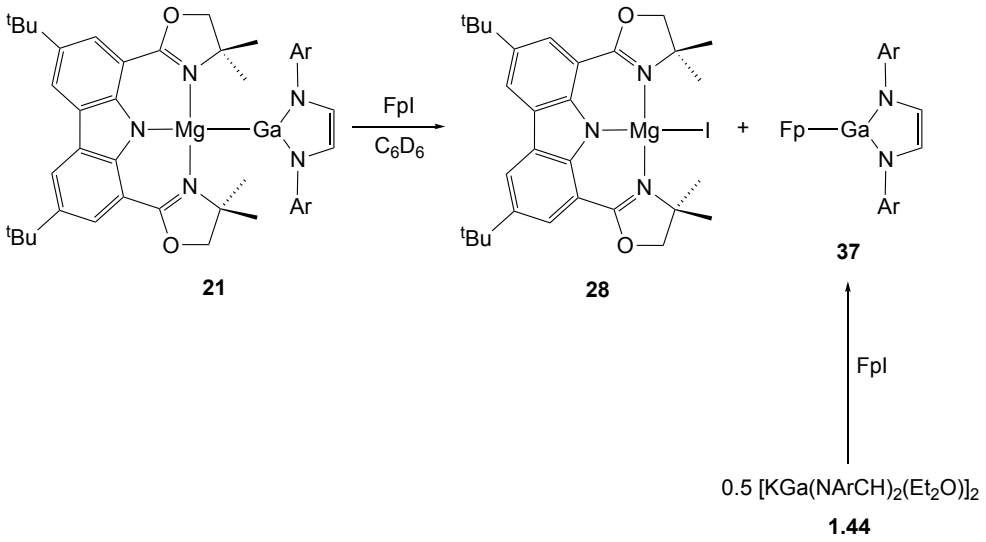

Scheme 3.8. Reaction of the $Mg(CzOx)\{Ga(NArCH)_2\}$ (**21**) complex with FpI and independent synthesis of the $FpGa(NArCH)_2$ (**37**) complex.

The reactivity of Mg(CzOx){Ga(NArCH)$_2$} (**21**) was further studied, this time with the Fp_2 dimer. Upon reaction of 1 equivalent of Fp_2 with **21** in C_6D_6, complex FpGa(NArCH)$_2$ **37** is formed along with a new species seemingly Mg(CzOx)Fp (**38**, Scheme 3.9). Subsequently, the independent synthesis of **38** was performed by reacting the base free Mg complex Mg(CzOx)I (**28**) and KFp in toluene giving a 63% yield. Upon isolation, the ^{1}H NMR spectrum of **28** corroborated its presence in the reaction of **21** with Fp_2. The THF adduct of **38**, Mg(CzOx)Fp(THF) (**38-THF**, Scheme 3.9), was observed by ^{1}H NMR after addition of 1 eq of THF to a fresh C_6D_6 solution of **28**. Alternatively, complex **38-THF** could be isolated (69% yield) from the reaction of Mg(CzOx)I(THF) (**3.14**) and KFp in toluene. The lack of a crystal structure for both **38** and **38-THF** makes difficult their structural assessment with regards to a direct Mg-Fe bond. However, both species present bands attributed to terminal carbonyls (**38**: 2014 cm^{-1} & 1959 cm^{-1}, **38-THF**: 2020 cm^{-1} & 1963 cm^{-1}) along with lower frequency bands in the 1700-1800 cm^{-1} region suggesting possible dimerisation or isocarbonyl linkages. Additionally, attempts to insert isopropyl carbodiimide were unsuccessful with both complexes, in contrast to other structurally authenticated complexes where direct Mg-Fe bonds have been observed.[44]

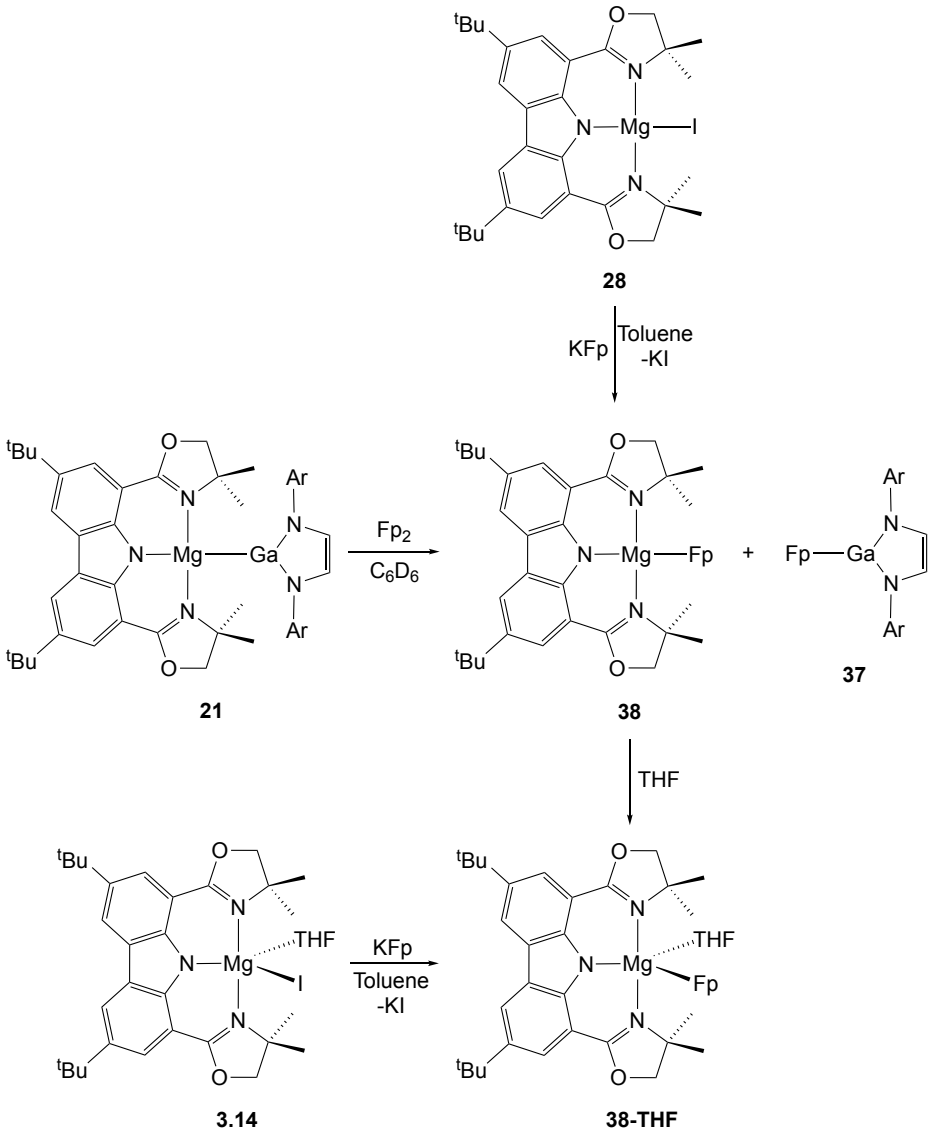

Scheme 3.9. Reaction of the Mg(CzOx){Ga(NArCH)$_2$} (**21**) complex with Fp_2 and independent synthesis of complexes Mg(CzOx)Fp (**38**) and Mg(CzOx)Fp(THF) (**38-THF**).

3.5 Conclusions

This Chapter has described the synthesis and reactivity of CzOx-supported Ae-Ga complexes. The use of the CzOx confers enhanced stability to these species in solution with respect to that of the ^{R}NacNac supported analogues. This has afforded the structural characterisation of a new Mg-Ga complex (**21**). In this species, the reactivity towards carbodiimides is dominated both by steric and electronic factors as observed by the lack of reactivity of complex **21** with TolNCNTol, in contrast with the successful reaction of **21** with CyNCNCy or the ^{R}NacNac supported analogue (**1**) with TolNCNTol, thus being the nucleophilicity of the carbodiimide determining in

its insertion into the Mg-Ga bond of **21**. A more feasible situation was found with the calcium variant of **21**, **22**, in which the steric hindrance of the system is reduced due to the larger atomic radius of Ca compared to Mg and the potential lability of the THF ligands. Along with the stability of Ae-Ga species, the CzOx ligand also afforded cleaner reactions than those obtained with the ^{R}NacNac ligand which translated into the structural authentication of products of the net insertion of carbodiimides into the Ca-Ga bond of **22** and the product of the oxygen abstraction of isobutene epoxide by the Mg-Ga bond of **21**. The stability of carbazolide supported Ae-Ga species in solution also offered a more varied reactivity than that of their ^{R}NacNac supported analogues resulting in the expansion of the study of the reactivity of **21** and **22** to cyclohexene- and norbornene epoxide, *tert*-butyl and phenyl azide, *tert*-butyl and ethyl isocyanate, azobenzene and Fp containing species. Of these, it is worthy of mention the reactions of **21** with cyclohexene- and norbornene epoxide which yielded the insertion of the epoxides rather than the oxygen abstraction product observed with isobutene epoxide.

3.6 References

1. M. Nakada and M. Inoue, *Heterocycles*, 2007, **72**, 133.
2. M. Inoue, T. Suzuki and M. Nakada, *J. Am. Chem. Soc.*, 2003, **125**, 1140.
3. T. Niwa and M. Nakada, *J. Am. Chem. Soc.*, 2012, **134**, 13538.
4. J. Zou, D. J. Berg, D. Stuart, R. McDonald and B. Twamley, *Organometallics*, 2011, **30**, 4958.
5. J. Zou, D. J. Berg, A. Oliver and B. Twamley, *Organometallics*, 2013, **32**, 6532.
6. B. Core, D. Phil Thesis, University of Oxford, 2015.
7. N. Grüger, H. Wadepohl and L. H. Gade, *Eur. J. Inorg. Chem.*, 2013, **2013**, 5358.
8. J. C. Ott, C. K. Blasius, H. Wadepohl and L. H. Gade, *Inorg. Chem.*, 2018, **57**, 3183.
9. J. Higuchi, S. Kuriyama, A. Eizawa, K. Arashiba, K. Nakajima and Y. Nishibayashi, *Dalton Trans.*, 2018, **47**, 1117.
10. H. B. Mansaray, M. Kelly, D. Vidovic and S. Aldridge, *Chem. Eur. J.*, 2011, **17**, 5381.

11. B. Cordero, V. Gomez, A. E. Platero-Prats, M. Reves, J. Echeverria, E. Cremades, F. Barragan and S. Alvarez, *Dalton Trans.*, 2008, 2832.
12. A. Seyboldt, B. Wucher, S. Hohnstein, K. Eichele, F. Rominger, K. W. Törnroos and D. Kunz, *Organometallics*, 2015, **34**, 2717.
13. L. M. A. Saleh, D. Phil Thesis, University of Oxford, 2014.
14. J. E. Huheey, E. A. Keiter and R. L. Keiter, *Inorganic Chemistry : Principles of Structure and Reactivity*, Harper Collins, New York, 4th edn., 1993.
15. O. Bonello, C. Jones, A. Stasch and W. D. Woodul, *Organometallics*, 2010, **29**, 4914.
16. D. Steinborn, T. Rüffer, C. Bruhn and F. W. Heinemann, *Polyhedron*, 1998, **17**, 3275.
17. D. A. Atwood, A. H. Cowley and R. A. Jones, *Organometallics*, 1993, **12**, 236.
18. C. Jones, D. P. Mills, J. A. Platts and R. P. Rose, *Inorg. Chem.*, 2006, **45**, 3146.
19. R. J. Baker, R. D. Farley, C. Jones, M. Kloth and D. M. Murphy, *J. Chem. Soc., Dalton Trans.*, 2002, 3844.
20. S. P. Green, C. Jones and A. Stasch, *Science*, 2007, **318**, 1754.
21. G. A. Pierce, S. Aldridge, C. Jones, T. Gans-Eichler, A. Stasch, N. D. Coombs and D. J. Willock, *Angew. Chem. Int. Ed.*, 2007, **46**, 2043.
22. S. P. Green, C. Jones and A. Stasch, *Angew. Chem. Int. Ed.*, 2008, **47**, 9079
23. M. Asay, C. Jones and M. Driess, *Chem. Rev.*, 2011, **111**, 354.
24. S. Nembenna, S. Singh, Sakya S. Sen, Herbert W. Roesky, H. Ott and D. Stalke, *Z. Anorg. Allg. Chem.*, 2011, **637**, 201.
25. S. Nembenna, H. W. Roesky, S. K. Mandal, R. B. Oswald, A. Pal, R. Herbst-Irmer, M. Noltemeyer and H.-G. Schmidt, *J. Am. Chem. Soc.*, 2006, **128**, 13056.
26. S. Sene, S. Bégu, C. Gervais, G. Renaudin, A. Mesbah, M. E. Smith, P. H. Mutin, A. van der Lee, J.-M. Nedelec, C. Bonhomme and D. Laurencin, *Chemistry of Materials*, 2015, **27**, 1242.
27. E. Bernabé-Pablo, V. Jancik and M. Moya-Cabrera, *Inorg. Chem.*, 2013, **52**, 6944.
28. M. H. Chisholm, D. Navarro-Llobet and J. Gallucci, *Inorg. Chem.*, 2001, **40**, 6506.

29. M. Veith, M. Burkhart and V. Huch, *Angew. Chem. Int. Ed.*, 2006, **45**, 5544.
30. S. P. Green, C. Jones, K. A. Lippert, D. P. Mills and A. Stasch, *Inorg. Chem.*, 2006, **45**, 7242.
31. T. Pott, P. Jutzi, B. Neumann and H.-G. Stammler, *Organometallics*, 2001, **20**, 1965.
32. S. A. Blum, P. J. Walsh and R. G. Bergman, *J. Am. Chem. Soc.*, 2003, **125**, 14276.
33. S. J. Bonyhady, S. P. Green, C. Jones, S. Nembenna and A. Stasch, *Angew. Chem. Int. Ed.*, 2009, **48**, 2973.
34. S. J. Bonyhady, C. Jones, S. Nembenna, A. Stasch, A. J. Edwards and G. J. McIntyre, *Chem. Eur. J.*, 2010, **16**, 938.
35. A. Stasch, *Angew. Chem. Int. Ed.*, 2014, **53**, 10200.
36. Y. Yang, M. D. Anker, J. Fang, M. F. Mahon, L. Maron, C. Weetman and M. S. Hill, *Chem. Sci.*, 2017, **8**, 3529.
37. C.-C. Chang, J.-H. Chen, B. Srinivas, M. Y. Chiang, G.-H. Lee and S.-M. Peng, *Organometallics*, 1997, **16**, 4980.
38. R. J. Baker, C. Jones and J. A. Platts, *Dalton Trans.*, 2003, 3673.
39. I. L. Fedushkin, V. G. Sokolov, V. M. Makarov, A. V. Cherkasov and G. A. Abakumov, *Russ. Chem. Bull.*, 2016, **65**, 1495.
40. X. He, R. A. Bartlett and P. P. Power, *Organometallics*, 1994, **13**, 548.
41. R. Frank, J. Howell, R. Tirfoin, D. Dange, C. Jones, D. M. P. Mingos and S. Aldridge, *J. Am. Chem. Soc.*, 2014, **136**, 15730.
42. L. Mercs, G. Labat, A. Neels, A. Ehlers and M. Albrecht, *Organometallics*, 2006, **25**, 5648.
43. B. N. Anand, I. Krossing and H. Nöth, *Inorg. Chem.*, 1997, **36**, 1979.
44. M. P. Blake, N. Kaltsoyannis and P. Mountford, *Chem. Commun.*, 2013, **49**, 3315.

Chapter Four

Synthesis and attempted reactivity of aluminium gallyl compounds

4.1 Overview

This Chapter describes the synthesis and attempted reactivity of Al-Ga complexes aiming to compare these with their counterparts of the same period presented in the previous chapters. An introductory section will briefly review all the literature complexes with unsupported Al-Ga interactions and their reactivity along with that of related species. The synthesis of the required aluminium bromide precursors and the structural characterisation of some of these species is then described. The further preparation of aluminium gallyl species and the structural authentication of three of these complexes is presented. The attempted reactivity will also be discussed.

4.2 Introduction

4.2.1 Al-Ga bonded complexes

To date, only four complexes with Al-Ga bonds have been reported, all which have been synthesised as donor-acceptor species. The first of these was prepared by Gorden *et. al.* in 2005 by reacting $Al(C_6F_5)_3$ with 1 eq. of Cp*Ga units in toluene to form the corresponding adduct (**4.1**, Figure 4.1).[1] In the solid state, two independent structures were contained in the asymmetric unit with Al-Ga bond distances of 2.5076(11) Å and 2.5229(11) Å which are longer than the sum of the respective covalent radii (2.43(5) Å).[2] Complexes **4.2** and **1.119** of Figure 4.1 were later isolated following a similar procedure by Schulz and co-workers.[3] Complex **1.119** has a longer Al-Ga bond distance (2.629(2) Å) than its previously reported analogue **4.1** which is consistent with the higher Lewis acidity of the $Al(C_6F_5)_3$ fragment in **4.1**. The longer Al-Ga bond distance in **1.119** also reflects the higher steric demand of $Al(^tBu)_3$ compared to $Al(C_6F_5)_3$. The Al-Ga bond distance in **4.2** (2.620(2) Å) is comparable to that of **1.119** (2.629(2) Å). In the ^1H NMR spectra, the ^{t}Bu resonace of **4.2** is shifted to lower field than in **1.119** as a consequence of Cp*Al being a stronger Lewis base than Cp*Ga. Indeed, a trend was found where the ^{t}Bu resonace shifts downfield with the basicity of the Cp*M' fragment in $M(^tBu)_3${Cp*M'} adducts of Group 13 metals presented in the same report. As expected, the geometries of the $M(^tBu)_3$ fragments deviate from planarity as a result of the donor-acceptor interaction. More recently, the preparation of $Ga(^{Dipp}NacNac)\{Al(C_6F_5)_3\}$ (**4.3**, Figure 4.1) has been reported.[4] The $Al(C_6F_5)_3$ fragment in **4.3** adopts a tetrahedral geometry around Al with an Al-Ga bond distance of 2.5482(4) Å which is intermediate between those of **4.1** and **1.119**.

The deviation of the Al-Ga bond distance in **4.3** from the sum of the covalent radii of Al and Ga (Alvarez: 2.43(5) Å,[2] Pyykkö: 2.50 Å[5]) is attributed to the electrostatic repulsion between the metal centres as a result of their high positive partial charges. The authors note that covalent radii are not helpful in the discussion of metal-metal bond distances in **4.3**.

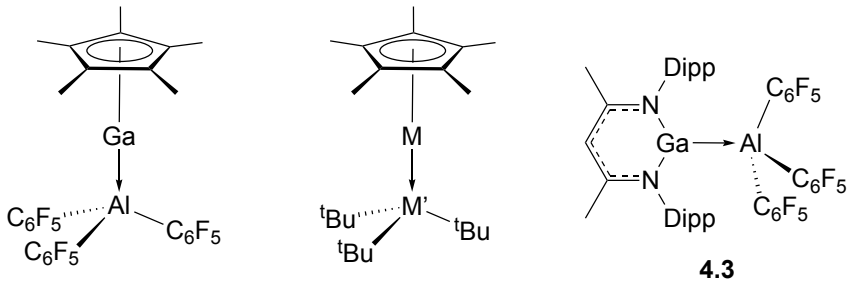

4.1 **1.119** M = Ga, M' = Al; **4.2** M = Al, M' = Ga **4.3**

Figure 4.1. Al-Ga bonded complexes[1, 3, 4]

4.2.2 Reactivity of Al-Ga and other Al-Group 13 bonded complexes

The reactivity of Al-Ga bonded species has only been reported with the aforementioned Ga(^{Dipp}NacNac){Al(C_6F_5)$_3$} (**4.3**) complex.[4] Complex **4.3** reacts with 1 equivalent of benzaldehyde to form complex **4.5** of Scheme 4.1 as a result of the non-innocence of the NacNac ligand. It is proposed that the insertion of PhCHO occurs in the early stages of the reaction to form complex **4.4** (Scheme 4.1) which then rearranges into **4.5**. No evidence for the formation of **4.4** was obtained, nonetheless, the Al-B analogue Ga(^{Dipp}NacNac){B(C_6F_5)$_3$} (**4.7**) could be isolated under the same conditions in which **4.4** is obtained. Heating of a solution of **4.5** forms the aluminium alkoxido complex [Al(C_6F_5)$_2$(μ-OCH$_2$Ph)]$_2$ (**4.6**, Scheme 4.1); however, the fate of the gallium heterocycle could not be determined.

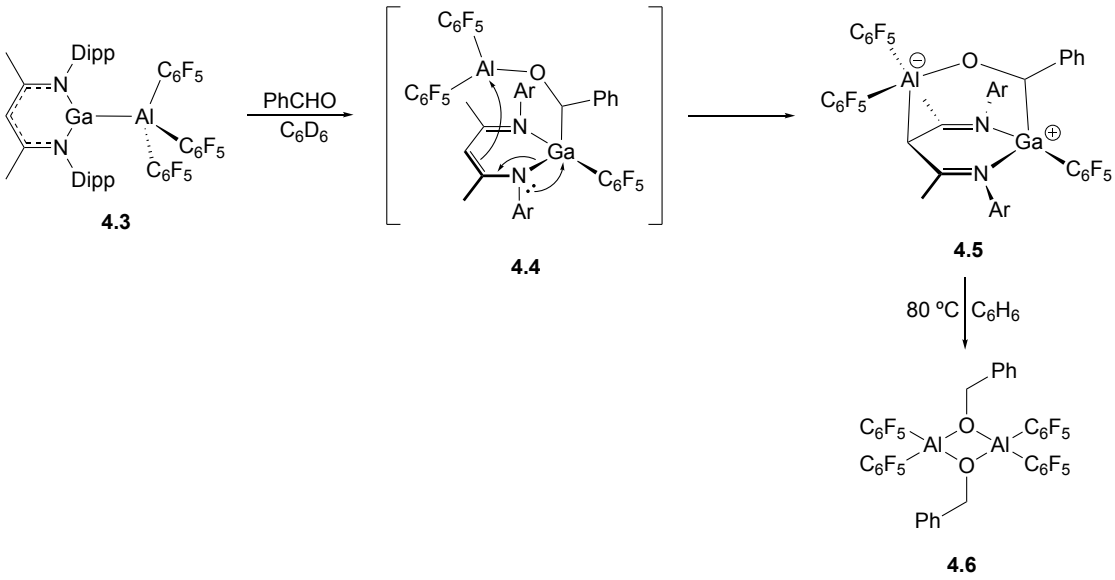

Scheme 4.1. Reactivity with Ga(^{Dipp}NacNac){Al(C_6F_5)$_3$} (**4.3**) with benzaldehyde.[4]

There are no other known reactions of complexes of aluminium bonded to gallium or heavier Group 13 elements. In contrast, the reactivity of Al-B and particularly Al-Al complexes have received great interest. In this context, one of the few reports on the reactivity of complexes containing unsupported Al-B bonds describes the coordination of the [Al{B(NArCH)$_2$}Me$_2$]$_2$ complex to trisalkyl lanthanide complexes (**4.7** and **4.8**, Equation 4.1).[6] The solid state structure of complex **4.9** was authenticated by X-ray diffraction revealing an hexamethyl coordination at the Lu centre. The Al-B bond distance elongates in **4.9** (2.153(3) Å average) with respect to its parent **4.7** (2.119(3) Å). The authors emphasise the terminal coordination of the boryl ligand as a result of the steric hindrance and the strong Al-B interaction, in contrast with other heteroaluminate complexes where the electronegative ligands, initially coordinated to aluminium in the starting materials, occupy bridging positions in the product. Other reactions of complexes containing unsupported Al-B involve the coordination of the Al centre to Fe[7] described in Chapter 1, coordination to complexes of rare earth elements[8, 9] or ligand displacement.[10] It is noteworthy that no reactions at the Al-B bond in these species, *e.g.,* insertions, have been reported.

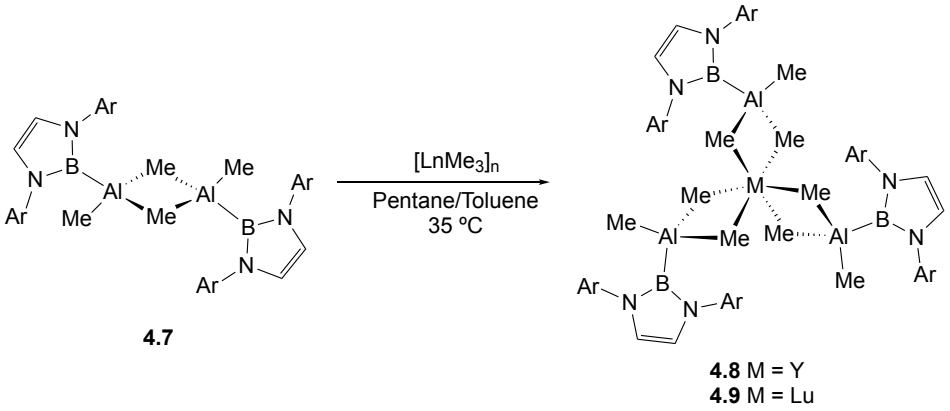

Equation 4.1[6]

The reactivity of the Al-Al complexes has been more widely explored than that of other Al-Group 13 complexes. In this context, Zhao and co-workers have reported the synthesis of an Al^{II}-Al^{II} complex (**4.10**) that can reduce azobenzene to form a bridged imido complex (**4.11**, Scheme 4.2).[11] In the formation of **4.11** the diazabutadiene ligand provides the electrons for the reduction of azobenzene yielding a diradical species. This reduction could be successfully applied to other non-symmetric azobenzene derivatives bearing methoxy- and dimethylamino substituents in *para* positions of one of the aromatic rings. The proposed mechanism for the reduction of azobenzene, supported by DFT calculations, suggests initial coordination of both of the N atoms of azobenzene to the Al centres, followed by cleavage of the N-N and Al-Al bonds and finalising with the isomerisation of the intermediate to form **4.11**. Later on, the same group reported the reactivity of **4.10** with stilbene and other alkenes. The reaction with stilbene with **4.10** yields the two-electron reduction of the alkene forming the corresponding insertion product **4.12** (Scheme 4.2). In **4.2**, the structural parameters determined by X-ray diffraction and the ^{1}H and ^{13}C NMR resonances of the inserted fragment are akin to those of an alkane consistent with the reduction of stilbene and the oxidation of Al. A similar reduction/insertion product is obtained when styrene is employed.

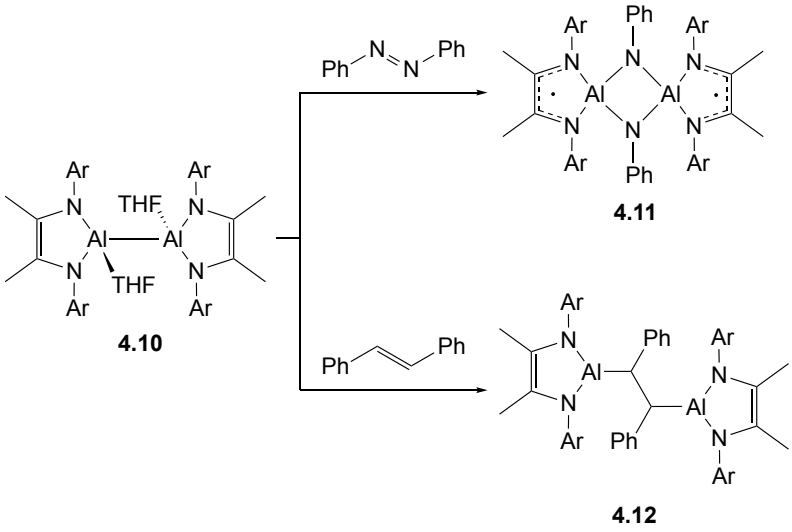

Scheme 4.2. Reactivity of an Al^{II}-Al^{II} complex (**4.10**) with azobenzene and stilbene in toluene.[11] Ar = Dipp.

Similar reactivity has been explored by Fedushkin *et al.* with the dialane [(Dipp-bian)Al]$_2$ (**4.13**, Scheme 4.3).[12] Upon reaction of **4.13** with phenylacetylene, the cycloaddition product (**4.14**, Scheme 4.3) is formed. The X-ray analysis of **4.14** confirmed the cycloaddition of the alkyne to **4.13**. In **4.14**, the Al-Al bond distance (2.600(1) Å) elongates with respect to **4.13** (2.522(1) Å), consistent with an increase in the coordination number of the Al atoms. Furthermore, heating of **4.14** in benzene, leads to the rearrangement of this complex with Al-Al bond cleavage. In going from **4.13** to **4.14**, the process can be seen as the oxidative addition of phenylacetylene to the Al-Al bond. The reduction of the alkyne involves the oxidation of the Al centres as well as the ligands which change their character from dianionic in **4.13** to diradical in **4.15**. The rearrangement of **4.14** to **4.15** is described to be governed by thermodynamic factors as the Al-C bonds are stronger than the Al-Al bond.

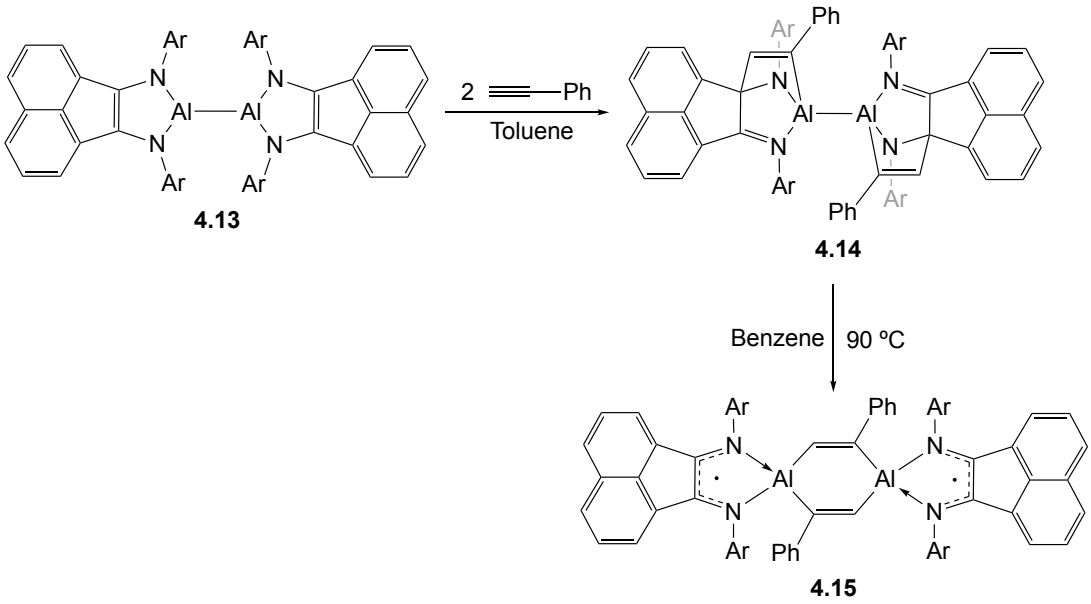

Scheme 4.3. Reactivity of the dialane [Al(Dipp-bian)]$_2$ (**4.13**) with phenylacetylene and further rearrangement of the cycloaddition product **4.14**.[12]

More recently, the activation of benzene with an Al^{II}-Al^{II} complex has been reported by Agou and co-workers.[13] The reduction of a dibromo-dialumane complex (**4.16**) in the presence of benzene yields the benzene adduct **4.17** (Equation 4.2). X-ray analysis of the crystals of **4.17** revealed 1,4-coordination of benzene. The interaction of benzene with the aluminium centres in **4.17** imposes folding of the aromatic ring. After dissolving **4.17** in C_6D_6, the signal for the coordinated C_6H_6 gradually disappears along with the increase of the resonance for free C_6H_6 consistent with an exchange between the coordinated C_6H_6 and C_6D_6. This exchange was observed with other aromatic hydrocarbons, namely, naphthalene and anthracene, forming the corresponding adducts.

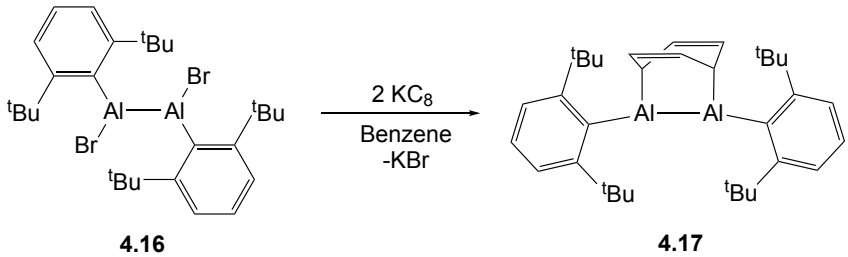

Equation 4.2[13]

4.3 Synthesis of aluminium amidinate complexes

After the study of the reactivity of Ae-Ga complexes described in Chapters 2 and 3, the formation of Al-Ga complexes and the study of their reactivity with small molecules was planned aiming to compare the structural properties and reactivity between both groups of complexes. Both aluminium and magnesium belong to the same period in the periodic table. However, their atomic properties such as covalent radius and electronegativity are rather different and those properties would confer different reactivities to the corresponding Mg-Ga and Al-Ga complexes.

Due to the lack of complexes with direct Al-Ga bonds, a proposed synthesis was conceived involving salt elimination in a manner similar to the Ae-Ga complexes described in the previous chapters. The possible formation of at least four-coordinate Al(III) complexes during the synthesis of Al-Ga complexes or their products suggested that the use of amidinates as supporting ligands due to their lower steric demand with respect to the previously employed ^{R}NacNac and carbazolide ligands and their facile preparation. The use of ligands with low steric demand are relevant with Al complexes due to its smaller covalent radius (1.21(4) Å) compared to Mg (1.41(7) Å).[2] Additionally, the reduction of the steric hindrance is particularly needed with the possibility of the formation of bis(gallyl) species when monoanionic ligands are supporting the Al centre.

Initial tests for the formation of Al-Ga species started with the synthesis of $Al\{(N^{i}Pr)_2CPh\}\{Ga(NArCH)_2\}_2$ (**46**) on the NMR tube scale *via* salt elimination between $[KGa(NArCH)_2(Et_2O)]_2$ (**1.44**) and the corresponding haloaluminium complexes $Al\{(N^{i}Pr)_2CPh\}X_2$ (X = Cl, Br) formed *in situ* (Equation 4.3). Overall, better selectivities and faster reaction times were observed with the use of $AlBr_3$ compared to $AlCl_3$. Therefore, the synthesis of the aluminium bromo amidinate complexes was envisaged. The synthesis of these species has not been reported as opposed to their chloride counterparts,[14-16] and hence the following sections describe their synthesis and characterisation.

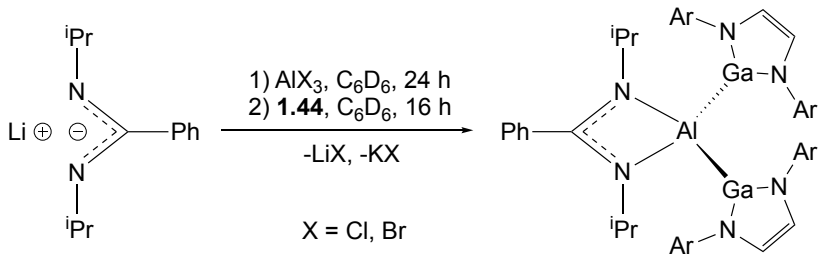

46

Equation 4.3

4.3.1 Synthesis of aluminium mono(amidinate) complexes

The synthesis of dibromo amidinate complexes with a series of steric and electronic modifications was performed by reactions between the lithium amidinates and $AlBr_3$ (Equation 4.4). The lithium amidinate Li{$(NCy)_2CPh$} (**4.20**)[17] necessary for the formation of Al{$(NCy)_2CPh$}Br_2 (**41**) was isolated as Li{$(NCy)_2CPh$}·0.3(Et_2O) (**4.20**·0.3(Et_2O)) according to NMR and elemental analyses. Consequently, the corresponding aluminium dibromoamidinate complex was isolated as the partial Et_2O solvate Al{$(NCy)_2CPh$}Br_2·0.3(Et_2O) (**41**·0.3(Et_2O)) (Equation 4.5). Both **4.20** and **41** could be structurally authenticated as base free species (*vide infra*). Complexes **39**, **40** and **41**·0.3(Et_2O) were isolated as white solids and exhibit one set of signals for the amidinate fragments in their ^1H NMR spectra, consistent with C_{2v}-symmetric species. The $^{13}C\{^1H\}$ spectra for these complexes present resonances for the NCN carbons in the range of 176.9-178.1 ppm in agreement with their chlorinated analogues.[14, 15] In the ^{27}Al spectra, complexes **39**, **40** and **41**·0.3(Et_2O) show a singlet in the 62.1-68.9 ppm range.

Crystals suitable for X-ray diffraction for **39** and **40** were obtained from saturated hexane solutions. Additionally, crystals of the base-free complexes **41** and **4.20** were also obtained by slow evaporation of hexane solutions of **41**·0.3(Et_2O) and **4.20**·0.3(Et_2O). The molecular structure and selected distances for these complexes are shown in Figures 4.2-4.6 and Tables 4.1-4.4.

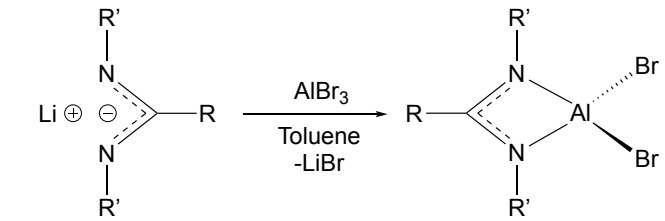

4.18 R = Me, R' = ^{i}Pr
4.19 R = Ph, R' = ^{i}Pr

39 R = Me, R' = ^{i}Pr
40 R = Ph, R' = ^{i}Pr

Equation 4.4

$$\text{Li}\{(\text{NCy})_2\text{CPh}\}\cdot 0.3(\text{Et}_2\text{O}) \xrightarrow[\text{Toluene}\ -\text{LiBr}]{\text{AlBr}_3} \text{Al}\{(\text{NCy})_2\text{CPh}\}\text{Br}_2\cdot 0.3(\text{Et}_2\text{O})$$

4.20·0.3(Et_2O) → **41**·0.3(Et_2O)

Equation 4.5

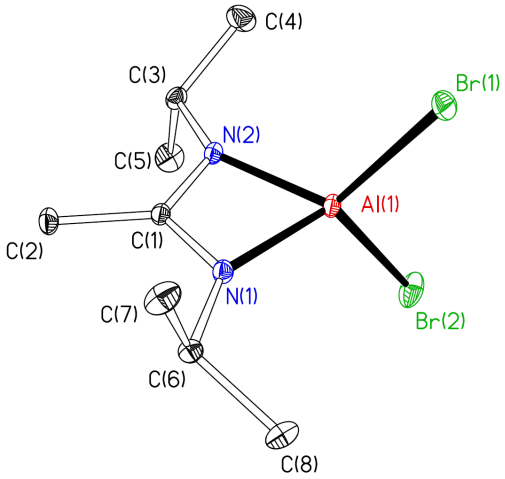

Figure 4.2. Displacement ellipsoid plot (20 % probability) of Al{(N^{i}Pr)$_2$CMe}Br$_2$ (**39**). H atoms omitted for clarity.

Table 4.1. Selected distances (Å) and angles (°) for Al{(N^{i}Pr)$_2$CPh}Br$_2$ (**39**).

Al(1)-Br(1)	2.2652(6)	N(2)-C(1)	1.335(2)
Al(1)-Br(2)	2.2634(6)	C(1)-C(2)	1.493(3)
Al(1)-N(1)	1.8739(16)	N(1)-C(6)	1.459(2)
Al(1)-N(2)	1.8784(17)	N(2)-C(3)	1.462(2)
N(1)-C(1)	1.335(2)		
Br(1)-Al(1)-Br(2)	110.93(2)	C(3)-N(2)-Al(1)	143.44(13)
N(1)-Al(1)-N(2)	71.20(7)	C(1)-N(1)-C(6)	125.54(16)
N(1)-Al(1)-Br(1)	117.34(6)	C(1)-N(2)-C(3)	125.74(16)
N(1)-Al(1)-Br(2)	117.64(6)	C(2)-C(1)-N(1)	125.46(17)
N(2)-Al(1)-Br(1)	119.83(6)	C(2)-C(1)-N(2)	124.73(18)
N(2)-Al(1)-Br(2)	115.01(6)	N(1)-C(1)-N(2)	109.80(16)
C(6)-N(1)-Al(1)	144.63(14)		

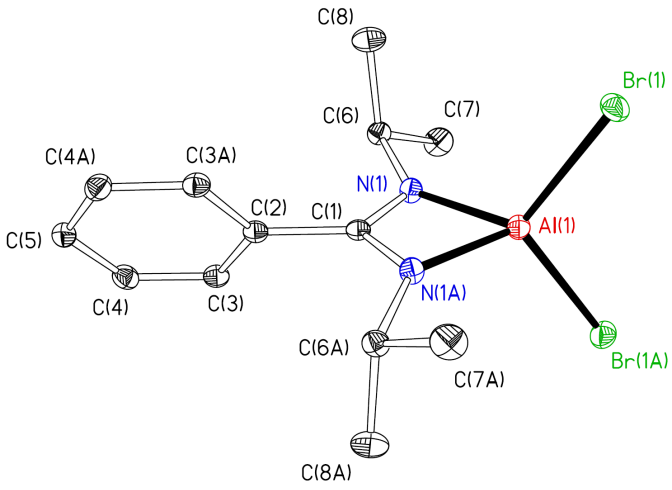

Figure 4.3. Displacement ellipsoid plot (20 % probability) of Al{(N^{i}Pr)$_2$CPh}Br$_2$ (**40**). Atoms carrying the suffix 'A' are related to their counterparts by the symmetry operator 1-x, y, ½-z. H atoms omitted for clarity.

Table 4.2. Selected distances (Å) and angles (°) for Al{(N^{i}Pr)$_2$CPh}Br$_2$ (**40**).

Al(1)-Br(1)	2.2673(8)	N(1)-C(6)	1.470(3)
Al(1)-N(1)	1.882(3)	C(1)-C(2)	1.480(5)
C(1)-N(1)	1.338(3)		
Br(1)-Al(1)-Br(1A)	111.23(5)	N(1A)-Al(1)-Br(1A)	116.75(8)
N(1)-Al(1)-N(1A)	71.49(14)	C(6)-N(1)-Al(1)	144.2(2)
N(1)-Al(1)-Br(1)	116.75(8)	C(1)-N(1)-C(6)	125.1(2)
N(1)-Al(1)-Br(1A)	117.82(7)	C(2)-C(1)-N(1)	124.76(17)
N(1A)-Al(1)-Br(1)	117.82(7)	N(1)-C(1)-N(1A)	110.5(3)

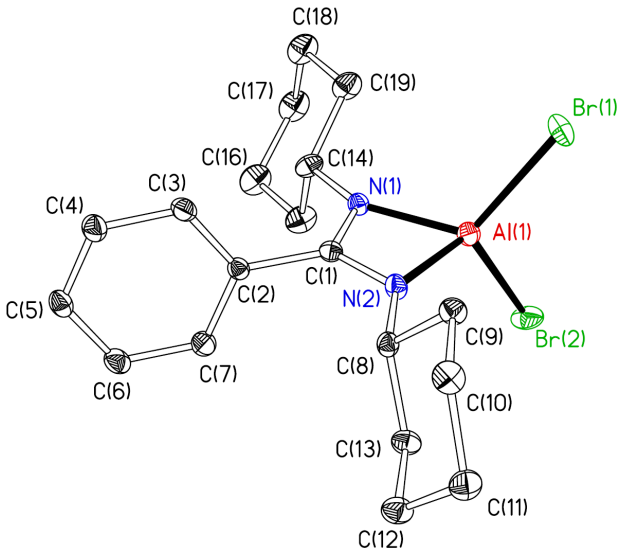

Figure 4.4. Displacement ellipsoid plot (20 % probability) of Al{(NCy)$_2$CPh}Br$_2$ (**41**). H atoms omitted for clarity.

Table 4.3. Selected distances (Å) and angles (°) for Al{(NCy)$_2$CPh}Br$_2$ (**41**).

Al(1)-Br(1)	2.2374(17)	N(2)-C(1)	1.329(6)
Al(1)-Br(2)	2.2739(17)	C(1)-C(2)	1.480(6)
Al(1)-N(1)	1.881(4)	N(1)-C(14)	1.448(7)
Al(1)-N(2)	1.852(4)	N(2)-C(8)	1.464(6)
N(1)-C(1)	1.329(6)		
Br(1)-Al(1)-Br(2)	110.85(7)	C(8)-N(2)-Al(1)	146.5(3)
N(1)-Al(1)-N(2)	72.25(17)	C(1)-N(1)-C(14)	126.4(4)
N(1)-Al(1)-Br(1)	118.51(14)	C(1)-N(2)-C(8)	124.9(4)
N(1)-Al(1)-Br(2)	114.75(14)	C(2)-C(1)-N(1)	124.0(4)
N(2)-Al(1)-Br(1)	119.81(16)	C(2)-C(1)-N(2)	124.2(4)
N(2)-Al(1)-Br(2)	115.96(17)	N(1)-C(1)-N(2)	111.8(4)
C(14)-N(1)-Al(1)	145.8(4)		

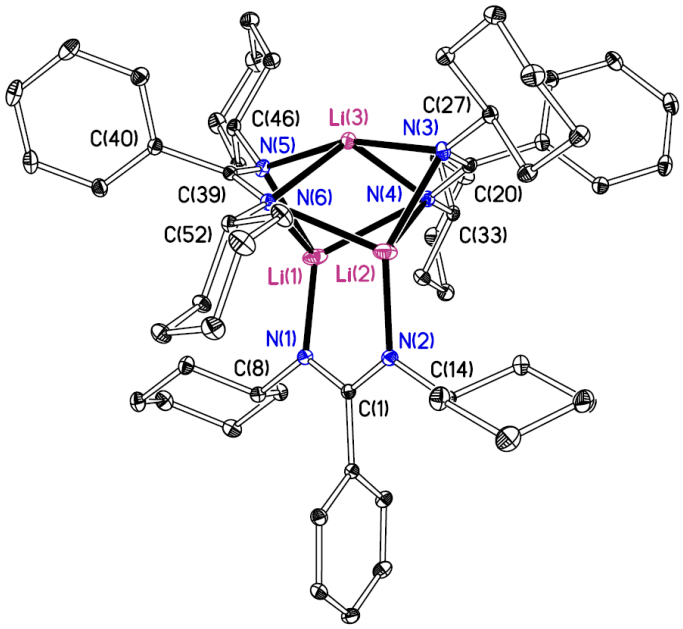

Figure 4.5. Displacement ellipsoid plot (20 % probability) of Li{(NCy)$_2$CPh} (**4.20**). H atoms omitted for clarity.

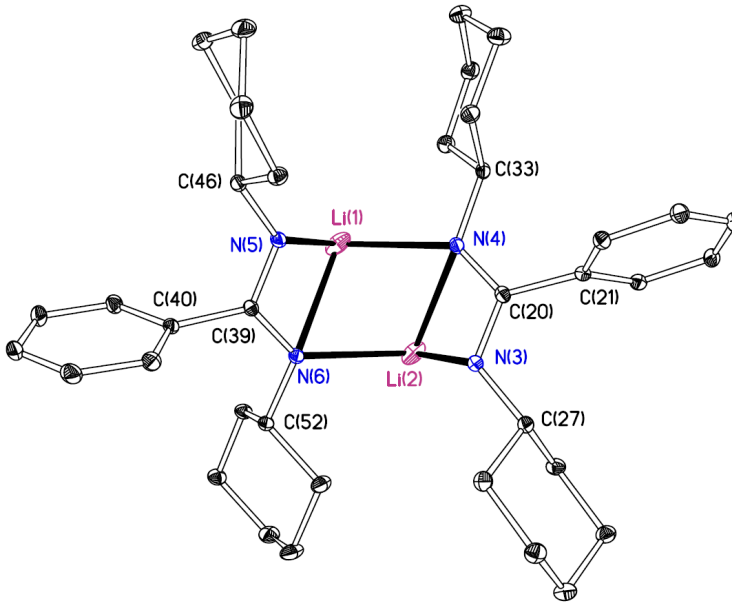

Figure 4.6. Displacement ellipsoid plot (20 % probability) of the $[Li(NCy)_2CPh]_2$ core of **4.20** viewed perpendicular to the approximate [N(3),N(4),N(5),N(6)] least-squares plane. Average deviation of atoms N(3)-N(6) from the plane = 0.385 ± 0.05 Å. H atoms omitted for clarity

Table 4.4. Selected distances (Å) and angles (°) for Li{$(NCy)_2CPh$} (**4.20**).

Li(1)-N(1)	1.952(2)	Li(3)-N(4)	2.095(2)
Li(1)-N(4)	2.457(2)	Li(3)-N(5)	2.114(2)
Li(1)-N(5)	2.018(3)	Li(3)-N(6)	2.119(2)
Li(1)-N(6)	2.402(2)	N(1)-C(1)	1.3253(13)
Li(2)-N(2)	1.988(2)	N(2)-C(1)	1.3321(13)
Li(2)-N(3)	2.136(2)	N(3)-C(20)	1.3383(13)
Li(2)-N(4)	2.396(3)	N(4)-C(20)	1.3304(13)
Li(2)-N(6)	2.355(3)	N(5)-C(39)	1.3392(13)
Li(3)-N(3)	2.107(2)	N(6)-C(39)	1.3310(13)
N(1)-Li(1)-N(4)	122.3(1)	N(4)-Li(2)-N(6)	96.99(9)
N(1)-Li(1)-N(5)	143.7(1)	N(3)-Li(3)-N(4)	65.31(7)
N(1)-Li(1)-N(6)	107.3(1)	N(3)-Li(3)-N(5)	160.3(1)
N(4)-Li(1)-N(5)	93.7(1)	N(3)-Li(3)-N(6)	105.42(9)
N(4)-Li(1)-N(6)	94.15(9)	N(4)-Li(3)-N(5)	102.28(9)
N(5)-Li(1)-N(6)	60.98(7)	N(4)-Li(3)-N(6)	115.2(1)
N(2)-Li(2)-N(3)	147.4(1)	N(5)-Li(3)-N(6)	64.75(7)
N(2)-Li(2)-N(4)	107.7(1)	N(1)-C(1)-N(2)	121.13(9)
N(2)-Li(2)-N(6)	115.1(1)	N(3)-C(20)-N(4)	116.33(9)
N(3)-Li(2)-N(4)	59.71(7)	N(5)-C(30)-N6(1)	116.18(9)
N(3)-Li(2)-N(6)	96.9(1)		

The X-ray structures of complexes **39**, **40** and **41** confirm their proposed formulations. All three species present distorted tetrahedral geometries around the aluminium centre formed by the bidentate amidinate and two bromine atoms. The Al-Br bond distances are in the range 2.2374(17)-2.2739(17) Å and are comparable to those found in related Al(N-N)Br_2 complexes, *e.g.,* [Al(en)Br_2][$AlBr_4$] 2.2467(16) Å and 2.2528(17) Å.[18] Expectedly, the Al-Br bond distances are longer than the Al-Cl distances in the chloride analogues consistent with the larger covalent radii of bromine with respect to chlorine.[14, 15] Other structural parameters of **39**, **40** and **41** are comparable to those of their chloride counterparts.

In the study of chloroamidinate aluminium complexes of the type $Al\{(NR')_2CR\}Cl_2$, Coles and co-workers found that the substituents in the amidinate carbon play an important role in the sterics of the complex.[15] The presence of sterically demanding substituents, *e.g., tert*-butyl, at the carbon of the amidinate, pushes the substituents of the nitrogen atoms towards the aluminium centre reducing the R'-N-Al and N-C-N angles. Consequently, the $Al\{(N^iPr)_2C^tBu\}Cl_2$ complex presents both narrower N-C-N (107.6(3)º) and Me_2HC-N-Al (135.8(3)º and 134.5(3)º) angles than its less sterically hindered counterpart $Al\{(N^iPr)_2C^tBu\}Cl_2$ (N-C-N: 109.7(2)º; Me_2HC-N-Al: 143.4(2)º and 143.9(2)º). In this context, the N(1)-C(1)-N(2) angles in **39** (109.80(16)º) and **40** (110.5(3)º) are comparable suggesting the similar steric demand of the methyl and phenyl fragments in the metallacycle. These similarities are also observed in the corresponding Me_2HC-N-Al angles of **39** (144.63(14)º and 143.44(13)º) and **40** (144.2(2)º) along with other parameters such as the N-C(1) and Al-Br bond distances. A more pronounced steric effect is observed with the presence of the cyclohexyl groups on the nitrogen atoms of complex **41** which increase the steric crowding in the vicinity of the aluminium centre. As a consequence, the N(1)-Al(1)-N(2) bite angle in **41** (72.25(17)º) is wider than in **39** (71.20(7)º) or **40** (71.49(14)º) which bear isopropyl substituents on the nitrogen atom. Additionally, the cyclohexyl rings are pushed towards the phenyl fragment in **41** resulting in the increase of the N(1)-C(1)-N(2) (111.8(4)º) and $(CH_2)_3HC$-N-Al (145.8(4)º and 146.5(3)º) angles and shortening of the N(1)-C(1) (1.329(6) Å) and N(2)-C(1) (1.329(6) Å) bond distances with respect to the equivalent parameters in **39** or **40**.

The solid state structure of base-free lithium amidinate **4.20** consists of three fused $Li(NCy)_2CPh$ moieties (Figure 4.5). A central dimeric $[Li(NCy)_2CPh]_2$ core (Figure 4.6) is capped on one face by Li(3) of the remaining $Li(NCy)_2CPh$ unit which bonds to atoms N(3)-N(6), and on the other face by the corresponding $(NCy)_2CPh$ group which bridges the Li(1)···Li(2) vector in an 'A-frame' manner. As a result, the N(1)-C(1)-N(2) angle (121.13(9)º) is significantly wider than the N(3)-C(20)-N(4) (116.33(9)º) and N(5)-C(30)-N6(1) (116.18(9)º) angles. However, the shortest Li-N bonds in the structure (Li(1)-N(1): 1.952(2) Å, Li(2)-N(2): 1.988(2) Å) are those of the C(1) amidinate due to the coordination of each nitrogen atom to only one lithium centre. This $[PhC(NCy)_2Li]_2$ motif is reminiscent of the structure of dimeric lithium amidinate complexes stabilised by Lewis bases, *e.g.,* $[Li\{(N^iPr)_2C^nBu\}(Et_2O)]_2$[19] or

$[Li\{(N^iPr)_2CCPh\}(THF)]_2$.[20] However, the presence of similar dimeric structures in base-free lithium amidinates and their aggregation into three moieties is rather uncommon.

4.3.2 Synthesis of aluminium bis(amidinate) complexes

In addition to the aforementioned complexes, the eventual formation of monogallyl complexes of aluminium was envisaged. As with the brominated mono(amidinates), the corresponding bis(amidinate) species have not been reported and hence these species were prepared following a similar procedure to that used in the synthesis of monoamidinates. Reaction of one equivalent of $AlBr_3$ with two equivalents of the corresponding lithium amidinate precursor yields the complexes $Al\{(NR')_2CR\}_2Br$ as depicted in Equation 4.6. As with $Al\{(NCy)_2CPh\}Br_2 \cdot 0.3(Et_2O)$ (**41**$\cdot 0.3(Et_2O)$) the formation of the corresponding bis(amidinate) complex was performed by using $Li\{(NCy)_2CPh\} \cdot 0.3(Et_2O)$ (**4.20**$\cdot 0.3(Et_2O)$). However, the Et_2O-free complex **44**, (Equation 4.6) was successfully isolated presumably as a result of the increased steric hindrance imposed by the four cyclohexyl substituents. In all cases, the salt metathesis reactions were completed in times between 20 to 24 h. The ^1H NMR spectra of complexes **42**-**44** suggest C_2 symmetry as only one set of signals is observed for the framework of the amidinato ligands. For instance, in the ^1H NMR spectrum of complex $Al\{(N^iPr)_2CMe\}_2Br$ (**42**, Equation 4.6) in C_6D_6, only one septet (3.40 ppm) and one doublet (1.26 ppm) corresponding to the isopropyl groups are observed. As mentioned, complex $Al\{(NCy)_2CPh\}_2Br$ (**44**) was isolated as a base-free species and crystals suitable for X-ray diffraction were grown from a saturated hexane solution. The molecular structure and selected distances and angles for complex **44** are shown in Figure 4.7 and Table 4.5.

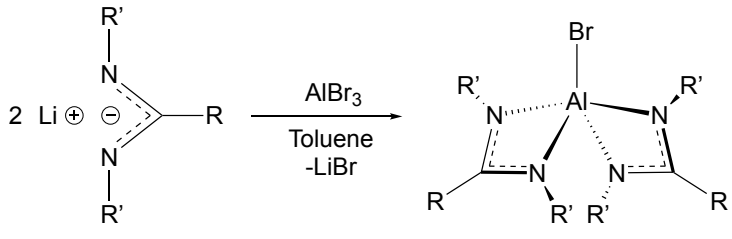

4.18 R = Me, R' = ^{i}Pr
4.19 R = Ph, R' = ^{i}Pr
4.20 R = Ph, R' = Cy

42 R = Me, R' = ^{i}Pr
43 R = Ph, R' = ^{i}Pr
44 R = Ph, R' = Cy

Equation 4.6. **4.20** used as **4.20**$\cdot 0.3(Et_2O)$

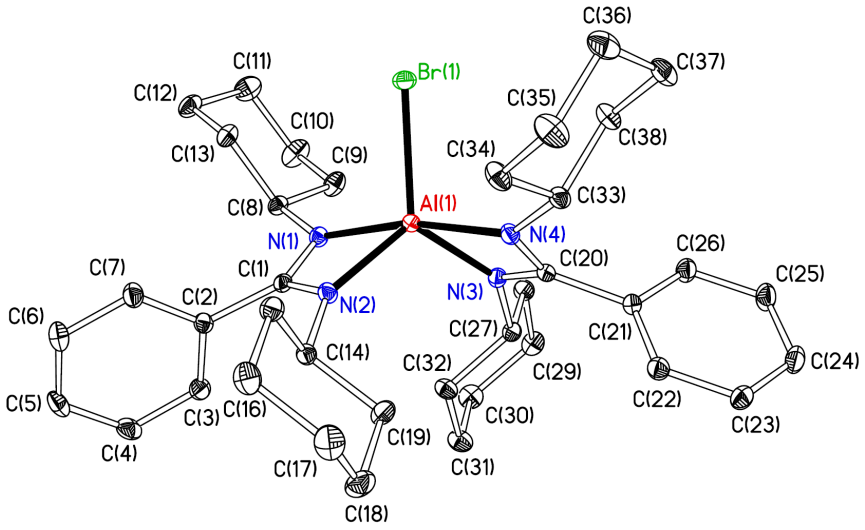

Figure 4.7. Displacement ellipsoid plot (20 % probability) of Al{(NCy)$_2$CPh}$_2$Br (**44**). H atoms omitted for clarity.

Table 4.5. Selected distances (Å) and angles (°) for Al{(NCy)$_2$CPh}$_2$Br (**44**).

Al(1)-Br(1)	2.3492(4)	C(20)-N(4)	1.3187(19)
Al(1)-N(1)	2.0110(13)	C(1)-C(2)	1.4932(19)
Al(1)-N(2)	1.9173(12)	C(20)-C(21)	1.4937(19)
Al(1)-N(3)	1.9182(13)	N(1)-C(8)	1.4673(19)
Al(1)-N(4)	1.9993(13)	N(2)-C(14)	1.4562(18)
C(1)-N(1)	1.3155(19)	N(3)-C(27)	1.4619(18)
C(1)-N(2)	1.3413(19)	N(4)-C(33)	1.4699(18)
C(20)-N(3)	1.3395(19)		
N(1)-Al(1)-Br(1)	95.86(4)	N(2)-Al(1)-N(3)	115.09(6)
N(2)-Al(1)-Br(1)	122.73(4)	C(8)-N(1)-Al(1)	146.34(10)
N(3)-Al(1)-Br(1)	122.18(4)	C(14)-N(2)-Al(1)	144.30(10)
N(4)-Al(1)-Br(1)	95.89(4)	C(27)-N(3)-Al(1)	142.07(10)
N(1)-Al(1)-N(2)	67.91(5)	C(33)-N(4)-Al(1)	145.84(10)
N(3)-Al(1)-N(4)	68.21(5)	N(1)-C(1)-N(2)	111.45(12)
N(1)-Al(1)-N(4)	168.22(6)	N(3)-C(20)-N(4)	111.52(12)

The X-ray structure depicted in Figure 4.7 confirms the proposed structure for complex **44**. This complex adopts a distorted trigonal bipyramidal geometry around

the aluminium centre formed by the two chelating amidinates and one bromine atom. Two nitrogen atoms from the amidinato ligands occupy the axial positions as expected for trigonal bipyramidal complexes while the most electronegative ligands occupy the axial positions.[21] The equatorial plane is thus formed by the remaining two nitrogen atoms and bromine. The Al(1)-Br(1) bond distance in **44** (2.3492(4) Å) is longer than those of the monoamidinate complex Al{(NCy)$_2$CPh}Br$_2$ (**41**, 2.2374(17) Å and 2.2379(17) Å), consistent with the higher coordination number of Al in **44**. The presence of the less electronegative Br in **44** slightly reduces the distortion compared to its chlorinated analogue Al{(NCy)$_2$CPh}$_2$Cl (**4.21**). Hence, the equatorial angle N(2)-Al(1)-Br(3) (115.09(6)º) increases with respect to that of **4.21** (112.73(8)º).[16] Similarly, the N(1)-Al(1)-N(4) axial bond angle (168.22(6)º) is slightly wider than that of Al{(NCy)$_2$CPh}$_2$Cl (167.92 (8)º).[16] As expected for complexes with trigonal bipyramidal geometry,[22] the axial Al(1)-N(1) (2.0110(13) Å) and Al(1)-N(4) (1.9993(13) Å) bonds are longer than the equatorial Al(1)-N(2) (1.9173(12) Å) and Al(1)-N(3) (1.9182(13) Å) bonds. Compared to its dibrominated analogue **41**, the presence of the two bulky amidinato ligands in **44** has a minimal steric effect on the structural parameters of the substituents on the nitrogen atoms of the amidinates and hence, the N(1)-C(1)-N(2) (111.45(12)º) and N(3)-C(20)-N(4) (111.52(12)º) angles are comparable to the N(1)-C(1)-N(2) angle of **41** (111.8(4)º).

4.3.3 Synthesis of aluminium bis(gallyl) complexes

Following the isolation of the dibrominated aluminium precursors, the synthesis of the corresponding aluminium bis(gallyl) species *via* salt elimination was attempted on the NMR tube scale. Addition of 1 eq. of [KGa(NArCH)$_2$(Et$_2$O)]$_2$ (**1.44**) to C_6D_6 solutions of the aluminium monoamidinate complexes resulted in the formation of red solutions and the precipitation of KBr (Equation 4.7). Compared to the synthesis of alkaline earth gallyl complexes described in the previous chapters, the formation of the amidinate supported aluminium gallyl species **45-47** proceeds over longer time periods, reaching completion after 10 to 16 h presumably as a result of the increased steric clash between the four Dipp groups of the gallyl ligands and the substituents of the amidinates.

The ^{1}H NMR spectra of complexes **45-47** show characteristic resonances for the vinyl protons of the gallyl fragments in the 6.28-6.32 ppm range which is upfield with respect to [KGa(NArCH)$_2$(Et$_2$O)]$_2$ (**1.44**) (6.48 ppm) and the Mg-Ga complexes

Mg(^{Dipp}NacNac){Ga(NArCH)$_2$}(THF) (**1**, 6.42 ppm) and Mg(CzOx){Ga(NArCH)$_2$} (**21**, 6.50 ppm). The observed upfield shift is consistent with the coordination of gallium in species **45-47** to a fragment more electronegative than potassium or magnesium. A similar effect was observed when carbodiimides were inserted into Mg-Ga, producing an upfield shift of the vinyl resonance due to the coordination of magnesium to carbon. In complexes **45-47** the resonances for the backbones of the amidinates exhibit upfield shifts with respect to those of their dibrominated precursors **39-41**. For instance, the methyl protons in Al{(N^{i}Pr)$_2$CPh}Br$_2$ (**40**) appear as a doublet (^3J = 4.2 Hz) centred at 0.96 ppm in C_6D_6 whereas in the bis(gallyl) complex Al{(N^{i}Pr)$_2$CPh}{Ga(NArCH)$_2$}$_2$ (**46**) the same protons resonate as a doublet (^3J = 6.3 Hz) at 0.27 ppm. The upfield shift of the resonances of the supporting ligand of aluminium are reminiscent of the same shift of the resonances of the ^{Dipp}NacNac ligand in the formation of the complex Mg(^{Dipp}NacNac){Ga(NArCH)$_2$}(THF) (**1**) described in Chapter 2. Complexes **45** and **46** could be isolated as orange solids in 32% and 43% yield, respectively. However, despite several attempts, complex **47** could not be isolated in a pure form and was hence characterised in solution. Fortunately, a few crystals of **47** suitable for X-ray diffraction were obtained by slow evaporation of the mixture containing this complex. The molecular structure and selected distances and angles for complex **47** are shown in Figure 4.8 and Table 4.6.

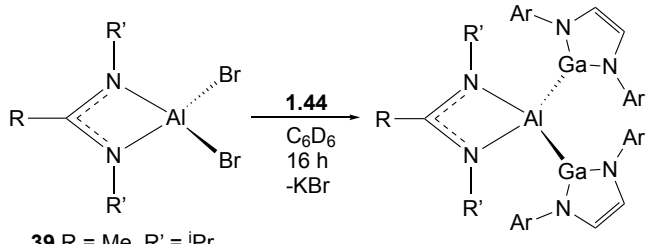

39 R = Me, R' = ^{i}Pr
40 R = Ph, R' = ^{i}Pr
41 R = Ph, R' = Cy

45 R = Me, R' = ^{i}Pr
46 R = Ph, R' = ^{i}Pr
47 R = Ph, R' = Cy

Equation 4.7

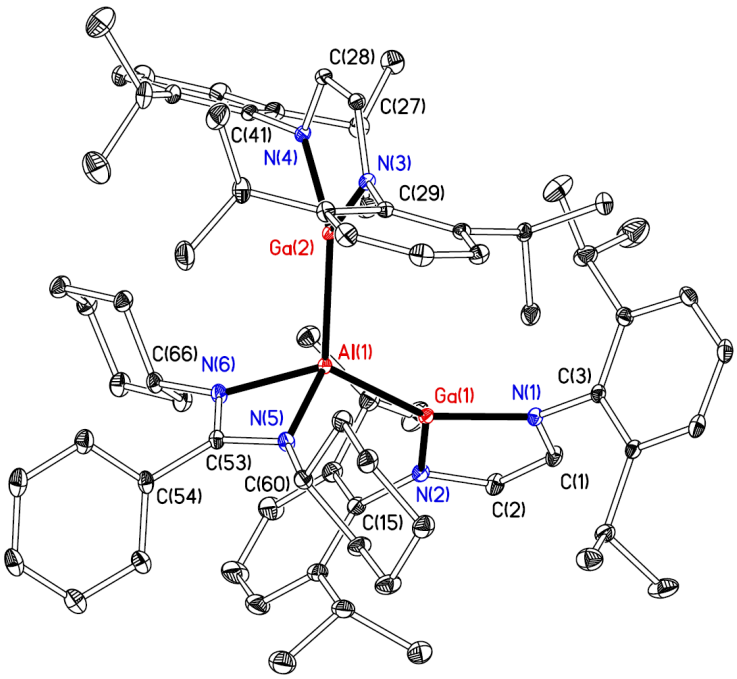

Figure 4.8. Displacement ellipsoid plot (20 % probability) of Al{(NCy)$_2$CPh}{Ga(NArCH)$_2$}$_2$ (**47**). H atoms and disorder omitted for clarity.

Table 4.6. Selected distances (Å) and angles (°) for Al{(NCy)$_2$CPh}{Ga(NArCH)$_2$}$_2$ (**47**).

Al(1)-Ga(1)	2.4829(7)	N(5)-C(60)	1.445(3)
Al(1)-Ga(2)	2.4727(7)	N(6)-C(66)	1.458(3)
Al(1)-N(5)	1.933(2)	Ga(1)-N(1)	1.876(2)
Al(1)-N(6)	1.923(2)	Ga(1)-N(2)	1.881(2)
C(53)-N(5)	1.346(3)	Ga(2)-N(3)	1.8750(19)
C(53)-N(6)	1.335(3)	Ga(2)-N(4)	1.8768(19)
Ga(1)-Al(1)-Ga(2)	121.82(3)	N(1)-Ga(1)-N(2)	87.33(9)
Ga(1)-Al(1)-N(5)	114.30(8)	C(1)-N(1)-Ga(1)	109.29(16)
Ga(1)-Al(1)-N(6)	115.80(8)	C(2)-N(2)-Ga(1)	109.68(17)
Ga(2)-Al(1)-N(5)	113.11(8)	N(3)-Ga(2)-N(4)	87.64(9)
Ga(2)-Al(1)-N(6)	110.67(8)	C(27)-N(3)-Ga(2)	109.54(15)
N(5)-Al(1)-N(6)	69.96(10)	C(28)-N(4)-Ga(2)	109.45(15)
N(5)-C(53)-N(6)	111.1(2)		

The solid state structure of complex **47** confirms its proposed structure. This complex presents a distorted tetrahedral geometry around the aluminium centre formed by two gallyl fragments and the bidentate amidinato ligand. Complex **47** represents the first complex with direct Al-Ga bonds as opposed to previously reported donor-acceptor species.[1, 3, 4] Both Al-Ga bonds in **47** are similar in distance (2.4829(7) Å and 2.4727(7) Å) and comparable to the sum of the Al and Ga covalent radii (2.43(5) Å).[2] Additionally, complex **47** contains the shortest Al-Ga bond distances observed to date, presumably due to the direct Al-Ga interaction. Previously, the shortest Al-Ga bond distance (2.5076(11) Å) was found in the donor-acceptor complex $Al(C_6F_5)_3GaCp^*$ (**4.1**, *vide supra*),[1] which contains the highly acidic $Al(C_6F_5)_3$ fragment. The tetrahedral geometry around the Al centre in **4.17** is noticeably more distorted than that of the parent $Al\{(NCy)_2CPh\}Br_2$ (**41**). For instance, the presence of the bulky gallyl fragments in **47** results in a Ga(1)-Al(1)-Ga(2) angle (121.82(3)º) considerably wider than the equivalent Br(1)-Al(1)-Br(1A) angle (111.23(5)º) in the dibromide precursor $Al\{(NCy)_2CPh\}Br_2$ (**41**). Additionally, the steric hindrance imposed by the presence of the gallyl moieties results in a narrower N(5)-Al(1)-N(6) bite angle (69.96(10)º) of the amidinate when compared to the N(1)-Al(1)-N(2) angle (72.25(17)º) in the parent complex **41**. This results in the elongation of the Al(1)-N(5) (1.933(2) Å) and Al(1)-N(6) (1.923(2) Å) bond distances in **47** with respect to the equivalent Al(1)-N(1)(1.881(4) Å) and Al(1)-N(2) (1.852(4) Å) distances in **41**. The gallacycles in **47** adopt inequivalent orientations with respect to the amidinate. For instance, the C(53)-Al(1)-Ga(1)-N(1) torsion angle is -138.2º whereas the C(53)-Al(1)-Ga(2)-N(3) torsion angle is 86.9º. These different orientations allow for the system to accommodate the isopropyl fragments of the Ga(1) gallacycle either between the isopropyl substituents of the Ga(2) gallyl or between the cyclohexyl substituents and the remaining isopropyl fragments of the Ga(2) gallacycle thus minimising the steric clash between all the *N*-substituents of the complex. Similar conformations are present in related tetrahedral bis(gallyl) species containing the $Ga(NArCH)_2$ fragment, e.g., $Zn(TMEDA)\{Ga(NArCH)_2\}_2$,[23] $Fe(TMEDA)\{Ga(NArCH)_2\}_2$[24] and $Pt(PEt_3)_2\{Ga(NArCH)_2\}_2$.[25] Both N(1)-Ga(1)-N(2) (87.33(9)º) and N(3)-Ga(2)-N(4) (87.64(9)º) angles are comparable and expectedly wider than that of $[KGa(NArCH)_2(Et_2O)]_2$ (**1.44**, 81.88(9)º)[26] or the Mg-Ga complexes $Mg(^{Dipp}NacNac)\{Ga(NArCH)_2(\kappa^1\text{-TMEDA})$ (**2.19**, 85.55(6)º)[27] and

Mg(CzOx){Ga(NArCH)$_2$(THF) (**21-THF**, 84.05(14)º) as a result of the coordination of gallium to aluminium being more electronegative than potassium or magnesium.

4.3.4 Synthesis of aluminium mono(gallyl) complexes

In a similar manner to the aforementioned bis(gallyl) species, the synthesis of aluminium mono(gallyl) species was attempted on the NMR tube scale. Addition of 0.5 eq. of [KGa(NArCH)$_2$(Et$_2$O)]$_2$ (**1.44**) to C_6D_6 solutions of 1 eq. of the aforementioned bis(amidinate) complexes results in the formation of red solutions and the precipitation of KBr (Equation 4.8). As with the formation of aluminium bis(gallyl) complexes, the full completion of these reactions was reached in *ca.* 16 h, which is considerably longer than the reactions yielding Ae-Ga species completed in 1 h. The ^{1}H NMR spectra of complexes **48-50** shows only one set of signals for both the amidinate and gallyl backbones suggesting C_2 symmetry. The vinyl resonances for these species appears in the 6.43-6.47 ppm range which is downfield with respect to their aluminium bis(gallyl) counterparts and comparable to the shifts observed in Ae-Ga species (*vide supra*). As with the aforementioned aluminium bis(gallyl) complexes, the resonances for the amidinate ligands shifts upfield with respect to the brominated percursors upon formation of the mono(gallyl) complexes. Compounds **48-50** could be successfully isolated as orange solids in 28-39% yield. Additionally, diffraction-quality crystals of **49** were grown from a concentrated benzene solution, in which all three **48-50** are highly soluble. The molecular structure and selected distances and angles are shown in Figure 4.9 and Table 4.6.

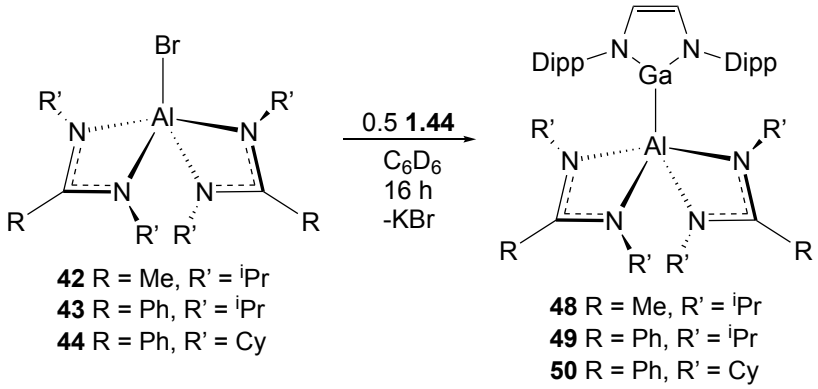

42 R = Me, R' = ^{i}Pr
43 R = Ph, R' = ^{i}Pr
44 R = Ph, R' = Cy

48 R = Me, R' = ^{i}Pr
49 R = Ph, R' = ^{i}Pr
50 R = Ph, R' = Cy

Equation 4.8

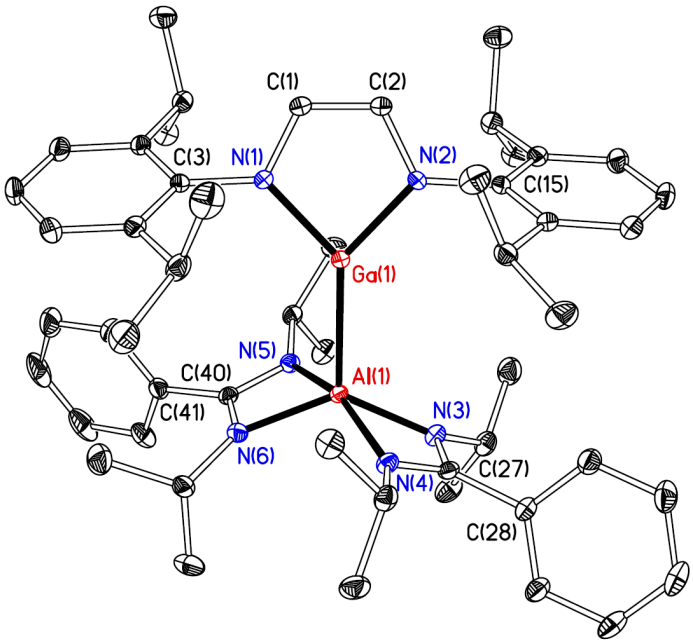

Figure 4.9. Displacement ellipsoid plot (20 % probability) of Al{(N^{i}Pr)$_2$CPh}$_2${Ga(NArCH)$_2$} (**49**). H atoms omitted for clarity.

Table 4.7. Selected distances (Å) and angles (°) for Al{(N^{i}Pr)$_2$CPh}$_2${Ga(NArCH)$_2$} (**49**).

Al(1)-Ga(1)	2.5015(5)	C(40)-N(6)	1.343(2)
Al(1)-N(3)	1.9308(14)	C(27)-C(28)	1.497(2)
Al(1)-N(4)	2.0229(13)	C(40)-C(41)	1.491(2)
Al(1)-N(5)	2.0314(14)	Ga(1)-N(1)	1.8970(11)
Al(1)-N(6)	1.9076(16)	Ga(1)-N(2)	1.8880(14)
C(27)-N(3)	1.335(2)	N(1)-C(1)	1.395(2)
C(27)-N(4)	1.316(2)	N(2)-C(2)	1.397(2)
C(40)-N(5)	1.322(2)	C(1)-C(2)	1.349(2)
N(3)-Al(1)-Ga(1)	116.41(5)	N(4)-Al(1)-N(6)	103.38(6)
N(4)-Al(1)-Ga(1)	103.60(4)	N(3)-C(27)-N(4)	111.36(14)
N(5)-Al(1)-Ga(1)	95.67(4)	N(5)-C(40)-N(6)	110.54(14)
N(6)-Al(1)-Ga(1)	111.93(5)	N(1)-Ga(1)-N(2)	86.28(7)
N(3)-Al(1)-N(4)	67.21(6)	Ga(1)-N(1)-C(1)	110.21(11)
N(5)-Al(1)-N(6)	67.50(6)	Ga(1)-N(2)-C(2)	110.79(11)
N(3)-Al(1)-N(5)	105.31(6)		

Complex Al{(N^{i}Pr)$_2$CPh}$_2${Ga(NArCH)$_2$} (**49**) exhibits a distorted trigonal bipyramidal geometry around the aluminium centre formed by two bidentate amidinate ligands and one gallyl ligand. Comparable to Mg(CzOx){Ga(NArCH)$_2$} (**21**), and as expected for a complex with a trigonal bipyramidal geometry, the most electronegative atoms occupy axial positions whereas the less electronegative groups, including gallyl, lie in the equatorial plane. The increase of the coordination number of aluminium in **49** with respect to Al{(NCy)$_2$CPh}{Ga(NArCH)$_2$}$_2$ (**47**), results in a slightly longer Al-Ga bond (2.5015(5) Å) with respect to those of **47** (2.4829(7)Å and 2.4727(7) Å). Despite this, the Al(1)-Ga(1) bond distance of **49** is still shorter than that of the donor-acceptor complex Al(C$_6$F$_5$)$_3$GaCp* (**4.1,** 2.5076(11) Å), [1] which, as mentioned, possesses the shortest Al-Ga bond distance reported to date. Expectedly, the axial Al-N bond distances (Al(1)-N(4): 2.0229(13) Å; Al(1)-N(5) 2.0314(14) Å) are longer that those of the equatorial ones (Al(1)-N(3): 1.9308(14); Al(1)-N(6): 1.9076(16)). The N(1)-Ga(1)-N(2) (86.28(7)º) angle of **49** is narrower than those

found in its bis(gallyl) analogue **47** (110.21(11)º and 110.79(11)º) although wider than that of its precursor $[KGa(NArCH)_2(Et_2O)]_2$ (**1.44**, 81.88(9)º)[26] or the Mg-Ga complexes $Mg(^{Dipp}NacNac)\{Ga(NArCH)_2(\kappa^1\text{-TMEDA})$ (**2.19**, 85.55(6)º)[27] and $Mg(CzOx)\{Ga(NArCH)_2(THF)$ (**21-THF**, 84.05(14)º). Along with **47**, complex **49** adds up to the first structurally authenticated complexes with direct Al-Ga bonds.

4.4 Synthesis of ^{R}NacNac supported aluminium gallyl complexes

After the isolation of the aforementioned aluminium gallyl complexes supported by amidinate ligands, the synthesis of Al-Ga species was expanded to the use of the ^{R}NacNac ligands. This is of particular interest in order to have a more direct comparison to the Mg-Ga complexes presented in this Thesis, *i.e.,* $Mg(^{Dipp}NacNac)\{Ga(NArCH)_2\}(THF)$ (**1**) or the literature complex $Mg(^{Dipp}NacNac)\{Ga(NArCH)_2\}(\kappa^1\text{-TMEDA})$ (**2.19**).[27] To do this, the use of ^{Dipp}NacNac and its less hindered analogue ^{Ph}NacNac were chosen as supporting frameworks for the aluminium centre. The preparation of one of the required precursors, $Al(^{Dipp}NacNac)Br_2$ (**4.22**), has been reported in the literature,[28] but not so that of $Al(^{Ph}NacNac)Br_2$; therefore, the following sections describe its preparation and the further synthesis of the ^{R}NacNac supported aluminium gallyl complexes.

4.4.1 Synthesis of $Al(^{Ph}NacNac)Br_2$

The synthesis of complex $Al(^{Ph}NacNac)Br_2$ (**51**) was performed by the salt elimination reaction of $K(^{Ph}NacNac)$[29] with $AlBr_3$ in toluene (Equation 4.9). After stirring for 16 h at RT and work up, **51** was isolated as a white solid in 64% yield. The ^{1}H NMR spectrum of **51** in C_6D_6 exhibits only one set of signals suggesting a C_{2v} symmetry. Additionally, the resonance for the γ-H of **51** appears as a sharp singlet at 4.69 ppm which is comparable to its analogue $Al(^{Dipp}NacNac)Br_2$ (**4.22**, 4.96 ppm).[28] Crystals of **51** suitable for X-ray diffraction could be grown from a concentrated benzene solution. The molecular structure and selected distances and angles are shown in Figure 4.10 and Table 4.8.

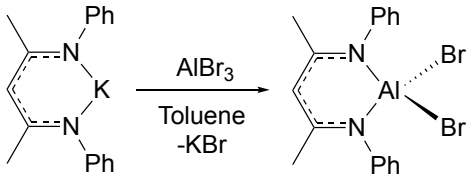

51

Equation 4.9

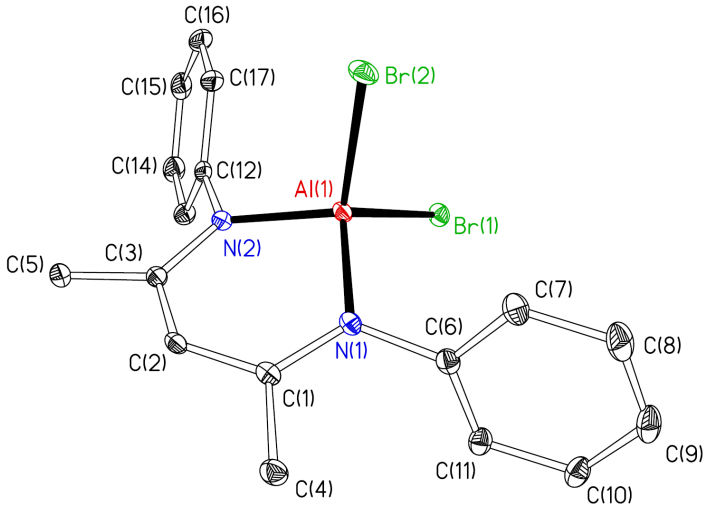

Figure 4.10. Displacement ellipsoid plot (20 % probability) of Al(^{Ph}NacNac)Br$_2$ (**51**). H atoms omitted for clarity.

Table 4.8. Selected distances (Å) and angles (°) for Al(^{Ph}NacNac)Br$_2$ (**51**).

Al(1)-Br(1)	2.2719(7)	Al(1)-N(1)	1.861(2)
Al(1)-Br(2)	2.3049(7)	Al(1)-N(2)	1.864(2)
Br(1)-Al(1)-Br(2)	111.42(3)	Br(2)-Al(1)-N(1)	109.85(7)
Br(1)-Al(1)-N(1)	112.25(7)	Br(2)-Al(1)-N(2)	110.42(7)
Br(1)-Al(1)-N(2)	112.03(7)	N(1)-Al(1)-N(2)	100.37(10)

Complex **51** exhibits a distorted tetrahedral geometry around Al formed by the bidentate ^{Ph}NacNac ligand and two Br atoms. Similar to other ^{R}NacNac Group 13 complexes,[30] the C_3N_2 ring fragment is almost planar and the aluminium centre lies out of the plane formed by the C_3N_2 fragment. The Al(1)-Br(1) and Al(1)-Br(2) bond distances (2.2719(7) Å and 2.3049(7) Å, respectively) of **51** are comparable to those of the only reported dibromo ^{R}NacNac aluminium complex Al(^{C_6F_5}NacNac)Br$_2$ (**4.23**, 2.267(1) Å and 2.271(1) Å)[31] and the related complex Al(^{Dipp}NacNac)(μ-Br){(μ-

$^{t\text{Bu}}$N)Nb($^{t\text{Bu}}$N)Br$_2$} (**4.24**, 2.3329(1) Å).[32] Likewise, the bite angle in **51** (100.37(10)º) is comparable to those of **4.23** (94.00(9)º),[31] **4.24** (99.31(12)º)[32] and the $^{\text{Dipp}}$NacNac aluminium dihalides Al($^{\text{Dipp}}$NacNac)Cl$_2$ (4.25, 99.36(4)º)[30] and Al($^{\text{Dipp}}$NacNac)I$_2$ (4.26, 99.9(1)º).[30]

4.4.2 Synthesis of Al($^{\text{Ph}}$NacNac){Ga(NArCH)$_2$}$_2$

Following the synthesis of Al($^{\text{Ph}}$NacNac)Br (**51**), the synthesis of the corresponding aluminium gallyl complexes was performed adapting the methodology used for the aforementioned aluminium (mono)amidinates. Addition of a C_6D_6 solution of 1eq. of [KGa(NArCH)$_2$(Et$_2$O)]$_2$ (**1.44**) to a C_6D_6 solution of **51** resulted in the formation of a dark red suspension. A new set of signals appeared in the ^{1}H NMR spectrum of the mixture consistent with the formation of the desired bis(amidinate) complex (52, Equation 4.10) whose formation from **51** and **1.44** was completed within 1 h. The integration for the resonance of the vinyl proton of **52** is four times higher than that of its γ-H suggesting substitution of both bromine atoms. This vinyl proton (6.23 ppm) is comparable to the range found in the bis(gallyl) complexes **45**-**47** (6.28-6.32 ppm) and expectedly shifted to high field with respect to the precursor [KGa(NArCH)$_2$(Et$_2$O)]$_2$ (**1.44**) (6.48 ppm) and the magnesium complex Mg($^{\text{Dipp}}$NacNac){Ga(NArCH)$_2$}(THF) (**1**, 6.42 ppm) or Mg($^{\text{Dipp}}$NacNac){Ga(NArCH)$_2$}(TMEDA) (**2.19**, 6.26 ppm).[27] Due to its extremely high solubility in hydrocarbons and despite several attempts, complex **52** could not be isolated in a pure form and was therefore only characterised spectroscopically in solution.

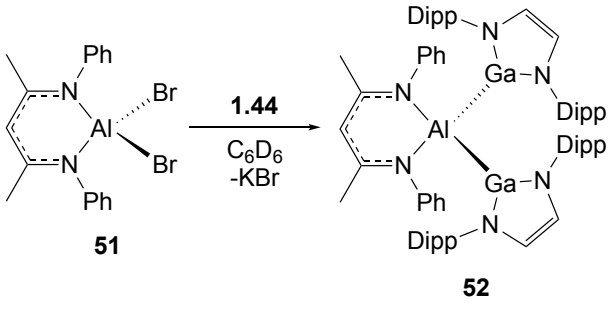

Equation 4.10

4.4.3 Synthesis of Al(^{Dipp}NacNac){Ga(NArCH)$_2$}Br

Similarly to the synthesis of **51**, addition of a C_6D_6 solution of 1 eq. of [KGa(NArCH)$_2$(Et$_2$O)]$_2$ (**1.44**) to a C_6D_6 solution of Al(^{Dipp}NacNac)Br$_2$ (**4.22**), resulted in the formation of a dark red suspension. However, 0.5 eq. of **1.44** did not appear to react even after 48 h at RT or heating the NMR tube at 80 ºC for 16 h, suggesting the substitution of only one bromide ligand in **4.22**. This was confirmed after reacting **1.44** with **4.22** in a 1:2 ratio, resulting in the clean formation of Al(^{Dipp}NacNac){Ga(NArCH)$_2$}Br (**53**, Equation 4.11). The formation of **53** and the impossibility to access a bis(gallyl) complex with **4.22** is seemingly due to the steric hindrance imposed by the isopropyl substituents of the ^{Dipp}NacNac ligand. The vinyl resonance in **53** (6.34 ppm) integrates for two protons with respect to the γ-H in the same complex corroborating the product of monosubstitution. Similarly to **52**, complex **53** is highly soluble in hydrocarbons and could not be isolated in a pure form. However, during the attempts to scale up the synthesis of **53**, a few diffraction-quality crystals were obtained by slow evaporation of the reaction mixture containing **53** in benzene. The molecular structure and selected distances and angles for complex **53** are shown in Figure 4.11 and Table 4.9.

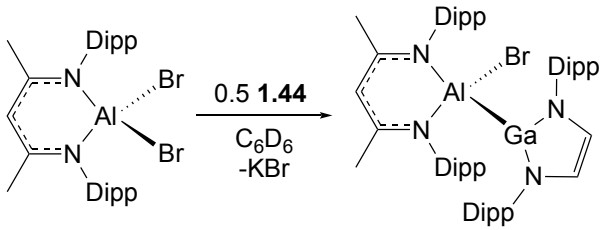

53

Equation 4.11

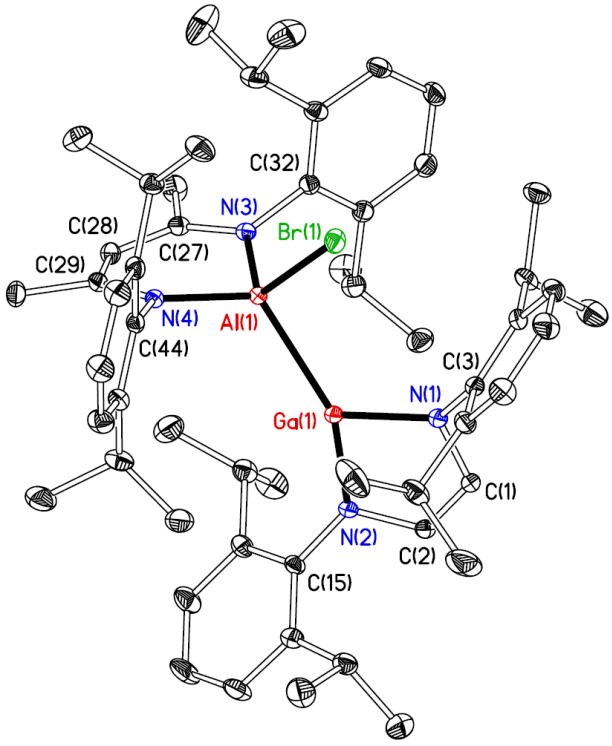

Figure 4.11. Displacement ellipsoid plot (20 % probability) of Al(^{Dipp}NacNac){Ga(NArCH)$_2$}Br (**53**). H atoms and solvent of crystallisation omitted for clarity.

Table 4.9. Selected distances (Å) and angles (°) for Al(^{Dipp}NacNac){Ga(NArCH)$_2$}Br (**53**).

Al(1)-Ga(1)	2.4930(5)	Al(1)-Br(1)	2.2856(5)
Al(1)-N(3)	1.8935(15)	Ga(1)-N(1)	1.8938(15)
Al(1)-N(4)	1.8930(15)	Ga(1)-N(2)	1.9020(14)
Br(1)-Al(1)-Ga(1)	97.274(19)	N(3)-Al(1)-N(4)	97.49(7)
Br(1)-Al(1)-N(3)	111.80(5)	N(1)-Ga(1)-N(2)	87.86(6)
Br(1)-Al(1)-N(4)	112.66(5)	C(1)-N(1)-Ga(1)	108.64(11)
Ga(1)-Al(1)-N(3)	116.91(5)	C(2)-N(2)-Ga(1)	108.40(11)
Ga(1)-Al(1)-N(4)	121.44(5)		

The solution of the structure of **53** confirms the formation of the monosubstituted product. In **53**, the aluminium centre exhibits a distorted tetrahedral geometry formed by the bidentate ^{Dipp}NacNac ligand, one gallyl fragment and one bromine atom. The

Al(1)-Ga(1) bond distance (2.4930(5) Å) is comparable to the sum of the Al and Ga covalent radii (2.43(5) Å)[2] and slightly shorter than that of $Al(C_6F_5)_3GaCp^*$ (**4.1**),[1] which contains the shortest Al-Ga interaction reported to date. However, the Al(1)-Ga(1) bond distance is longer than those of $Al\{(NCy)_2CPh\}\{Ga(NArCH)_2\}_2$ (**47**, 2.4829(7)Å and 2.4727(7) Å) and comparable to that of the mono(gallyl) complex $Al\{(N^iPr)_2CPh\}_2\{Ga(NArCH)_2\}$ (**49**, 2.5015(5) Å). Complex **53** is structurally similar to $Mg(^{Dipp}NacNac)\{Ga(NArCH)_2\}(\kappa^1\text{-TMEDA})$ (**2.19**)[27] in the way that both are ^{Dipp}NacNac supported mono(gallyl) complexes of metals of the 3rd Period. In this context, as expected for the reduction of the covalent radius in the period, the Al(1)-Ga(1) bond distance is shorter than the Mg-Ga bond in **2.19** (2.7470(7) Å). The smaller covalent radius of Al also gives shorter Al(1)-N(3) and Al(1)-N(4) bonds (1.8935(15) Å and 1.8930(15) Å, respectively) compared to the equivalent bonds in **2.19** (2.0678(15) Å and 2.0822(14) Å), which results in a wider bite angle for **53** (97.49(7)º) with respect to **2.19** (91.50(6)º).[27] The N(1)-Ga(1)-N(2) angle (87.86(6)º) is expectedly wider than that of **2.19** (85.55(6)º)[27] due to the higher electronegativity of Al with respect to Mg, which increases the *s* character in the Ga-N bonds.[33, 34] The N(1)-Ga(1)-N(2) angle of **53** is thus comparable to the equivalent angles in **47** (87.33(9)º and 87.64(9)º) and **49** (86.28(7)º).

4.5 Attempted reactivity of Al-Ga complexes

Aiming to establish comparison between the reactivity of aluminium gallyl complexes and the alkaline earth gallyl species presented in the previous chapters, a series of reactions with complexes **45-52** and small molecules were performed on the NMR-tube scale. These included reactions with carbodiimides, epoxides, Me_3NO, MeI, isocyanates, azobenzene and azides. However, surprisingly, no reaction occurred in any case. Additionally, attempts to react $Al\{(^{Dipp}NacNac)\{Ga(NArCH)_2\}Br$ (**53**) with MeI aiming to form the methylated derivative or with $Na[B(C_6H_5)_4]$ to form the bromide-free complex were also unsuccessful. This lack of reactivity of these species could be due to the steric hindrance in these species as inferred by the long reaction times in the formation of amidinate supported Al-Ga complexes, the difficulties in the scaling up of the synthesis of the bis(gallyl) complex $Al\{(NCy)_2CPh\}\{Ga(NArCH)_2\}_2$ (**47**), or the access to only the monosubstituted product (**52**) with the use of $Al(^{Dipp}NacNac)Br_2$ (**4.22**). In this context, in the majority of the reactions with the above-mentioned small molecules, the first step is the

coordination of a donor atom in the substrate, e.g., carbodiimide or epoxide, followed by nucleophilic attack by the gallium atom. The reduced covalent radius of Al compared to Mg would result in a less accessible metal centre which would then be encumbered by the supporting ligand. Additionally, in all the structurally authenticated Al-Ga presented in this Chapter, the Al-Ga bond distances are shorter than the Al-Ga species reported in the literature, which suggests that these direct Al-Ga bonds are stronger and have a higher covalent character than their more polarised counterparts in the donor-acceptor species. For instance, the only reported reaction of a Al-Ga complex has been reported as the insertion of benzaldehyde into the Al-Ga bond of the complex Ga(^{Dipp}NacNac){Al(C_6F_5)$_3$} (**4.3,** *vide supra*)[4], which contains the highly acidic and polarising Al(C_6F_5)$_3$ fragment.

4.6 Conclusions

In this Chapter, the synthesis of aluminium gallyl complexes has been presented. These species were formed by salt metathesis between the precursor [KGa(NArCH)$_2$(Et_2O)]$_2$ (**1.44**) and the corresponding amidinate or β-diketiminate aluminium bromide complexes. The synthesis of the required aluminium amidinate aluminium bromide complexes and the structural authentication for all three mono(amidinates) and one bis(amidinate) complex proceeded successfully. In the mono(amidinate) complexes, the presence of either methyl or phenyl substituents was found to have a minimal effect in the sterics of the complex with N(1)-C(1)-N(2) angles in those species. A significant change was found only with the presence of cyclohexyl substituents on the nitrogen atoms of the amidinate, which results in the increase of the N(1)-C(1)-N(2) angle. Following the synthesis of the aluminium amidinate precursors, the synthesis of the aluminium gallyl complexes on the NMR-tube scale and subsequent scaling up was possible in most cases. The X-ray analysis of mono- and bis(gallyl) complexes resulted in the structural authentication of the first complexes containing direct unsupported Al-Ga bonds. A similar approach with the ^{R}NacNac ligands allowed the elucidation of the structure of Al(^{Dipp}NacNac){Ga(NArCH)$_2$}Br (**53**). In all cases, shorter bond distances were found with respect to the literature Al-Ga species indicative of stronger and more covalent interactions. These interactions, along with the steric hindrance in these complexes resulted in rather stable complexes as no reactivity with small molecules was found in contrast with the polarised gallylene Ga(^{Dipp}NacNac){Al(C_6F_5)$_3$} (**4.3**) or their Ae-Ga

counterparts.

The study of these species is still in its infancy but future approaches aiming to enhance the reactivity could include the use of less bulky amidinates, ^{R}NacNac ligands, the installation of electron-withdrawing substituents (*e.g.,* C_6F_5) on the nitrogen atoms of either the amidinates or the ^{R}NacNac ligands and further attempts to displace the bromine atom in Al{(^{Dipp}NacNac){Ga(NArCH)$_2$}Br (**53**) with different salts of tetraphenylborate bearing electron-withdrawing substituents.

4.7 References

1. J. D. Gorden, C. L. B. MacDonald and A. A. H. Cowley, *Main Group Chemistry*, 2005, **4**, 33.
2. B. Cordero, V. Gomez, A. E. Platero-Prats, M. Reves, J. Echeverria, E. Cremades, F. Barragan and S. Alvarez, *Dalton Trans.*, 2008, 2832.
3. S. Schulz, A. Kuczkowski, D. Schuchmann, U. Flörke and M. Nieger, Organometallics, 2006, 25, 5487.
4. C. Ganesamoorthy, M. Matthias, D. Blaser, C. Wolper and S. Schulz, Dalton Trans, 2016, 45, 11437.
5. P. Pyykkö and M. Atsumi, Chem. Eur. J., 2009, 15, 186.
6. N. Dettenrieder, H. M. Dietrich, C. Schadle, C. Maichle-Mossmer, K. W. Tornroos and R. Anwander, Angew. Chem. *Int. Ed.*, 2012, **51**, 4461.
7. D. Dange, C. P. Sindlinger, S. Aldridge and C. Jones, *Chem. Commun.*, 2017, **53**, 149.
8. N. Dettenrieder, C. O. Hollfelder, L. N. Jende, C. Maichle-Mössmer and R. Anwander, *Organometallics*, 2014, **33**, 1528.
9. M. Bonath, C. O. Hollfelder, D. Schädle, C. Maichle-Mössmer, P. Sirsch and R. Anwander, *Eur. J. Inorg. Chem.*, 2017, **2017**, 4683.
10. W. Lu, H. Hu, Y. Li, R. Ganguly and R. Kinjo, *J. Am. Chem. Soc.*, 2016, **138**, 6650.
11. Y. Zhao, Y. Liu, L. Yang, J. G. Yu, S. Li, B. Wu and X. J. Yang, *Chem. Eur. J.*, 2012, **18**, 6022.
12. I. L. Fedushkin, M. V. Moskalev, A. N. Lukoyanov, A. N. Tishkina, E. V. Baranov and G. A. Abakumov, *Chem. Eur. J.*, 2012, **18**, 11264.
13. T. Agou, K. Nagata and N. Tokitoh, *Angew. Chem. Int. Ed.*, 2013, **52**, 10818.

14. I. M. Riddlestone, J. Urbano, N. Phillips, M. J. Kelly, D. Vidovic, J. I. Bates, R. Taylor and S. Aldridge, *Dalton Trans.*, 2013, **42**, 249.
15. M. P. Coles, D. C. Swenson, R. F. Jordan and V. G. Young, *Organometallics*, 1997, **16**, 5183.
16. D. H. Mayo, Y. Peng, P. Zavalij, K. H. Bowen and B. W. Eichhorn, *Acta Crystallogr., Sect. C: Struct. Chem.*, 2013, **69**, 1120.
17. J. Richter, J. Feiling, H. G. Schmidt, M. Noltemeyer, W. Brüser and F. T. Edelmann, *Z. Anorg. Allg. Chem.*, 2004, **630**, 1269.
18. C. Trinh, M. Bodensteiner, A. V. Virovets, E. V. Peresypkina, M. Scheer, S. M. Matveev and A. Y. Timoshkin, *Polyhedron*, 2010, **29**, 414.
19. T. Chlupatý, Z. Padělková, A. Lyčka and A. Růžička, *J. Organomet. Chem.*, 2011, **696**, 2346.
20. F. Sroor, C. Hrib and F. Edelmann, *Inorganics*, 2015, **3**, 429.
21. J. E. Huheey, E. A. Keiter and R. L. Keiter, *Inorganic Chemistry : Principles of Structure and Reactivity*, Harper Collins, New York, 4th edn., 1993.
22. T. A. Albright, J. K. Burdett and M.-H. Whangbo, *Orbital Interactions in Chemistry*, Wiley-Interscience, New York, 1985.
23. C. Jones, R. P. Rose and A. Stasch, *Dalton Trans.*, 2007, 2997.
24. C. Jones, D. P. Mills, R. P. Rose, A. Stasch and W. D. Woodul, *J. Organomet. Chem.*, 2010, **695**, 2410.
25. C. Jones, D. P. Mills, R. P. Rose and A. Stasch, *Dalton Trans.*, 2008, 4395.
26. R. J. Baker, R. D. Farley, C. Jones, M. Kloth and D. M. Murphy, *J. Chem. Soc., Dalton Trans.*, 2002, 3844.
27. O. Bonello, C. Jones, A. Stasch and W. D. Woodul, *Organometallics*, 2010, **29**, 4914.
28. Y. Yang, T. Schulz, M. John, A. Ringe, H. W. Roesky, D. Stalke, J. Magull and H. Ye, *Inorg. Chem.*, 2008, **47**, 2585.
29. Y. K. Radwan, A. Maity and T. S. Teets, *Inorg. Chem.*, 2015, **54**, 7122.
30. M. Stender, B. E. Eichler, N. J. Hardman, P. P. Power, J. Prust, M. Noltemeyer and H. W. Roesky, *Inorg. Chem.*, 2001, **40**, 2794.
31. Z. Yang, H. Zhu, X. Ma, J. Chai, H. W. Roesky, C. He, J. Magull, H.-G. Schmidt and M. Noltemeyer, *Inorg. Chem.*, 2006, **45**, 1823.
32. L. N. Grant, B. M. Kriegel and J. Arnold, *Polyhedron*, 2016, **114**, 53.
33. L. M. A. Saleh, D. Phil Thesis, University of Oxford, 2014.

34. H. A. Bent, *Chem. Rev.*, 1961, **61**, 275.

Chapter Five

Experimental details and characterising data

5.1 General methods and instrumentation

All manipulations were carried out using standard Schlenk line or dry-box techniques under an atmosphere of argon or dinitrogen. Solvents were degassed by sparging with dinitrogen and dried by passing through a column of the appropriate drying agent (benzene, pentane and hexane).[1] Alternatively, solvents were predried over activated 4 Å molecular sieves and refluxed over sodium (toluene), Na/K alloy (Et_2O) or potassium (THF) and distilled. Deuterated solvents were dried over potassium (C_6D_6 and THF-d_8), distilled under reduced pressure and stored under argon in Teflon valve ampoules. NMR samples were prepared under dinitrogen in 5 mm Wilmad 507-PP tubes fitted with J. Young Teflon valves. ^{1}H, $^{13}C\{^{1}H\}$, ^{7}Li and ^{27}Al spectra were recorded on a Bruker Ascend 400 NMR spectrometer, a Bruker Avance III 500 NMR spectrometer or on a Bruker AVC 500 spectrometer fitted with a ^{13}C cryoprobe. Unless otherwise stated, all NMR spectra were recorded at 298 K. ^{1}H and $^{13}C\{^{1}H\}$ spectra are referenced internally to residual protio-solvent (^{1}H) or solvent (^{13}C) resonances, and are reported relative to tetramethylsilane (δ = 0 ppm). Assignments were confirmed as necessary with the use of two-dimensional ^{1}H-^{1}H and ^{13}C-^{1}H NMR correlation experiments. Chemical shifts are quoted in δ (ppm) and coupling constants in Hz. IR spectra were recorded on a Perkin Elmer Paragon 1000 FTIR or Thermo Scientific Nicolet iS5 FTIR spectrometer and samples prepared in a dry-box as Nujol mulls between NaCl plates. The data are quoted in wavenumbers (cm^{-1}). Mass spectra were recorded by the Mass Spectrometry Service of Oxford University's Department of Chemistry. Elemental analyses were carried out by the Elemental Analysis Service of London Metropolitan University.

5.2 X-ray data collection and processing parameters

Crystals were mounted on glass fibres using perfluoropolyether oil and cooled rapidly in a stream of cold N_2 using an Oxford Cryosystems Cryostream unit. Diffraction data were measured using an Enraf-Nonius KappaCCD diffractometer or Agilent Technologies Supernova diffractometer using Mo-κα or Cu-κα, respectively. As appropriate, absorption and decay corrections were applied to the data and equivalent reflections merged.[2, 3] The structures were solved using SIR92[4] or Superflip[5] and further refinements and all other crystallographic calculations were performed using the CRYSTALS program suite.[6] Other details of the structure solution and refinements are given in the CD Appendix.

5.3 Literature preparations

Unless stated, starting materials were purchased from Sigma Aldrich, Strem Chemicals or Alfa Aesar and used without further purification. HMPA, DME, isobutene epoxide, cyclohexene epoxide, EtNCO, ^{t}BuNCO, MeI were dried over CaH_2, filtered and distilled under reduced pressure. $[KGa(NArCH)_2(Et_2O)]_2$,[7] Mg(^{Dipp}NacNac){Ga(NArCH)$_2$}(κ^1-TMEDA),[8] KFp,[9] Mg(^{Dipp}NacNac)I(Et$_2$O),[10] Mg(^{Dipp}NacNac)I(THF),[10] Mg(^{Mes}NacNac)I(THF),[10] [Ca(^{Dipp}NacNac)I(THF)]$_2$,[11] [Sr(^{Dipp}NacNac)I(THF)]$_2$,[11] Ca{Ga(NArCH)$_2$}$_2$(THF)$_4$,[12] H-CzOx[13] Mg(CzOx)I(THF),[14] Ca(CzOx)I(THF)$_2$,[14] Li[(N^{i}Pr)$_2$CMe],[15] Li[(N^{i}Pr)$_2$CPh],[16] K(^{Ph}NacNac),[17] Al(^{Dipp}NacNac)Br$_2$[18] were synthesised according to published procedures.

5.4 Experimental details and characterising data for Chapter Two

Mg(^{Dipp}NacNac){Ga(NArCH)$_2$}(THF) (1). A solid mixture of Mg(^{Dipp}NacNac)I(THF) (**2.31**, 386 mg, 0.543 mmol) and $[KGa(NArCH)_2(Et_2O)]_2$ (**1.44**, 304 mg, 0.271 mmol) was cooled to -78. °C. To this cooled mixture was added, with stirring, toluene (20 mL). The resulting suspension was allowed to warm to room temperature and react for 1 h. The reaction mixture was filtered and the volatiles were removed from the filtrate. The resulting orange solid was washed with hexane (2 x 5 mL) then dried *in vacuo* to afford **1** as a bright orange solid. Yield: 0.438 g (84%). ^{1}H NMR (C_6D_6, 400.2 MHz): δ 7.19 (4 H, *m*-C_6H_3 of Ga(NArCH)$_2$), 7.14 – 7.11 (2 H, m, *p*-C_6H_3 of Ga(NArCH)$_2$), 7.07 – 6.97 (6 H, overlapping 2 x m, *m*- & *p*-C_6H_3 of ^{Dipp}NacNac), 6.42 (2 H, s, NCH), 4.79 (1 H, s, NC(Me)C<u>H</u>), 3.84 – 3.68 (4 H, br. m, C<u>H</u>Me$_2$ of Ga(NArCH)$_2$), 3.27 – 3.11 (4 H, br. m, C<u>H</u>Me$_2$ of ^{Dipp}NacNac), 2.94 (4 H, br. s, OCH_2), 1.53 (6 H, s, NCMe), 1.39 (12 H, d, ^3J = 6.5 Hz, CH<u>Me</u>$_2$ of Ga(NArCH)$_2$), 1.21 (12 H, d, ^3J = 6.5 Hz, CH<u>Me</u>$_2$ of Ga(NArCH)$_2$), 1.19 – 1.11 (12 H, br. m, CH<u>Me</u>$_2$ of ^{Dipp}NacNac), 1.09 (12 H, d, ^3J = 6.8 Hz, CH<u>Me</u>$_2$ of ^{Dipp}NacNac), 0.82 (4 H, br. s, $OCH_2\underline{CH_2}$). ^{13}C{^{1}H} NMR (C_6D_6, 100.6 MHz): δ 169.0 (N<u>C</u>Me), 148.6 (*i*-C_6H_3 of Ga(NArCH)$_2$), 145.5 (*o*-C_6H_3 of Ga(NArCH)$_2$), 145.0 (*i*-C_6H_3 of ^{Dipp}NacNac), 142.5 (*o*-C_6H_3 of ^{Dipp}NacNac), 125.9 (*m*-C_6H_3 of ^{Dipp}NacNac), 123.8 (*p*-C_6H_3 of Ga(NArCH)$_2$), 123.3 (*m*-C_6H_3 of Ga(NArCH)$_2$), 123.2 (NCH), 96.1 (NC(Me)<u>C</u>H), 69.1 (OCH_2), 28.40 (<u>C</u>HMe$_2$ of ^{Dipp}NacNac), 28.3 (<u>C</u>HMe$_2$ of Ga(NArCH)$_2$), 27.1 (CH<u>Me</u>$_2$ of Ga(NArCH)$_2$), 24.7 (CH<u>Me</u>$_2$ of ^{Dipp}NacNac), 24.6 (CH<u>Me</u>$_2$ of Ga(NArCH)$_2$), 24.5 (CH<u>Me</u>$_2$ of ^{Dipp}NacNac), 24.4 ($OCH_2\underline{CH_2}$), 24.3

(NC<u>Me</u>). IR (NaCl plates, Nujol mull, cm^{-1}): 1681 (w), 1563 (w), 1542 (m), 1519 (m), 1460 (s), 1402 (s), 1377 (m), 1315 (m), 1260 (m), 1207 (w), 1175 (w), 1099 (m), 1021 (m), 931 (w), 869 (w), 800 (m), 757 (w), 720 (w), 668 (w), 492 (w). Anal. found (calcd. for $C_{59}H_{85}GaMgN_4O$): C, 73.43 (73.79); H, 8.42 (8.92); N, 5.67 (5.83)%.

Alternative NMR tube-scale synthesis of Mg(^{Dipp}NacNac){Ga(NArCH)$_2$}(THF) (1). To a solution of Mg(^{Dipp}NacNac){Ga(NArCH)$_2$}(TMEDA) (**2.19**, 20.0 mg, 19.9 μmol) in C_6D_6 (0.6 mL) at RT was added THF (1.6 μL, 20.0 μmol). The NMR tube was gently shaken and volatiles were removed under reduced pressure. The resulting orange solid was redissolved in C_6D_6 (0.6 ml). ^{1}H NMR analysis was consistent with the displacement of TMEDA by THF to form **1**.

Ca(^{Dipp}NacNac){Ga(NArCH)$_2$}(THF) (2). A solid mixture of [Ca(^{Dipp}NacNac)I(THF)]$_2$ (**2.32**, 400 mg, 0.305 mmol) and [KGa(NArCH)$_2$(Et$_2$O)]$_2$ (341 mg, 0.305 mmol) was cooled to -78. °C. To this cooled mixture was added, with stirring, toluene (20 mL). After stirring the solution 1 h at -78 ºC the mixture was allowed to warm to room temperature and then react for a further 1 h. The solution was filtered and the volatiles were removed from the filtrate. The resulting orange solid was washed with hexane (2 x 5 mL) then dried *in vacuo* to afford **2** as a yellow solid. Yield: 0.211 g (71%). ^{1}H NMR (C_6D_6, 400.2 MHz): δ 7.30 (4 H, d, ^3J = 6.5 Hz, *m*-C_6H_3 of Ga(NArCH)$_2$), 7.27 – 7.24 (2 H, m, *p*-C_6H_3 of Ga(NArCH)$_2$), 7.18 – 7.14 (overlapping with solvent, m, *m*- & *p*-C_6H_3 of ^{Dipp}NacNac), 6.56 (2 H, s, NCH), 4.80 (1 H, s, NC(Me)C<u>H</u>), 3.93 (4 H, sept, ^3J = 6.8 Hz, C<u>H</u>Me$_2$ of Ga(NArCH)$_2$), 3.32 – 3.25 (4 H, br. m, OCH$_2$), 3.06 (4 H, sept, ^3J = 6.4 Hz, C<u>H</u>Me$_2$ of ^{Dipp}NacNac), 1.63 (6 H, s, NCMe), 1.48 (12 H, d, ^3J = 6.8 Hz, CH<u>Me</u>$_2$ of Ga(NArCH)$_2$), 1.26 (12 H, d, ^3J = 6.8 Hz, CH<u>Me</u>$_2$ of Ga(NArCH)$_2$), 1.24 – 1.18 (24 H, m, CH<u>Me</u>$_2$ of ^{Dipp}NacNac), 1.13 (4 H, br. s, OCH$_2$<u>C</u>H$_2$). ^{13}C{^{1}H} NMR (C_6D_6, 100.6 MHz): δ 166.5 (N<u>C</u>Me), 149.8 (*i*-C_6H_3 of Ga(NArCH)$_2$), 145.7 (*o*-C_6H_3 of Ga(NArCH)$_2$), 144.9 (*i*-C_6H_3 of ^{Dipp}NacNac), 141.7 (*o*-C_6H_3 of ^{Dipp}NacNac), 125.2 (*p*-C_6H_3 of ^{Dipp}NacNac), 124.2 (*m*-C_6H_3 of ^{Dipp}NacNac), 123.5 (*p*-C_6H_3 of Ga(NArCH)$_2$), 122.8 (overlapping resonances for *m*-C_6H_3 of Ga(NArCH)$_2$ & NCH), 93.8 (NC(Me)<u>C</u>H), 69.1 (OCH$_2$), 28.6 (<u>C</u>HMe$_2$ of ^{Dipp}NacNac), 28.2 (<u>C</u>HMe$_2$ of Ga(NArCH)$_2$), 26.0 (CH<u>Me</u>$_2$ of Ga(NArCH)$_2$), 25.8 (CH<u>Me</u>$_2$ of ^{Dipp}NacNac), 25.5 (CH<u>Me</u>$_2$ of Ga(NArCH)$_2$), 24.9 (OCH$_2$<u>CH$_2$</u>), 24.5 (NC<u>Me</u>), 24.3 (CH<u>Me</u>$_2$ of ^{Dipp}NacNac). IR (NaCl plates, Nujol mull, cm^{-1}): 1585 (w), 1541 (m), 1511 (m), 1459 (s), 1378 (s), 1358 (s), 1313 (s), 1259 (s), 1226 (w), 1213

(m), 1169 (w), 1099 (w), 1057 (w), 1016 (w), 925 (w), 894 (w), 863 (w), 837 (w), 801 (w), 790 (m), 762 (m), 751 (w), 722 (w), 666 (w), 486 (w). Anal. found (calcd. for $C_{59}H_{85}CaGaN_4O$): C, 72.37 (72.60); H, 8.83 (8.78); N, 5.55 (5.74)%.

NMR tube-scale synthesis of Sr(^{Dipp}NacNac){Ga(NArCH)$_2$}(THF) (3). To a solution of [Sr(^{Dipp}NacNac)I(THF)]$_2$ (20.0 mg, 14.2 μmol) in C_6D_6 (0.6 mL) at RT was added [KGa(NArCH)$_2$(Et$_2$O)]$_2$ (**1.44**, 15.9 mg, 14.2 μmol). The solution was immediately analysed by ^{1}H and ^{13}C NMR spectroscopies which showed the formation of **3** and other minor unknown products. ^{1}H NMR (C_6D_6, 400.2 MHz): δ 7.24 – 7.17 (6 H, m, *m*- & *p*-C_6H_3 of Ga(NArCH)$_2$), 7.09 – 7.05 (6 H, m, *m*- & *p*-C_6H_3 of ^{Dipp}NacNac), 6.47 (2 H, br. s, NCH), 4.65 (1 H, s, NC(Me)C<u>H</u>), 3.96 (4 H, br. s, C<u>H</u>Me$_2$ of Ga(NArCH)$_2$), 3.23 – 3.18 (4 H, br. m, OCH$_2$), 2.98 (4 H, br. s, C<u>H</u>Me$_2$ of ^{Dipp}NacNac), 1.57 (6 H, s, NCMe), 1.40 (12 H, br. s, CH<u>Me</u>$_2$ of Ga(NArCH)$_2$), 1.26 – 1.18 (24 H, m centred at 1.25 & 1.21, overlapping CH<u>Me</u>$_2$ of Ga(NArCH)$_2$ & ^{Dipp}NacNac), 1.15 (12 H, d, ^3J = 6.6 Hz, CH<u>Me</u>$_2$ of ^{Dipp}NacNac), 1.12 – 1.10 (6 H, br. m, OCH$_2$C<u>H</u>$_2$). ^{13}C{^{1}H} NMR (C_6D_6, 125.7 MHz): δ 164.8 (N<u>C</u>Me), 151.4 (*i*-C_6H_3 of Ga(NArCH)$_2$), 150.5 (*o*-C_6H_3 of Ga(NArCH)$_2$), 142.0 (*i*-C_6H_3 of ^{Dipp}NacNac), 141.1 (*o*-C_6H_3 of ^{Dipp}NacNac), 125.1 (*p*-C_6H_3 of Ga(NArCH)$_2$), 124.4 (*m*-C_6H_3 of Ga(NArCH)$_2$), 123.9 (*m*-C_6H_3 of ^{Dipp}NacNac), 122.7 (NCH), 92.8 (NC(Me)<u>C</u>H), 65.9 (OCH$_2$), 28.0 (<u>C</u>HMe$_2$ of Ga(NArCH)$_2$), 27.7 (<u>C</u>HMe$_2$ of ^{Dipp}NacNac), 26.1 (CH<u>Me</u>$_2$ of Ga(NArCH)$_2$), 24.9 (NC<u>Me</u>), 24.4 (OCH$_2$<u>C</u>H$_2$), 24.3 (CH<u>Me</u>$_2$ of ^{Dipp}NacNac), 24.0 (CH<u>Me</u>$_2$ of Ga(NArCH)$_2$), 23.1 (CH<u>Me</u>$_2$ of Ga(NArCH)$_2$).

Mg(^{Ph}NacNac)I(THF) (4). To a stirred solution of H(^{Ph}NacNac) (2.00 g, 8.00 mmol) in Et$_2$O (20 mL) a 3.0 M solution of MeMgI (4.00 mL, 8.00 mmol) in Et$_2$O was added dropwise at -20 °C. The resulting suspension was allowed to warm to RT and stirred for 30 min. The precipitate was isolated by filtration then dried under reduced pressure. The white solid was dissolved in THF (20 mL) and stirred at RT for 1 h. The volatiles were removed under reduced pressure and the resulting white solid washed with pentane (2 x 5 mL) then dried *in vacuo* to afford **4** as a white solid. Yield: 2.24 g (59%). ^{1}H NMR (C_6D_6, 400.2 MHz): δ 7.21 (4 H, d, ^3J = 7.4 Hz, *o*-C_6H_5), 7.11 (4 H, t, ^3J = 7.7 Hz, *m*-C_6H_5), 6.90 (2 H, t, ^3J = 7.2, Hz, *p*-C_6H_5), 4.77 (1 H, s, NC(Me)C<u>H</u>), 3.33 (4 H, br s, OCH$_2$), 1.79 (6 H, s, NCMe), 0.90 (4 H, br s, OCH$_2$C<u>H</u>$_2$). ^{13}C{^{1}H} NMR (C_6D_6, 100.6 MHz): δ 167.9 (N<u>C</u>Me), 149.9 (*i*-C_6H_5), 129.3 (*p*-C_6H_5), 125.2 (*p*-C_6H_5), 124.2 (*o*-C_6H_5), 97.2 (NC(Me)<u>C</u>H), 69.9 (OCH$_2$), 24.8 (NC<u>Me</u>), 23.5

($OCH_2\underline{C}H_2$). IR (NaCl plates, Nujol mull, cm^{-1}): 1515 (w), 1306 (m), 1156 (m), 1018 (m), 879 (w), 803 (m). Anal. found (calcd. for $C_{21}H_{24}IMgN_2O$): C, 49.57 (53.48); H, 5.04 (5.13); N, 5.39 (5.94)%.

Mg(^{Mes}NacNac){Ga(NArCH)$_2$}(THF) (5). To a stirred solution of Mg(^{Mes}NacNac)I(THF) (0.420 g, 7.50 mmol) in toluene (15 mL) was added a solution of [KGa(NArCH)$_2$(Et$_2$O)]$_2$ (**1.44**, 0.422 g, 3.80 mmol) in toluene (15 mL) at -78 °C. The resulting suspension was allowed to warm to RT and stirred for 1 h then filtered to give an orange solution. The volatiles were removed under reduced pressure to afford **5** as an orange-brown solid. Yield: 0.491 g (74%). ^{1}H NMR (C_6D_6, 400.2 MHz): δ 7.20 (4 H, d, ^3J = 7.5 Hz, *m*-C_6H_3), 7.15 (2 H, m overlapping with solvent, *p*-C_6H_3), 6.76 (4 H, s, *m*-C_6H_2), 6.46 (2 H, s, NCH) 4.79 (1 H, s, NC(Me)C$\underline{H}$), 3.75 (4 H, sept, ^3J = 6.9 Hz, C$\underline{H}$Me$_2$), 3.11 (4 H, br s, OC$\underline{H}_2$), 2.15 (6 H, s, *p*-$C_6H_2\underline{Me}_3$), 2.04 (12 H, s, *o*-$C_6H_2\underline{Me}_3$), 1.49 (6 H, s, NCMe), 1.38 (12 H, d ^3J = 6.9 Hz, CH$\underline{Me}_2$), 1.21 (12 H, d ^3J = 6.9 Hz, CH$\underline{Me}_2$), 1.00 (4 H, br s, $OCH_2C\underline{H}_2$). ^{13}C{^{1}H} NMR (C_6D_6, 100.6 MHz): δ 168.3 (N$\underline{C}$Me), 148.9 (*i*-$\underline{C}_6H_3$), 145.6 (*o*-C_6H_3), 145.3 (*i*-C_6H_2), 133.5 (*p*-C_6H_2), 129.9 (*m*-C_6H_2), 124.1 (*o*-C_6H_2), 123.4 (*p*-C_6H_3), 123.2 (NCH), 123.0 (*m*-C_6H_3), 95.3 (NC(Me)$\underline{C}$H), 68.8 (OCH_2), 28.3 ($\underline{C}$HMe$_2$), 25.9 (CH$\underline{Me}_2$), 25.2 ($OCH_2\underline{C}H_2$), 25.1 (CH$\underline{Me}_2$), 23.2 (NC$\underline{Me}$), 20.9 (*p*-$C_6H_2\underline{Me}_3$), 18.9 (*o*-$C_6H_2\underline{Me}_3$). IR (NaCl plates, Nujol mull, cm^{-1}): 2752 (w), 1522 (w), 1459 (s), 1377 (s), 1260 (m), 1198 (w), 1147 (w), 1020 (m), 722 (m). EI-MS: *m/z* = 445 (50%) [Ga(NArCH)$_2$]$^+$, 357 (30%) [Mg(^{Mes}NacNac)]$^+$, 333 (60%) [^{Mes}NacNac]$^+$. Anal. found (calcd. for $C_{53}H_{72}GaMgN_4O$): C, 72.48 (72.73); H, 8.29 (8.29); N, 6.33 (6.40)%.

NMR tube-scale synthesis of Mg(^{Ph}NacNac){Ga(NArCH)$_2$}(THF) (6). To Mg(^{Ph}NacNac)I(THF) (**4**, 8.4 mg, 18 μmol) was added a solution of [KGa(NArCH)$_2$(Et$_2$O)]$_2$ (**1.44**, 10 mg, 8.9 μmol) in C_6D_6 (0.5 mL). The solution was immediately analysed by ^{1}H and ^{13}C NMR spectroscopies. ^{1}H NMR (C_6D_6, 400.2 MHz) δ 7.32 (4 H, d ^3J = 6.7 Hz, *m*-C_6H_3), 7.26 (2 H, t, ^3J = 7.5 Hz, *p*-C_6H_5), 6.98 (4 H, t, ^3J = 7.9 Hz, *m*-C_6H_5), 6.85 (2 H, t, ^3J = 7.2 Hz, *p*-C_6H_3), 6.58 (2 H, s, NCH) 6.56 (4 H, d, ^3J = 7.2 Hz, *o*-C_6H_5), 4.70 (1 H, s, NC(Me)C$\underline{H}$), 3.94 (4 H, sept, ^3J = 6.9 Hz, C$\underline{H}$Me$_2$), 3.15 (4 H, br s, OCH_2), 1.70 (6 H, s, NCMe), 1.42 (12 H, d, ^3J = 6.9 Hz, CH$\underline{Me}_2$), 1.33 (12 H, d, ^3J = 6.9 Hz, CH$\underline{Me}_2$), 0.90 (4 H, br s, $OCH_2C\underline{H}_2$). ^{13}C{^{1}H} NMR (C_6D_6, 100.6 MHz): δ 167.5 (N$\underline{C}$Me), 150.0 (*i*-C_6H_5), 148.8 (*i*-C_6H_3), 146.1 (*o*-C_6H_3), 129.7 (*m*-C_6H_5), 124.7 (*p*-C_6H_5), 124.4 (*o*-C_6H_5), 123.7 (*p*-$\underline{C}_6H_3(^iPr)_2$), 123.2

(*m*-C$_6$H$_3$(^{i}Pr)$_2$), 122.8 (NCH), 97.3 (NC(Me)CH), 69.1 (OCH$_2$), 28.4 (CHMe$_2$), 25.7 (CHMe$_2$), 25.2 (CHMe$_2$), 24.9 (OCH$_2$CH$_2$), 23.2 (NCMe).

Mg(^{Dipp}NacNac){(N^{i}Pr)$_2$CGa(NArCH)$_2$} (7). To a solution of Mg(^{Dipp}NacNac){Ga(NArCH)$_2$}(THF) (**1**, 0.400 g, 0.420 mmol) in toluene (15 mL) at -78 ºC was added a solution of ^{i}PrNCN^{i}Pr (0.0530 g, 0.420 mmol) in toluene (5 mL). The solution was allowed to warm to RT then stirred for a further 1 h to give an orange solution. The solution was filtered and the volatiles were removed from the filtrate under reduced pressure. The resultant solid was washed with cold hexane (2 x 5 mL) and dried *in vacuo* to afford **7** as an orange solid. Yield: 0.356 g (84%). Diffraction-quality crystals were grown by slow evaporation from a concentrated benzene solution at RT. ^{1}H NMR (C$_6$D$_6$, 400.2 MHz): δ 7.19 – 7.18 (2 H, m, *p*-C$_6$H$_3$ of Ga(NArCH)$_2$), 7.15 – 7.13 (4 H, m, *m*-C$_6$H$_3$ of ^{Dipp}NacNac), 7.12 – 7.10 (2 H, m, *p*-C$_6$H$_3$ of ^{Dipp}NacNac), 7.10 – 7.08 (6 H, m, *m*-C$_6$H$_3$ of Ga(NArCH)$_2$), 6.13 (2 H, s, ArNCH), 4.80 (1 H, s, NC(Me)CH), 3.43 (4 H, sept, ^3J = 6.8 Hz, CHMe$_2$ of Ga(NArCH)$_2$), 3.29 (4 H, sept, ^3J = 6.8 Hz, CHMe$_2$ of ^{Dipp}NacNac), 3.13 (2 H, sept, ^3J = 6.3 Hz, NCHMe$_2$), 1.63 (6 H, s, NCMe), 1.24 (12 H, d, ^3J = 6.8 Hz, CHMe$_2$ of Ga(NArCH)$_2$), 1.18 (12 H, d, ^3J = 6.8 Hz, CHMe$_2$ of ^{Dipp}NacNac), 1.16 (12 H, d, ^3J = 6.8 Hz, CHMe$_2$ of Ga(NArCH)$_2$), 1.13 (12 H, d, ^3J = 6.8 Hz, CHMe$_2$ of ^{Dipp}NacNac), 0.78 (12 H, d, ^3J = 6.3 Hz, NCHMe$_2$). ^{13}C{^{1}H} NMR (C$_6$D$_6$, 100.6 MHz): δ 181.3 (NCN), 169.8 (NCMe), 145.7 (*o*-C$_6$H$_3$ of Ga(NArCH)$_2$), 145.6 (*i*-C$_6$H$_3$ of ^{Dipp}NacNac), 144.7 (*i*-C$_6$H$_3$ of Ga(NArCH)$_2$), 142.4 (*o*-C$_6$H$_3$ of ^{Dipp}NacNac), 126.1 (*p*-C$_6$H$_3$ of Ga(NArCH)$_2$), 125.3 (*p*-C$_6$H$_3$ of ^{Dipp}NacNac), 123.9 (*m*-C$_6$H$_3$ of Ga(NArCH)$_2$), 123.6 (*m*-C$_6$H$_3$ of ^{Dipp}NacNac), 121.1 (ArNCH), 94.82 (NC(Me)CH), 52.7 (NCHMe$_2$), 28.6 (CHMe$_2$ of Ga(NArCH)$_2$), 28.2 (CHMe$_2$ of ^{Dipp}NacNac), 26.5 (NCHMe$_2$), 26.3 (CHMe$_2$ of Ga(NArCH)$_2$), 25.2 (CHMe$_2$ of ^{Dipp}NacNac), 24.5 (CHMe$_2$ of ^{Dipp}NacNac), 24.4 (NCMe), 23.85 (CHMe$_2$ of Ga(NArCH)$_2$). IR (NaCl plates, Nujol mull, cm^{-1}): 1541 (w), 1516 (m), 1460 (s), 1402 (s), 1377 (s), 1350 (s), 1316 (s), 1260 (m), 1201 (m), 1173 (m), 1111 (m), 1055 (m), 1027 (m), 932 (w), 850 (w), 791(m), 759 (m), 721 (m), 676 (w). Anal. found (calcd. for C$_{62}$H$_{91}$GaMgN$_6$): C, 73.28 (73.41); H, 8.95 (9.04); N, 8.19 (8.28)%.

Alternative NMR tube-scale synthesis of Mg(^{Dipp}NacNac){(N^{i}Pr)$_2$CGa(NArCH)$_2$} (7). To a solution of Mg(^{Dipp}NacNac){Ga(NArCH)$_2$}(TMEDA) (**2.19**, 20.0 mg, 19.9 μmol) in C$_6$D$_6$ (0.6 mL) at RT was added ^{i}PrNCN^{i}Pr (2.5 mg, 20 μmol). The solution

was immediately analysed by ^{1}H NMR spectroscopy. The spectrum was consistent with the formation of **7** and the release of TMEDA.

NMR tube-scale synthesis of Mg(^{Mes}NacNac){(N^{i}Pr)$_2$CGa(NArCH)$_2$} (**8**). To a solution of Mg(^{Mes}NacNac){Ga(NArCH)$_2$}(THF) (**5**, 20 mg, 25 μmol) in C_6D_6 (0.6 mL) was added ^{i}PrNCN^{i}Pr (3.5 μL, 25 μmol). The solution was immediately analysed by ^{1}H NMR spectroscopy. The spectrum was consistent with the formation of **8** and the release of THF. ^{1}H NMR (C_6D_6, 400.2 MHz): δ 7.15 (6 H, overlapping 2 x m, *m*- & *p*-C_6H_3), 6.76 (4 H, s, *m*-C_6H_2), 6.28 (2 H, s, NCH), 4.90 (1 H, s, NC(Me)C<u>H</u>), 3.50 (4 H, sept, ^{3}J = 6.8 Hz, ArC<u>H</u>Me$_2$), 3.07 (2 H, sept, ^{3}J = 6.2 Hz, NC<u>H</u>Me$_2$), 2.22 (6 H, s, *p*-C_6H_2), 2.15 (12 H, s, *o*-C_6H_2<u>Me$_3$</u>), 1.61 (6 H, s, NC(<u>Me</u>)CH), 1.23 (12 H, d, ^{3}J = 6.9 Hz, ArCH<u>Me$_2$</u>), 1.12 (12H, d, ^{3}J = 6.9 Hz, ArCH<u>Me$_2$</u>), 0.67 (12H, d, ^{3}J = 6.1 Hz, NCH<u>Me$_2$</u>). ^{13}C{^{1}H} NMR (C_6D_6, 100.6 MHz): δ 181.5 (NCN), 166.9 (N<u>C</u>Me), 145.5 (*i*-C_6H_2), 145.03 (*o*-C_6H_3), 144.2 (*i*-C_6H_3), 133.1 (*p*-$C_6H_2Me_3$), 131.3 (*o*-C_6H_2), 129.4 (*m*-$C_6H_2Me_3$), 125.7 (*p*-C_6H_3(iPr)$_2$), 123.6 (*m*-C_6H_3(^{i}Pr)$_2$), 120.3 (GaNCH), 95.1 (NC(Me)<u>C</u>H), 55.0 (N<u>C</u>HMe$_2$), 28.6 (Ar<u>C</u>HMe$_2$), 26.2 (NCH<u>Me$_2$</u>), 25.8 (ArCH<u>Me$_2$</u>), 24.4 (ArCH<u>Me$_2$</u>), 23.2 (NC<u>Me</u>), 20.9 (*p*-C_6H_2<u>Me$_3$</u>), 19.4 (*o*-C_6H_2<u>Me$_3$</u>).

NMR tube-scale synthesis of Mg(^{Ph}NacNac){(N^{i}Pr)$_2$CGa(NArCH)$_2$} (9). To a solution of Mg(^{Ph}NacNac){Ga(NArCH)$_2$}(THF) (**6**, 20 mg, 25 μmol) in C_6D_6 (0.5 mL) was added ^{i}PrNCN^{i}Pr (3.9 μL, 25 μmol). The reaction was accompanied by a colour change from pale yellow to orange. The solution was immediately analysed by ^{1}H and ^{13}C NMR spectroscopies. ^{1}H NMR (C_6D_6, 400.2 MHz): δ 7.15 (6 H, overlapping 2 x m, *o*-C_6H_5 & *p*-C_6H_3), 7.08 (4 H, d, ^{3}J = 7.7 Hz, *m*-C_6H_5), 6.91 (6 H, overlapping 2 x m, *p*-C_6H_5 & *m*-C_6H_3(^{i}Pr)$_2$), 6.30 (2 H, s, GaNCH), 4.79 (1 H, s, NC(Me)C<u>H</u>), 3.55 (4 H, sept, ^{3}J = 7.0 Hz, ArC<u>H</u>Me$_2$), 3.13 (2 H, sept, ^{3}J = 6.1 Hz, NC<u>H</u>Me$_2$), 1.80 (6 H, s, NCMe), 1.26 (12 H, d, ^{3}J = 6.9 Hz, ArCH<u>Me$_2$</u>), 1.21 (12 H, d, ^{3}J = 6.9 Hz, ArCH<u>Me$_2$</u>), 0.70 (12 H, d, ^{3}J = 6.1 Hz, NCH<u>Me$_2$</u>). ^{13}C{^{1}H} NMR (C_6D_6, 100.6 MHz): δ 178.1 (NCN), 167.4 (N<u>C</u>Me), 150.6 (*i*-C_6H_5), 145.4 (*i*-C_6H_3), 129.07 (*m*-C_6H_5), 125.9 (*p*-C_6H_5), 124.9 (*m*-C_6H_3), 123.8 (*o*-C_6H_3), 123.6 (*o*-C_6H_5), 123.4 (*p*-C_6H_3), 120.6 (GaNCH), 96.8 (NC(Me)<u>C</u>H), 55.0 (N<u>C</u>HMe$_2$), 28.7 (Ar<u>C</u>HMe$_2$), 26.7 (NCH<u>Me$_2$</u>), 25.9 (ArCH<u>Me$_2$</u>), 24.6 (ArCH<u>Me$_2$</u>), 23.6 (NC<u>Me</u>).

Mg(^{Dipp}NacNac){(NCy)$_2$CGa(NArCH)$_2$} (10). To a solution of Mg(^{Dipp}NacNac){Ga(NArCH)$_2$}(THF) (**1**, 0.400 g, 0.42 mmol) in toluene (15 mL) at -78 ºC was added a solution of CyNCNCy (0.0867 g, 0.42 mmol) in toluene (5 mL).

The mixture was allowed to warm to RT then stirred for a further 1 h to give an orange solution. The solution was filtered and the volatiles were removed from the filtrate under reduced pressure. The resultant solid was washed with cold hexane (2 x 5 mL) and dried *in vacuo* to afford **10** as yellow solid. Yield: 0.310 g (68%). ^{1}H NMR (C_6D_6, 400.2 MHz): δ 7.24 – 7.17 (6 H, overlapping 2 x m, *m*- & *p*-C_6H_3 of $Ga(NArCH)_2$), 7.08 (6 H, s, *m*- & *p*-C_6H_3 of ^{Dipp}NacNac), 6.13 (2 H, s, ArNC<u>H</u>), 4.82 (1 H, s, NC(Me)C<u>H</u>), 3.50 (4 H, sept, ^{3}J = 7.1 Hz, C<u>H</u>Me_2 of $Ga(NArCH)_2$), 3.34 (4 H, sept, ^{3}J = 7.1 Hz, C<u>H</u>Me_2 of ^{Dipp}NacNac), 2.99 (2 H, br. s, 1-C_6H_{11}), 1.63 (6 H, s, NCMe), 1.49, 1.45, 1.40, 1.24, 1.08 (20 H, m, 2,3,4,5,6-C_6H_{11}), 1.30 (12 H, d, ^{3}J = 6.8 Hz, CH<u>Me$_2$</u> of $Ga(NArCH)_2$), 1.29 (12 H, d, ^{3}J = 6.8 Hz, CH<u>Me$_2$</u> of $Ga(NArCH)_2$), 1.19 (12 H, d, ^{3}J = 6.8 Hz, CH<u>Me$_2$</u> of ^{Dipp}NacNac), 1.12 (12 H, d, ^{3}J = 6.8 Hz, CH<u>Me$_2$</u> of ^{Dipp}NacNac). ^{13}C{^{1}H} NMR (C_6D_6, 100.6 MHz): δ 178.7 (NCN), 170.1 (N<u>C</u>Me), 145.8 (*i*-C_6H_3 of $Ga(NArCH)_2$), 145.5 (*o*-C_6H_3 of $Ga(NArCH)_2$), 145.2 (*i*-C_6H_3 of ^{Dipp}NacNac), 142.6 (*p*-C_6H_3 of ^{Dipp}NacNac), 126.0 (*p*-C_6H_3 of $Ga(NArCH)_2$), 125.3 (*p*-C_6H_3 of ^{Dipp}NacNac), 124.0 (*m*-C_6H_3 of ^{Dipp}NacNac), 123.8 (*m*-C_6H_3 of $Ga(NArCH)_2$), 121.8 (ArN<u>C</u>H), 94.4 (NC(Me)<u>C</u>H), 59.6 (1-C_6H_{11}), 37.5 (2,6-C_6H_{11}), 29.0 (<u>C</u>HMe_2 of $Ga(NArCH)_2$), 28.0 (<u>C</u>HMe_2 of ^{Dipp}NacNac), 26.4 (CH<u>Me$_2$</u> of $Ga(NArCH)_2$), 26.1 (3,5-C_6H_{11}), 25.2 (CH<u>Me$_2$</u> of ^{Dipp}NacNac), 24.7 (CH<u>Me$_2$</u> of ^{Dipp}NacNac), 24.4 (N<u>CMe</u>), 24.3 (4-C_6H_{11}), 23.7 (CH<u>Me$_2$</u> of $Ga(NArCH)_2$). IR (NaCl plates, Nujol mull, cm^{-1}): 1541 (m), 1517 (m), 1460 (s), 1404 (s), 1379 (s), 1360 (s), 1350 (m), 1316 (m), 1254 (m), 1207 (w), 1175 (w), 1114 (m), 1053 (w), 1020 (w), 930 (w), 804 (w), 792 (w), 759 (m), 721 (w), 687 (w), 672(w). Anal. found (calcd. for $C_{68}H_{99}GaMgN_6$): C, 74.07 (74.62); H, 9.33 (9.12); N, 7.18 (7.68)%.

Mg(^{Dipp}NacNac){$(NTol)_2CGa(NArCH)_2$} (11). To a solution of Mg(^{Dipp}NacNac){$Ga(NArCH)_2$}(THF) (**1**, 0.400 g, 0.420 mmol) in toluene (15 mL) at -78 ºC was added a solution of TolNCNTol (0.0926 g, 0.420 mmol) in toluene (5 mL). The suspension was allowed to warm to RT then stirred for a further 16 h to give an orange solution. The solution was filtered and the volatiles were removed from the filtrate under reduced pressure. The resultant solid was washed with cold hexane (2 x 5 mL) and dried *in vacuo* to afford **11** as a bright orange solid. Yield: 0.432 g (92%). ^{1}H NMR (C_6D_6, 400.2 MHz): δ 7.15 – 7.10 (8 H, overlapping 3 x m, *m*- & *p*-C_6H_3 of $Ga(NArCH)_2$ and *p*-C_6H_3 of ^{Dipp}NacNac), 7.08 – 7.00 (4 H, m, *m*-

C_6H_3 of ^{Dipp}NacNac), 6.72 (4 H, d, ^3J = 7.8 Hz, *m*-C_6H_4), 6.43 (4 H, d, ^3J = 7.8 Hz, *m*-C_6H_4), 6.12 (2 H, s, NCH), 4.88 (1 H, s, NC(Me)C<u>H</u>), 3.19 (4 H, sept, ^3J = 6.5 Hz, C<u>H</u>Me_2 of ^{Dipp}NacNac), 3.07 (4 H, sept, ^3J = 6.5 Hz, C<u>H</u>Me_2 of Ga(NArCH)$_2$), 2.08 (6 H, s, <u>Me</u>C_6H_4), 1.67 (6 H, s, NCMe), 1.19 (12 H, d, ^3J = 6.8 Hz, CH<u>Me</u>$_2$ of Ga(NArCH)$_2$), 1.13 (12 H, d, ^3J = 6.8 Hz, CH<u>Me</u>$_2$ of ^{Dipp}NacNac), 0.89 (12 H, d, ^3J = 6.8 Hz, CH<u>Me</u>$_2$ of Ga(NArCH)$_2$), 0.71 (12 H, d, ^3J = 6.8 Hz, CH<u>Me</u>$_2$ of ^{Dipp}NacNac). $^{13}C\{^1H\}$ NMR (C_6D_6, 100.6 MHz): δ 180.8 (NCN), 169.8 (N<u>C</u>Me), 146.7 (*i*-C_6H_4), 145.1 (*i*-C_6H_3 of Ga(NArCH)$_2$), 145.0 (*o*-C_6H_3 of Ga(NArCH)$_2$), 144.6 (*i*-C_6H_3 of ^{Dipp}NacNac), 142.6 (*o*-C_6H_3 of ^{Dipp}NacNac), 132.5 (*p*-C_6H_4), 130.6 (*m*-C_6H_4), 125.5 (*p*-C_6H_3 of ^{Dipp}NacNac), 125.3 (*p*-C_6H_3 of Ga(NArCH)$_2$), 124.0 (*m*-C_6H_3 of ^{Dipp}NacNac), 123.7 (*m*-C_6H_3 of Ga(NArCH)$_2$), 121.9 (*o*-C_6H_4), 120.8 (N<u>C</u>H), 95.3 (NC(Me)<u>C</u>H), 28.6 (<u>C</u>HMe_2 of Ga(NArCH)$_2$), 28.4 (<u>C</u>HMe_2 of ^{Dipp}NacNac), 26.0 (CH<u>Me</u>$_2$ of Ga(NArCH)$_2$), 24.4 (CH<u>Me</u>$_2$ of ^{Dipp}NacNac), 24.0 (NC<u>Me</u>), 23.9 (CH<u>Me</u>$_2$ of ^{Dipp}NacNac), 23.5 (CH<u>Me</u>$_2$ of Ga(NArCH)$_2$), 20.9 (C_6H_4<u>Me</u>). EI-MS: *m/z* = 668 (12%) $[(NTol)_2CGa(NArCH)_2 + H]^+$, 445 $[Ga(NArCH)_2]^+$, 403 (70%) $[^{Dipp}$NacNac-Me + H$]^+$. IR (NaCl plates, Nujol mull, cm^{-1}): 1646 (w), 1621 (w), 1567 (w), 1542 (m), 1518 (m), 1503 (s), 1463 (s), 1377 (sh), 1350 (s), 1315 (m), 1261 (m), 1226 (m), 1212 (m), 1177 (w), 1107 (w), 1053 (m), 1021 (m), 959 (w), 932 w), 853 (m), 821 (m), 793 (m), 757 (m), 721 (m), 690 (w), 668 (m), 655 (w). Anal. found (calcd. for $C_{70}H_{91}GaMgN_6$): C, 75.81 (75.71); H, 8.35 (8.26); N, 7.54 (7.57)%.

NMR tube scale synthesis of Mg(^{Ph}NacNac){(NTol)$_2$CGa(NArCH)$_2$} (12). To TolNCNTol (2.9 mg, 13 μmol) was added a solution of Mg(^{Ph}NacNac){Ga(NArCH)$_2$}(THF) (**6**, 10 mg, 13 μmol) in C_6D_6 (0.5 mL). The reaction mixture was stirred until the carbodiimide had dissolved and then the solution transferred to an NMR tube. The solution was then analysed by ^1H and ^{13}C NMR spectroscopies. ^1H NMR (C_6D_6, 400.2 MHz): δ 7.28-7.22 (6 H, overlapping 2 x m, *m*-C_6H_3 & *p*-C_6H_5), 6.87-6.78 (14 H, overlapping 4 x m, *m*-C_6H_5, *m*-C_6H_3, *o*-C_6H_4 & *o*-C_6H_5), 6.71 (4 H, d, ^3J = 8.0 Hz, *m*-C_6H_4), 6.25 (2 H, s, NCH), 4.88 (1 H, s, NC(Me)C<u>H</u>), 3.40 (4 H, sept, ^3J = 6.8 Hz, C<u>H</u>Me_2), 2.10 (6 H, s, C_6H_4<u>Me</u>), 1.89 (6 H, s, NCMe), 1.29 (12 H, d, ^3J = 6.8 Hz, CH<u>Me</u>$_2$), 1.16 (12 H, d, ^3J = 6.9 Hz, , CH<u>Me</u>$_2$). $^{13}C\{^1H\}$ NMR (C_6D_6, 100.6 MHz): δ 189.0 (NCN) 166.3 (N<u>C</u>Me), 151.8 (*i*-C_6H_5), 148.2 (*i*-C_6H_4), 145.5 (*i*-C_6H_3), 145.4 (*o*-$C_6H_3(^iPr)_2$), 131.0 (*p*-C_6H_4), 130.8 (*o*-C_6H_4), 129.2 (*m*-C_6H_5), 125.4 (*p*-C_6H_5), 124.8 (*o*-C_6H_5), 124.0 (*m*-C_6H_3), 123.2 (*p*-C_6H_3),

120.7 (*m*-C_6H_4), 120.7 (NCH), 95.6 (NC(Me)CH), 28.7 ($\underline{C}HMe_2$), 26.0 ($CH\underline{Me}_2$), 24.0 ($CH\underline{Me}_2$), 23.5 (NC$\underline{Me}$), 20.8 ($C_6H_4\underline{Me}$).

Ca(^{Dipp}NacNac){(N^iPr)$_2$C(Ga(NArCH)$_2$}(THF) (13). To a solution of Ca(^{Dipp}NacNac){Ga(NArCH)$_2$}(THF) (**2**, 0.400 g, 0.410 mmol) in toluene (15 mL) at -78 ºC was added a solution of $^iPrNCN^iPr$ (0.0517 g, 0.410 mmol) in toluene (5 mL). The solution was allowed to warm to RT then stirred for a further 1 h to give an orange solution. The solution was filtered and the volatiles were removed from the filtrate under reduced pressure. The resultant solid was washed with cold hexane (2 x 5 mL) and dried *in vacuo* to afford **13** as a yellow solid. Yield: 0.276 g (61%). ^{1}H NMR (C_6D_6, 400.2 MHz): 7.28 – 7.20 (7 H, overlapping 2 x m, *m*- & *p*-C_6H_3 of Ga(NArCH)$_2$), 7.12 – 7.04 (7 H, m, overlapping 2 x m, *m*- & *p*-C_6H_3 of ^{Dipp}NacNac), 6.33 (2 H, s, ArNC$\underline{H}$), 4.83 (1 H, s, NC(Me)C$\underline{H}$), 3.70 (4 H, sept, ^3J = 6.8 Hz, C$\underline{H}Me_2$ of Ga(NArCH)$_2$), 3.25 (4 H, sept, ^3J = 6.8 Hz, C$\underline{H}Me_2$ of ^{Dipp}NacNac), 3.18 (4 H, br. s, OCH_2), 1.68 (6 H, s, NCMe), 1.41 (12 H, d, ^3J = 6.8 Hz, CH$\underline{Me}_2$ of Ga(NArCH)$_2$), 1.36 (12 H, d, ^3J = 6.8 Hz, CH$\underline{Me}_2$ of Ga(NArCH)$_2$), 1.19 (12 H, d, ^3J = 6.8 Hz, CH$\underline{Me}_2$ of ^{Dipp}NacNac), 1.14 (12 H, d, ^3J = 6.8 Hz, CH$\underline{Me}_2$ of ^{Dipp}NacNac), 1.07 (4 H, br. s, $OCH_2C\underline{H}_2$), 0.85 (12 H, br. s, NCH$\underline{Me}_2$). ^{13}C{^{1}H} NMR (C_6D_6, 100.6 MHz): δ 165.5 (N$\underline{C}$Me), 147.9 (*i*-C_6H_3 of ^{Dipp}NacNac), 146.0 (*i*-C_6H_3 of Ga(NArCH)$_2$), 145.7 (*o*-C_6H_3 of Ga(NArCH)$_2$), 141.6 (*o*-C_6H_3 of ^{Dipp}NacNac), 125.6 (*p*-C_6H_3 of Ga(NArCH)$_2$), 124.2 (*p*-C_6H_3 of ^{Dipp}NacNac), 123.8 (*m*-C_6H_3 of ^{Dipp}NacNac), 123.5 (*m*-C_6H_3 of Ga(NArCH)$_2$), 121.3 (ArN$\underline{C}$H), 93.2 (NC(Me)$\underline{C}$H), 68.5 (OCH_2), 60.5 (N$\underline{C}HMe_2$), 29.0 ($\underline{C}HMe_2$ of Ga(NArCH)$_2$), 28.2 ($\underline{C}HMe_2$ of ^{Dipp}NacNac), 27.4 (NCH$\underline{Me}_2$), 26.6 (CH$\underline{Me}_2$ of Ga(NArCH)$_2$), 26.1 (CH$\underline{Me}_2$ of ^{Dipp}NacNac), 25.1 ($OCH_2\underline{C}H_2$), 24.9 (NC$\underline{Me}$), 24.4 (CH$\underline{Me}_2$ of ^{Dipp}NacNac), 24.0 (CH$\underline{Me}_2$ of Ga(NArCH)$_2$). IR (NaCl plates, Nujol mull, cm^{-1}): 3059 (w), 2924 (s), 2854 (s), 1543 (s), 1507 (s), 1466 (s), 1403 (s), 1379 (s), 1363 (s), 1353 (s), 1320 (m), 1257 (m), 1227 (m), 1209 (w), 1173 (m), 1112 (m), 1056 (w), 1034 (w), 1017 (w), 926 (w), 879 (w), 800 (w), 787 (w), 757 (m), 722 (w), 674 (w). Anal. found (calcd. for $C_{66}H_{99}CaGaN_6O$): C, 71.70 (71.91); H, 8.90 (9.05); N, 7.56 (7.62)%.

Ca(^{Dipp}NacNac){(NCy)$_2$C(Ga(NArCH)$_2$}(THF) (14). To a solution of Ca(^{Dipp}NacNac){Ga(NArCH)$_2$}(THF) (**2**, 0.400 g, 0.410 mmol) in toluene (15 mL) at -78 ºC was added a solution of CyNCNCy (0.0846 g, 0.410 mmol) in toluene (5 mL). The solution was allowed to warm to RT then stirred for a further 1 h to give an

orange solution. The solution was filtered and the volatiles were removed from the filtrate under reduced pressure. The resultant solid was washed with cold hexane (2 x 5 mL) and dried *in vacuo* to afford **14** as a yellow solid. Yield: 0.368 g (76%). ^{1}H NMR (C_6D_6, 400.2 MHz): 7.31 – 7.23 (6 H, overlapping 2 x m, *m*- & *p*-C_6H_3 of $Ga(NArCH)_2$), 7.11 – 7.03 (6 H, overlapping 2 x m, *m*- & *p*-C_6H_3 of ^{Dipp}NacNac), 6.28 (2 H, s, ArNC<u>H</u>), 4.86 (1 H, s, NC(Me)C<u>H</u>), 3.67 (4 H, sept, ^{3}J = 6.9 Hz, C<u>H</u>Me_2 of $Ga(NArCH)_2$), 3.26 (4 H, sept, ^{3}J = 6.3 Hz, C<u>H</u>Me_2 of $Ga(NArCH)_2$), 3.11 (4 H, br. s, OCH_2), 2.95 – 2.86 (2 H, m, 1-C_6H_{11}), 1.71 (6 H, s, NCMe), 1.62 (12 H, m, 2,4,6-C_6H_{11}), 1.47 (12 H, d, ^{3}J = 6.8 Hz, CH<u>Me</u>$_2$ of $Ga(NArCH)_2$), 1.40 (12 H, d, ^{3}J = 6.8 Hz, CH<u>Me</u>$_2$ of $Ga(NArCH)_2$), 1.38 – 1.30 (6 H, m, 3,5-C_6H_{11}), 1.17 (12H, d, ^{3}J = 6.8 Hz, CH<u>Me</u>$_2$ of ^{Dipp}NacNac), 1.10 (12H, d, ^{3}J = 6.8 Hz, CH<u>Me</u>$_2$ of ^{Dipp}NacNac), 1.06 (4 H, br. s, OCH_2C<u>H</u>$_2$). ^{13}C{^{1}H} NMR (C_6D_6, 100.6 MHz): δ 176.3 (NCN), 165.5 (N<u>C</u>Me), 147.8 (*i*-C_6H_3 of ^{Dipp}NacNac), 146.4 (*i*-C_6H_3 of $Ga(NArCH)_2$), 145.6 (*o*-C_6H_3 of $Ga(NArCH)_2$), 141.6 (*p*-C_6H_3 of ^{Dipp}NacNac), 125.5 (*p*-C_6H_3 of $Ga(NArCH)_2$), 124.2 (*p*-C_6H_3 of ^{Dipp}NacNac), 123.7 (*m*-C_6H_3 of ^{Dipp}NacNac), 123.6 (*o*-C_6H_3 of $Ga(NArCH)_2$), 121.8 (ArN<u>C</u>H), 93.1 (NC(Me)<u>C</u>H), 68.4 (OCH_2), 67.9 (1-C_6H_{11}), 38.1 (2,6-C_6H_{11}), 29.0 (<u>C</u>HMe_2 of $Ga(NArCH)_2$), 28.2 (<u>C</u>HMe_2 of ^{Dipp}NacNac), 26.8 (CH<u>Me</u>$_2$ of $Ga(NArCH)_2$), 26.2 (4-C_6H_{11}), 26.1 (3,5-C_6H_{11}), 26.1 (CH<u>Me</u>$_2$ of ^{Dipp}NacNac), 25.3 (OCH_2<u>C</u>H_2), 24.9 (NC<u>Me</u>), 24.5 (CH<u>Me</u>$_2$ of ^{Dipp}NacNac), 23.9 (CH<u>Me</u>$_2$ of $Ga(NArCH)_2$). IR (NaCl plates, Nujol mull, cm^{-1}): 2723 (w), 2559 (w), 2521 (w), 2121 (w), 1917 (w), 1855 (w), 1541(s), 1531 (s), 1255 (s), 1228 (s), 1207 (s), 1170 (s), 1158 (s), 1108 (s), 1055 (s), 1038 (m), 987 (m), 960 (m), 925 (w), 906 (w), 885 (w), 833 (w), 800 (w), 788 (m), 758 (m), 708 (m), 687 (w), 666 (w), 587 (w). A satisfactory elemental analysis could not be obtained.

Ca(^{Dipp}NacNac){(NTol)$_2$C(Ga(NArCH)$_2$}(THF) (15). To a solution of Ca(^{Dipp}NacNac){Ga(NArCH)$_2$}(THF) (**2**, 0.300 g, 0.307 mmol) in toluene (15 mL) at -78 ºC was added a solution of TolNCNTol (0.0683 g, 0.307 mmol) in toluene (5 mL). The solution was allowed to warm to RT then stirred for a further 16 h to give a bright orange solution. The solution was filtered and the volatiles were removed from the filtrate under reduced pressure. The resultant solid was washed with cold hexane (2 x 5 mL) and dried *in vacuo* to afford **15** as a yellow solid. Yield: 0.250 g (68%). ^{1}H NMR (C_6D_6, 400.2 MHz): δ 7.26 – 7.19 (6 H, overlapping 2 x m, *m*- & *p*-C_6H_3 of $Ga(NArCH)_2$), 7.13 – 7.07 (6 H, overlapping 2 x m, *m*- & *p*-C_6H_3 of ^{Dipp}NacNac),

6.84 (4 H, d, ^3J = 7.8 Hz, *m*-C_6H_4), 6.36 (4 H, d, ^3J = 7.8 Hz, *p*-C_6H_4), 6.22 (2 H, s, NCH), 4.87 (1 H, s, NC(Me)C<u>H</u>), 3.26 – 3.10 (12H, overlapping 3 x m, C<u>H</u>Me_2 of Ga(NArCH)$_2$, C<u>H</u>Me_2 of ^{Dipp}NacNac & OCH_2), 2.17 (6 H, s, C_6H_4<u>Me</u>), 1.67 (6 H, s, NCMe), 1.20 (12H, d, ^3J = 6.7 Hz, CH<u>Me</u>$_2$ of Ga(NArCH)$_2$), 1.18 (12H, d, ^3J = 6.7 Hz, CH<u>Me</u>$_2$ of Ga(NArCH)$_2$), 1.16 (12H, m, CH<u>Me</u>$_2$ of ^{Dipp}NacNac), 1.01 (4 H, s, OCH_2C<u>H</u>$_2$), 0.96 (12H, d, ^3J = 6.9 Hz, CH<u>Me</u>$_2$ of ^{Dipp}NacNac). $^{13}C\{^1H\}$ NMR (C_6D_6, 100.6 MHz): δ 165.5 (N<u>C</u>Me), 149.9 (*i*-C_6H_4), 149.4 (*p*-C_6H_4), 145.9 (*i*-C_6H_3 of ^{Dipp}NacNac), 145.5 (*i*-C_6H_3 of Ga(NArCH)$_2$), 145.0 (*o*-C_6H_3 of Ga(NArCH)$_2$), 141.5 (*o*-C_6H_3 of ^{Dipp}NacNac), 130.4 (*m*-C_6H_4), 124.1 (*p*-C_6H_3 of Ga(NArCH)$_2$), 123.9 (*p*-C_6H_3 of ^{Dipp}NacNac), 123.7 (*m*-C_6H_3 of ^{Dipp}NacNac), 123.5 (*m*-C_6H_3 of Ga(NArCH)$_2$), 120.2 (NCH), 120.1 (*o*-C_6H_4), 94.9 (NC(Me)<u>C</u>H), 68.3 (OCH_2), 28.2 (<u>C</u>HMe_2 of Ga(NArCH)$_2$), 27.9 (<u>C</u>HMe_2 of ^{Dipp}NacNac), 25.7 (CH<u>Me</u>$_2$ of Ga(NArCH)$_2$), 24.8 (OCH_2<u>C</u>H_2), 24.8 (CH<u>Me</u>$_2$ of ^{Dipp}NacNac), 24.2 (NC<u>Me</u>), 24.0 (CH<u>Me</u>$_2$ of ^{Dipp}NacNac), 25.7 (CH<u>Me</u>$_2$ of Ga(NArCH)$_2$), 20.5 C_6H_4<u>Me</u>). IR (NaCl plates, Nujol mull, cm^{-1}): 1540 (m), 1501 (s), 1433 (s), 1406 (s), 1378 (s), 1364 (s), 1352 (s), 1315 (m), 1257 (s), 1228 (s), 1195 (s), 1171 (s), 1109 (s), 1054 (s), 1031 (s), 935 (w), 905 (s), 878 (s), 817 (s), 799 (s), 788 (m), 758(m), 722 (w). Anal. found (calcd. for $C_{74}H_{99}CaGaN_6O$): C, 73.99 (74.16); H, 8.43 (8.33); N, 6.90 (7.01)%.

Ca{(NTol)$_2$C(Ga(NArCH)$_2$}$_2$(THF)$_2$ (16) To a solution of Ca{Ga(NArCH)$_2$}$_2$(THF)$_4$ (**1.12**, 0.500 g, 0.409 mmol) in THF (20 mL) at -78 ºC was added a solution of TolNCNTol (0.1820 g, 0.819 mmol) in THF (10 mL). The suspension was allowed to warm to RT then stirred for a further 16 h to give an orange solution. The solution was filtered and the volatiles were removed from the filtrate under reduced pressure. The resultant solid was washed with hexane (3 x 5 mL) and dried *in vacuo* to afford **16** as a bright yellow solid. Yield: 0.380 g (61%). ^1H NMR (THF-d_8, 400.2 MHz): δ 7.11 – 6.98 (12 H, overlapping 2 x m, *m*- & *p*-C_6H_3), 6.61 (8 H, d, ^3J = 8.1 Hz, *m*-C_6H_4), 6.49 (8 H, d, ^3J = 8.1 Hz, *o*-C_6H_4), 5.82 (4 H, s, NCH), 3.64 – 3.59 (8 H, m, OCH_2), 2.97 (8 H, sept, ^3J = 6.6 Hz, C<u>H</u>Me_2), 2.14 (12H, s, C_6H_4Me), 1.77 (8 H, m, OCH_2C<u>H</u>$_2$), 1.02 – 0.91 (48H, m, CH<u>Me</u>$_2$). $^{13}C\{^1H\}$ NMR (THF-d_8, 100.6 MHz): δ 151.3 (*p*-C_6H_4), 146.3 (*i*-C_6H_3), 145.6 (*o*-C_6H_3), 130.8 (*m*-C_6H_4), 130.0 (*i*-C_6H_4), 123.8 (*p*-C_6H_3), 123.7 (*m*-C_6H_3), 120.4 (*o*-C_6H_4), 120.4 (NCH), 68.0 (OCH_2), 28.6 (<u>C</u>HMe_2), 26.2 (CH<u>Me</u>$_2$), 25.9 (OCH_2<u>C</u>H_2), 24.1 (CH<u>Me</u>$_2$), 20.65 (C_6H_4Me). IR (NaCl plates, Nujol mull, cm^{-1}): 2728 (w), 1654 (w),

1605 (w), 1589 (w), 1562 (w), 1501 (s), 1434 (s), 1378 (s), 1360 (s), 1350 (s), 1320 (m), 1256 (m), 1230 (m), 1210 (m), 1194 (m), 1171 (m), 1110 (s), 1074 (m), 1054 (m), 1037 (m), 939 (m), 905 (m), 881 (m), 818 (s), 800 (m), 757 (s), 722 (w), 688 (w), 653 (w), 611 (w). Anal. found (calcd. for $C_{90}H_{116}CaGa_2N_8O_2$): C, 71.50 (71.05); H, 7.90 (7.69); N, 7.56 (7.36)%.

NMR tube-scale synthesis of Mg(^{Dipp}NacNac){O(Ga(NArCH)$_2$}(THF) (17) Mg(^{Dipp}NacNac){Ga(NArCH)$_2$}(THF) (**1**, 20.0 mg, 20.8 μmol) in C_6D_6 (0.6 mL) at RT was added isobutene epoxide (1.5 mg, 21 μmol). The solution was immediately analysed by ^{1}H and ^{13}C NMR spectroscopies which showed the formation of **17**, isobutene and other minor unknown species. ^{1}H NMR (C_6D_6, 400.2 MHz): δ 7.13 (6 H, s, *m*- & *p*-C_6H_3 of Ga(NArCH)$_2$), 7.11 – 7.03 (6 H, m, *m*- & *p*-C_6H_3 of ^{Dipp}NacNac), 6.02 (2 H, s, NCH), 4.75 (1 H, s, NC(Me)C<u>H</u>), 3.63 (4 H, sept, ^3J = 6.8 Hz, C<u>H</u>Me$_2$ of Ga(NArCH)$_2$), 3.18 (4 H, br. s, OCH$_2$), 3.06 (4 H, sept, ^3J = 6.7 Hz, C<u>H</u>Me$_2$ of ^{Dipp}NacNac), 1.57 (6 H, s, NCMe), 1.33 (12H, d, ^3J = 6.8 Hz, CH<u>Me$_2$</u> of Ga(NArCH)$_2$), 1.17 – 1.08 (36H, br. m centred at 1.15 & 1.10, overlapping resonaces for CH<u>Me$_2$</u> of Ga(NArCH)$_2$ & CH<u>Me$_2$</u> of ^{Dipp}NacNac), 0.84 (4 H, br. s, OCH$_2$C<u>H$_2$</u>). ^{13}C{^{1}H} NMR (C_6D_6, 100.6 MHz): δ 168.8 (N<u>C</u>Me), 146.1 (*o*-C_6H_3 of Ga(NArCH)$_2$), 145.7 (*i*-C_6H_3 of Ga(NArCH)$_2$), 145.6 (*i*-C_6H_3 of ^{Dipp}NacNac), 142.3 (*o*-C_6H_3 of ^{Dipp}NacNac), 124.8 (*p*-C_6H_3 of Ga(NArCH)$_2$), 124.2 (*m*-C_6H_3 of ^{Dipp}NacNac), 123.6 (*p*-C_6H_3 of ^{Dipp}NacNac), 123.3 (*m*-C_6H_3 of Ga(NArCH)$_2$), 118.2 (NCH), 94.6 (NC(Me)<u>C</u>H), 69.3 (OCH$_2$), 28.4 (<u>C</u>HMe$_2$ of ^{Dipp}NacNac), 28.3 (<u>C</u>HMe$_2$ of Ga(NArCH)$_2$), 25.6 (CH<u>Me$_2$</u> of Ga(NArCH)$_2$), 25.2 (OCH$_2$<u>CH$_2$</u>), 24.4 (CH<u>Me$_2$</u> of Ga(NArCH)$_2$), 24.3 (CH<u>Me$_2$</u> of ^{Dipp}NacNac), 24.2 (CH<u>Me$_2$</u> of ^{Dipp}NacNac), 24.1 (NC<u>Me</u>).

Ca(^{Dipp}NacNac){O(Ga(NArCH)$_2$}(THF) (18). To a solution of Ca(^{Dipp}NacNac){Ga(NArCH)$_2$}(THF) (**2**, 0.300 g, 0.307 mmol) in toluene (15 mL) at -78 ºC was added a solution of isobutene epoxide (0.0221 g, 0.307 mmol) in toluene (5 mL). The solution was allowed to warm to RT then stirred for a further 2 h to give a yellow solution. The solution was filtered and the volatiles were removed from the filtrate under reduced pressure. The resultant solid was washed with cold hexane (2 x 2 mL) and dried *in vacuo* to afford **18** as a yellow solid. Yield: 0.192 g (63%). ^{1}H NMR (C_6D_6, 400.2 MHz): δ 7.16 (overlapping with solvent, m, *m*- & *p*-C_6H_3 of Ga(NArCH)$_2$), 7.10 – 7.06 (6 H, m, *m*- & *p*-C_6H_3 of ^{Dipp}NacNac), 6.04 (2 H, s, NCH),

4.74 (1 H, s, NC(Me)C<u>H</u>), 3.73 (4 H, sept, ^{3}J = 6.9 Hz, C<u>H</u>Me$_2$ of Ga(NArCH)$_2$), 3.19 (4 H, sept, ^{3}J = 6.9 Hz, C<u>H</u>Me$_2$ of ^{Dipp}NacNac), 3.11 (4 H, br. s, OCH$_2$), 1.65 (6 H, s, NCMe), 1.36 (12 H, d, ^{3}J = 6.9 Hz, CH<u>Me</u>$_2$ of Ga(NArCH)$_2$), 1.25 (12 H, d, ^{3}J = 6.9 Hz, CH<u>Me</u>$_2$ of Ga(NArCH)$_2$), 1.17 (24 H, overlapping 2 x d, ^{3}J = 6.9 Hz, CH<u>Me</u>$_2$ of ^{Dipp}NacNac), 1.05 (4 H, br. s, OCH$_2$CH$_2$). ^{13}C{^{1}H} NMR (C$_6$D$_6$, 100.6 MHz): δ 165.6 (N<u>C</u>Me), 146.7 (*i*-C$_6$H$_3$ of ^{Dipp}NacNac), 146.2 (*i*-C$_6$H$_3$ of Ga(NArCH)$_2$), 146.1 (*o*-C$_6$H$_3$ of Ga(NArCH)$_2$), 141.7 (*o*-C$_6$H$_3$ of ^{Dipp}NacNac), 124.8 (*p*-C$_6$H$_3$ of Ga(NArCH)$_2$), 124.4 (*p*-C$_6$H$_3$ of ^{Dipp}NacNac), 123.8 (*m*-C$_6$H$_3$ of ^{Dipp}NacNac), 123.4 (*m*-C$_6$H$_3$ of Ga(NArCH)$_2$), 118.1 (NCH), 93.2 (NC(Me)<u>C</u>H), 69.0 (OCH$_2$), 28.4 (<u>C</u>HMe$_2$ of Ga(NArCH)$_2$), 28.3 (<u>C</u>HMe$_2$ of ^{Dipp}NacNac), 25.3 (CH<u>Me</u>$_2$ of ^{Dipp}NacNac), 25.1 (OCH$_2$<u>C</u>H$_2$), 25.0 (CH<u>Me</u>$_2$ of Ga(NArCH)$_2$), 24.7 (CH<u>Me</u>$_2$ of Ga(NArCH)$_2$), 24.4 (CH<u>Me</u>$_2$ of ^{Dipp}NacNac), 24.3 (OCH$_2$<u>C</u>H$_2$). IR (NaCl plates, Nujol mull, cm^{-1}): 1585 (w), 1541 (w), 1511 (s), 1459 (s), 1378 (s), 1358 (m), 1313 (m), 1259 (m), 1213 (w), 1169 (m), 1099 (m), 1057 (m). Anal. found (calcd. for C$_{59}$H$_{85}$CaGaN$_4$O$_2$): C, 70.99 (71.43); H, 8.33 (8.64); N, 5.10 (5.65)%.

Alternative NMR tube-scale synthesis of Ca(^{Dipp}NacNac){O(Ga(NArCH)$_2$}(THF) (18). To a solution of Ca(^{Dipp}NacNac){Ga(NArCH)$_2$}(THF) (**2**, 20.0 mg, 20.2 μmol) in C$_6$D$_6$ (0.6 mL) at RT was added trimethylamine *N*-oxide (1.5 mg, 20 μmol). The solution was immediately analysed by ^{1}H NMR spectroscopy. The spectrum was consistent with the formation of **18**, trimethylamine and other minor unknown species.

NMR tube-scale reaction of Ca(^{Dipp}NacNac){O(Ga(NArCH)$_2$}(THF) (18) with Me$_3$SiI. To a solution of Ca(^{Dipp}NacNac){OGa(NArCH)$_2$}(THF) (**18**, 20.0 mg, 20.2 μmol) in C$_6$D$_6$ (0.6 mL) at RT was Me$_3$SiI (2.9 μL, 20 μmol). The solution was immediately analysed by ^{1}H NMR which showed the formation of a complex mixture where [Ca(^{Dipp}NacNac)I(THF)]$_2$ (**2.32**) could be indentified.

NMR tube-scale reaction of Mg(^{Dipp}NacNac){Ga(NArCH)$_2$}(THF) (1) with MeI. To a solution of Mg(^{Dipp}NacNac){Ga(NArCH)$_2$}(THF) (**1**, 20.0 mg, 20.8 μmol) in C$_6$D$_6$ (0.6 mL) at RT was MeI (1.7 μL, 21 μmol). The solution was immediately analysed by ^{1}H NMR which showed the formation of a complex mixture where Mg(^{Dipp}NacNac)I(THF) (**2.31**) could be indentified.

NMR tube-scale reaction of Ca(^{Dipp}NacNac){Ga(NArCH)$_2$}(THF) (2) with MeI. To a solution of Ca(^{Dipp}NacNac){Ga(NArCH)$_2$}(THF) (**2**, 20.0 mg, 20.5 μmol) in C_6D_6 (0.6 mL) at RT was MeI (1.3 μL, 21 μmol). The solution was immediately analysed by ^{1}H NMR which showed the formation of a complex mixture where [Ca(^{Dipp}NacNac)I(THF)]$_2$ (**2.32**) could be indentified.

(Me$_3$Si)Ga(NArCH)$_2$ (19) To a solution of KGa(NArCH)$_2$ (**20**, 0.300 g, 0.618 mmol) in toluene (15 mL) at -78 ºC was added a solution of Me$_3$SiI (0.125 g, 0.618 mmol) in toluene (5 mL). The solution was allowed to warm to RT then stirred for a further 1 h then filtered to give an orange solution. Volatiles were removed under reduced pressure and the resultant solid was extracted into hexane (20 mL) and then filtered. The volatiles were removed from the filtrate under reduced pressure and the resulting solid was dried *in vacuo* to afford **19** as a yellow solid. Yield: 1.05 g (84%). Diffraction-quality crystals were grown by slow evaporation from a concentrated benzene solution at RT. ^{1}H NMR (C_6D_6, 400.2 MHz): δ 7.20 (6 H, s, *m*- & *p*-C_6H_3), 6.33 (2 H, s, NCH), 3.59 (4 H, sept, ^3J = 6.9 Hz, C<u>H</u>Me$_2$), 1.28 (12 H, d, ^3J = 6.9 Hz, CH<u>Me</u>$_2$), 1.27 (12 H, d, ^3J = 6.9 Hz, CH<u>Me</u>$_2$), 0.00 (9 H, s, SiMe$_3$). ^{13}C{^{1}H} NMR (C_6D_6, 100.6 MHz): δ 145.5 (*i*-C_6H_3), 145.4 (*o*-C_6H_3), 126.0 (*p*-C_6H_3), 123.3 (*m*-C_6H_3), 122.2 (NCH), 28.5 (<u>C</u>HMe$_2$), 25.1 (CH<u>Me</u>$_2$), 24.7 (CH<u>Me</u>$_2$), 0.8 (SiMe$_3$). IR (NaCl plates, Nujol mull, cm^{-1}): 1918 (w), 1856 (w), 1663 (w), 1589 (m), 1460 (s), 1379 (s), 1356 (s), 1323 (s), 1261 (s), 1213 (s), 1197 (s), 1178 (s), 1159 (m), 1120 (m), 1058 (m), 1043 (m), 962 (m), 933 (m), 841 (s), 802 (s), 758 (s), 697 (m), 682 (m), 663 (m), 620 (m), 478 (m). Anal. found (calcd. for $C_{56}H_{74}GaMgN_5O_2$): C, 66.96 (67.05); H, 8.92 (8.73); N, 5.45 (5.39)%.

K[Ga(NArCH)$_2$] (20) THF (40 mL) was added to a mixture of Ga(NArCH)I$_2$ (1.00 g, 1.43 mmol) and K (0.172 g, 4.29 mmol) at RT. The dark brown suspension was sonicated for 8 h at RT to give a yellow suspension. The suspension was filtered and the volatiles were removed from the filtrate under reduced pressure. The resultant dark yellow solid was redissolved in benzene (50 mL) and then filtered. The fitrate was concentrated to *ca*. 20 mL and placed in a fridge at 4 ºC overnight to afford **20** as orange crystals. Yield: 0.146 g (21%). ^{1}H NMR (C_6D_6, 400.2 MHz): 7.19 (4 H, d, ^3J = 7.6 Hz, *m*-C_6H_3), 7.09 (2 H, t, ^3J = 7.6 Hz, *p*-C_6H_3), 6.30 (2 H, s, NCH), 3.65 (4 H, sept, ^3J = 7.0 Hz, C<u>H</u>Me$_2$), 1.28 (24 H, dd, ^3J = 7.0 Hz, CH<u>Me</u>$_2$). ^{13}C{^{1}H} NMR (C_6D_6, 100.6 MHz): δ 149.8 (*i*-C_6H_3), 146.0 (*o*-C_6H_3), 123.5 (*p*-C_6H_3), 123.1 (*m*-

C_6H_3), 122.8 (NCH), 28.3 (CHMe$_2$), 25.6 (CHMe$_2$), 25.6 (CHMe$_2$). IR (NaCl plates, Nujol mull, cm^{-1}): 1586 (m), 1556 (m), 1459 (s), 1432 (s), 1378 (s), 1352 (s), 1326 (s), 1309 (s), 1245 (s), 1203 (s), 1185 (m), 1158 (w), 1113 (m), 1097 (m), 1082 (m), 1055 (m), 1037 (m), 931 (w), 885 (w), 858 (m), 800 (m), 758 (m), 744 (w), 722 (w), 694 (m), 678 (m), 647 (w). Anal. found (calcd. for $C_{26}H_{36}GaKN_2$): C, 64.70 (64.33); H, 7.67 (7.48); N, 5.46 (5.77)%.

NMR tube-scale reaction of Mg(^{Dipp}NacNac){Ga(NArCH)$_2$}(THF) (1) with Me$_3$SiI. To a solution of Mg(^{Dipp}NacNac){Ga(NArCH)$_2$}(THF) (**1**, 20.0 mg, 20.8 μmol) in C_6D_6 (0.6 mL) at RT was added Me_3SiI (3.0 μL, 21 μmol). The solution was immediately analysed by ^{1}H NMR. The spectrum was consistent with the formation of Mg(^{Dipp}NacNac)I(THF) (**2.31**) and $Me_3SiGa(NArCH)_2$ **(19)** along with other minor unknown species.

5.5 Ligand numbering system for HCzOx (3.7)

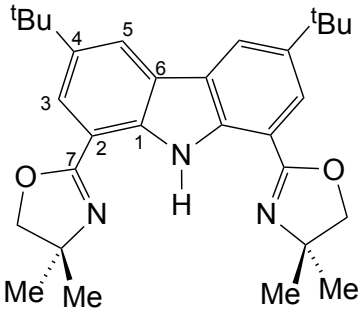

HCzOx (**3.7**)

5.6 Experimental details and characterising data for Chapter Three

Mg(CzOx){Ga(NArCH)$_2$} (21). Toluene (40 mL) was added to Mg(CzOx)I(THF) (**3.14**, 1.00 g, 1.44 mmol) and [KGa(NArCH)$_2$(Et$_2$O)]$_2$ (**1.44**, 0.804 g, 0.718 mmol) at -78 ºC to give an orange suspension. The suspension was allowed to warm to RT, stirred for 1 h then filtered to give an orange solution. Volatiles were removed under reduced pressure and the resultant orange solid washed with hexane (3 × 5 mL) at 0 ºC and dried *in vacuo* to afford **21** as a bright orange solid. Yield: 1.05 g (77%). Diffraction-quality crystals of the THF adduct (**21-THF**) were obtained by slow evaporation of a benzene/THF solution. ^{1}H NMR (C_6D_6, 400.2 MHz): δ 8.54 (2 H, d, ^4J = 1.8 Hz, C_5–H), 8.28 (2 H, d, ^4J = 1.8 Hz, C_3–H), 7.24 – 7.18 (6 H, overlapping 2 × m, *m*- & *p*-C_6H_3), 6.50 (2 H, s, NCH), 3.68 (4 H, sept, ^3J = 6.9 Hz, CHMe$_2$), 3.45 (4 H, s, CH_2), 1.47 (18 H, s, CMe_3), 1.25 (12 H, d, ^3J = 6.9 Hz, CHMe$_2$), 1.10 (12 H, d,

^{3}J = 6.9 Hz, CHMe$_2$), 0.92 (6 H, s, CMe$_2$), 0.81 (6 H, s, CMe$_2$). ^{13}C{^{1}H} NMR (C_6D_6, 100.6 MHz): δ 168.9 (C_7), 149.6 (C_1), 149.1 (*i*-C_6H_3), 145.9 (*o*-C_6H_3), 139.9 (C_4), 127.1 (C_6), 124.2 (C_3), 124.0 (*p*-C_6H_3), 123.3 (C_5), 122.9 (NCH), 122.8 (*m*-C_6H_3), 108.4 (C_2), 78.2 (CH_2), 66.1 (CMe$_2$), 35.0 (CMe$_3$), 32.3 (CMe$_3$), 29.5 (CMe$_2$), 28.6 (CMe$_2$), 28.2 (CHMe$_2$), 25.8 (CHMe$_2$), 24.7 (CHMe$_2$). IR (NaCl plates, Nujol mull, cm^{-1}): 1634 (w), 1597 (w), 1570 (s), 1568 (sh), 1460 (s), 1396 (w), 1377 (m), 1359 (m), 1322 (w), 1272 (m), 1233 (w), 1185 (m), 1074 (m), 1026 (m), 884 (m), 801 (m), 756 (m), 729 (w), 668 (w), 517 (w). Anal. found (calcd. for $C_{56}H_{74}GaMgN_5O_2$): C, 71.14 (71.31); H, 7.81 (7.91); N, 7.40 (7.42)%.

Ca(CzOx){Ga(NArCH)$_2$}(THF)$_2$ (22) Toluene (40 mL) was added to Ca(CzOx)I(THF)$_2$ (**3.16**, 2.00 g, 2.55 mmol) and [KGa(NArCH)$_2$(Et$_2$O)]$_2$ (**1.44**, 1.43 g, 1.28 mmol) at -78 ºC to give a yellow suspension. The suspension was allowed to warm to RT, stirred for 1 h then filtered to give a yellow solution. Volatiles were removed under reduced pressure and the resultant solid washed with hexane (3 × 10 mL) at 0 ºC and dried *in vacuo* to afford **22** as a bright yellow solid. Yield: 2.05 g (73%). ^{1}H NMR (C_6D_6, 400.2 MHz): δ 8.67 (4 H, s, C_5–H & C_3–H), 7.26 (4 H, d, ^{3}J = 6.8 Hz, *m*-C_6H_3), 7.20 – 7.17 (2 H, m, *p*-C_6H_3), 6.54 (2 H, s, NCH), 4.09 (4 H, sept, ^{3}J = 6.9 Hz, CHMe$_2$), 3.65 (4 H, s, CH$_2$CMe$_2$), 3.24 (8 H, br. s, OCH$_2$CH$_2$), 1.52 – 1.48 (30 H, m centred at 1.50 & 1.49, overlapping CMe$_3$ & CHMe$_2$), 1.44 (12 H, s, CMe$_2$), 1.33 (12 H, d, ^{3}J = 6.9 Hz, CHMe$_2$), 0.88 (8 H, br. s, OCH$_2$CH$_2$). ^{13}C{^{1}H} NMR (C_6D_6, 100.6 MHz): δ 167.0 (C_7), 152.3 (*i*-C_6H_3), 149.2 (C_1), 146.1 (*o*-C_6H_3), 138.3 (C_4), 127.0 (C_6), 126.2 (C_3), 123.4 (*p*-C_6H_3), 123.1 (NCH), 122.7 (*m*-C_6H_3), 121.4 (C_5), 109.8 (C_2), 78.3 (CH$_2$CMe$_2$), 69.1 (OCH$_2$CH$_2$), 68.5 (CMe$_2$), 34.7 (CMe$_3$), 32.3 (CMe$_3$), 29.8 (CMe$_2$), 28.8 (CHMe$_2$), 27.2 (CHMe$_2$), 25.0 (OCH$_2$CH$_2$), 24.3 (CHMe$_2$). EI-MS: *m/z* = 512 (5%) [(CzOx)Ca]$^{+}$, 445 (2%) [Ga(NArCH)$_2$]$^{+}$. IR (NaCl plates, Nujol mull, cm^{-1}): 1639 (m), 1599 (s), 1464 (s), 1377 (s), 1318 (m), 1307 (w), 1289 (w), 1255 (w), 1225 (w), 1167 (m), 1116 (w), 1098 (w), 1067 (m), 1030 (m), 963 (w), 933 (w), 882 (w), 822 (w), 801 (w), 775 (w), 765 (w), 722 (m), 672 (w), 645 (w), 632 (w). Anal. found (calcd. for $C_{64}H_{90}CaGaN_5O_4$): C, 69.50 (69.68); H, 8.12 (8.22); N, 6.42 (6.35)%.

Mg(CzOx){(N^{i}Pr)$_2$CGa(NArCH)$_2$} (23). To a solution of Mg(CzOx){Ga(NArCH)$_2$} (**21**, 0.400 g, 0.424 mmol) in toluene (15 mL) at -78 ºC was added a solution of ^{i}PrNCN^{i}Pr (0.0535 g, 0.424 mmol) in toluene (5 mL). The solution was allowed to

warm to RT then stirred for a further 1 h to give an orange solution. The solution was filtered and the volatiles were removed from the filtrate under reduced pressure. The resultant solid was washed with cold hexane (2 × 5 mL) and dried *in vacuo* to afford **23** as an orange solid. Yield: 0.218 g (48%). ^{1}H NMR (C_6D_6, 400.2 MHz): δ 8.58 (2 H, d, ^{4}J = 1.8 Hz, C_5–H), 8.36 (2 H, d, ^{4}J = 1.8 Hz, C_3–H), 7.11 – 7.06 (6 H, overlapping 2 × m, *m*- & *p*-C_6H_3), 6.21 (2 H, s, ArNCH), 3.62 (4 H, s , CH_2), 3.54 (4 H, sept, ^{3}J = 6.7 Hz, ArCHMe$_2$), 3.33 – 3.19 (2 H, m, NCHMe$_2$), 1.45 (18 H, s, CMe$_3$), 1.32 (12 H, s, CMe$_2$), 1.23 (12 H, d, ^{3}J = 6.7 Hz, ArCHMe$_2$), 1.19 (12 H, d, ^{3}J = 6.7 Hz, ArCHMe$_2$), 0.66 (12 H, br. s, NCHMe$_2$). ^{13}C{^{1}H} NMR (C_6D_6, 100.6 MHz): δ 168.7 (C_7), 149.97 (C_1), 145.4 (*o*-C_6H_3), 145.0 (*i*-C_6H_3), 138.6 (C_4), 127.0 (C_6), 125.5 (*p*-C_6H_3), 123.5 (*m*-C_6H_3), 123.2 (C_3), 122.2 (C_5), 120.5 (ArNCH), 109.0 (C_2), 79.57 (CH_2), 67.3 (CMe$_2$), 55.7 (NCHMe$_2$), 34.9 (CMe$_3$), 32.4 (CMe$_3$), 28.7 (ArCHMe$_2$), 27.8 (CMe$_2$), 26.7 (NCHMe$_2$), 26.1 (ArCHMe$_2$), 24.1 (ArCHMe$_2$). EI-MS: *m/z* = 571 (<1%) [(N^{i}Pr)$_2$CGa(NArCH)$_2$]$^{+}$, 497 (20%) [(CzOx)Mg + H]$^{+}$, 473 (60%) [CzOx + H]$^{+}$. IR (NaCl plates, Nujol mull, cm^{-1}): 1638 (m), 1599 (m), 1582 (s), 1558 (w), 1507 (w), 1463 (s), 1377 (m), 1362 (m), 1351 (w), 1339 (w), 1318 (m), 1272 (w), 1232 (w), 1185 (m), 1112 (w), 1074 (m), 1016 (m), 959 (w), 881 (w), 800 (w), 784 (w), 758 (w), 728 (w), 668 (w), 491 (w). A satisfactory elemental analysis could not be obtained.

Mg(CzOx){(NCy)$_2$CGa(NArCH)$_2$} (24). To a solution of Mg(CzOx){Ga(NArCH)$_2$} (**21**, 0.400 g, 0.424 mmol) in toluene (15 mL) at -78 ºC was added a solution of CyNCNCy (0.0874 g, 0.424 mmol) in toluene (5 mL). The solution was allowed to warm to RT then stirred for a further 1 h to give an orange solution. The solution was filtered and the volatiles were removed from the filtrate under reduced pressure. The resultant solid was washed with cold hexane (2 × 5 mL) and dried *in vacuo* to afford **24** as yellow solid. Yield: 0.253 g (54%). ^{1}H NMR (C_6D_6, 400.2 MHz): 8.58 (2 H, d, ^{4}J = 2.0 Hz, C_5–H), 8.34 (2 H, d, ^{4}J = 1.8 Hz, C_3–H), 7.16 – 7.11 (6 H, overlapping 2 × m, *m*- & *p*-C_6H_3), 6.26 (2 H, s, ArNCH), 3.67 – 3.57 (8 H, overlapping 2 × m, OCH_2 & CHMe$_2$), 2.96 – 2.86 (2 H, m, 1-C_6H_{11}), 1.47 (18 H, s, CMe$_3$), 1.30 (12 H, d, ^{3}J = 6.8 Hz, CHMe$_2$), 1.29 – 1.25 (24 H, m, CHMe$_2$ & CMe$_2$), 1.44 – 0.86 (12 H, m, 2,4,6-C_6H_{11}), 0.73 – 0.53 (8 H, m, 3,5-C_6H_{11}). ^{13}C{^{1}H} NMR (C_6D_6, 100.6 MHz): δ 168.6 (C_7), 150.0 (C_1), 145.6 (*i*-C_6H_3), 144.7 (*o*-C_6H_3), 138.7 (C_4), 127.2 (C_6), 125.0 (*p*-C_6H_3), 123.9 (*m*-C_6H_3), 123.1 (C_3), 121.8 (C_5), 120.8 (ArNCH), 109.3 (C_2), 79.6

(OCH_2), 67.3 ($\underline{C}Me_2$), 63.5 (1-C_6H_{11}), 37.7 (2,6-C_6H_{11}), 34.9 ($\underline{C}Me_3$), 32.4 ($C\underline{Me}_3$), 28.8 ($\underline{C}HMe_2$), 27.8 ($C\underline{Me}_2$), 26.2 ($CH\underline{Me}_2$), 25.7 (4-C_6H_{11}), 25.4 (3,5-C_6H_{11}), 24.2 ($CH\underline{Me}_2$). EI-MS: *m/z* = 985 (10%) $[Mg(CzOx)\{(NCy)_2CGa(NArCH)_2\} - Ar]^+$, 652 (20%) $[(NCy)_2CGa(NArCH)_2 + H]^+$, 496 (30%) $[(CzOx)Mg]^+$, 473 (60%) $[(CzOx) + H]^+$. IR (NaCl plates, Nujol mull, cm^{-1}): 2723 (w), 1639 (m), 1600 (m), 1583 (s), 1463 (s), 1377 (s), 1350 (sh), 1322 (m), 1271 (m), 1231 (w), 1202 (w), 1184 (m), 1158 (w), 1108 (w), 1074 (m), 1030 (w), 960 (w), 880 (w), 824 (w), 799 (w), 783 (w), 757 (w), 727 (m), 694, 668 (m). Anal. found (calcd. for $C_{56}H_{74}GaMgN_5O_2$): C, 72.15 (72.09); H, 8.37 (8.42); N, 8.40 (8.53)%.

Ca(CzOx){(N^{i}Pr)$_2$CGa(NArCH)$_2$}(THF) (25) To a solution of $Ca(CzOx)\{Ga(NArCH)_2\}(THF)_2$ (**22**, 0.400 g, 0.363 mmol) in toluene (15 mL) at -78 ºC was added a solution of ^{i}PrNCN^{i}Pr (0.0458 g, 0. 363 mmol) in toluene (5 mL). The solution was allowed to warm to RT then stirred for 1 h to give a yellow solution. The solution was filtered and the volatiles were removed from the filtrate under reduced pressure. The resultant solid was washed with cold hexane (2 × 5 mL) and dried *in vacuo* to afford **25** as a yellow solid. Yield: 0.214 g (51%). Crystals suitable for X-ray diffraction were grown by slow evaporation from a concentrated hexane solution at RT. ^{1}H NMR (C_6D_6, 400.2 MHz): δ 8.67 (2 H, d, ^4J = 2.1 Hz, C_3–H), 8.65 (2 H, d, ^4J = 2.1 Hz, C_5–H), 7.18 (6 H, s, *m*- & *p*-C_6H_3), 6.25 (2 H, s ArNC$\underline{H}$), 3.69 (4 H, s, $C\underline{H}_2CMe_2$), 3.62 (4 H, sept, ^3J = 6.9 Hz, ArC$\underline{H}Me_2$), 3.38 – 3.28 (6 H, m, overlapping NC$\underline{H}Me_2$ & $OC\underline{H}_2CH_2$), 1.49 (18 H, s, CMe_3), 1.30 (12 H, d, ^3J = 5.9 Hz, ArCH$\underline{Me}_2$), 1.28 (12 H, d, ^3J = 5.9 Hz, ArCH$\underline{Me}_2$), 1.23 (12 H, s, CMe_2), 0.94 – 0.90 (4 H, m, $OCH_2C\underline{H}_2$), 0.88 (12 H, d, ^3J = 6.9 Hz, NC$\underline{H}Me_2$). $^{13}C\{^1H\}$ NMR (C_6D_6, 100.6 MHz): δ 166.8 (C_7), 149.5 (C_1), 145.9 (*o*-C_6H_3), 145.9 (*i*-C_6H_3), 137.6 (C_4), 126.5 (*p*-C_6H_3), 125.6 (C_3), 123.3 (*m*-C_6H_3), 121.4 (C_5), 121.2 (NCH), 109.9 (C_2), 78.1 ($\underline{C}H_2CMe_2$), 68.9 ($O\underline{C}H_2CH_2$), 68.1 ($\underline{C}Me_2$), 58.71 ($N\underline{C}HMe_2$), 34.7 ($\underline{C}Me_3$), 32.3 ($C\underline{Me}_3$), 28.8 ($Ar\underline{C}HMe_2$), 28.4 ($C\underline{Me}_2$), 27.8 ($NCH\underline{Me}_2$), 26.5 ($ArCH\underline{Me}_2$), 25.0 ($OCH_2\underline{C}H_2$), 24.0 ($ArCH\underline{Me}_2$). IR (NaCl plates, Nujol mull, cm^{-1}): 1634 (m), 1601 (s), 1550 (sh), 1463 (s), 1377 (s), 1360 (s), 1321 (s), 1305 (s), 1286 (s), 1256 (s), 1224 (m), 1203 (m), 1169 (s), 1130 (m), 1113 (m), 1064 (s), 1034 (m), 1000 (m), 980 (w), 960 (w), 933 (w), 908 (w), 882 (m), 860 (w), 840 (w), 822 (w), 801 (w), 776 (w), 759 (m), 731 (w), 669 (w), 646 (w), 633 (w). Anal. found (calcd. for $C_{67}H_{96}CaGaN_7O_3$): C, 69.08 (69.53); H, 8.78 (8.36); N, 8.14 (8.47)%.

Ca(CzOx){(NCy)$_2$CGa(NArCH)$_2$}(THF) (26) To a solution of Ca(CzOx){Ga(NArCH)$_2$}(THF)$_2$ (**22**, 0.400 g, 0.363 mmol) in toluene (15 mL) at -78 ºC was added a solution of CyNCNCy (0.0749 g, 0. 363 mmol) in toluene (5 mL). The solution was allowed to warm to RT then stirred for 1 h to give a yellow solution. The solution was filtered and the volatiles were removed from the filtrate under reduced pressure. The resultant solid was washed with cold hexane (2 × 5 mL) and dried *in vacuo* to afford **26** as a yellow solid. Yield: 0.265 g (59%). ^{1}H NMR (C_6D_6, 400.2 MHz): δ 8.68 – 8.64 (4 H, m, overlapping C_3–H & C_5–H), 7.24 – 7.19 (6 H, m, overlapping *m*- & *p*-C_6H_3), 6.22 (2 H, s, ArNC<u>H</u>), 3.67 (8 H, m, overlapping C<u>H</u>$_2$CMe$_2$ & C<u>H</u>Me$_2$), 3.38 (4 H, s, OC<u>H</u>$_2$CH$_2$), 3.17 (2 H, br. s, 1-C_6H_{11}), 1.77 – 1.65 (4 H, m, 2,6- C_6H_{11}), 1.59 – 1.44 (20 H, m centred at 1.51 & 1.49, overlapping CMe$_3$ & 3,5-C_6H_{11}), 1.38 (12 H, d, ^3J = 6.8 Hz, CH<u>Me</u>$_2$), 1.35 (12 H, d, ^3J = 6.8 Hz, CH<u>Me</u>$_2$), 1.31 – 1.13 (17 H, m centred at 1.24, overlapping CMe$_2$, 2',6'-C_6H_{11}, 3',5'-C_6H_{11} & 4-C_6H_{11}), 0.93 (4 H, m, OCH$_2$C<u>H</u>$_2$), 0.82 – 0.63 (2 H, m, 4'-C_6H_{11}). ^{13}C{^{1}H} NMR (C_6D_6, 100.6 MHz): δ 166.7 (C_7), 149.7 (C_1), 146.4 (*i*-C_6H_3), 145.8 (*o*-C_6H_3), 137.5 (C_4), 127.5 (C_6), 125.7 (C_3), 125.3 (*p*-C_6H_3), 123.5 (*m*-C_6H_3), 121.6 (ArN<u>C</u>H), 121.3 (C_5), 110.0 (C_2), 78.1 (<u>C</u>H$_2$CMe$_2$), 69.0 (O<u>C</u>H$_2$CH$_2$), 68.2 (<u>C</u>Me$_2$), 67.1 (1-C_6H_{11}), 38.5 (2,6-C_6H_{11}), 34.7 (<u>C</u>Me$_3$), 32.3 (C<u>Me</u>$_3$), 28.8 (<u>C</u>HMe$_2$), 28.5 (C<u>Me</u>$_2$), 26.8 (CH<u>Me</u>$_2$), 26.2 (4-C_6H_{11}), 25.1 (3,5-C_6H_{11}), 25.1 (OCH$_2$<u>C</u>H$_2$), 24.0 (CH<u>Me</u>$_2$). IR (NaCl plates, Nujol mull, cm^{-1}): 1780 (w), 1635 (s), 1601 (s), 1459 (s), 1378 (s), 1361 (s), 1305 (s), 1286 (s), 1256 (s), 1224 (s), 1204 (s), 1169 (s), 1108 (m), 1065 (s), 1036 (w), 983 (w), 960 (w), 933 (w), 882 (m), 859 (w), 841 (w), 823 (w), 801 (w), 776 (m), 758 (m), 730 (m), 670 (w), 647 (w), 633 (m), 584 (w). Anal. found (calcd. for $C_{73}H_{104}CaGaN_7O_3$): C, 69.08 (69.53); H, 8.78 (8.36); N, 8.14 (8.47)%.

Ca(CzOx){(NTol)$_2$CGa(NArCH)$_2$}(THF) (27) To a solution of Ca(CzOx){Ga(NArCH)$_2$}(THF)$_2$ (**22**, 0.400 g, 0.363 mmol) in toluene (15 mL) at -78 ºC was added a solution of TolNCNTol (0.0806 g, 0. 363 mmol) in toluene (5 mL). The solution was allowed to warm to RT then stirred for a further 16 h to give a yellow solution. The solution was filtered and the volatiles were removed from the filtrate under reduced pressure. The resultant solid was washed with cold hexane (2 × 5 mL) and dried *in vacuo* to afford **27** as a yellow solid. Yield: 0.378 g (83%). Crystals suitable for X-ray diffraction were grown by slow evaporation from a concentrated hexane solution at RT. ^{1}H NMR (C_6D_6, 400.2 MHz): δ 8.67 (4 H, s, C_5–

H & C_3–H), 7.29 – 7.20 (6 H, m, *m*- & *p*-C_6H_3), 6.99 (4 H, d, ^3J = 8.2 Hz, *o*-C_6H_4), 6.80 (4 H, d, ^3J = 8.2 Hz, *m*-C_6H_4), 6.21 (2 H, s, NCH), 3.55 (4 H, s, C$\underline{H}_2$CMe$_2$), 3.33 – 3.29 (4 H, br. m, OC$\underline{H}_2$CH$_2$), 3.22 (4 H, sept, ^3J = 6.7 Hz, C$\underline{H}$Me$_2$), 2.09 (6 H, s, $C_6H_4\underline{Me}$), 1.50 (18 H, s, CMe$_3$), 1.25 (12 H, d, ^3J = 6.7 Hz, CH$\underline{Me}_2$), 1.19 (12 H, d, ^3J = 6.7 Hz, CH$\underline{Me}_2$), 1.11 (12 H, s, CMe$_2$), 0.89 – 0.85 (4 H, br. m, OCH$_2$C$\underline{H}_2$). $^{13}C\{^1H\}$ NMR (C_6D_6, 100.6 MHz): δ 167.0 (C_7), 150.2 (*i*-C_6H_4), 149.6 (C_1), 146.6 (*i*-C_6H_3), 146.0 (*o*-C_6H_3), 137.8 (C_4), 131.3 (*m*-C_6H_4), 130.6 (*p*-C_6H_4), 128.6 (C_6), 126.3 (C_3), 125.1 (*p*-C_6H_3), 123.8 (*m*-C_6H_3), 121.4 (C_5), 120.8 (NCH), 119.8 (*o*-C_6H_4), 110.1 (C_2), 78.0 ($\underline{C}H_2CMe_2$), 69.0 (O$\underline{C}H_2CH_2$), 68.3 ($\underline{C}Me_2$), 35.7 ($\underline{C}Me_3$), 32.4 (C$\underline{Me}_3$), 28.8 ($\underline{C}HMe_2$), 28.0 (C$\underline{Me}_2$), 26.2 (CH$\underline{Me}_2$), 24.0 (OCH$_2\underline{C}H_2$), 24.2 (CH$\underline{Me}_2$), 20.8 ($C_6H_4\underline{Me}$). IR (NaCl plates, Nujol mull, cm^{-1}): 1634 (m), 1600 (s), 1534 (w), 1500 (m), 1460 (s), 1377 (m), 1361 (m), 1318 (m), 1305 (m), 1286 (m), 1256 (m), 1225 (m), 1193 (m), 1169 (s), 1109 (m), 1065 (s), 1034 (m), 979 (s), 960 (w), 934 (m), 904 (w), 882 (m), 860 (m), 821 (w), 801 (m), 776 (m), 759 (m), 730 (m), 675 (m), 647 (w), 633 (w), 611 (w). Anal. found (calcd. for $C_{75}H_{96}CaGaN_7O_3$): C, 71.93 (71.87); H, 7.82 (7.72); N, 7.64 (7.82)%.

Mg(CzOx)I (28). A 3M Et_2O solution of MeMgI (1.70 mL, 5.10 mmol) was added dropwise to a stirred Et_2O (50 mL) solution of CzOx-H (2.00 g, 4.22 mmol) cooled to -78 °C. The resultant suspension was warmed to RT and stirred for 1 h. The suspension was filtered and the residue was washed with pentane (4 × 10 mL). The volatiles were removed *in vacuo* to yield the final product as a yellow powder. Yield: 2.30 g (87%). %). ^1H NMR (C_6D_6, 400.2 MHz): δ 8.52 (2 H, d, ^4J = 1.8 Hz, C_5–H), 8.30 (2 H, d, ^4J = 1.8 Hz, C_3–H), 3.50 (4 H, s, CH_2), 1.48 (18 H, s, CMe$_3$), 1.35 (12 H, s, m, CMe$_2$). $^{13}C\{^1H\}$ NMR (C_6D_6, 100.6 MHz): δ 169.1 (C_7), 149.5 (C_1), 139.9 (C_4), 127.3 (C_6), 124.2 (C_3), 123.5 (C_5), 108.3 (C_2), 78.8 (CH_2), 66.6 ($\underline{C}Me_2$), 35.0 ($\underline{C}Me_3$), 32.4 (C$\underline{Me}_3$), 29.5 (C$\underline{Me}_2$). EI-MS: *m/z* = 623 (10%) $[Mg(CzOx)I]^+$, 496 (100%) $[Mg(CzOx)]^+$, 473 (50%) $[(CzOx) + H]^+$. IR (NaCl plates, Nujol mull, cm^{-1}): 1631 (m), 1595 (m), 1562 (s), 1463 (s), 1396 (s), 1378 (s), 1366 (s), 1340 (w), 1312 (s), 1301 (s), 1269 (w), 1235 (m), 1207 (s), 1187 (m), 1078 (m), 1028 (m), 1013 (w), 965 (w), 917 (w), 887 (m), 825 (w), 805 (w), 785 (w), 770 (w), 734 (w), 721 (w), 668 (w), 650 (w). Anal. found (calcd. for $C_{56}H_{74}GaMgN_5O_2$): C, 57.71 (57.76); H, 6.55 (6.14); N, 6.34 (6.74)%.

NMR tube-scale reaction of Mg(CzOx){Ga(NArCH)$_2$} (21) with MeI. To a solution of Mg(CzOx){Ga(NArCH)$_2$} (**21**, 20.0 mg, 21.2 μmol) in C_6D_6 (0.6 mL) at RT was MeI (1.3 μL, 21 μmol). The solution was immediately analysed by ^{1}H NMR spectroscopy which showed the formation of a complex mixture where Mg(CzOx)I (**28**) could be identified. A similar result was found with the use of ^{t}BuI, AcI and I_2.

NMR tube-scale reaction of Ca(CzOx){Ga(NArCH)$_2$}(THF)$_2$ (22) with MeI. To a solution of Ca(CzOx){Ga(NArCH)$_2$}(THF)$_2$ (**22**, 20.0 mg, 18.1 μmol) in C_6D_6 (0.6 mL) at RT was MeI (1.1 μL, 18 μmol). The solution was immediately analysed by ^{1}H NMR spectroscopy which showed the formation of a complex mixture where Ca(CzOx)I(THF)$_2$ (**3.16**) could be identified.

NMR tube-scale reaction of Mg(CzOx){Ga(NArCH)$_2$} (21) with Me$_3$SiI. To a solution of Mg(CzOx){Ga(NArCH)$_2$} (**21**, 20.0 mg, 21.2 μmol) in C_6D_6 (0.6 mL) at RT was Me_3SiI (3.0 μL, 21 μmol). The solution was immediately analysed by ^{1}H NMR spectroscopy. The spectrum was consistent with the formation of Mg(CzOx)I (**28**), $Me_3SiGa(NArCH)_2$ (**19**) and [Ga(NArCH)$_2$]$_2$ (**1.68**).

Mg(CzOx){(O)Ga(NArCH)$_2$} (29) To a solution of Mg(CzOx){Ga(NArCH)$_2$} (**21**, 0.400 g, 0.424 mmol) in toluene (15 mL) at -78 ºC was added a solution of isobutylene oxide (0.0306 g, 0.424 mmol) in toluene (5 mL). The solution was allowed to warm to RT then stirred for 30 min to give a yellow solution. The solution was filtered and the volatiles were removed from the filtrate under reduced pressure. The resultant solid was washed with cold hexane (2 × 2 mL) and dried *in vacuo* to afford **29** as yellow solid. Yield: 0.183 g (45%). Diffraction-quality crystals were grown by slow evaporation from a concentrated benzene solution at RT. ^{1}H NMR (C_6D_6, 400.2 MHz): δ 8.56 (2 H, d, ^4J = 1.8 Hz, C_5–H), 8.32 (2H, d, ^4J = 1.8 Hz, C_3–H), 7.10 (6 H, m, *m*- & *p*-C_6H_3), 6.01 (2 H, s, NCH), 3.63 (4 H, sept, ^3J = 6.9 Hz, C<u>H</u>Me$_2$), 3.52 (4 H, s, CH_2), 1.50 (18 H, s, CMe_3), 1.22 (12 H, d, ^3J = 6.9 Hz, CH<u>Me</u>$_2$), 1.11 (12 H, d, ^3J = 6.9 Hz, CH<u>Me</u>$_2$), 1.07 (12 H, s, CMe_2). ^{13}C{^{1}H} NMR (C_6D_6, 100.6 MHz): δ 168.3 (C_7), 149.6 (C_1), 146.3 (*o*-C_6H_3), 145.6 (*i*-C_6H_3), 139.5 (C_4), 127.6 (C_6), 125.2 (*p*-C_6H_3), 123.7 (C_3), 123.1 (*m*-C_6H_3), 122.6 (C_5), 117.8 (NCH), 108.6 (C_2), 78.6 (CH_2), 66.4 (<u>C</u>Me$_2$), 35.0 (<u>C</u>Me$_3$), 32.4 (C<u>Me</u>$_3$), 28.4 (C<u>Me</u>$_2$), 28.3 (<u>C</u>HMe$_2$), 24.5 (CH<u>Me</u>$_2$), 24.4 (CH<u>Me</u>$_2$). IR (NaCl plates, Nujol mull, cm^{-1}): 1635 (m), 1581 (s), 1463 (s), 1377 (s), 1362 (s), 1352 (s), 1323 (m), 1309 (m), 1271

(s), 1232 (m), 1184 (s), 1112 (m), 1073 (s), 1056 (m), 1015 (m), 961 (m), 923 (m), 883 (m), 827 (m), 801 (m), 784 (m), 757 (m), 733 (m), 668 (w), 651 (w), 634 (w). Anal. found (calcd. for $C_{56}H_{74}GaMgN_5O_3$): C, 69.99 (70.12); H, 7.89 (7.78); N, 7.26 (7.30)%.

Alternative NMR tube-scale synthesis of Mg(CzOx){(O)Ga(NArCH)$_2$} (29) To a solution of Mg(CzOx){Ga(NArCH)$_2$} (**21**, 20.0 mg, 21.2 μmol) in C_6D_6 (0.6 mL) at RT was trimethylamine *N*-oxide (1.6 mg, 21 μmol). The solution was immediately analysed by ^{1}H NMR spectroscopy. The spectrum was consistent with the formation of Mg(CzOx){(O)Ga(NArCH)$_2$} (**29**) and other minor unknown species.

Mg(CzOxMe){(OC$_6$H$_{10}$)Ga(NArCH)$_2$} (30) To a solution of Mg(CzOx){Ga(NArCH)$_2$} (**21**, 0.400 g, 0.424 mmol) in toluene (15 mL) at -78 ºC was added a solution of cyclohexene oxide (0.0416 g, 0.424 mmol) in toluene (5 mL). The solution was allowed to warm to RT then stirred for 1 h to give a yellow solution. The solution was filtered and the volatiles were removed from the filtrate under reduced pressure. The resultant solid was washed with cold hexane (2 × 2 mL) and dried *in vacuo* to afford **30** as yellow solid. Yield: 0.331 g (75%). ^{1}H NMR (C_6D_6, 400.2 MHz): δ 8.48 (2 H, app. d, ^3J = 1.3 Hz, C_3–H), 8.39 (2 H, br. s, C_5–H)), 7.26 – 7.18 (6 H, m, overlapping *m*- & *p*-C_6H_3), 6.08 (2 H, s, NCH), 4.02 (2 H, sept, ^3J = 6.7 Hz, C<u>H</u>Me$_2$), 3.85 (2 H, sept, ^3J = 6.7 Hz, C<u>H</u>Me$_2$), 3.68 – 3.55 (5 H, m, OC<u>H$_2$</u>CMe$_2$ & MgOCH$_2$), 2.78 (1 H, br. s, GaCH), 1.95 – 1.56 (8 H, m centred at 1.82, 1.79, 1.72 & 1.67, overlapping CH_2 resonances of C_6H_{10}), 1.45 (30 H, br. s, overlapping CMe$_3$, CMe$_2$ & CH<u>Me$_2$</u>), 1.40 (6 H, d, ^3J = 6.7 Hz, CH<u>Me$_2$</u>), 1.35 (6 H, d, ^3J = 6.7 Hz, CH<u>Me$_2$</u>), 1.27 – 1.21 (12 H, m, ovlerapping CH<u>Me$_2$</u> & C<u>Me$_2$</u>). ^{13}C{^{1}H} NMR (C_6D_6, 100.6 MHz): δ 163.5 (C_7), 148.9 (C_1), 142.8 (*o*-C_6H_3), 142.2 (*i*-C_6H_3), 138.7 (C_4), 127.0 (C_6), 125.6 (C_5), 125.0 (C_3), 124.0 (*m*-C_6H_3), 123.6 (*p*-C_6H_3), 117.3 (NCH), 109.0 (C_2), 79.5 (<u>C</u>H$_2$CMe$_2$), 78.5 (OCH), 67.5 (<u>C</u>Me$_2$), 34.9 (<u>C</u>Me$_3$), 34.8 (GaCH<u>C</u>H$_2$), 32.3 (C<u>Me$_3$</u>), 32.1 (OCH<u>C</u>H$_2$), 28.5 (<u>C</u>HMe$_2$), 28.3 (<u>C</u>HMe$_2$), 27.9 (C<u>Me$_2$</u>), 27.7 (C<u>Me$_2$</u>), 24.4 (OCHCH$_2$<u>C</u>H$_2$), 24.3 (GaCHCH$_2$<u>C</u>H$_2$), 24.2 (CH<u>Me$_2$</u>), 23.5 (CH<u>Me$_2$</u>), 22.6 (GaCH). IR (NaCl plates, Nujol mull, cm^{-1}): 1635 (m), 1575 (s), 1463 (s), 1377 (s), 1351 (s), 1314 (s), 1270 (s), 1232 (m), 1185 (s), 1102 (m), 1075 (m), 1052 (m), 1028 (m), 961 (w), 933 (w), 882 (w), 828 (w), 800 (w), 784 (w), 758 (w), 722 (w), 654 (w), 633 (w). A satisfactory elemental analysis could not be obtained.

Mg(CzOxMe){(OC$_7$H$_{10}$)Ga(NArCH)$_2$} **(31)** To a solution of Mg(CzOx){Ga(NArCH)$_2$} (**21**, 0.400 g, 0.424 mmol) in toluene (15 mL) at -78 ºC was added a solution of *exo*-2,3-Epoxynorbornane (0.0467 g, 0.424 mmol) in toluene (5 mL). The solution was allowed to warm to RT then stirred for 48 h to give a yellow solution. The solution was filtered and the volatiles were removed from the filtrate under reduced pressure. The resultant solid was washed with cold hexane (2 × 2 mL) and dried *in vacuo* to afford **31** as yellow solid. Yield: 0.183 g (83%). ^{1}H NMR (C$_6$D$_6$, 400.2 MHz): 8.56 (2 H, d, ^3J = 1.9 Hz, C$_5$–H), 8.40 (2 H, d, ^3J = 1.9 Hz, C$_3$–H), 7.25 – 7.16 (6 H, m, overlapping *m*- & *p*-C$_6$H$_3$), 6.22 (2 H, s, NCH), 4.22 – 4.18 (1 H, m, OCH), 3.75 – 3.58 (8 H, m, overlapping C$\underline{H}_2$CMe$_2$ & C$\underline{H}$Me$_2$), 2.01 (1 H, br. s, MgOCHC$\underline{H}$), 1.68 – 1.51 (6 H, overlapping CH$_2$ and CH resonances of C$_6$H$_{10}$), 1.46 (18 H, s, CMe$_3$), 1.33 (12 H, d, ^3J = 6.7 Hz, CH$\underline{Me}_2$), 1.30 (12 H, d, ^3J = 6.7 Hz, CH$\underline{Me}_2$), 1.29 – 1.23 (13 H, m, centred at 1.27, 1.24 & 1.24, overlapping CMe$_2$ & GaCH). ^{13}C{^{1}H} NMR (C$_6$D$_6$, 100.6 MHz): δ C$_6$D$_6$) δ 168.0 (C$_7$), 149.8 (C$_1$), 146.1 (*i*-C$_6$H$_3$), 145.9 (*o*-C$_6$H$_3$), 139.5 (C$_4$), 128.6 (C$_6$), 125.5 (*p*-C$_6$H$_3$), 123.9 (C$_3$), 123.3 (*m*-C$_6$H$_3$), 122.9 (C$_5$), 120.5 (NCH), 108.5 (C$_2$), 79.5 (OCH), 78.8 (C$\underline{H}_2$CMe$_2$), 66.7 (C$\underline{Me}_2$), 51.3 (GaCH$\underline{C}$HCH$_2$), 47.9 (OCH$\underline{C}$HCH$_2$), 39.0 (OCHCH$\underline{C}$H$_2$CH), 34.9 (C$\underline{Me}_3$), 32.4 (C$\underline{Me}_3$), 28.6 (C$\underline{H}$Me$_2$), 28.5 (C$\underline{Me}_2$), 28.4 (C$\underline{Me}_2$), 28.2 (CH$\underline{Me}_2$), 25.9 (GaCH), 25.2 (CH$\underline{Me}_2$), 25.1 (GaCHCH$\underline{C}$H$_2$CH$_2$), 24.5 (OCHCH$\underline{C}$H$_2$CH$_2$). IR (NaCl plates, Nujol mull, cm^{-1}): 1636 (m), 1598 (s), 1582 (s), 1463 (s), 1377 (s), 1361 (s), 1322 (m), 1269 (s), 1231 (m), 1184 (s), 1115 (s), 1073 (s), 1027 (s), 963 (m), 933 (w), 882 (m), 847 (w), 802 (m), 784 (w), 759 (m), 733 (w), 676 (w), 634 (w). Anal. found (calcd. for C$_{63}$H$_{84}$GaMgN$_5$O$_3$): C, 71.99 (71.83); H, 7.89 (8.04); N, 6.26 (6.65)%.

Mg(CzOxMe){(^{t}BuN)(O)CGa(NArCH)$_2$} **(32)** To a solution of Mg(CzOx){Ga(NArCH)$_2$} (**21**, 0.300 g, 0.318 mmol) in toluene (15 mL) at -78 ºC was added a solution of *tert*-butyl isocyanate (0.0364 g, 0.318 mmol) in toluene (5 mL). The solution was allowed to warm to RT then stirred for 2 h to give a yellow solution. The solution was filtered and the volatiles were removed from the filtrate under reduced pressure. The resultant solid was washed with cold hexane (2 × 2 mL) and dried *in vacuo* to afford **32** as yellow solid. Yield: 0.282 g (85%). ^{1}H NMR (C$_6$D$_6$, 400.2 MHz): δ 8.58 (2 H, d, ^4J = 1.9 Hz, C$_5$–H), 8.38 (2 H, d, ^4J = 1.9 Hz, C$_3$–H), 7.19 – 7.17 (6 H, m, *m*- & *p*-C$_6$H$_3$), 6.16 (2 H, s, NCH), 3.79 (2 H, d, ^2J = 8.0 Hz,

OCH_2), 3.64 (4 H, sept, ^3J = 7.0 Hz, C<u>H</u>Me_2), 3.49 (2 H, d, ^2J = 8.0 Hz, OCH_2), 1.45 (18 H, s, ArC<u>Me</u>$_3$), 1.34 – 1.28 (30 H, m, overlapping CH<u>Me</u>$_2$ & CMe_2), 1.15 (6 H, s, CMe_2), 0.43 (9 H, s, NC<u>Me</u>$_3$). $^{13}C\{^1H\}$ NMR (C_6D_6, 100.6 MHz): δ 180.4 (^{t}BuN<u>C</u>O), 168.4 (C_7), 149.6 (C_1), 145.9 (*o*-C_6H_3), 145.6 (*i*-C_6H_3), 138.7 (C_4), 127.1 (C_6), 125.8 (*p*-C_6H_3), 123.6 (C_3), 123.4 (*m*-C_6H_3), 122.4 (C_5), 120.3 (NCH), 109.1 (C_2), 79.5 (CH_2), 67.5 (<u>C</u>Me_2), 49.8 (N<u>C</u>Me_3), 34.9 (Ar<u>C</u>Me_3), 32.3 (ArC<u>Me</u>$_3$), 32.1 (NC<u>Me</u>$_3$), 28.7 (<u>C</u>HMe_2), 27.3 (C<u>Me</u>$_2$), 27.1 (C<u>Me</u>$_2$), 25.8 (CH<u>Me</u>$_2$), 24.1 (CH<u>Me</u>$_2$). IR (NaCl plates, Nujol mull, cm^{-1}): 1638 (m), 1589 (s), 1512 (m), 1463 (s), 1377 (s), 1362 (s), 1289 (w), 1263 (m), 1230 (m), 1184 (s), 1126 (w), 1076 (m), 1032 (w), 934 (w), 882 (w), 822 (w), 801 (w), 780 (w), 770 (w), 757 (w), 722(w), 635 (w). Anal. found (calcd. for $C_{61}H_{83}GaMgN_6O_3$): C, 69.99 (70.29); H, 7.79 (8.03); N, 7.98 (8.06)%.

Ca(CzOx){(EtN)(O)CGa(NArCH)$_2$}(THF) (33) To a solution of Ca(CzOx){Ga(NArCH)$_2$}(THF)$_2$ (**22**, 0.300 g, 0.272 mmol) in toluene (15 mL) at -78 ºC was added a solution of EtNCO (0.0193 g, 0. 363 mmol) in toluene (5 mL). The solution was allowed to warm to RT then stirred for 1 h to give an orange solution. The solution was filtered and the volatiles were removed from the filtrate under reduced pressure. The resultant solid was washed with cold hexane (2 × 5 mL) and dried *in vacuo* to afford **33** as an orange solid. Yield: 0.218 g (73%). ^1H NMR (C_6D_6, 400.2 MHz): δ 8.71 (2 H, d, ^4J = 2.1 Hz, C_3–H), 8.67 (2 H, d, ^4J = 2.1 Hz, C_5–H), 7.13 – 7.06 (6 H, m, *m*- & *p*-C_6H_3), 5.84 (2 H, s, NCH), 3.81 – 3.67 (4 H, br m, C<u>H</u>Me_2), 3.64 (4 H, s, C<u>H</u>$_2$CMe_2), 3.45 (2 H, q, ^3J = 7.3 Hz), 3.28 (4 H, br s, OC<u>H</u>$_2$CH_2), 1.53 (18 H, s, CMe_3), 1.39 (3 H, t, ^3J = 7.3 Hz, CH_2C<u>H</u>$_3$), 1.18 (12 H, d, ^3J = 6.7 Hz, CH<u>Me</u>$_2$), 1.13 – 1.04 (12 H, m, CH<u>Me</u>$_2$), 0.95 – 0.84 (16 H, m, overlapping CMe_2 & OCH_2C<u>H</u>$_2$). $^{13}C\{^1H\}$ NMR (C_6D_6, 100.6 MHz): δ 169.9 (EtN<u>C</u>O), 167.3 (C_7), 149.2 (C_1), 147.5 (*o*-C_6H_3), 145.8 (*i*-C_6H_3), 138.0 (C_4), 127.7 (C_6), 125.9 (C_3), 124.8 (*p*-C_6H_3), 123.3 (*m*-C_6H_3), 121.6 (C_5), 119.0 (NCH), 110.1 (C_2), 77.7 (<u>C</u>H_2CMe_2), 68.7 (O<u>C</u>H_2CH_2), 67.9 (<u>C</u>Me_2), 38.6 (NCH_2), 34.8 (<u>C</u>Me_3), 32.3 (C<u>Me</u>$_3$), 28.0 (<u>C</u>HMe_2), 26.6 (C<u>Me</u>$_2$), 25.2 (OCH_2<u>C</u>H_2), 25.0 (CH<u>Me</u>$_2$), 24.1 (CH<u>Me</u>$_2$), 16.4 (CH_2<u>C</u>H_3). IR (NaCl plates, Nujol mull, cm^{-1}): 1621 (m), 1596 (s), 1536 (w), 1463 (s), 1416 (w), 1377 (s), 1363 (s), 1349 (m), 1305 (m), 1286 (m), 1262 (m), 1224 (m), 1201 (m), 1169 (m), 1129 (w), 1100 (m), 1066 (m), 1035 (m), 968 (w), 935 (w), 883 (w), 861 (w), 820 (w), 801 (m), 776 (w), 755 (w), 730 (w), 722 (w), 669 (w), 647 (w), 633 (w). A satisfactory elemental analysis could not be obtained.

Mg(CzOx){N(Ph)N(Ph)Ga(NArCH)$_2$} (34) To a solution of Mg(CzOx){Ga(NArCH)$_2$} (**21**, 0.400 g, 0.424 mmol) in benzene (15 mL) was added a solution of azobenzene (0.0773 g, 0.424 mmol) in benzene (5 mL) at RT. The solution was stirred for 10 min to give a red solution. The volatiles were removed from the solution and the resultant solid was dried *in vacuo* to afford **34** as dark orange solid. Yield: 0.429 g (90%). ^{1}H NMR (C_6D_6, 400.2 MHz): δ 8.39 (2 H, d, ^4J = 1.6 Hz, C_5–H), 8.10 (2 H, d, ^4J = 1.6 Hz, C_3–H), 7.14 – 7.13 (2 H, m, *p*-C_6H_3), 7.13 – 7.10 (2 H, m, 3,5-C_6H_5), 7.11 – 7.08 (4 H, m, *m*-C_6H_3), 6.70 (2 H, d, ^3J = 7.8 Hz, 2,6-C_6H_5), 6.49 (1 H, t, ^3J = 7.1 Hz, 4-C_6H_5), 6.23 (3 H, m, 3',4',5'-C_6H_5), 6.15 (2 H, d, ^3J = 6.9 Hz, 2',6'-C_6H_5), 5.91 (2 H, s, NCH), 3.42 (4 H, s, CH_2), 3.41 – 3.34 (4 H, m, C<u>H</u>Me$_2$), 1.45 (18 H, s, CMe$_3$), 1.27 (12 H, d, ^3J = 6.9 Hz, CH<u>Me</u>$_2$), 1.12 (12 H, d, ^3J = 6.9 Hz, CH<u>Me</u>$_2$), 1.04 (12 H, s, CMe$_2$). ^{13}C{^{1}H} NMR (C_6D_6, 100.6 MHz): δ 169.5 (C_7), 161.0 (1-C_6H_5), 150.1 (C_1), 146.4 (*o*-C_6H_3), 146.3 (*i*-C_6H_3), 139.0 (C_4), 128.6 (3',5'-C_6H_5), 128.6 (1'-C_6H_5), 127.3 (C_6), 127.0 (*p*-C_6H_3), 125.8 (3,5-C_6H_5), 123.8 (C_4), 123.4 (*m*-C_6H_3), 122.9 (C_5), 120.1 (NCH), 118.7 (2,6-C_6H_5), 118.6 (4'-C_6H_5), 115.5 (2',6'-C_6H_5), 114.5 (4-C_6H_5), 108.1 (C_5), 78.0 (CH_2), 65.9 (<u>C</u>Me$_2$), 34.9 (<u>C</u>Me$_3$), 32.4 (C<u>Me</u>$_3$), 28.5 (<u>C</u>HMe$_2$), 28.3 (C<u>Me</u>$_2$), 25.7 (CH<u>Me</u>$_2$), 23.9 (CH<u>Me</u>$_2$). IR (NaCl plates, Nujol mull, cm^{-1}): 1634 (w), 1597 (w), 1570 (s), 1568 (sh), 1460 (s), 1396 (w), 1377 (m), 1359 (m), 1322 (w), 1272 (m), 1233 (w), 1185 (m), 1074 (m), 1026 (m), 884 (m), 801 (m), 756 (m), 729 (w), 668 (w), 517 (w). A satisfactory elemental analysis could not be obtained.

Mg(CzOx){N(SiMe$_3$)Ga(NArCH)$_2$} (35) To a solution of Mg(CzOx){Ga(NArCH)$_2$} (**21**, 0.400 g, 0.424 mmol) in toluene (15 mL) at -78 ºC was added a solution of trimethylsilyl azide (0.0488 g, 0.424 mmol) in toluene (5 mL). The solution was allowed to warm to RT then stirred for 30 min to give a yellow solution. The solution was filtered and the volatiles were removed from the filtrate under reduced pressure. The resultant solid was washed with cold hexane (2 × 2 mL) and dried *in vacuo* to afford **35** as yellow solid. Yield: 0.184 g (41%). ^{1}H NMR (C_6D_6, 400.2 MHz): δ 8.53 (2 H, d, ^4J = 1.8 Hz, C_5–H), 8.37 (2 H, d, ^4J = 1.8 Hz, C_3–H), 7.23 – 7.17 (6 H, m, *m*- & *p*-C_6H_3), 6.19 (2 H, s, NCH), 3.99 – 3.69 (4 H, br m, C<u>H</u>Me$_2$), 3.80 (2 H, d, ^2J = 8.3 Hz, CH_2), 3.55 (2 H, d, ^2J = 8.3 Hz, CH_2), 1.46 (18 H, s, CMe$_3$), 1.45 – 1.35 (24 H, br m, CH<u>Me</u>$_2$), 1.35 (6 H, s, CMe$_2$), 0.89 (6 H, s, CMe$_2$), -0.53 (9 H, s, SiMe$_3$). ^{13}C{^{1}H} NMR (C_6D_6, 125.7 MHz): δ 168.6 (C_7), 150.0 (C_1), 148.2 (*o*-C_6H_3), 146.5 (*i*-

C_6H_3), 139.7 (C_4), 127.13 (C_6), 124.8 (*m*-C_6H_3), 124.2 (*p*-C_6H_3), 123.8 (C_3), 123.4 (C_5), 119.5 (NCH), 108.6 (C_2), 78.0 (CH_2), 66.2 ($\underline{C}Me_2$), 35.0 ($\underline{C}Me_3$), 32.3 ($C\underline{Me}_3$), 29.8 ($C\underline{Me}_2$), 29.5 ($C\underline{Me}_2$), 28.5 ($\underline{C}HMe_2$), 26.7 ($CH\underline{Me}_2$), 6.2 ($SiMe_3$). IR (NaCl plates, Nujol mull, cm^{-1}): 2149 (m), 1635 (m), 1594 (m) 1578 (s), 1463 (s), 1377 (s), 1352 (s), 1317 (m), 1270 (s), 1234 (m), 1208 (m), 1185 (s), 1105 (m), 1073 (m), 1012 (m), 962 (w), 918 (m), 883 (w), 827 (m), 799 (w), 786 (w), 759 (w), 722 (w), 662 (w), 633 (w). Anal. found (calcd. for $C_{59}H_{83}GaMgN_8O_2Si$): C, 68.99 (68.77); H, 7.89 (8.12); N, 8.26 (8.16)%.

Ca(CzOx){N(Ph)Ga(NArCH)$_2$}(THF) (37) To a solution of Ca(CzOx){Ga(NArCH)$_2$}(THF)$_2$ (**22**, 0.300 g, 0.272 mmol) in toluene (15 mL) at -78 ºC was added a solution of PhN_3 (0.0324 g, 0.272 mmol) in toluene (5 mL). The solution was allowed to warm to RT then stirred for 1 h to give a yellow solution. The solution was filtered and the volatiles were removed from the filtrate under reduced pressure. The resultant solid was washed with cold hexane (2 × 5 mL) and dried *in vacuo* to afford **37** as a yellow solid. Yield: 0.200 g (66%). ^{1}H NMR (C_6D_6, 400.2 MHz): δ 8.66 (2 H, s, C_5–H), 8.60 (2 H, s, C_3–H), 7.57 (2 H, d, ^3J = 7.7 Hz, *o*-C_6H_5), 7.24 – 7.18 (6 H, m, *m*- & *p*-C_6H_3), 7.12 – 7.03 (4 H, m, *o*-C_6H_5), 6.72 (1 H, t, ^3J = 7.2 Hz, *p*-C_6H_5), 6.19 (2 H, s, NCH), 4.00 (4 H, sept, ^3J = 6.5 Hz), 3.43 (4 H, s, $C\underline{H}_2CMe_2$), 3.30 (8 H, br. s, $OC\underline{H}_2CH_2$), 1.53 – 1.44 (30 H, m, overlapping CMe_3 & $CH\underline{Me}_2$), 1.05 (12 H, d, ^3J=6.5 Hz, $CH\underline{Me}_2$), 0.90 (8 H, br. s, $OCH_2C\underline{H}_2$), 0.81 (12 H, s, CMe_2). ^{13}C{^{1}H} NMR (C_6D_6, 125.7 MHz): δ 167.9 (C_7), 149.1 (C_1), 147.8 (*i*-C_6H_3), 147.3 (*o*-C_6H_3), 147.1 (*i*-C_6H_5), 138.7 (C_4), 129.5 (*m*-C_6H_5), 128.0 (overlapping with C_6D_6 resonance, C_6), 126.4 (C_3), 124.0 (*p*-C_6H_3), 123.5 (*m*-C_6H_3), 121.9 (C_5), 121.7 (*p*-C_6H_5), 119.1 (NCH), 117.1 (*o*-C_6H_5), 109.7 (C_2), 77.9 ($\underline{C}H_2CMe_2$), 68.8 ($O\underline{C}H_2CH_2$), 68.0 ($\underline{C}Me_2$), 34.7 ($\underline{C}Me_3$), 32.2 ($C\underline{Me}_3$), 28.5 ($\underline{C}HMe_2$), 27.8 ($C\underline{Me}_2$), 26.7 ($CH\underline{Me}_2$), 25.3 ($OCH_2\underline{C}H_2$), 23.6 ($CH\underline{Me}_2$). IR (NaCl plates, Nujol mull, cm^{-1}): 1624 (m), 1536 (w), 1464 (s), 1430 (w), 1357 (s), 1363 (s), 1321 (m), 1306 (m), 1286 (m), 1262 (m), 1224 (m), 1200 (m), 1140 (m), 1111 (w), 1100 (m), 1066 (m), 1025 (m), 968 (w), 962 (w), 918 (m), 883 (w), 822 (m), 799 (w), 786 (w), 755 (w), 721 (w), 668 (w), 638 (w). A satisfactory elemental analysis could not be obtained.

Ga(NArCH)$_2$Fp (37). A solution of [KGa(NArCH)$_2$(Et_2O)]$_2$ (**1.44**, 0.400 g, 0.357 mmol) in benzene (15 mL) was added to a solution of FpI (0.217 g, 0.715 mmol) in

benzene at RT. The solution was heated, with sirring, at 60 ºC for 48 h to give a black suspension. The suspension was filtered and the volatiles were removed from the filtrate under reduced pressure. The resultant solid was washed with cold pentane (2 × 5 mL) and dried *in vacuo* to afford **37** as a black sticky solid. Yield: 0.182 g (41%). ^{1}H NMR (C_6D_6, 400.2 MHz): δ 7.22 (6 H, app s, *m*- & *p*-C_6H_3), 6.52 (2 H, s, NCH), 3.96 (5 H, br. s, Cp), 3.76 (4 H, sept, ^{3}J = 6.9 Hz, C<u>H</u>Me$_2$), 1.34 (24 H, dd, ^{3}J = 6.9, CH<u>Me</u>$_2$). ^{13}C{^{1}H} NMR (C_6D_6, 125.7 MHz): δ δ 212.7 (CO), 146.0 (*i*-C_6H_3), 145.9 (*o*-C_6H_3), 125.9 (*p*-C_6H_3), 123.6 (*m*-C_6H_3), 123.4 (NCH), 80.5 (Cp), 28.6 (<u>C</u>HMe$_2$), 25.7 (CH<u>Me</u>$_2$), 24.1 (CH<u>Me</u>$_2$). IR (NaCl plates, Nujol mull, cm^{-1}): 2851 (s), 2725 (s), 2010 (w), 1964 (w), 1791 (w), 1590 (s), 1460 (s), 1377 (m), 1353 (m), 1322 (m), 1261 (m), 1213 (w), 1114 (m), 1019 (m), 801 (m), 759 (m), 722 (m), 634 (m), 586 (m). Anal. found (calcd. for $C_{33}H_{41}FeGaN_2O_2$): C, 63.21 (63.59); H, 6.14 (6.63); N, 4.26 (4.49)%.

Mg(CzOx)Fp (38). Toluene (30 mL) was added to Mg(CzOx)I (0.500 g, 0.801 mmol) and KFp (0.173 g, 0.801 mmol) at -78 ºC to give a brown suspension. The suspension was allowed to warm to RT, stirred for 4 h and then filtered. Volatiles were removed under reduced pressure and the resultant orange solid washed with hexane (3 × 5 mL) at 0 ºC and dried *in vacuo* to afford **38** as brown solid. Yield: 0.238 g (44%). ^{1}H NMR (C_6D_6, 400.2 MHz): δ 8.55 (2 H, br. s, C_5–H), 8.33 (2 H, s, C_3–H), 4.02 (5 H, s, Cp), 3.55 (4 H, br. s, OCH_2), 1.47 (18 H, s, C<u>Me</u>$_3$), 1.36 (12 H, s, C<u>Me</u>$_2$). ^{13}C{^{1}H} NMR (C_6D_6, 125.7 MHz): δ 169.0 (C_7), 149.6 (C_1), 139.9 (C_4), 127.2 (C_6), 124.1 (C_3), 123.5 (C_5), 108.5 (C_2), 78.8 (OCH), 78.7 (Cp), 66.6 (<u>C</u>Me$_2$), 35.0 (<u>C</u>Me$_3$), 32.3 (C<u>Me</u>$_3$), 29.3 (<u>C</u>Me$_2$) (δ(CO) not observed). IR (NaCl plates, Nujol mull, cm^{-1}): 2014 (m), 1959 (m), 1827 (m), 1762 (m), 1712 (m), 1635 (m), 1584 (s), 1463 (m), 1376 (m), 1364 (w), 1341 (m), 1311 (m), 1268 (m), 1231 (m), 1184 (m), 1124 (w), 1073 (m), 1015 (m), 977 (w), 964 (w), 881 (m), 820 (m), 803 (m), 780 (m), 733 (m), 668 (w), 649, (w) 634 (w), 475 (w). A satisfactory elemental analysis could not be obtained.

Mg(CzOx)Fp(THF) (38-THF). Toluene (40 mL) was added to Mg(CzOx)I(THF) (0.500 g, 0.718 mmol) and KFp (0.155 g, 0.718 mmol) at -78 ºC to give a brown suspension. The suspension was allowed to warm to RT, stirred for 1 h then filtered to give an orange brown solution. Volatiles were removed under reduced pressure and the resultant orange solid washed with hexane (3 × 5 mL) at 0 ºC and dried *in vacuo*

to afford **38-THF** as brown solid. Yield: 0.370 g (69%). ^{1}H NMR (C_6D_6, 400.2 MHz): δ 8.61 (2 H, s, C_5–H), 8.48 (2 H, s, C_3–H), 4.52 (5 H, s, Cp), 3.65 (4 H, s, C$\underline{H_2}$CMe$_2$), 3.25 (4 H, br. s, OC$\underline{H_2}$CH$_2$), 1.52 (12 H, s, CMe$_2$), 1.47 (18 H, s, CMe$_3$, 0.89 (4 H, br. s, OCH$_2$C$\underline{H_2}$). ^{13}C{^{1}H} NMR (C_6D_6, 100.6 MHz): δ 217.9 (CO), 168.1 (C_7), 149.1 (C_1), 139.4 (C_4), 127.1 (C_6), 124.5 (C_3), 122.5 (C_5), 109.1 (C_2), 79.3 (Cp), 79.1 ($\underline{C}$H$_2$CMe$_2$), 68.8 (O$\underline{C}$H$_2$CH$_2$), 68.1 ($\underline{C}$Me$_2$), 34.9 ($\underline{C}$Me$_3$), 32.3 (C$\underline{Me}_3$), 28.3 (C$\underline{Me}_2$), 25.0 (OCH$_2\underline{C}$H$_2$). IR (NaCl plates, Nujol mull, cm^{-1}): 2020 (m), 1963 (m), 1950 (m), 1882 (w), 1827 (s), 1779 (s), 1715 (m), 1635 (m), 1596 (s), 1464 (s), 1377 (s), 1314 (w), 1267 (m), 1229 (w), 1182 (m), 1127 (w), 1072 (m), 1032 (w), 880 (w), 820 (w), 779 (w), 729 (w), 668 (w), 634 (w). Anal. found (calcd. for $C_{41}H_{51}FeMgN_3O_5$): C, 66.07 (66.01); H, 7.10 (6.89); N, 5.79 (5.63)%.

NMR tube-scale reaction of Mg(CzOx)Fp (38) with THFs. To a solution of Mg(CzOx)Fp (**38**, 20.0 mg, 29.7 μmol) in C_6D_6 (0.6 mL) at RT was THF (2.4 μL, 30 μmol). The solution was immediately analysed by ^{1}H NMR spectroscopy. The spectrum was consistent with the formation of Mg(CzOx)I(THF) (**38-THF**).

5.7 Experimental details and characterising data for Chapter Four

Al{(N^{i}Pr)$_2$CMe}Br$_2$ (39) A suspension of Li{(N^{i}Pr)$_2$CMe} (**4.18**, 0.556 g, 3.75 mmol) in toluene (20 mL) was added to a solution of $AlBr_3$ (1.00 g, 3.75 mmol) in toluene (15 mL) at -78 ºC. The mixture was allowed to warm to RT then stirred for 20 h to give a white suspension. The suspension was filtered and the volatiles were removed from the filtrate under reduced pressure. The resultant solid was washed with hexane (2 x 5 mL) and dried *in vacuo* to afford **39** as a white solid. Yield: 1.07 g (60%). Diffraction-quality crystals were grown by slow evaporation from a concentrated hexane solution at RT. ^{1}H NMR (C_6D_6, 400.2 MHz): δ 2.93 (2 H, br s, C$\underline{H}$Me$_2$), 1.02 (3 H, s, CMe), 0.94 (12 H, d, ^{3}J = 4.2 Hz, CH$\underline{Me}_2$). ^{13}C{^{1}H} NMR (C_6D_6, 100.6 MHz): δ 176.9 (NCN), 45.5 ($\underline{C}$HMe$_2$), 24.5 (CH$\underline{Me}_2$), 10.8 (C$\underline{Me}$). ^{27}Al NMR (C_6D_6, 104.3 MHz): δ 69.0. IR (NaCl plates, Nujol mull, cm^{-1}): 1610 (w), 1463 (s), 1377 (m), 1339 (m), 1283 (m), 1173 (w), 1151 (w), 1129 (w), 1022 (w), 937 (w), 843 (w), 722 (w), 590 (m). Anal. found (calcd. for $C_8H_{17}AlBr_2N_2$): C, 28.72 (29.29); H, 5.33 (5.22); N, 8.42 (8.54)%.

Al{(N^{i}Pr)$_2$CPh}Br$_2$ (40) A suspension of Li{(N^{i}Pr)$_2$CPh} (**4.19**, 1.58 g, 7.50 mmol) in toluene (20 mL) was added to a solution of $AlBr_3$ (2.00 g, 7.50 mmol) in toluene

(15 mL) at -78 ºC. The mixture was allowed to warm to RT then stirred for 20 h to give a white suspension. The suspension was filtered and the volatiles were removed from the filtrate under reduced pressure. The resultant solid was washed with hexane (2 x 5 mL) and dried *in vacuo* to afford **40** as a white solid. Yield: 1.35 g (46%). Diffraction-quality crystals were grown by slow evaporation from a concentrated hexane solution at RT. ^{1}H NMR (C_6D_6, 400.2 MHz): δ 7.00 – 6.86 (3 H, m, overlapping *m*- & *p*-C_6H_5), 6.63 (2 H, d, ^{3}J = 7.3 Hz, *o*-C_6H_5), 3.15 – 3.01 (2 H, m, C<u>H</u>Me$_2$), 0.96 (12 H, d, ^{3}J = 4.2 Hz, CH<u>Me</u>$_2$). ^{13}C{^{1}H} NMR (C_6D_6, 100.6 MHz): δ 177.7 (NCN), 130.4 (*p*-C_6H_5), 129.1 (*m*-C_6H_5), 126.8 (*o*-C_6H_3), 46.3 (<u>C</u>HMe$_2$), 24.8 (CH<u>Me</u>$_2$). ^{27}Al NMR (C_6D_6, 104.3 MHz): δ 62.1 (br s). IR (NaCl plates, Nujol mull, cm^{-1}): 1992 (w), 1966 (w), 1921 (w), 1895 (w), 1814 (w), 1772 (w), 1709 (w), 1628 (m), 1604 (m), 1581 (m), 1513 (m), 1365 (s), 1284 (s), 1172 (s), 1129 (s), 1080 (s), 1064 (s), 1049 (s), 1023 (s), 1001 (m), 954 (w), 944 (m), 926 (m), 881 (w), 839 (m), 780 (s), 757 (s), 727 (s), 704 (s), 667 (m), 613 (m), 583 (m). Anal. found (calcd. for $C_{13}H_{19}AlBr_2N_2$): C, 39.91 (40.03); H, 5.10 (4.91); N, 6.82 (7.18)%.

Li{(NCy)$_2$CPh}·0.3(Et$_2$O) (4.20·0.3(Et$_2$O)) A 1.9 M solution of phenyllithium in Et_2O (37.9 mL, 72.0 mmol) was added dropwise to a stirring solution of CyNCNCy (14.9 g, 72.2 mmol) in Et_2O (20 mL) at -78 ºC. The mixture was allowed to warm to RT then stirred for 16 h to give a white suspension. The suspension was filtered and the volatiles were removed from the filtrate under reduced pressure. The resultant solid was washed with hexane (2 x 5 mL) and dried *in vacuo* to afford **4.20·0.3(Et$_2$O)** as a white solid. Yield: 18.3 g (81%). Diffraction-quality crystals of the base-free compound (**4.20**) were obtained by slow evaporation of a concentrated hexane solution of **4.20·0.3(Et$_2$O)** at RT. ^{1}H NMR (C_6D_6, 400.2 MHz): δ 7.32 (2 H, d, ^{3}J = 7.6 Hz, *o*-C_6H_5), 7.26 (2 H, t, ^{3}J = 7.6 Hz, *m*-C_6H_5), 7.13 (1 H, t, ^{3}J = 7.6 Hz, *p*-C_6H_5), 3.27 (1.2 H, q, ^{3}J = 7.5 Hz, OCH_2), 2.96 (2 H, br s, 1-C_6H_{11}), 2.06 (4 H, m, 2,6-C_6H_{11}), 1.84 – 1.67 (8 H, m, overlapping 2',6'-C_6H_{11} & 3,5-C_6H_{11}), 1.52 (2 H, m, 4-C_6H_{11}), 1.32 – 1.19 (2 H, m, 4'-C_6H_{11}), 1.19 – 1.05 (5.8 H, m, 2,6-C_6H_{11} & CH_3). ^{13}C{^{1}H} NMR (C_6D_6, 100.6 MHz): δ 175.0 (NCN), 139.6 (*i*-C_6H_5), 128.5 (*m*-C_6H_5), 127.3 (*p*-C_6H_5), 126.9 (*p*-C_6H_5), 65.9 (OCH_2), 57.5 (1-C_6H_{11}), 38.2 (2,6-C_6H_{11}), 26.4 (overlapping 4-C_6H_{11} & 3,5-C_6H_{11}), 15.6 (CH_3). ^{7}Li NMR (C_6D_6, 155.5 MHz): δ 1.96. IR (NaCl plates, Nujol mull, cm^{-1}): 1615 (w), 1598 (w), 1575 (w), 1464 (s), 1378 (m), 1359 (s), 1345 (s), 1312 (m), 1258 (m), 1242 (m), 1185 (m), 1153 (m), 1092 (s), 1064

(s), 1026 (m), 986 (s), 912 (m), 887 (m), 843 (m), 800 (m), 775 (s), 758 (w), 723 (m), 702 (s), 661 (m), 499 (m). Anal. found (calcd. for $C_{20.2}H_{30}LiN_2O_{0.3}$): C, 77.59 (77.61); H, 9.13 (9.67); 8.79 (8.96)%.

Al{(NCy)$_2$CPh}Br$_2$·0.3(Et$_2$O) (41·0.3(Et$_2$O)) A suspension of Li{(NCy)$_2$CPh}·0.3(Et$_2$O) (**4.20·0.3(Et$_2$O)**, 1.17 g, 3.75 mmol) in toluene (20 mL) was added to a solution of $AlBr_3$ (1.00 g, 3.75 mmol) in toluene (15 mL) at -78 ºC. The mixture was allowed to warm to RT then stirred for 20 h to give a white suspension. The suspension was filtered and the volatiles were removed from the filtrate under reduced pressure. The resultant solid was washed with cold hexane (2 x 5 mL) and dried *in vacuo* to afford **41·0.3(Et$_2$O)** as a white solid. Yield: 1.18 g (64%). Diffraction-quality crystals of the base-free compound (**41**) were obtained by slow evaporation of a concentrated hexane solution of **41·0.3(Et$_2$O)** at RT ^{1}H NMR (C_6D_6, 400.2 MHz): δ 6.94 (3 H, m, *o*- & *p*-C_6H_5), 6.82 – 6.73 (2 H, m, *m*-C_6H_5), 3.51 (1.2 H, q, ^3J = 6.6 Hz, OCH_2), 2.90 (2 H, s, 1-C_6H_{11}), 1.77 – 1.66 (4 H, m, , 2,6-C_6H_{11}), 1.56 – 1.37 (8 H, m, 2',6'-C_6H_{11} & 3,5-C_6H_{11}), 1.22 (2 H, m, , 4-C_6H_{11}), 0.99 – 0.73 (6 H, br m, overlapping 3',5'-C_6H_{11} & 4'-C_6H_{11}), 1.8 (2 H, t, ^3J = 6.6 Hz, CH_3). $^{13}C\{^1H\}$ NMR (C_6D_6, 100.6 MHz): δ 178.1 (NCN), 130.5 (*p*-C_6H_5), 129.1 (*o*-C_6H_5), 126.8 (*m*-C_6H_5), 71.0 (OCH_2), 53.8 (1-C_6H_{11}), 35.6 (2,6-C_6H_{11}), 25.3 (4-C_6H_{11}), 25.0 (3,5-C_6H_{11}), 13.1 (CH_3). ^{27}Al NMR (C_6D_6, 104.3 MHz): δ 64.9 (br s). IR (NaCl plates, Nujol mull, cm^{-1}): 1886 (w), 1808 (w), 1762 (w), 1603 (m), 1580 (m), 1512 (m), 1456 (s), 1365 (s), 1348 (s), 1283 (s), 1264 (s), 1241 (m), 1190 (m), 1148 (m), 1107 (m), 1092 (m), 1079 (m), 1049 (m), 1025 (m), 994 (s), 924 (s), 889 (s), 873 (s), 844 (s), 831 (w), 800 (s), 773 (s), 717 (s), 698 (s), 657, 605 (s). Anal. found (calcd. for $C_{20.2}H_{30}AlBr_2N_2O_{0.3}$): C, 42.62 (42.97); H, 6.73 (6.14); N, 5.26 (5.69)%.

Al{(N^{i}Pr)$_2$CMe}$_2$Br (42) A suspension of Li{(N^{i}Pr)$_2$CMe} (1.11 g, 7.50 mmol) in toluene (20 mL) was added to a solution of $AlBr_3$ (1.00 g, 3.75 mmol) in toluene (15 mL) at -78 ºC. The mixture was allowed to warm to RT then stirred for 20 h to give a white suspension. The suspension was filtered and the volatiles were removed from the filtrate under reduced pressure. The resultant solid was washed with hexane (2 x 5 mL) and dried *in vacuo* to afford **42** as a white solid. Yield: 0.803 g (55%). ^{1}H NMR (C_6D_6, 400.2 MHz): δ 3.40 (4 H, sept, ^3J = 7.0 Hz, C<u>H</u>Me$_2$), 1.45 (6 H, s, CMe), 1.26 (24 H, d, ^3J = 7.0 Hz, CH<u>Me</u>$_2$). $^{13}C\{^1H\}$ NMR (C_6D_6, 100.6 MHz): δ 173.2 (NCN), 45.8 (<u>C</u>HMe$_2$), 24.43 (CH<u>Me</u>$_2$), 11.7 (C<u>Me</u>). ^{27}Al NMR (C_6D_6, 104.3 MHz): δ 58.3.

IR (NaCl plates, Nujol mull, cm^{-1}): 1652 (w), 1530 (s), 1460 (s), 1378 (s), 1338 (m), 1236 (m), 1174 (m), 1152 (m), 1127 (m), 1017 (m), 835 (m), 820 (m), 722 (m), 685 (w), 619 (m), 594 (m), 471 (m). Anal. found (calcd. for $C_{16}H_{34}AlBrN_4$): C, 49.00 (49.36); H, 8.75 (8.80); N, 14.47 (14.39)%.

Al{(N^{i}Pr)$_2$CPh}$_2$Br (43) A suspension of Li{(N^{i}Pr)$_2$CPh} (3.16 g, 15.0 mmol) in toluene (40 mL) was added to a solution of $AlBr_3$ (2.00 g, 7.50 mmol) in toluene (15 mL) at -78 ºC. The mixture was allowed to warm to RT then stirred for 20 h to give a white suspension. The suspension was filtered and the volatiles were removed from the filtrate under reduced pressure. The resultant solid was washed with hexane (2 x 10 mL) and dried *in vacuo* to afford **43** as a white solid. Yield: 2.16 g (56%). ^{1}H NMR (C_6D_6, 400.2 MHz): δ 7.15 – 7.02 (10 H, m, overlapping *o*-, *m*- & *p*-C_6H_5), 3.46 (4 H, sept, ^3J = 4.2 Hz, C<u>H</u>Me$_2$), 1.32 (24 H, d, ^3J = 4.2 Hz, CH<u>Me</u>$_2$). ^{13}C{^{1}H} NMR (C_6D_6, 100.6 MHz): δ 175.9 (NCN), 132.5 (*i*-C_6H_5), 128.9 (*p*-C_6H_5), 128.8 (*i*-C_6H_5), 128.4 (*m*-C_6H_5), 127.0 (*o*-C_6H_5), 46.4 (<u>C</u>HMe$_2$), 24.4 (CH<u>Me</u>$_2$). ^{27}Al NMR (C_6D_6, 104.3 MHz): δ 58.6. IR (NaCl plates, Nujol mull, cm^{-1}): 1963 (w), 1895 (w), 1826 (w), 1773 (w), 1703 (w), 1633 (w), 1605 (w), 1578 (m), 1522 (s), 1479 (s), 1380 (s), 1345 (s), 1325 (s), 1262 (s), 1170 (s), 1154 (s), 1127 (s), 1109 (s), 1077 (m), 1055 (w), 1039 (w), 1020 (s), 954 (w), 941 (w), 922 (m), 832 (w), 782 (s), 752 (s), 739 (s), 729 (s), 706 (s), 663 (w), 613 (m), 593 (m), 562 (w). Anal. found (calcd. for $C_{26}H_{38}AlBrN_4$): C, 60.78 (60.81); H, 7.53 (7.46); N, 10.79 (10.91)%.

Al{(NCy)$_2$CPh}$_2$Br (44) A suspension of Li{(NCy)$_2$CPh}·0.3(Et$_2$O) (**4.20·0.3(Et$_2$O)**, 2.34 g, 7.50 mmol) in toluene (20 mL) was added to a solution of $AlBr_3$ (1.00 g, 3.75 mmol) in toluene (15 mL) at -78 ºC. The mixture was allowed to warm to RT then stirred for 20 h to give a white suspension. The suspension was filtered and the volatiles were removed from the filtrate under reduced pressure. The resultant solid was washed with hexane (2 x 5 mL) and dried *in vacuo* to afford **44** as a white solid. Yield: 1.69 g (67%). Diffraction-quality crystals were grown by slow evaporation from a concentrated hexane solution at RT. ^{1}H NMR (C_6D_6, 400.2 MHz): δ 7.26 (4 H, d, ^3J = 7.0 Hz, *o*-C_6H_5), 7.14 – 7.00 (6 H, m, overlapping *m*-C_6H_5 & *p*-C_6H_5), 3.17 (4 H, s, 1-C_6H_{11}), 2.15 – 1.99 (16 H, m, 2,6-C_6H_{11}), 1.69 (8 H, m, 3,5-C_6H_{11}), 1.43 (4 H, m, 4-C_6H_{11}), 1.23 – 1.09 (4 H, m, 4′-C_6H_{11}), 1.08 – 0.94 (8 H, m, 3',5'-C_6H_{11}). ^{13}C{^{1}H} NMR (C_6D_6, 100.6 MHz): δ 176.4 (NCN), 133.2 (*i*-C_6H_5), 129.4 (*p*-C_6H_5), 128.8 (*m*-C_6H_5), 127.4 (*o*-C_6H_5), 55.5 (1-C_6H_{11}), 35.2 (2,6-C_6H_{11}), 26.3 (3,5-C_6H_{11}),

25.9 (4-C_6H_{11}). ^{27}Al NMR (C_6D_6, 104.3 MHz): δ 64.2. IR (NaCl plates, Nujol mull, cm^{-1}): 1607 (w), 1579 (w), 1520 (m), 1464 (s), 1376 (m), 1346 (m), 1312 (m), 1258 (m), 1237 (m), 1188 (m), 1155 (w), 1108 (m), 1080 (m), 1049 (m), 1024 (m), 993 (m), 925 (m), 890 (m), 843 (w), 803 (m), 776 (m), 724 (m), 704 (m), 682 (m), 595 (m). Anal. found (calcd. for $C_{38}H_{54}AlBrN_4$): C, 67.72 (67.74); H, 8.33 (8.08); N, 8.42 (8.32)%.

Al{(N^{i}Pr)$_2$CMe}{Ga(NArCH)$_2$}$_2$ (45) Toluene (20 mL) was added to Al{(N^{i}Pr)$_2$CMe}Br$_2$ (**39**, 0.300 g, 0.914 mmol) and [KGa(NArCH)$_2$(Et$_2$O)]$_2$ (1.02 g, 0.914 mmol) at -78 ºC to give a red suspension. The suspension was allowed to warm to RT, stirred for 1 h then filtered to give a red solution. Volatiles were removed under reduced pressure and the resultant solid washed with cold hexane (2 x 1 mL) at 0 ºC and dried *in vacuo* to afford **45** as an orange solid. Yield: 0.310 g (32%). ^{1}H NMR (C_6D_6, 400.2 MHz): δ 7.18 – 7.14 (12 H, s, *m*- & *p*-C_6H_3), 6.28 (4 H, s, ArNC<u>H</u>), 3.55 (8 H, sept, ^3J = 6.9 Hz, ArC<u>H</u>Me$_2$), 2.74 (2 H, sept, ^3J = 6.2 Hz, NC<u>H</u>Me$_2$), 1.32 (24 H, d, ^3J = 6.9 Hz, ArCH<u>Me</u>$_2$), 1.17 (24 H, d, ^3J = 6.9 Hz, ArCH<u>Me</u>$_2$), 1.11 (3 H, s, CMe), 0.29 (12 H, d, ^3J = 6.2 Hz, NCH<u>Me</u>$_2$). ^{13}C{^{1}H} NMR (C_6D_6, 100.6 MHz): δ 172.5 (NCN), 146.7 (*i*-C_6H_3), 145.4 (*o*-C_6H_3), 125.5 (*p*-C_6H_3), 123.3 (*m*-C_6H_3), 123.0 (ArN<u>C</u>H), 44.9 (N<u>C</u>HMe$_2$), 28.3 (Ar<u>C</u>HMe$_2$), 25.3 (ArCH<u>Me</u>$_2$), 25.2 (ArCH<u>Me</u>$_2$), 23.8 (NCH<u>Me</u>$_2$), 11.5 (C<u>Me</u>). ^{27}Al NMR (C_6D_6, 104.3 MHz): δ 73.8. IR (NaCl plates, Nujol mull, cm^{-1}): 1636 (w), 1589 (w), 1460 (s), 1379 (s), 1358 (s), 1325 (s), 1260 (s), 1212 (m), 1176 (w), 1119 (m), 1105 (m), 1057 (w), 1041 (w), 1022 (w), 934 (w), 907 (w), 838 (w), 802 (m), 759 (m), 746 (w), 722 (w), 680 (w), 661 (w). Anal. found (calcd. for $C_{60}H_{89}AlGa_2N_6$): C, 67.62 (67.93); H, 8.33 (8.46); N, 7.60 (7.92)%.

Al{(N^{i}Pr)$_2$CPh}{Ga(NArCH)$_2$}$_2$ (46) Toluene (20 mL) was added to Al{(N^{i}Pr)$_2$CPh}Br$_2$ (**40**, 0.300 g, 0.769 mmol) and [KGa(NArCH)$_2$(Et$_2$O)]$_2$ (0.861 g, 0.769 mmol) at -78 ºC to give a red suspension. The suspension was allowed to warm to RT, stirred for 1 h then filtered to give a red solution. Volatiles were removed under reduced pressure and the resultant solid washed with cold hexane (2 x 1 mL) at 0 ºC and dried *in vacuo* to afford **46** as an orange solid. Yield: 0.370 g (43%). ^{1}H NMR (C_6D_6, 400.2 MHz): δ 7.17 – 7.15 (12 H, m, *o*- & *m*-C_6H_3), 6.99 – 6.93 (5 H, m, *o-, m-* & *p*-C_6H_5), 6.32 (4 H, s, ArNC<u>H</u>), 3.63 (8 H, sept, ^3J = 6.9 Hz, ArC<u>H</u>Me$_2$), 2.86 (2 H, sept, ^3J = 6.3 Hz, NC<u>H</u>Me$_2$), 1.36 (24 H, d, ^3J = 6.9 Hz, ArCH<u>Me</u>$_2$), 1.27

(24 H, d, ^3J = 6.9 Hz, ArCH$\underline{Me}_2$), 0.27 (12 H, d, ^3J = 6.3 Hz, NCH$\underline{Me}_2$). $^{13}C\{^1H\}$ NMR (C_6D_6, 100.6 MHz): δ 174.4 (NCN), 146.6 (*i*-C_6H_3), 145.2 (*o*-C_6H_3), 130.6 (*i*-C_6H_5), 128.6 (*p*-C_6H_5), 127.4 (*m*-C_6H_5), 126.7 (*o*-C_6H_5), 123.4 (ArN$\underline{C}$H), 123.4 (*m*-C_6H_3), 123.2 (*p*-C_6H_3), 45.6 (N$\underline{C}$HMe$_2$), 28.4 (Ar$\underline{C}$HMe$_2$), 25.6 (ArCH$\underline{Me}_2$), 25.3 (ArCH$\underline{Me}_2$), 24.3 (NCH$\underline{Me}_2$). ^{27}Al NMR (C_6D_6, 104.3 MHz): δ 69.2. IR (NaCl plates, Nujol mull, cm^{-1}): 1921 (w), 1856 (w), 1655 (w), 1625 (w), 1588 (w), 1460 (s), 1380 (s), 1359 (s), 1323 (s), 1258 (s), 1210 (m), 1177 (m), 1145 (m), 1120 (m), 1057 (m), 1042 (w), 1023 (w), 955 (m), 934 (m), 907 (w), 802 (m), 785 (m), 759 (m), 723 (m), 703 (m), 688 (m), 661 (w). A satisfactory elemental analysis could not be obtained.

NMR tube-scale synthesis of Al{(NCy)$_2$CPh}{Ga(NArCH)$_2$}$_2$ (47) To Al{(NCy)$_2$CPh}Br$_2$·0.3(Et$_2$O) (**41·0.3(Et$_2$O)**) 10.0 mg, 20.3 μmol) was added a solution of [KGa(NArCH)$_2$(Et$_2$O)]$_2$ (22.7 mg, 20.3 μmol) in C_6D_6 (0.6 mL). The solution was analysed by ^{1}H NMR spectroscopy showing completion of the reaction after 24 h. Diffraction-quality crystals were grown by slow evaporation from a concentrated benzene solution at RT. ^{1}H NMR (C_6D_6, 400.2 MHz): δ 7.24 – 7.17 (8 H, m, *m*-C_6H_3), 7.18 (4 H, app s, *p*-C_6H_3), 7.15 – 7.00 (5 H, m, *o-, m-* & *p*-C_6H_5), 6.31 (4 H, s, NCH), 3.67 (8 H, sept, ^3J = 6.9 Hz, C$\underline{H}$Me$_2$), 3.58 – 3.51 (2 H, m, 1-C_6H_{11}), 1.92 – 1.75 (8 H, m, 2,6-C_6H_{11}), 1.43 – 1.41 (4 H, m, 3,5-C_6H_{11}), 1.32 – 1.26 (56 H, overlapping 2 x m & d, ^3J = 6.9 Hz, CH$\underline{Me}_2$, 3',5'-C_6H_{11} & 4-C_6H_{11}). $^{13}C\{^1H\}$ NMR (C_6D_6, 100.6 MHz): δ 174.9 (NCN), 150.5 (*i*-C_6H_3), 149.5 (*o*-C_6H_3), 133.8 (*i*-C_6H_5), 129.0 (*p*-C_6H_5), 125.0 (*p*-C_6H_3), 124.4 (*m*-C_6H_3), 123.9 (*m*-C_6H_5), 123.4 (*o*-C_6H_5), 122.7 (ArN$\underline{C}$H), 67.8 (1-C_6H_{11}), 36.4 (2,6-C_6H_{11}), 28.7 (3,5-C_6H_{11}), 28.3 ($\underline{C}$HMe$_2$), 25.8 (4-C_6H_{11}), 25.5 (CH$\underline{Me}_2$).). ^{27}Al NMR (C_6D_6, 104.3 MHz): δ 70.36.

Al{(N^{i}Pr)$_2$CMe}$_2${Ga(NArCH)$_2$} (48) Toluene (20 mL) was added to Al{(N^{i}Pr)$_2$CMe}$_2$Br (**42**, 0.300 g, 0.770 mmol) and [KGa(NArCH)$_2$(Et$_2$O)]$_2$ (0.431 g, 0.385 mmol) at -78 ºC to give a red suspension. The suspension was allowed to warm to RT, stirred for 1 h then filtered to give a red solution. Volatiles were removed under reduced pressure and the resultant solid washed with cold hexane (2 x 0.5 mL) at 0 ºC and dried *in vacuo* to afford **48** as an orange solid. Yield: 0.167 g (28%). ^{1}H NMR (C_6D_6, 400.2 MHz): δ 7.27 – 7.24 (4 H, m, *m*-C_6H_3), 7.21 – 7.18 (2 H, m, *p*-C_6H_3), 6.43 (2 H, s, ArNC$\underline{H}$), 3.81 (4 H, sept, ^3J = 6.9 Hz, ArC$\underline{H}$Me$_2$), 3.29 (4 H, sept, ^3J = 6.7 Hz, NC$\underline{H}$Me$_2$), 1.46 (6 H, s, CMe), 1.40 (12 H, d, ^3J = 6.9 Hz, ArCH$\underline{Me}_2$), 1.33 (12 H, d, ^3J = 6.9 Hz, ArCH$\underline{Me}_2$), 0.98 (24 H, d, ^3J = 6.7 Hz,

NCH$\underline{Me}_2$). $^{13}C\{^1H\}$ NMR (C_6D_6, 100.6 MHz): δ 172.2 (NCN), 148.9 (*i*-C_6H_3), 145.2 (*o*-C_6H_3), 124.2 (*p*-C_6H_3), 123.1 (*m*-C_6H_3), 122.0 (ArN$\underline{C}$H), 46.5 (N$\underline{C}$HMe$_2$), 28.7 (Ar$\underline{C}$HMe$_2$), 26.1 (ArCH$\underline{Me}_2$), 25.6 (NCH$\underline{Me}_2$), 25.5 (ArCH$\underline{Me}_2$), 13.2 (C$\underline{Me}$). ^{27}Al NMR (C_6D_6, 104.3 MHz): δ 64.5. IR (NaCl plates, Nujol mull, cm^{-1}): 1655 (w), 1603 (w), 1588 (w), 1529 (s), 1494 (s), 1463 (s), 1378 (s), 1355 (s), 1338 (s), 1322 (s), 1262 (s), 1244 (s), 1212 (m), 1197 (m), 1173 (s), 1152 (m), 1139 (m), 1122 (m), 1081 (m), 1057 (m), 1041 (m), 1017 (m), 968 (w), 933 (w), 903 (w), 875 (w), 824 (m), 803 (m), 763 (m), 745 (w), 727 (w), 687 (w), 672 (w), 655 (w), 620 (w), 600 (m), 482 (w). Anal. found (calcd. for $C_{42}H_{70}AlGaN_6$): C, 66.81 (66.75); H, 9.68 (9.34); N, 10.69 (11.12)%.

Al{(N^{i}Pr)$_2$CPh}$_2${Ga(NArCH)$_2$} (49) Toluene (20 mL) was added to Al{(N^{i}Pr)$_2$CPh}$_2$Br (**43**, 0.200 g, 0.389 mmol) and [KGa(NArCH)$_2$(Et$_2$O)]$_2$ (0.218 g, 0.195 mmol) at -78 ºC to give a red suspension. The suspension was allowed to warm to RT, stirred for 1 h then filtered to give a red solution. Volatiles were removed under reduced pressure and the resultant solid washed with cold hexane (2 x 1 mL) at 0 ºC and dried *in vacuo* to afford **49** as an orange solid. Yield: 0.133 g (39%). Diffraction-quality crystals were grown by slow evaporation from a concentrated benzene solution at RT. ^{1}H NMR (C_6D_6, 400.2 MHz): δ 7.35 – 7.31 (4 H, m, *m*-C_6H_3), 7.30 – 7.27 (2 H, m, *p*-C_6H_3), 7.15 – 7.11 (2 H, m, *o*-C_6H_5), 7.10 (2 H, m, *m*-C_6H_3), 7.09 – 7.07 (2 H, m, *o*-C_6H_3), 7.07 – 7.03 (2 H, m, *p*-C_6H_3), 6.47 (2 H, s, ArNC$\underline{H}$), 3.97 (4 H, sept, ^3J = 6.7 Hz, ArC$\underline{H}$Me$_2$), 3.27 (4 H, sept, ^3J = 6.6 Hz, NC$\underline{H}$Me$_2$), 1.42 (12 H, d, ^3J = 6.7 Hz, ArCH$\underline{Me}_2$), 1.39 (12 H, d, ^3J = 6.7 Hz, ArCH$\underline{Me}_2$), 1.11 (24 H, d, ^3J = 6.6 Hz, NCH$\underline{Me}_2$). $^{13}C\{^1H\}$ NMR (C_6D_6, 100.6 MHz): δ 174.6 (NCN), 149.9 (*i*-C_6H_3), 145.7 (*o*-C_6H_3), 133.3 (*i*-C_6H_5), 129.1 (*m*-C_6H_5), 128.6 (*p*-C_6H_5), 124.4 (*p*-C_6H_3), 123.6 (*o*-C_6H_5), 123.4 (*m*-C_6H_3), 122.2 (ArN$\underline{C}$H), 46.8 (N$\underline{C}$HMe$_2$), 29.0 (Ar$\underline{C}$HMe$_2$), 26.6 (ArCH$\underline{Me}_2$), 25.6 (NCH$\underline{Me}_2$), 24.1 (ArCH$\underline{Me}_2$). ^{27}Al NMR (C_6D_6, 104.3 MHz): δ 70.6. IR (NaCl plates, Nujol mull, cm^{-1}): 1663 (w), 1640 (w), 1602 (w), 1587 (w), 1577 (w), 1568 (w), 1520 (m), 1481 (s), 1465 (s), 1379 (s), 1355 (s), 1340 (s), 1321 (m), 1262 (s), 1213 (w), 1198 (w), 1170 (m) 1152 (m), 1127 (m), 1117 (m), 1104 (m), 1076 (m), 1058 (m), 1041 (m), 1020 (m), 957 (w), 933 (w), 923 (w), 901 (w), 799 (m), 780 (m), 759 (m), 750 (m), 730 (w), 708 (m), 677 (w), 656 (w), 610 (w), 594 (w). Anal. found (calcd. for $C_{52}H_{74}AlGaN_6$): C, 70.86 (70.98); H, 8.45 (8.48); N, 9.40 (9.55)%.

Al{(NCy)$_2$CPh}$_2${Ga(NArCH)$_2$} (50) Toluene (20 mL) was added to Al{(NCy)$_2$CPh}$_2$Br (**44**, 0.200 g, 0.297 mmol) and [KGa(NArCH)$_2$(Et$_2$O)]$_2$ (0.166 g, 0.148 mmol) at -78 ºC to give a red suspension. The suspension was allowed to warm to RT, stirred for 1 h then filtered to give a red solution. Volatiles were removed under reduced pressure and the resultant solid washed with cold hexane (2 x 1 mL) at 0 ºC and dried *in vacuo* to afford **50** as an orange solid. Yield: 0.117 g (38%). ^{1}H NMR (C$_6$D$_6$, 400.2 MHz): δ 7.39 – 7.35 (4 H, m, *m*-C$_6$H$_3$), 7.34 – 7.28 (2 H, m, *p*-C$_6$H$_3$), 7.14 – 7.00 (10 H, m, overlapping *o-, m-* & *p*-C$_6$H$_5$), 6.44 (2 H, s, ArNC<u>H</u>), 3.98 (4 H, sept, ^3J = 6.9 Hz, C<u>H</u>Me$_2$), 2.95 – 2.83 (4 H, m, 1-C$_6$H$_{11}$), 1.87 – 1.55 (24 H, m, overlapping 2,6-C$_6$H$_{11}$ & 3,5-C$_6$H$_{11}$), 1.45 (12 H, d, ^3J = 6.9 Hz, CH<u>Me</u>$_2$), 1.40 (12 H, d, ^3J = 6.9 Hz, CH<u>Me</u>$_2$), 1.12 – 0.86 (16 H, m, overlapping 3',5'-C$_6$H$_{11}$ & 4-C$_6$H$_{11}$). ^{13}C{^{1}H} NMR (C$_6$D$_6$, 100.6 MHz): δ 174.9 (NCN), 149.54 (*i*-C$_6$H$_3$), 145.9 (*o*-C$_6$H$_3$), 133.8 (*i*-C$_6$H$_5$), 129.0 (*p*-C$_6$H$_5$), 128.6 (*m*-C$_6$H$_5$), 127.4 (*o*-C$_6$H$_5$), 124.0 (*p*-C$_6$H$_3$), 123.3 (*m*-C$_6$H$_3$), 122.3 (ArN<u>C</u>H), 55.4 (1-C$_6$H$_{11}$), 36.4 (2,6-C$_6$H$_{11}$), 28.4 (<u>C</u>HMe$_2$), 26.6 (CH<u>Me</u>$_2$), 26.4 (3,5-C$_6$H$_{11}$), 25.9 (4-C$_6$H$_{11}$), 23.7 (CH<u>Me</u>$_2$). ^{27}Al NMR (C$_6$D$_6$, 104.3 MHz): δ 64.6. IR (NaCl plates, Nujol mull, cm^{-1}): 1640 (w), 1590 (w), 1523 (m), 1463 (s), 1377 (s), 1366 (s), 1353 (s), 1318 (m), 1258 (m), 1211 (w), 1177 (w), 1152 (w), 1102 (m), 1076 (m), 1060 (m), 1025 (m), 993 (w), 962 (w), 925 (w), 889 (w), 844 (w), 799 (w), 775 (w), 759 (m), 727 (m), 703 (m), 680 (w), 654 (w). Anal. found (calcd. for C$_{64}$H$_{90}$AlGaN$_6$): C, 73.74 (73.90); H, 8.88 (8.72); N, 7.97 (8.08)%.

Al(^{Ph}NacNac)Br$_2$ (51) A suspension of K(^{Ph}NacNac) (1.17 g, 3.75 mmol) in toluene (20 mL) was added to a solution of AlBr$_3$ (1.00 g, 3.75 mmol) in toluene (15 mL) at -78 ºC. The mixture was allowed to warm to RT then stirred for 16 h to give a white suspension. The suspension was filtered and the volatiles were removed from the filtrate under reduced pressure. The resultant solid was washed with hexane (2 x 5 mL) and dried *in vacuo* to afford **44** as a white solid. Yield: 1.35 g (64%). Diffraction-quality crystals were grown by slow evaporation from a concentrated benzene solution at RT. ^{1}H NMR (C$_6$D$_6$, 400.2 MHz): δ 7.20 (4 H, d, ^3J = 8.1 Hz, *o*-C$_6$H$_5$), 7.05 (4 H, t, ^3J = 7.7 Hz, *m*-C$_6$H$_5$), 6.93 (2 H, t, ^3J = 7.4 Hz, *p*-C$_6$H$_5$), 4.69 (1 H, s, CH, NC(Me)C<u>H</u>), 1.39 (6 H, s, CMe). ^{13}C{^{1}H} NMR (C$_6$D$_6$, 100.6 MHz): δ 170.8 (N<u>C</u>Me), 142.9 (*i*-C$_6$H$_5$), 129.6 (*m*-C$_6$H$_5$), 127.4 (*o*-C$_6$H$_5$), 127.3 (*p*-C$_6$H$_5$), 99.0 (NC(Me)<u>C</u>H), 23.2 (NC<u>Me</u>). ^{27}Al NMR (C$_6$D$_6$, 104.3 MHz): δ 70.5. IR (NaCl plates,

Nujol mull, cm^{-1}): 1594 (w), 1585 (w), 1533 (s), 1484 (s), 1450 (s), 1377 (s), 1365 (s), 1305 (m), 1260 (w), 1197 (w), 1171 (w), 1154 (w), 1092 (w), 1071 (w), 1025 (m), 1001 (m), 947 (m), 926 (m), 880 (m), 799 (m), 781 (m), 771 (m), 757 (m), 722 (w), 701 (m), 692 (m), 682 (w), 643 (w), 565 (m), 521 (m). Anal. found (calcd. for $C_{17}H_{17}AlBr_2N_2$): C, 73.74 (46.82); H, 8.88 (3.93); N, 7.97 (6.42)%.

NMR tube-scale synthesis of Al(^{Ph}NacNac){Ga(NArCH)$_2$}$_2$ (52) To Al(^{Ph}NacNac)Br_2 (**51**, 10.0 mg, 22.9 μmol) was added a solution of $[KGa(NArCH)_2(Et_2O)]_2$ (25.7 mg, 22.9 μmol) in C_6D_6 (0.6 mL). The solution was analysed by ^{1}H NMR spectroscopy showing completion of the reaction after 2 h. ^{1}H NMR (C_6D_6, 400.2 MHz): δ 7.20 – 7.18 (12 H, m, *m*- & *p*-C_6H_3), 7.14 – 7.11 (2 H, m, *o*-C_6H_5), 6.87 – 6.78 (6 H, m, *m*- & *p*-C_6H_5), 6.23 (4 H, s, NCH), 4.66 (1 H, s, NC(Me)C<u>H</u>), 3.43 (8 H, sept, ^3J = 6.8 Hz, CH<u>Me</u>$_2$), 1.29 – 1.25 (30 H, m, overlapping NCMe & CH<u>Me</u>$_2$), 1.03 (24 H, d, ^3J = 6.8 Hz, CH<u>Me</u>$_2$). ^{13}C{^{1}H} NMR (C_6D_6, 100.6 MHz): δ 171.3 (N<u>C</u>Me), 147.7 (*i*-C_6H_3), 145.5 (*o*-C_6H_3), 143.9 (*i*-C_6H_5), 130.5 (*m*-C_6H_5), 127.0 (*p*-C_6H_5), 125.2 (*p*-C_6H_3), 123.9 (*o*-C_6H_5), 123.6 (*m*-C_6H_3), 123.2 (NCH), 100.7 (NC(Me)<u>C</u>H), 28.4 (<u>C</u>HMe$_2$), 25.4 (CH<u>Me</u>$_2$), 25.2 (CH<u>Me</u>$_2$), 23.7 (NC<u>Me</u>). ^{27}Al NMR (C_6D_6, 104.3 MHz): δ 69.6 (s).

NMR tube-scale synthesis of Al(^{Dipp}NacNac){Ga(NArCH)$_2$}Br (53) To Al{^{Dipp}NacNac)Br_2 (**51**, 10 mg, 16 μmol) was added a solution of $[KGa(NArCH)_2(Et_2O)]_2$ (9.3 mg, 8.2 μmol) in C_6D_6 (0.6 mL). The solution was analysed by ^{1}H NMR spectroscopy showing completion of the reaction after 2 h. Diffraction-quality crystals were grown by slow evaporation from a concentrated benzene solution at RT. ^{1}H NMR (C_6D_6, 400.2 MHz): δ 7.23 – 7.17 (6 H, m, overlapping *m*- & *p*-C_6H_3 of Ga(NArCH)$_2$), 7.14 – 7.11 (2 H, m, *p*-C_6H_3 of ^{Dipp}NacNac), 7.07 – 7.02 (2 H, m, *m*-C_6H_3 of ^{Dipp}NacNac), 6.98 – 6.94 (2 H, m, *m*-C_6H_3 of ^{Dipp}NacNac), 6.34 (2 H, s, NCH), 4.87 (1 H, s, NC(Me)C<u>H</u>), 3.54 – 3.44 (4 H, m, C<u>H</u>Me$_2$ of Ga(NArCH)$_2$), 3.38 (2 H, sept, ^3J = 6.7 Hz, C<u>H</u>Me$_2$ of ^{Dipp}NacNac), 2.97 (2 H, sept, ^3J = 6.7 Hz, C<u>H</u>Me$_2$ of ^{Dipp}NacNac), 1.36 (6 H, s, NCMe), 1.32 (12 H, d, ^3J = 6.9 Hz, CH<u>Me</u>$_2$ of Ga(NArCH)$_2$), 1.27 (6 H, d, ^3J = 6.7 Hz, CH<u>Me</u>$_2$ of ^{Dipp}NacNac), 1.20 (6 H, d, ^3J = 6.7 Hz, CH<u>Me</u>$_2$ of ^{Dipp}NacNac), 1.15 (12 H, d, , ^3J = 6.9 Hz, CH<u>Me</u>$_2$ of Ga(NArCH)$_2$), 1.01 – 0.96 (12 H, dd, ^3J = 6.7 & 3.3 Hz). ^{13}C{^{1}H} NMR (C_6D_6, 100.6 MHz): δ 171.9 (N<u>C</u>Me), 146.9 (*i*-C_6H_3 of Ga(NArCH)$_2$), 144.9 (*o*-C_6H_3 of Ga(NArCH)$_2$), 144.8 (*o*-C_6H_3 of ^{Dipp}NacNac), 144.3 (*o*-C_6H_3 of ^{Dipp}NacNac),

125.1 (*m*-C_6H_3 of ^{Dipp}NacNac), 124.6 (*m*-C_6H_3 of ^{Dipp}NacNac), 123.7 (*p*-C_6H_3 of ^{Dipp}NacNac), 123.6 (*p*-C_6H_3 of Ga(NArCH)$_2$), 123.5 (*m*-C_6H_3 of Ga(NArCH)$_2$), 123.0 (NCH), 100.3 (NC(Me)CH), 29.3 ($\underline{C}HMe_2$ of ^{Dipp}NacNac), 29.1 ($\underline{C}HMe_2$ of ^{Dipp}NacNac), 28.4 ($\underline{C}HMe_2$ of Ga(NArCH)$_2$), 26.9 ($CH\underline{Me}_2$ of Ga(NArCH)$_2$), 26.4 ($CH\underline{Me}_2$ of ^{Dipp}NacNac), 25.0 ($CH\underline{Me}_2$ of ^{Dipp}NacNac), 24.8 ($CH\underline{Me}_2$ of ^{Dipp}NacNac), 24.8 ($CH\underline{Me}_2$ of ^{Dipp}NacNac), 24.5 ($CH\underline{Me}_2$ of Ga(NArCH)$_2$), 24.1 (NC$\underline{Me}$). ^{27}Al NMR (C_6D_6, 104.3 MHz): δ 71.8.

5.8 References

1. A. B. Pangborn, M. A. Giardello, R. H. Grubbs, R. K. Rosen and F. J. Timmers, *Organometallics*, 1996, **15**, 1518.
2. Z. Otwinowski and W. Minor, *Processing of X-ray Diffraction Data Collected in Oscillation Mode*, Academic press, New York, 1997.
3. *Journal*, 2011.
4. A. Altomare, G. Cascarano, G. Giacovazzo, A. Guagliardi, M. C. Burla, G. Polidori and M. Camalli, *J. Appl. Crystallogr.*, 1994, **27**, 435.
5. L. Palatinus and G. Chapuis, *J. Appl. Cryst.*, 2007, **40**, 786.
6. P. W. Betteridge, J. R. Cooper, R. I. Cooper, K. Prout and D. J. Watkin, *J. Appl. Cryst.*, 2003, **36**, 1487.
7. R. J. Baker, R. D. Farley, C. Jones, M. Kloth and D. M. Murphy, *J. Chem. Soc., Dalton Trans.*, 2002, 3844.
8. O. Bonello, C. Jones, A. Stasch and W. D. Woodul, *Organometallics*, 2010, **29**, 4914.
9. J. S. Plotkin and S. G. Shore, *Inorg. Chem.*, 1981, **20**, 284.
10. S. J. Bonyhady, C. Jones, S. Nembenna, A. Stasch, A. J. Edwards and G. J. McIntyre, *Chem. Eur. J.*, 2010, **16**, 938.
11. S. Pillai Sarish, A. Jana, H. W. Roesky, T. Schulz, M. John and D. Stalke, *Inorg. Chem.*, 2010, **49**, 3816.
12. C. Jones, D. P. Mills, J. A. Platts and R. P. Rose, *Inorg. Chem.*, 2006, **45**, 3146.
13. J. Zou, D. J. Berg, D. Stuart, R. McDonald and B. Twamley, *Organometallics*, 2011, **30**, 4958.
14. B. Core, D. Phil Thesis, University of Oxford, 2015.
15. M. P. Coles and R. F. Jordan, *J. Am. Chem. Soc.*, 1997, **119**, 8125.

16. J. Richter, J. Feiling, H. G. Schmidt, M. Noltemeyer, W. Brüser and F. T. Edelmann, *Z. Anorg. Allg. Chem.*, 2004, **630**, 1269.
17. Y. K. Radwan, A. Maity and T. S. Teets, *Inorg. Chem.*, 2015, **54**, 7122.
18. Y. Yang, T. Schulz, M. John, A. Ringe, H. W. Roesky, D. Stalke, J. Magull and H. Ye, *Inorg. Chem.*, 2008, **47**, 2585.